Engineered Floating Wetlands as a Secondary Oil Spill Remediation Strategy for Freshwater Shorelines

by

Madeline J. Stanley

A Thesis submitted to the Faculty of Graduate Studies of

The University of Manitoba

in partial fulfilment of the requirements of the degree of

DOCTOR OF PHILOSOPHY

Department of Biosystems Engineering

University of Manitoba

Winnipeg, Manitoba, Canada

Abstract

Conventional oil spill recovery methods are not desirable for sensitive freshwater shorelines due to damage caused from physical recovery efforts. This, in addition to the residual oil, causes long term impacts to the environment. With increasing production and transport of oil across Canada, there is a need for non-invasive alternatives for oil spill remediation. This thesis has assessed the use of Engineered Floating Wetlands (EFW) as a non-invasive strategy for remediating oil spills in sensitive habitats, through a series of in-lake model oil spill and microcosm experiments conducted at the International Institute for Sustainable Development Experimental Lakes Area. The in-lake experiments monitored changes to the EFW root microbial community upon exposure to model spills of diluted bitumen and conventional heavy crude oil following primary recovery in shoreline enclosures. These experiments found that EFWs support a diverse microbial community, with high richness and evenness of prokaryotes, and variable dominance of eukaryotes. While direct roles in degradation were not assessed, total polycyclic aromatic compounds (PACs) declined to near background conditions in the aqueous environment after ~60-70 days, likely a result of various biotic and abiotic processes. To confirm whether plants can enhance removal of PACs, a microcosm experiment was conducted to assess the removal of 1 mg/L phenanthrene by three emergent plants from freshwater over 21 days. All treatments resulted in successful removal of phenanthrene (≥ 89% from initial measured concentration). *Typha* sp. had a greater removal rate than *Carex lasiocarpa*, but not *C. utriculata*. However, the control with no vegetation also resulted in successful phenanthrene removal, likely from biostimulation. There were no differences between the control and planted microcosms, however *Typha* generally had greater removal rates than the control. While all treatments had successful removal, it was clear there were plant specific functions influencing water quality and removal.

This thesis has demonstrated that EFWs may be a successful alternative to conventional strategies for sensitive environments. A number of recommendations are made throughout this thesis to help advance knowledge in this field to protect freshwater ecosystems. Specifically, future research is recommended to further identify factors driving successful bioremediation mediated by EFWs.

Acknowledgements

I acknowledge my gratitude to be able to conduct this research at the International Institute for Sustainable Development Experimental Lakes Area (IISD-ELA) in northwestern Ontario, the traditional land of the Anishanaabe Nation in Treaty 3 territory and the Homeland of the Métis Nation. As well at the University of Manitoba, located in Treaty 1 territory, the traditional land of the Anishinaabeg, Cree, Ojibwe-Cree, Dakota, and Dene Peoples, and the Homeland of the Métis Nation.

Funding for this research was primarily provided by Genome Canada [GAPP R13-6336] and Mitacs Accelerate [Grant Number IT15202], and an NSERC Collaborative Research and Development Grant awarded to Dr. Gregg Tomy [NSERC File CRDPJ 532225-18] supported analyses in the Centre for Oil and Gas Research and Development (COGRAD) laboratory. The overall FOReSt and FLOWTER study had numerous supporters and collaborators including Canadian Association of Petroleum Producers, Canadian Energy Pipeline Association (defunct), Canada Energy Regulator, COGRAD, Enbridge Inc., Environment and Climate Change Canada, Genome Canada, Genome Prairie, Genome Quebec, IISD-ELA, Institute national de la recherche scientific, IISD, Jacor LLC, McGill University, Mitacs, Myera Group, National Research Council-Conseil national de recherches Canada, Natural Resources Canada, Natural Sciences and Engineering Research Council of Canada, Polaris Applied Science, Stantec Consulting Ltd., TransCanada Pipelines, TransMountain Pipelines, University of Manitoba, and University of Saskatchewan.

I would also like to thank the IISD-ELA for the IISD-ELA Graduate Research Fellowship and the IISD-ELA Student Support Fund which helped to support my stay at the research facility over the duration of the 2021 and 2022 field seasons, the University of Manitoba

for nominating and awarding me the Price Graduate Scholarship for Women in Engineering (2020-2021), the Faculty of Graduate Studies Research Completion Scholarship (2021-2022), and the Faculty of Graduate Studies Travel Award (2023). Thank you as well to SETAC North America for providing travel award to attend the 2022 conference.

The IISD Experimental Lakes Area research facility is like no other, it is truly the only place around the world to conduct this scale of ecosystem research. I have had the absolute pleasure to work and study at this field station and learn from some incredible scientists and colleagues. Other than the ground-breaking science, one of the greatest joys of working at the IISD-ELA and one of my greatest outcomes are the friendships made. I have had the honor to work alongside some of the most kind and supportive people, who bring so much joy to my life. Thank you to the amazing toxicology field crew members and graduate students over the years, who have made this research possible; Adam Scott, Aidan Guttormson, Carolyn Currie, Cody Jackson, Danielle Desrocher, Hakeem Omilowo, Heather Jovanovic, Holly Kajpust, Jamie Dearnley, Dr. José Luis Rodríguez-Gil, Katarina Djordjevic, Krista Robertson, Leah Dickenson, Lauren Timlick, Dr. Lisa Peters, McKenzie Perry, Nicholas Blandford, Patrique Bulloch, Phil Ankley, Rebecca Castel, Dr. Richard Grosshans, Sonya Michaleski, Tyler Black, Dr. Vince Palace, and the entire IISD-ELA research team. I am especially grateful for my field partners and pals over the years, to Aidan and Lauren- I could not have done this without you. To Sonya, Adam, and Heather, your friendship and encouragement throughout this degree is so appreciated. To Lisa, this entire project relied heavily on the countless hours you spent in the lab, I appreciate all that you have done to make this happen. Thank you to Pepe, for being available and supporting my many questions in R, and for being an excellent friend throughout this journey.

Another immense thank you goes to Vince. You have created a really supportive and wonderful Tox family, and I am so grateful to be apart of it.

Another thank you goes to Blake Cooney and Michael Opyr for providing laboratory support and patience during failing experiments, to Dr. Ryan Sestric for support in Dr. Levin's lab, and to Dr. Gregg Tomy and Dr. Thor Halldorson for guiding me through my many chemistry questions and supporting analyses in the COGRAD laboratory.

To my advisor, Dr. David Levin. Thank you for your guidance and kindness while navigating through grad school, and while working from home during the COVID-19 pandemic. You have always provided a great trust and confidence in me as I have worked through this research, and I want to thank you for that. It has been an absolute pleasure to work under your advisement. I would also like to thank my entire PhD committee for many years of meetings, review, and comments, and challenging me to create the best research possible; Dr. David Levin, Dr. Belay Ayele, Dr. Ivan Oresnik, Dr. Vince Palace, and Dr. Richard Grosshans.

As I close my long list of acknowledgments, I would like to thank my family, Gail, Nan, Katherine, Jordon, Audrey, Margaret, Marcel, David, Susan, Andrew, Kristen, Josh, and Anthony, for all of their encouragement and love. Especially to my parents, for genuinely thinking I can do anything. This future may be different than you had imagined, and while I am not living on a beach somewhere, I do get to work on the water and that's a pretty close second.

Finally, to my partner, David. I am so thankful for you, and for your love and support over my PhD journey. After many years of stress and long distance during field work, I know you are as equally excited that I have completed this degree as I am.

Table of Contents

List of Tables

List of Figures

List of Acronyms

ANOVA	Analysis of variance
aPAC	Alkylated polycyclic aromatic compound
ASV	Amplicon sequence variant
BPD	Barrels per day
CCME	Canadian Council of Ministers of the Environment
CHV	Conventional heavy crude oil
Dilbit	Diluted bitumen
EE	Experimental Enclosure (oiled)
EFW	Engineered Floating Wetland
FLOWTER	FLOating Wetland Treatments to Enhance Remediation
FOReSt	Freshwater Oil spill Remediation Study
GAMM	Generalized Additive Mixed Models
IISD-ELA	International Institute for Sustainable Development Experimental Lakes Area
IPIS	Instrument Performance Internal Standard
LR	Lake Reference (unoiled)
NRC	National Research Council
OTU	Operational Taxonomic Unit
PAC	Polycyclic aromatic compound
PAH	Polycyclic aromatic hydrocarbon
PCoA	Principal Coordinate Analyses
RA	Relative Abundance
RE	Reference Enclosure (unoiled)
RIS	Recovery Internal Standard
rRNA	Ribosomal ribonucleic acid
SD	Standard deviation
US EPA	United States Environmental Protection Agency

Permission to Use Copyright Material in Thesis

Chapter 2: This manuscript has been previously published in the Journal of Environmental Management (Stanley et al., 2022). Elsevier journals allow authors to retain rights to include published work in academic theses with full acknowledgement. The original article can be accessed here: Stanley, M., Palace, V., Grosshans, R., Levin, D.B. (2022). Floating treatment wetlands for the bioremediation of oil spills: A review. *Journal of Environmental Management*. 317, 115416. https://doi.org/10.1016/j.jenvman.2022.115416

Chapters 3-5: These chapters have not been published but have been written as stand alone manuscripts and will be reviewed by co-authors prior to submission for peer review. Some co-authors have already provided review to Chapter 3. Manuscript titles are listed for each chapter title, and author contributions are described in Section 1.2.1. Statements of previous publication in an academic thesis will be included with submission for peer review.

Chapter 1. Introduction

Canada is host to the third largest crude oil reserve in the world, with 168 billion barrels remaining in established reserves (Natural Resources Canada, 2020), mostly in the Alberta Oil Sands region (Dupuis & Ucan-Marin, 2015; Natural Resources Canada, 2020). Canada is also the fifth largest producer and fourth largest exporter of crude oil (Natural Resources Canada, 2019, 2020), transporting globally by rail, tanker ships, and pipelines to meet energy needs (Canada Energy Regulator, 2023). Over the last 30 years (1990 to 2019), Canadian crude oil production has increased four-fold from 1.7 million barrels per day (bpd) to 4.7 million bpd, and export has increased approximately six-fold from 656 thousand bpd to 3.8 million bpd, mostly contributed to an increase in bitumen products (Canada Energy Regulator, 2021c, 2021a, 2021b)[1]. With increased production and transport across in-land freshwater systems, there is risk of release events (Chang et al., 2014; Murray et al., 2018).

Upon accidental release, spills are most commonly met with mechanical and chemical recovery techniques, such as dredging or skimming, or applying emulsifiers or dispersants, depending on oil product, environment type, conditions, and local regulations (Etkin & Tebeau, 2003; Lee et al., 2015; Zhu et al., 2001). Unfortunately, some techniques can cause further destruction to sensitive habitat and biota. Specifically, mechanical recovery efforts of oil coated shoreline habitat may include significant human activity to remove oiled material through washing, dredging, excavation, or vegetation removal (Hoff, 1995; Lee et al., 2015; Pezeshki et al., 2000; Zhu et al., 2001). Often despite efforts, significant volumes of oil are left behind (Das

[1] Data presented from the Canadian Crude Oil Exports: A 30 Year Review (Canada Energy Regulator, 2021a; 2021b) contains information licensed under the Open Government Licence-Canada. https://open.canada.ca/en/open-government-licence-canada

& Chandran, 2011; Etkin & Tebeau, 2003; Zhu et al., 2001). This can result in chronic exposure and toxicity to interacting biota and nearby communities.

The Royal Society of Canada released a report in 2015 that included a list of high priority research needs to better understand the behaviour and impact of crude oil in aquatic environments. Including a need to understand the effectiveness of oil spill response and to develop and improve methods for remediation in freshwater habitats. As well as a need for baseline research for areas that may be affected by oil spills (Lee et al., 2015). These led to the development of in-lake research led by the International Institute for Sustainable Development Experimental Lakes Area (IISD-ELA) and various collaborators/funders (see acknowledgements). The *FLOating Wetland Treatments to Enhance Remediation* (FLOWTER) and the *Freshwater Oil spill Remediation Study* (FOReSt), were two projects conducted at the International Institute for Sustainable Development Experimental Lakes Area (IISD-ELA) to understand the efficacy of minimally invasive primary and secondary remediation efforts for oil spills in freshwater shoreline environments.

This research took place on Lake 260, at the IISD-ELA[2], in northwestern Ontario, Canada. The IISD-ELA began operation in 1968 to conduct whole ecosystem scale experiments to understand human impacts on freshwater systems and inform decision makers with detailed science. The facility is located in the boreal ecozone and is located in a region with limited anthropogenic influence, so the research observations reflect those either applied to the lakes through experimental manipulation or through climate change. The IISD-ELA consists of 58 lakes designated for scientific research including both experimental lakes and reference lakes.

---

https://www.iisd.org/ela/

The reference lakes are part of the long-term ecological research program that allow researchers to identify changes related to ecosystem manipulation and climate.

The benefit of conducting this research at the IISD-ELA is the capacity to manipulate freshwater ecosystems, the long-term baseline dataset, and the location within the boreal ecozone. One of the needs highlighted by the Royal Society of Canada was the need to understand baseline conditions prior to oil spills to understand effectiveness of spill response (Lee et al., 2015). The IISD-ELA has over 50 years of long term research in boreal lakes, and research at this facility may allow us to understand how oil spills may impact and be treated successfully in similar boreal environments, which occupy 28% of Canada (Brandt et al., 2013).

FOReSt was initiated as a pilot project in 2018 to compare monitored natural recovery of conventional heavy crude oil (CHV) and diluted bitumen (dilbit) in shoreline enclosures (Palace et al., 2021). In 2019, the FOReSt began their second objective, which was to conduct a field application study to determine the effectiveness of minimally invasive, secondary remediation methods for Cold Lake Winter Blend dilbit in two shoreline environments, wetland and rock cobble (2019), and for CHV in a wetland shoreline environment (2021). In this research, secondary remediation refers to techniques implemented to recover residual oil after primary recovery efforts of shoreline washing. The FLOWTER project was integrated with FOReSt to study the effectiveness of engineered floating wetlands (EFWs) as a secondary remediation option for oil spills in freshwater shoreline environments. This PhD thesis research specifically focuses on Objective 1 of the FLOWTER project which was to *optimize the microbiome associated with floating wetland rhizomes to enhance degradation of oil*. Within these two projects there were many collaborators, funders, graduate students, and summer students who

monitored other ecosystem components (e.g., periphyton to fish), contributing to a greater understanding of oil spill recovery and its impacts on interacting biota (see acknowledgements).

1.1 Thesis Objectives and Hypotheses

The overall objective of the FLOWTER study was to optimize EFWs as a non-invasive and secondary remediation option for oil spills in freshwater shoreline environments, by assessing the potential of the root microbial community to degrade residual oil following primary efforts (shoreline washing), specifically polycyclic aromatic compounds (PACs). Over the duration of this research, this was achieved through experiments directed to elucidate a number of specific objectives conducted in field studies and a replicated microcosm experiment:

Objective 1: Monitor changes to the EFW root biofilm microbial community upon exposure to model oil spills of **(1a)** diluted bitumen (2019) and **(1b)** conventional heavy crude oil (2021) in wetland shoreline enclosures of a boreal lake at the IISD-ELA. And to monitor changes to water quality and polycyclic aromatic compound chemistry in water and sediment. I hypothesized that the rhizosphere microbial community would shift in the presence of oil to microorganisms known to consume and degrade hydrocarbon compounds. This objective was conducted in two separate field-based research trials in 2019 with diluted bitumen (Chapter 3) and in 2021 with conventional heavy crude oil (Chapter 4).

Objective 2: Assess the efficacy of three emergent wetland plants in enhancing the removal of phenanthrene from freshwater microcosms. Further to compare removal rates among plant treatments. I hypothesized that the plants would contribute to the removal of phenanthrene, and that removal rates would vary by plant type (Chapter 5).

Objective 3: Communicate results and contribute guidance to industry experts on the use of EFWs for secondary oil spill remediation (synthesis) (Chapter 6).

1.2 Thesis Structure and Preface

This thesis includes a series of manuscripts that have been published or will soon be submitted for peer review publication in scientific journals. Detailed use of copyrighted material are included above on page xxiv. Due to the formatting of this thesis, there is no standalone methods chapter as it is included in detail in each of the chapters. The structure of the thesis is as follows.

Chapter 2 is a literature review, previously published in the Journal of Environmental Management (Stanley et al., 2022), that introduces challenges with using conventional methods of oil spill recovery in sensitive environments, like freshwater shorelines or wetlands, and discusses non-invasive biological remediation alternatives. Chapter 2 specifically highlights the potential of engineered floating wetlands (EFWs) for oil spill recovery and discusses the need for research conducted in large scale field-based trials, under variable environmental conditions. This chapter sets-up the rest of the thesis, which explores the use of EFWs in model oil spills conducted in larger-scale, shoreline enclosures of a boreal lake at the IISD-ELA.

Chapters 3 and 4 describe two field-based research experiments that investigated changes to the root microbial community on EFWs upon exposure to modelled oil spills of diluted bitumen (Chapter 3) and conventional heavy crude oil (Chapter 4) following primary recovery efforts of shoreline washing in wetland shoreline enclosures. In addition, monitored changes to polycyclic aromatic compound chemistry in water and sediment of experimental and reference sites.

Chapter 5 describes a microcosm-scale experiment designed to determine whether plants, and specific plant types, contribute to the removal of phenanthrene from freshwater. The overall research will be used to confirm potential of EFWs for oil spill remediation.

Chapter 6 concludes this thesis by synthesizing research to provide recommendations and guidance on the use of EFWs for oil spill remediation and future research, as well as discussing significance and contribution of this research for the oil spill response industry.

1.2.1 Contribution of Authors

Because this thesis is structured as a series of co-authored manuscripts, the following section will describe my contribution to each chapter, as well as highlighting the roles of other authors in conducting this work. Noting I am the primary author of each chapter.

Chapter 2 is a published literature review (Stanley et al., 2022) for which I developed the concept, wrote in its entirety, and integrated comments and edits from co-authors and journal editors. Co-authors, including Dr. Vince Palace, Dr. Richard Grosshans, and Dr. David Levin, contributed to editing and review of the manuscript.

Chapters 3 and 4 describe research on model diluted bitumen spills in 2019 (Chapter 3) and model conventional crude oil spill in 2021 (Chapter 4) as part of a large collaborative study at the IISD-ELA. I wrote the entirety of these chapters and was responsible for conducting the research in relation to my PhD objectives on the FLOWTER project, as well as analyzing and synthesizing data. This included project set up, oil spill application and recovery, microbial sampling, water sampling, and floating wetland monitoring. This was a large collaborative project, and many individuals listed in the acknowledgements contributed to the overall success of this project. Co-authors directly contributed to the development of this manuscript through project design and deployment, sample collecting and processing, and the editing and review

process. Specifically, Aidan Guttormson and Lauren Timlick supported project deployment and sample collection. Dr. Lisa Peters, conducted all PAC chemical analyses in the COGRAD laboratory, run by Dr. Gregg Tomy. Dr. Thor Halldorson conducted PAC chemical analyses for sediment in the COGRAD laboratory. Dr. Julien Tremblay, Jessica Wasserscheid, and Dr. Charles Greer contributed to microbial rRNA gene amplicon sequencing, and supported microbial analyses by providing R scripts and guidance on analyses. As well Dr. Charles Greer is a principal investigator on the FLOWTER project and provided the written methods included in Chapter 3, Section 3.2.3.1. Dr. Richard Grosshans is one of the principal investigators on the FLOWTER project and supported EFW and project design. Dr. José Luis Rodríguez-Gil was a post doctoral fellow on the FLOWTER project. Dr. Sonya Havens leads the IISD-ELA chemistry facility and conducted water quality nutrient analyses. Dr. David Levin is my academic advisor and oversaw much of my research plans and design. Dr. Vince Palace is the overall principal investigator on the FLOWTER and FOReSt projects and led project design, deployments, and sampling plans. Most co-authors have contributed to review of Chapter 3, and will review Chapter 4 prior to submission for peer review publication.

Chapter 5 describes the microcosm scale phenanthrene removal experiment. I wrote the entirety of this chapter, and was responsible for designing and conducting this research experiment, as well as the analyses and synthesis of all samples and data. Co-authors were involved in various roles in the success of this research. Aidan Guttormson supported project set up and sample collection and processing through the duration of the experiment, as well as supported discussions and developments of generalized additive mixed models. Dr. Lisa Peters supported methods of phenanthrene sampling and extractions, as well as laboratory support in COGRAD laboratory. Dr. Thor Halldorson and Dr. Gregg Tomy supported the analyses of

phenanthrene samples on GC-MS/MS in the COGRAD laboratory. Dr. José Luis Rodríguez-Gil provided valued support and review of statistical analyses and modelling. Blake Cooney conducted photoelectrochemical oxygen demand analyses. Dr. Richard Grosshans is one of the principal investigators on the FLOWTER project who supported discussions on design. Dr. David Levin is my academic advisor and oversaw much of my research plans and design. Dr. Vince Palace is the overall principal investigator on the FLOWTER project and supported much of my research design plans. All co-authors will review this manuscript prior to submission for peer review publication.

There is no manuscript associated with the concluding synthesis chapter (Chapter 6). I am responsible for the entirety of this chapter, however acknowledging that my thesis committee and examiners have contributed to its review.

Chapter 2. Literature Review

2.1 Preface

This chapter introduces challenges with current conventional oil spill remediation methods and engineered floating wetlands as a non-invasive alternative for spill response, discussing potential through an in-depth literature review analysis, and highlights research needs for field-based trials under variable environmental conditions. This chapter has been published as a review manuscript in the Journal of Environmental Management, titled *Floating Treatment Wetlands for the Bioremediation of Oil Spills: A Review* (Stanley et al., 2022). However slight modifications have been made for thesis consistency and terms, as well as addressing examiner suggestions. For example, the article refers to floating treatment wetlands (FTW), but they will be called engineered floating wetlands (EFWs) in this chapter for consistency throughout this thesis. Author contributions are outlined in Section 1.2.1.

2.2 Introduction

Oil is a non-renewable energy source that is extracted from the earth, formed from organic matter of plants, animals, and microorganisms (Lee et al., 2015). While it is a naturally occurring substance, crude oil is made of thousands of compounds, some of which can be extremely harmful when released in high concentrations, such as during oil spills. The fate and impact of an oil spill is determined by the physical and chemical characteristics of the oil products, spill location (e.g. freshwater, marine, or terrestrial habitat), environmental conditions, and local response capacity, suggesting no two oil spills are ever the same (Dupuis & Ucan-Marin, 2015; Lee et al., 2015; Zhu et al., 2001). Although oil spill recovery tends to prioritize mechanical and chemical methods, there is growing interest in biological recovery due to its cost-effectiveness and less invasive approach (Rehman et al., 2018). Of particular interest is the

use of plants to stimulate microbial biodegradation for oil spills in freshwater, a habitat that has received far less attention compared to marine spill events and requires increased knowledge and research to improve recovery methods (Lee et al., 2015). Phytoremediation efforts in freshwater environments may be limited to regions of plant growth, such as the periphery of the site, or shallow depths (Pilon-Smits, 2005). Researchers are assessing the use of engineered floating wetlands (EFWs), platforms that support emergent vegetation and a microbial biofilm community in the rhizosphere, to increase plant surface area for phytoremediation and microbial biodegradation of aquatic contaminants. Here we review the literature and assess the use of EFWs as a non-invasive method for oil spill recovery.

2.3 Oil Spill Recovery

2.3.1 Mechanical and Chemical Remediation

Conventional oil spill recovery includes mechanical and chemical methods to facilitate oil removal or breakdown in the environment. Mechanical efforts use physical techniques to remove oil from the water surface, sediments, or shoreline habitat, including the use of sorbent pads, skimmers, booms, and dredging. When oil adheres and coats shoreline habitat, spill responders may create trenches to collect and remove oil, use vacuums, wash and scrub shoreline material, apply pressure washing and flushing, remove sediment, cut back and dispose of vegetation, actively disperse oil with bioventing or air sparging, or conduct an in-situ burn (Lee et al., 2015; Zhu et al., 2001). The selection of mechanical efforts is influenced by oil type, habitat type, biota, weather conditions, nearby communities, and local capacity (Etkin & Tebeau, 2003; Lee et al., 2015; Zhu et al., 2001). Some mechanical efforts may be costly (Atlas, 1995; Yavari et al., 2015), and can cause significant damage to shoreline habitat due to increased human activity, dredging, vegetation and soil compaction from foot traffic or heavy machinery,

or vegetation removal (Lee et al., 2015; Zhu et al., 2001). Shoreline habitat and the littoral zone are some of the most productive regions in aquatic environments, and are an important habitat for littoral benthic algae at the base of the food web (Devlin et al., 2016). In addition to impacts to the ecosystem, habitat changes in this region have potential to impact fish, as most fish species tend to occupy the littoral zone and are supported more by benthic primary production in this region than pelagic environments (Vander Zanden et al., 2011). The removal of, or damage to, shoreline material further reduces habitat availability for native species and productivity, and can also create conditions ideal for invasive species establishment (Lee et al., 2015).

Chemical recovery includes the application of products such as dispersants, demulsifiers, and solidifiers to increase degradation of oil products or enhance recovery. Dispersants break down oil into smaller droplets in the water column to increase surface area for more efficient biodegradation or dilution. Demulsifiers disperse oil-water emulsions and solidifiers are used to solidify or stabilize oil to support physical recovery (Lee et al., 2015; Zhu et al., 2001). Surface film chemicals can also be applied to remove oil adhered to shoreline environments, to enhance oil removal and recovery during shoreline washing (Zhu et al., 2001). Compared to other recovery efforts, chemical methods are less desirable due to the introduction of additional contaminants, its use is influenced by oil type and environmental conditions, and can increase exposure of aquatic life to oil compounds and thus toxicity (Lee et al., 2015).

Despite the myriad of methods available to remove oil from the environment, some conventional oil spill cleanup efforts are not fully effective (Das & Chandran, 2011; Zhu et al., 2001). Mechanical recovery efforts are estimated to remove 10-30 % of spilled oil, and with occasional recovery of 50% or more (Etkin & Tebeau, 2003). Data from the United States Department of Transportation, Pipeline and Hazardous Materials Safety Administration (2022)

indicated that all reported pipeline incidences for hazardous liquids (crude oil and refined petroleum products) in all states over the last 20 years (2002 to 2021; total of 6,419 incidents and over 1.09 million barrels spilled) had a mean (± standard deviation [SD]) recovery of 66 ± 15%, ranging from 38% to 86% (Figure 2.1). Noting, these data are only for pipeline transport and does not include details of recovery methods. Residual oil in the environment may continue to have negative impacts for interacting organisms and affect long term ecosystem health. Natural recovery (bioremediation) is a promising secondary recovery method, tested at a large scale first during the marine Exxon Valdez oil spill in Prince William Sound, Alaska (Rosenberg & Ron, 1996; Zhu et al., 2001), where intensive efforts only recovered 10% of the spilled oil, while other processes (weathering and biodegradation) were very important for long term recovery (Lee et al., 2015). Bioremediation may also be far less invasive than conventional efforts as noted during historic spills.

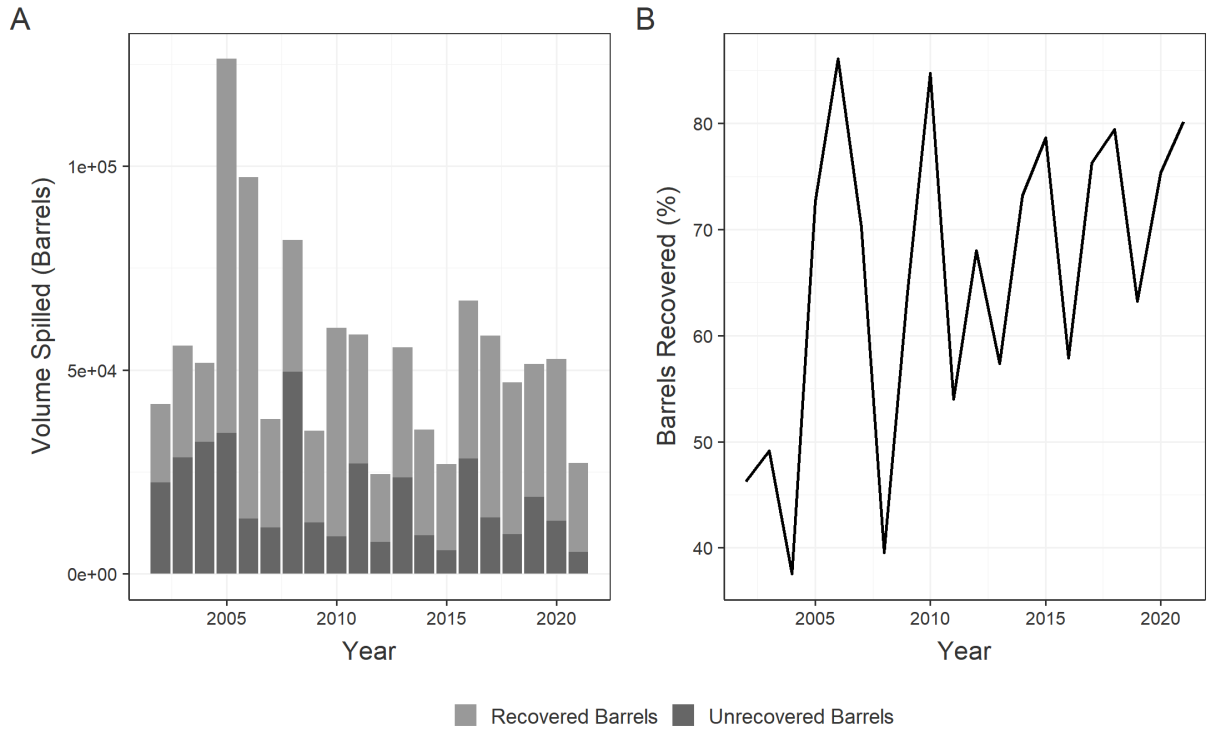

Figure 2.1. A. Total annual barrels spilled (recovered/unrecovered), and B. annual percent recovery from all reported pipeline incidents (N=6,419) of hazardous liquid (crude oil and refined petroleum products) in all states from 2002 to 2021. Publicly Available Data Source: United States Department of Transportation, Pipeline and Hazardous Materials Safety Administration, 2022.

Gilfillan et al. (1995) studied the impacts of cleaning oil from coastal marshes during the Amoco Cadiz spill in 1978, where 221,000 tonnes of light crude oil spilled into the sea and oiled 300 km of shoreline, coating many marshes. Using remote sensing, they compared vegetation composition and area between four marshes that received clean-up methods and one marsh that did not. The un-treated marsh had a 21% increase in vegetative area between 1971 and 1987, while the vegetative area declined by 22% to 38% in the treated marshes between 1971 and 1990. They also observed that vegetation type and composition were significantly altered in the treated marshes, likely due to removal of sediment (up to 50 cm) causing changes to intertidal

height, while there were no changes to vegetation composition in the untreated marsh. Beazley et al. (2012) highlighted this research as a case example to suggest that non-invasive methods, such as natural attenuation, may be preferred for sensitive habitats to reduce habitat loss.

In 2010, 819,000 gallons of diluted bitumen and unconventional heavy sour crude oil spilled into Talmadge Creek and the Kalamazoo River, Michigan, from a ruptured pipeline. Intensive recovery efforts were employed as part of the response efforts including excavation, dredging, and sediment disturbance (e.g. sparging of sediments with pressurized air to mobilize entrapped oil). Recovery efforts may have had greater impacts to the benthic community than direct oil toxicity, and it was suggested that it may be better to rely on natural recovery processes because invasive recovery efforts can be damaging (Lee et al., 2015).

2.3.2 Biological Remediation

Biological remediation (also known as "bioremediation") is driven by natural processes in the environment, including biodegradation by microorganisms or phytoremediation and rhizoremediation by plants (Czaplicki & Gunsch, 2016; Das & Chandran, 2011; Malla et al., 2018; Raju & Scalvenzi, 2018). It is a cost-effective method that can reduce environmental impacts during on-site remediation (Rehman et al., 2018). While it is driven by natural processes in the environment, oil spill bioremediation can also include human intervention to enhance recovery (Lee et al., 2015).

2.3.2.1 Biodegradation. Biodegradation of oil spills is often referred to as natural attenuation or monitored natural recovery, and is built on the basis of native microorganisms consuming carbon-based compounds for energy through various metabolic pathways. This method is often implemented in remote locations or in sensitive environments (Lee et al., 2015;

Magar et al., 2009; Zhu et al., 2001), and its success is influenced by native microorganisms, environmental conditions, and enzymatic activity (Chakraborty et al., 2012).

Hydrocarbons are a major component of oil, made of carbon and hydrogen atoms and can be further classified as saturates, aromatics, resins, and asphaltenes (Dupuis & Ucan-Marin, 2015; Lee et al., 2015). Each of these categories differ in structure and complexity, molecular weight, abundance, toxicity, solubility and resistance to degradation (Lee et al., 2015; Raju & Scalvenzi, 2018). Compounds of particular concern due to their recalcitrant properties and potential chronic toxicity, are polycyclic aromatic hydrocarbons/compounds (PAHs or PACs; further referred to as PACs), aromatic compounds made of two or more fused six-carbon atom aromatic rings (Dupuis & Ucan-Marin, 2015; Lee et al., 2015; Raju & Scalvenzi, 2018; Zhu et al., 2001). In order to breakdown complex hydrocarbon compounds, microorganisms produce enzymes that catalyze biological pathways to facilitate degradation (Das & Chandran, 2011). Aerobic degradation of PACs depends on the opening or cleavage of the aromatic rings, through oxygen insertion, with oxidoreductase enzymes, such as oxidases, laccases, and/or peroxidases (Atlas, 1995; Cao et al., 2009; Das & Chandran, 2011; Haritash & Kaushik, 2009). These intermediate compounds continue to be degraded with metabolites (e.g. acetyl-CoA), eventually entering microbial catabolic pathways, including the tricarboxylic acid cycle (TCA). The TCA cycle completes the degradation pathway, ultimately resulting in non-harmful end-products of carbon dioxide, water, and increased microbial cell biomass (Al-Hawash et al., 2018; Das & Chandran, 2011; Dhir, 2013; Lee et al., 2015). Anaerobic organisms are also important PAC degraders for harsh environments with low oxygen availability (Peixoto et al., 2011). These organisms use various terminal electron acceptors in place of oxygen, such as nitrate, sulfate, or metals (Yang et al., 2009), often forming benzoyl-CoA (Cao et al., 2009).

PAC metabolism is also influenced by compound bioavailability and the microbial community. Bioavailability determines whether compounds can be taken up and metabolized by microorganisms, and is influenced by compound solubility and its ability to bind with organic matter and sediment (Al-Hawash et al., 2018; Ghosal et al., 2016; Lee et al., 2015). As PACs increase in molecular weight and complexity, their bioavailability decreases, as does degradation potential (Ghosal et al., 2016). Some microorganisms can release biosurfactants that can enhance compound bioavailability by increasing solubility in water, allowing for uptake and metabolism, similar to chemical dispersants (Lee et al., 2015), as described in Section 2.3.1.

Bacteria are well known for their capacity to adapt to variable environmental conditions and contaminants, and some (such as Alphaproteobacteria, Betaproteobacteria, Gammaproteobacteria, Actinomycetes, Firmicutes) for their PAC degradation potential. PAC degrading bacteria are mostly known to use dioxygenase and monooxygenase enzymes for aerobic metabolism, but can also use anaerobic metabolic pathways. Other prokaryotic (e.g. archaea) and eukaryotic (e.g. fungi and algae) organisms are able to degrade PACs (Ghosal et al., 2016) using different metabolic capabilities. PAC degrading fungi include ligninolytic and non-ligninolytic groups, who produce peroxidases and laccases, or monooxygenases (e.g. cytochrome P450), respectively (Ghosal et al., 2016 and citations therein; Haritash and Kaushik, 2009). Some fungal groups may not use PACs as their sole carbon source but may be involved in co-metabolism, and some can excrete enzymes extracellularly which can support PAC degradation in the environment (e.g. ligninolytic, white rot fungi) (Ghosal et al., 2016). Ligninolytic enzymes are particularly beneficial for degrading different types of compounds, as they have low substrate specificity (Haritash & Kaushik, 2009). Algae have been far less studied for PAC degradation compared to other microorganisms, however, there are some groups of microalgae that have

metabolic potential, such as cyanobacteria or strains of diatoms (Ghosal et al., 2016 and citations therein; Haritash and Kaushik, 2009 and citations therein). Not all microorganisms can fully degrade oil compounds into end-products, and some are specific to compound type (e.g. saturate vs. aromatic hydrocarbons), so it is essential to have a microbial consortia for co-metabolism and to maximize degradation potential. This is particularly important for complex hydrocarbons, such as 5+ ring PACs, or a mixture of compounds (Cao et al., 2009; Ghosal et al., 2016; Lee et al., 2015; Zhu et al., 2001), that may be more difficult to break down and that are especially difficult to recover from the environment. For example, some white-rot fungi (ligninolytic fungi) co-metabolize PACs with bacteria by increasing compound bioavailability (Ghosal et al., 2016, and citations therein).

Microbial degradation has proven successful, but it can be time consuming and is influenced by environmental conditions (Das & Chandran, 2011; Dhir, 2013; Lee et al., 2015; Raju & Scalvenzi, 2018; Zhu et al., 2001). This can be enhanced with biostimulation or bioaugmentation for both in-situ or ex-situ recovery efforts. During an oil spill, the influx of carbon (C) may result in an unbalanced ratio of nitrogen (N) and phosphorus (P) (Lee et al., 2015). Based on the Redfield Ratio of 106:16:1 (C:N:P), there are 150 mg N and 30 mg P used for every 1,000 mg of hydrocarbon consumed and transformed to microbial cells (Rosenberg & Ron, 1996). To ensure there are proper ratios to maximize biodegradation, spill responders may conduct biostimulation by adding nutrients to the ecosystem. If biodegrading organisms are not present, or are insufficiently abundant, spill responders may inoculate the system with microorganisms known to degrade the targeted contaminant, termed bioaugmentation (Das & Chandran, 2011; Haritash & Kaushik, 2009; Lee et al., 2015; Raju & Scalvenzi, 2018; Zhu et al., 2001). However, its success is often limited by *in-situ* conditions and competition with native

organisms (Peixoto et al., 2011). As discussed above, degradation of oil spills and complex compounds may require a diverse community of microorganisms that have different gene expression, produce various enzymes, and have different roles in metabolism (Cao et al., 2009; Lee et al., 2015; Zhu et al., 2001), as one microorganism may only use or consume specific oil compounds (Rosenberg & Ron, 1996). Rohrbacher and St-Arnaud (2016) noted that the use of plants may be more effective in stimulating the microbial community than bioaugmentation.

2.3.2.2 Phytoremediation. Phytoremediation is a cost-effective method that uses plants to remediate contaminated sites (Lee et al., 2015; Phillips et al., 2012; Pilon-Smits, 2005). Of particular interest for the treatment of oil spills is phytostimulation, also known as rhizoremediation or rhizodegradation, where plants stimulate microbial degradation of contaminants, forming less toxic or unavailable compounds (Bisht et al., 2015; Dhir, 2013; Lee et al., 2015; Muratova et al., 2009). Plants provide root surface area for microbial colonization and are able to release exudates into the rhizosphere and rhizoplane, such as oxygen, nutrients, amino acids, and/or enzymes, that may stimulate the microbial community with potential to facilitate degradation, enhance compound bioavailability, or directly degrade the contaminant (Bisht et al., 2015; Dhir, 2013; Lee et al., 2015; Martin et al., 2014; Muratova et al., 2009; Pilon-Smits, 2005; Shahzad et al., 2016). Ferrera-Rodríguez et al. (2013) found that vegetation increased microbial abundance in the rhizosphere compared to bulk soil through laboratory experiments of samples collected in contaminated Arctic soils fourteen years after a diesel spill. The rhizosphere samples also had higher cultivable heterotrophic and diesel degrading bacteria by two orders of magnitude.

Oxygen is an important factor influencing hydrocarbon biodegradation pathways (Das & Chandran, 2011; Dhir, 2013; Lee et al., 2015). Aerobic degradation is the fastest

metabolic/enzymatic pathway which requires oxygen as the terminal electron acceptor (Cao et al., 2009; Das & Chandran, 2011; Rohrbacher & St-Arnaud, 2016) as described in Section 2.3.2.1. During an oil spill, the slick on the water surface can inhibit atmospheric oxygen mixing (Chen, 2018; Freitas et al., 2016), photosynthesis and respiration (Freitas et al., 2016), and the oil may become limited in subsurface sediments (Zhu et al., 2001), depending on wave and wind aeration (Lee et al., 2015). Certain plant species can transfer oxygen into the rhizosphere, creating potential to provide oxygen to the microbial community that may otherwise be deficient. The ability to transfer oxygen varies by plant species and is influenced by their morphology and anatomy, such as biomass, surface area, stomata, and aerenchyma, and environmental conditions (Randerson et al., 2011; Wieβner et al., 2002). Ferrera-Rodríguez et al. (2013) notes that the mechanism that allows plants to grow in harsh conditions (e.g. low oxygen environments) may be the same used to grow in hydrocarbon contaminated environments. Jouanneau et al. (2005) studied pyrene degradation in sediment by *Phragmites australis* and/or bacterial inoculant *Mycobacterium* sp. 6PY1 over 61 days. *P. australis* increased pyrene degradation compared to the control with no plants, and through redox measurements, suggested that it was enhanced through the release of oxygen into the sediment, stimulating the microbial community. However, they also observed that *Mycobacterium* had greater degradation alone than when in conjunction with *P. australis*, unlike many studies where plants enhance microbial degradation. Out of a series of hypotheses, they suggested it may have been due to carbon sources from root exudates that were more readily available than pyrene. They also observed that plants were able to bioaccumulate pyrene into plant tissue when alone, however, bioaccumulation decreased 10 to 20 fold when in the presence of the inoculum, possibly due to microbial metabolism and reduced availability of pyrene.

Plants also release other exudates, that help to stimulate the microbial community including photosynthetic products, amino acids, sugars, nutrients, and enzymes (Afzal et al., 2019; Dhir, 2013; Rohrbacher & St-Arnaud, 2016). Enzymes can specifically enhance or support the microbial community, or directly degrade the hydrocarbon contaminant (Lee et al., 2015; Muratova et al., 2009). For example, some plants can release laccases, phenol oxidases, or peroxidases, which help to breakdown hydrocarbons (Rohrbacher and St-Arnaud, 2016 and citations therein). In addition, the microbial community can also protect and support plants. For example, some microorganisms provide indole acetic acid, a plant growth hormone, through PAC degradation, offering support and protection to the plant (Afzal et al., 2019; Golubev et al., 2009; Hussain et al., 2019; Rehman et al., 2018).

Toyama et al. (2011) studied biodegradation of pyrene and benzo[a]pyrene with *P. australis* and its associated root exudates and microbial communities. Through a series of experiments, they found that *P. australis* enhanced the removal of pyrene and benzo[a]pyrene in contaminated sediment by microbial biodegradation, and root exudation enhanced microbial cell growth of *Mycobacterium gilvum* and pyrene degradation. Cellular growth and benzo[a]pyrene degradation was only observed in the presence of root exudates, and was enhanced with root exudates from plants previously exposed to pyrene contamination. They found that the plant increased phenolic exudation upon exposure to pyrene, which was essential to the biodegradation of benzo[a]pyrene. Toyama et al. (2011) highlighted the importance of oxygen and exudate release for biodegradation of high molecular weight-PACs.

Phillips et al. (2012) studied the impact of root exudates of *Medicago sativa* L. (alfalfa) and *Elymus angustus* Trin. (Altai wildrye) on microbial communities from weathered hydrocarbon contaminated soil amended with hexadecane, naphthalene, or phenanthrene.

Initially, root exudation repressed degradation of the hydrocarbons causing a lag period compared to control eluates. No changes were observed to the microbial community structure or abundance when exposed to root exudates or control eluates, but rather were observed for microbial gene expression. Degradation was correlated with microbial gene expression of catechol 2,3 dioxygenase and naphthalene dioxygenase, which increased in presence of root exudates, acetate and alanine, and decreased with malonate. They noted the type and concentration of exudates varied with exposure conditions (e.g. with and without PACs) and between plant species, suggesting that conditions that enhance root exudation vary by plant species.

While much of the literature on phytoremediation of oil, not summarized here, has focused on terrestrial environments, similar characteristics and features are also present in aquatic plants. Phytoremediation potential is limited by root protrusion in soil of terrestrial environments or shoreline habitat and water depth in aquatic environments (Pilon-Smits, 2005). Of particular interest is the use of EFWs to enhance surface area of roots for microbial colonization, and ultimately the biodegradation of crude oil contaminated sites.

2.3.2.3 Engineered Floating Wetlands. Engineered floating wetlands, also referred to as artificial islands or hydroponic root mats, are floating platforms that support vegetation allowing their roots to grow into the water column creating a dense surface area that facilitates microbial biofilm colonization. EFWs have various functions to treat contaminated aquatic environments, including filtration, or nutrient and metal uptake by the plants, for example (Shahid et al., 2018). Of particular interest for remediating crude oil contamination, is their potential to enhance microbial colonization on their roots. Roots and the rhizoplane are the most active/complex site of plants due to their microbial communities, and are often the first point of contact with

contaminants in aquatic or terrestrial environments (Dhir, 2013; Srivastava et al., 2017 and citations therein). EFWs can be established in various depths of water, increasing plant surface area and contaminant interaction, and thus increasing microbial development and phytoremediation/biodegradation potential (Shahid et al., 2018; Tanner & Headley, 2011). Not only does increasing surface area improve microbial colonization, but the biofilm layer can provide important protection for microorganisms when exposed to environmental contamination or stress, and the interaction between organisms in the biofilm may increase degradation rates (Cao et al., 2009). The synergistic relationship between plants and microorganisms on EFWs may be successful at remediating oil or hydrocarbon contamination, which we have explored by conducting a literature review analysis.

2.4 Engineered Floating Wetlands and Oil: Literature Review Analysis

A literature review analysis was conducted to identify research on the use of EFWs for bioremediation of oil, diesel, or oil degradation by-products. Table 2.1 summarizes available literature partially identified in a Web of Science search using key words identified in title or topic of publications most recently on February 10, 2022. Key words included ‘floating wetland(s)’, ‘floating treatment wetland(s)’, ‘hydroponic root mat(s)’, ‘artificial island(s)’, ‘constructed floating wetland(s)’, ‘floating island(s)’, ‘floating island system(s)’, ‘artificial floating bed(s)’, ‘floating bed(s)’, ‘floating bioplato(s)’, ‘oil(s)’, ‘crude oil(s)’, ‘oil spill(s)’, ‘hydrocarbon(s)’, ‘polycyclic aromatic hydrocarbon(s)’, ‘polycyclic aromatic compound(s)’, ‘petroleum(s)’, ‘diluted bitumen(s)’, and ‘diesel(s)’. The various names for EFWs used in the literature search were collated from Shahid et al. (2018). After screening, a total of eight relevant research articles were identified, while 58 other papers were excluded as they did not focus on the use of EFWs for remediation of oil or related contaminants. The Web of Science literature

search results did not include Effendi et al., 2017, Phenrat et al. (2017), Saleem et al. (2019; 2018) or Rehman et al. (2021), however are relevant and are included in Table 2.1. Phenrat et al., 2017 and Saleem et al., (2019; 2018) focus on phenol and not specifically oil or diesel remediation. However, these papers are included in the analysis in Table 2.1, as phenol is an aromatic organic compound and may be a by-product of oil degradation pathways. Details from these three reports may help to inform how compounds, specifically benzene rings, are degraded. Table 2.1 summarizes data from thirteen selected research articles that inform the potential for EFW and oil spill recovery. Each study used a form of EFW planted with various vegetation species. Two of them tested the role of plant density in degrading contaminants (Effendi et al., 2017; Phenrat et al., 2017). Effendi et al. (2017) found that *Vetiveria zizanoides* (L.) Nash planted in three or six pot plants had 90.29 % (final concentration = 0.013 mg/L) and 91.39 % (final concentration = 0.015 mg/L) reduction of oil content in water (initial concentration = 0.151 mg/L), respectively, and the control had 84.77 % (final concentration = 0.023 mg/L) after four weeks. During the first to second week, the oil declined by 43.70%, 56.07%, and 62.47%, for the control, three pot plant, and six plot plant, respectively, and noted that greater number of plants resulted in increased oil reduction. Suggesting the degradation processes may be driven by plant uptake, biodegradation by root microorganisms, or phyto/rhizodegradation. They also observed that plants did better under oil contamination than without, recorded through the percent of living shoots, biomass, growth rate, and morphology, and suggested it was due to nutrient availability from degradation products.

Table 2.1. Summary of engineered floating wetland remediation case studies for oil, diesel, or oil degradation by-products as identified in part by a Web of Science search (as of February 10, 2022).

Plant Species	Inoculated Bacterial Strains	Contaminant Source	Study Location/ Type	Study Duration	Initial Concentration	Total Reduction	Source
Geophila herbacea O Kumtze; *Lolium perenn* c. 'Caddieshack' *Lolium perenne* Topone *Lolium perenne* L.	None	Refinery wastewater from Hangzhou Petrochemical Company Limited	Zhejiang University, China. Mesocosm, 75 L plastic containers	35 days from October to December, 2008	1720 mg/L total petroleum hydrocarbons	Control: ~18 % (visually estimated from figures in the publication) *L. perenn cv.* 'Caddieshack*:* 40.0'% *G. herbacea* O Kumtze*:* 48.2 % *L. perenne* Topone: 51.9 % *L. perenne* L.: 55.6 %	Li et al., 2012
Brachiaria mutica	*Acinetobacter* sp. BRSI56 *Bacillus cereus* BRSI57 *Bacillus licheniformis* BRSI58	Sewage effluent from Paharang and Madhuana drains	National Institute for Biotechnology and Genetic Engineering (NIBGE), Faisalabad, Pakistan. Microcosm, 30 L polyethylene tanks.	Paharang: 96 hours. Madhuana: 192 hours. From September to October 2014.	Paharang: 8.5 ± 1.3 mg/L oil and grease (±SD) Madhuana: 15.7 ± 2.7 mg/L oil and grease (±SD)	No numerical reduction data was provided. However, based on visual interpretation, plants and bacteria had the greatest oil and grease percent reduction, followed by plants alone,	Ijaz et al., 2015*

Plant Species	Inoculated Bacterial Strains	Contaminant Source	Study Location/ Type	Study Duration	Initial Concentration	Total Reduction	Source
						bacteria alone, and the control.	
Vetiveria zizanioides (L) Nash	None	Crude oil from the Oil and Gas Institute Jakarta	Bogor Agricultural University, Indonesia. Mesocosm, 25 L.	Four weeks from February to March, 2016	0.151 mg/L oil	Control: 84.77 % 3 potted plants: 90.29 % 6 potted plants: 91.39%	Effendi et al., 2017
Vetiveria zizanioides (L.) Nash	None	Phenol	Thailand Mesocosms, 35 L glass containers	Eight weeks (1400 hours)	500 mg/L phenol in illegally dumped industrial wastewater	Days to reduce < 1mg/L with aeration. Control: 235; 20 plants: 122; 40 plants: 66.6; 60 plants: 50.6; 80 plants: 56.8; 100 plants: 31.9	Phenrat et al., 2017
Brachiaria mutica *Phragmites australis*	*Bacillus cereus* LCR H93 *Acinetobacter junii* TYRH47 *Bacillus amyloquefaciens* BRRI53 *Klebsiella* sp. LCRI87	Oil field produced wastewater from Fimkassar, Chakwal, Pakistan	NIBGE, Faisalabad, Pakistan Microcosm, 20L plastic tank	Six weeks from May to June, 2016	325 ± 10.1 mg/L oil (± SD) in wastewater effluent	Plants and bacteria: 93-97% oil content. Note: no numerical reduction data was provided for controls, or plants and bacteria alone. However plants	Rehman et al., 2018

Plant Species	Inoculated Bacterial Strains	Contaminant Source	Study Location/ Type	Study Duration	Initial Concentration	Total Reduction	Source
	Acinetobacter sp. BRSI56 *Bacillus licheniformis* BRSI58 *Acinetobacter* sp. CYRH21 *Acinetobacter* sp. LCRH81 *Bacillus subtilis* LORI66					alone had greater reduction than bacteria alone, and treatments with *P. australis* had the greatest reduction.	
Typha domingensis	*Acinetobacter lwofii* ACRH76 *Bacillus cereus* LORH97 *Pseudomonas* sp. LCRH90	Phenol	NIBGE, Faisalabad, Pakistan Microcosm, 20 L polyethylene tanks	15 days March 2017	500 mg/L phenol	Phenol removal rate (15 days): Control: 0.058 $g/m^2/day$ Plants: 0.146 $g/m^2/day$ Bacteria: 0.107 $g/m^2/day$ Plants and bacteria: 0.166 $g/m^2/day$ (maximum removal was on days 0-5)	Saleem et al., 2018
Phragmites australis *Typha domingensis*	*Ochrobacterum intermedium* R2 *Microbacterium oryzae* R4	Crude oil contaminated water in a water	Chakwal, Pakistan Water stabilization	March 2016 to September 2017	319 ± 9.7 mg/L of hydrocarbons (± SD)	99.1 %	Afzal et al., 2019

Plant Species	Inoculated Bacterial Strains	Contaminant Source	Study Location/ Type	Study Duration	Initial Concentration	Total Reduction	Source
Leptochloa fusca *Brachiaria mutica*	*Pseudomonas aeruginosa* R25 *Pseudomonas aeruginosa* R21 *Acinetobacter.* sp. LCRH81 *Klebsiella* sp. LCRI-87 *Acinetobacter* sp. BRSI56 *Pseudomonas aeruginosa* BRRI54 *Bacillus subtilus* LORI66 *Acinetobacter junii* TYRH47	stabilization pit	pit (22.326 m^3)				
Leptochloa fusca	*Acinetobacter* sp. ACRH82 *Acinetobacter.* sp. BRRH61 *Bacillus niabensis* ACSI85	Hexadecane	NIBGE, Faisalabad, Pakistan Microcosm, 20 L polyethylene tanks, with 15 L of tap water.	50 days from August to September 2017	150 mg/L hexadecane	Control: 31% Plants: 69% Bacteria: 58% Plants and Bacteria: 92%	Hussain et al., 2019
Leptochloa fusca	*Bacillus subtilis* LORI66	Oil field produced wastewater	Pakistan Mesocosm, 20 L	Six weeks from April	304 ± 10.25 mg/L of total	Control: 16% Plants: 75- 78% Bacteria: 38%	Rehman et al., 2019

Plant Species	Inoculated Bacterial Strains	Contaminant Source	Study Location/ Type	Study Duration	Initial Concentration	Total Reduction	Source
Typha domingensis	*Klebsiella* sp. LCR187 *Acinetobacter junii* TYRH47 *Acinetobacter* sp. LCRH81	from Fimkassar, Chakwal, Pakistan	polyethylene tanks	to June 2017	hydrocarbons (TH) (±SE)**	Plants and bacteria: 93- 97%	
Phragmites australis (Cav.)	*Acinetobacter lwofii* ACRH76 *Bacillus cereus* LORH97 *Pseudomonas* sp. LCRH90	Phenol	NIBGE, Faisalabad, Pakistan Microcosm, 20L polyethylene tank	15 days March 2017	500 mg/L phenol	Control: 33% Plants: 66% Bacteria: 61% Plants and bacteria: 96%	Saleem et al., 2019
Cyperus laevigatus L.	*Acinetobacter* sp. 61KJ620863 *Bacillus megaterium* 65KF478214 *Acinetobacter* sp. 82KF478231	Diesel oil	NIBGE, Faisalabad, Pakistan Microcosm, 20L polyethylene tanks	Twelve weeks from April to June 2018	10,000 mg/L oil (visually estimated from figures in the publication)	Control: 9.30% Plants:56.56% Bacteria: 37.46% Plants and bacteria: 73.48%	Fahid, Ali, et al., 2020
Phragmites australis	*Acinetobacter* sp. BRRH61 *Bacillus megaterium* RGR14 *Acinetobacter iwoffii* AKR1	Diesel	NIBGE, Faisalabad, Pakistan Microcosm, 20 L polyethylene tanks	Twelve weeks from April to June 2018	10,000 mg/L oil (visually estimated from figures in the publication)	Control:10.3 % Plants: 68.7 % Bacteria: 39.5% Plants and bacteria: 97.5%	Fahid, Arslan, et al., 2020

Plant Species	Inoculated Bacterial Strains	Contaminant Source	Study Location/ Type	Study Duration	Initial Concentration	Total Reduction	Source
Phragmites australis *Typha domingensis*	*Acinetobacter junii* TYRH47 *Acinetobacter* sp. LCRH81 *Bacillus subtilis* LORI66 *Klebsiella* sp. LCRI87	Contaminated water from oil production site near Fimkassar, Chakwal, Pakistan	NIBGE, Faisalabad Pakistan. Macrocosm, 1000 L plastic tanks	36 days	300 mg/L total hydrocarbons	Control: 8% *P. australis:* 81% *T. domingensis:* 72% Bacteria: 61 % *P. australis* and bacteria: 95 % *T. domingensis* and bacteria: 85%	Rehman et al., 2021

*This study (Ijaz et al., 2015) is not specific to oil or hydrocarbons as their contaminant source is sewage effluent, however is included as oil and grease was a metric of sewage effluent bioremediation.

** SE= standard error

Phenrat et al. (2017) also tested *V. zizanoides* (L.) Nash planted on hydroponic root mats with 20, 40, 60, 80, or 100 individual plantlets in an aerated 35 L tank of 500 mg/L of phenol in industrial wastewater. They observed that increasing plant numbers decreased the total number of days to reduce phenol to less than 1 mg/L in an aerated system, ranging from 31.9 days to 122 days for 100 and 20 plants, respectively, while aeration alone would take 235 days. The phenol degradation rate constant was three times higher with aeration than without, and the addition of plants to the aerated system significantly increased degradation. Throughout the exposure they monitored plants for morphometric features and observed a phenol dose-dependent toxicity, through weight reduction, leaf browning and death, and root deterioration for all treatments due to the high initial concentration, until approximately 400-600 hours of exposure when phenol concentrations started to decline. However, they also observed an increase in root release of peroxidases after 400 hours, which later decreased once phenol concentrations were reduced (766 hours). They suggested that the increase in plant numbers resulted in an increase in peroxidase release and thus greater phenol degradation. Phenol toxicity to *Typha domingensis* and *P. australis* (Cav.), recorded as inhibition of plant growth and development, and root necrosis in *P. australis* was also observed by Saleem et al. (2019, 2018). However, they noted that impacts were reduced in the presence of inoculated bacteria, selected for phenol degradation potential and plant growth promotion (ACC deaminase enzyme) (Saleem et al., 2018). Similarly, Fahid, Ali, et al. (2020) and Fahid, Arslan, et al. (2020) observed impacts to *Cyperus laevigatus* L and *P. australis* biomass and length in diesel contaminated environments relative to control plants not exposed to diesel and that impacts were reduced in the presence of bacterial inoculants, due to reduced toxicity and plant growth promotion (Fahid, Arslan, et al., 2020).

Phenrat et al. (2017) assessed microbial communities (bacteria, yeasts, and moulds) and found phenol degrading organisms in industrial wastewater including, *Rhodococcus* sp., *Pseudomonas* sp., *Bacillus* sp., *Enterobacter* sp., *Alcaligenes* sp., *Trichosporon* sp., *Rhodotorula* sp., and *Fusarium* sp. The total viable counts revealed phenol toxicity to microorganisms, that later recovered at the end of the first phase of phenol degradation, likely due to reduced toxicity from plant exudation of peroxidases and hydrogen peroxide. This was observed while comparing the microbial community between roots and water, where roots had greater total viable counts from 43 to 838 hours. Based on the recovery of the microorganisms, they proposed the degradation of phenol occurred over two phases. The first phase was driven by phytopolymerization, phyto-oxidation and release of peroxidases and hydrogen peroxide by the roots, and the second phase included phase one paired with microbial degradation, which had a much higher degradation rate. Concluding that increasing plant density on the hydroponic root mats enhanced degradation rates of phenol.

Ten studies in Table 2.1 examined the addition of endophytic and rhizospheric bacteria inoculants to EFWs for enhancing biodegradation of various contaminants including oil field wastewater, oil production contaminated water, sewage effluent, phenol, hexadecane, crude oil, and diesel.

Nine of the studies assessed plants and bacteria alone or together, and in all cases, plants and inoculated bacteria together had the highest degradation capacity. However, plants alone had greater degradation potential than the inoculated bacteria alone, suggesting that plants are a more important factor in degradation success (Table 2.1). For example, Rehman et al. (2019) studied EFWs planted with *T. domingensis* or *Leptochloa fusca* with and without inoculation of *Bacillus subtilis* LORI66, *Klebsiella* sp. LCR187, *Acinetobacter junii* TYRH47, and *Acinetobacter* sp.

LCRH81 for remediation of oil field wastewater using small-scale mesocosms. After six weeks of treatment, total hydrocarbons (mean initial concentration ± SE = 304 ± 10.25 mg/L) were reduced by over 90% in mesocosms treated with inoculated floating wetlands of either plant species (93-97%). While plants alone reduced total hydrocarbons from 75 to 78% and bacteria inoculation alone only reduced total hydrocarbons by 38%. The inoculated bacteria colonized successfully among all compartments and were highest in the rhizoplane, followed by root interior, water, and shoot interior. Over the duration of the study, the bacteria colonization in the water declined but increased in the roots and shoots, and the overall bacterial persistence was greater in treatments with vegetation, and higher in *T. domingensis*. Inoculated *T. domingensis* trials also had higher abundance and expression of the *alkB* gene in all compartments compared to inoculated *L. fusca* and bacteria alone, which was positively correlated with crude oil mineralization ($r^2 = 0.83$). The *alkB* gene has an important role for hydrocarbon degradation, specifically encoding for the alkane hydroxylase enzyme. There was a reduction in plant growth when plants alone were exposed to the oil wastewater, however, EFWs treated with bacterial inoculation improved plant growth. Rehman et al. (2019) also identified that fish (*Labeo rohita*) toxicity, measured as mortality over four days (n=10), was reduced from complete mortality after 24 hours in the untreated control (16% degradation) to zero mortality in the inoculated floating wetland treatments, whereas vegetation (2-3 mortalities) and bacteria alone (6 mortalities) only partially reduced mortality.

Similar relationships and results have been observed in terrestrial phytoremediation and biodegradation trials. Fatima et al. (2016) studied crude oil degradation potential *Brachiaria mutica* and *L. fusca* inoculated with a consortium of endophytic bacteria, *Acinetobacter* sp. strain BRSI56 and *Pseudomonas aeruginosa* strain BRRI54, in crude oil contaminated soil in *ex-situ*

pot experiments, with an initial concentration of 25.6 g crude oil/kg soil. Maximum crude oil degradation was observed for plants and bacteria together ranging from 71 to 78% after 93 days. Significantly higher than plants alone (60-66%), bacteria alone (52%), and the control with no treatment (40%). They observed reduction of growth metrics when plants were grown in the contaminated soil, but were improved in the presence of bacterial inoculants, with lower impacts for *B. mutica.* While both inoculated plant treatments had significantly higher degradation than the other treatments, *B. mutica* had higher crude oil degradation than *L. fusca*, and also had higher endophyte persistence and *alkB* gene expression and abundance in the endosphere and rhizosphere. Similar to Rehman et al. (2019), the *alkB* gene abundance was positively correlated with hydrocarbon removal (r = 0.87).

Fatima et al. (2018) also studied *B. mutica* and *L. fusca* inoculated with *Acinetobacter* sp. strain BRSI56, *P. aeruginosa* strain BRRI54, and *Klebsiella* sp. strain LCRI87 in field based, plot trials of crude oil contaminated soil at an oil exploration and production facility in Chakwal, Pakistan, with an initial concentration of 46.8 ± 1.6 g oil/kg (mean ± SE). Maximum crude oil degradation was observed for plants and inoculant treatment (78-85%) after three months. Vegetation alone had significantly higher degradation (51-61%) than bacteria alone (40%), and the control with no treatment had 12% reduction. Inoculated *B. mutica* treatments had greater oil removal than inoculated *L. fusca*, and removal was positively correlated with bacterial colonization (r = 0.71). The inoculated trials had greater abundance and expression of the *alkB* gene when vegetated compared to low bacterial survival and activity in unvegetated trials, and that expression was positively correlated with oil degradation (r = 0.73), suggesting that the plants enhance bacterial persistence and activity. Similar to their 2016 study, there was an impact to plant growth to both plant species when grown in contaminated soil, however, this impact was

reduced in the presence of endophytes. They further tested the soil toxicity after recovery through seed germination bioassay with wheat and found that the untreated contaminated soil had significantly less germination than treated soil, and where plant and inoculated bacteria treatments resulted in the greater germination, higher for *B. mutica*. Fatima et al. (2018) concluded that both plant species had potential for remediating crude oil contaminated soil, however, this was enhanced with endophytic inoculation.

Afzal et al. (2019) was the only study in Table 2.1 to conduct EFW and bacterial inoculation trials in a large-scale field application. The study was conducted at a crude oil contaminated, closed basin water stabilization pit in Chakwal, Pakistan, with an initial mean (± SD) hydrocarbon concentration of 319 ± 9.7 mg/L. They established a large EFW (3058 m^2/ 25% surface area of pit) planted with *P. australis*, *T. domingensis*, *L. fusca*, and *B. mutica* and inoculated with a bacterial consortium selected for hydrocarbon degradation, biosurfactant production (rhamnolipid), and plant growth promotion (indole acetic acid/amino-cyclopropane-1-carboxylic acid) capabilities. From March 2016 to September 2017, they monitored contaminant concentration, plant growth, bacterial colonization, and metabolic activity, and added fertilizer every three months. Hydrocarbon concentration decreased over the duration of the study, most rapidly during the first six months, reaching a final concentration of 2.8 mg/L after 18 months (99.1% reduction). The inoculants were applied to both the roots of the EFW and the contaminated water. The rhizoplane supported the highest number of the inoculated bacteria, followed by plant interior and water, however location of colonization and activity varied by bacteria type (e.g. endophytic vs. rhizospheric).

Afzal et al. (2019) observed a decrease in bacterial abundance and *alkB* gene expression in the water over the duration of the study. However, they also observed an increase in the

rhizoplane and plant tissue during the first six months followed by a decline, possibly due to the bioavailability of compounds. Of the plant species, *P. australis* had the highest bacterial numbers and the highest abundance and expression of *alkB* gene as well as the largest dry biomass and heights/lengths of roots and shoots. Toxicity of the water was tested at different time points by measuring mortality of fish (*L. rohita*) exposed to water for 96 hours (n = 10). Full mortality was observed in the first 24 hours of exposure on day 0 of the study, followed by partial mortality after 72 hours of exposure at both six (total mortalities at 96 h=3) and twelve months (total mortalities at 96 h=2) of treatment, while no mortalities were observed over the experimental period after 18 months of treatment, suggesting the site was no longer toxic and that EFWs can be used as a successful approach for remediating oil contaminated water.

2.4.1 Research Needs

The studies, described in Table 2.1, indicate that the use of EFWs may be a successful option for oil spill recovery. While some the results indicate a significant decline of total hydrocarbons with the use of bacterially inoculated EFWs, results may vary for real-world scenarios and in different climates. Eleven studies were conducted in small-scale (20-75 L) mesocosm experiments, one was conducted in a larger (1000 L) mesocosm experiment (Rehman et al., 2021), and only one was conducted at a large field-scale in a water stabilization pit (Afzal et al., 2019). While this research is useful for identifying the potential for utilizing plant-bacterial symbiosis for oil spill recovery, there is a need to further understand how these systems perform during real spill scenarios in freshwater and marine environments. Small-scale microcosms, with limited volume and energy inputs, represent 100% interaction between oil compounds and the treatment (e.g. root surface area is high relative to mesocosm volume; Rehman et al., 2021), which is not the case during an oil spill event, where oil can become bound to shoreline material,

soil, or sediment, and may remobilize into the water column with wave activity, changes in water level, or weather events (Lee et al., 2015). Changes in environmental conditions and chemical pulses may influence the success of this treatment and should be studied in larger context field-based trials. For example, temperature will affect the solubility and bioavailability of oil compounds (Ghosal et al., 2016), the microbial community and activity (Al-Hawash et al., 2018; Das & Chandran, 2011), as well as plant growth. Optimal temperature for biodegradation varies by environment type; marine, freshwater, and soil environments observe maximum degradation between 15-20 ℃, 20-30 ℃, and 30-40 ℃, respectively (Al-Hawash et al., 2018 and citations therein; Das and Chandran, 2011 and citations therein).

Most of the studies in Table 2.1 are conducted in temperate, semi-arid, or tropical regions; ten of which were conducted in Pakistan. For example, the Afzal et al. (2019) study was located in Chakwal, Pakistan, and was conducted over 1.5 years. The average air temperatures noted in this study ranged from 15 ℃ to 40 ℃ in the summer and -4 ℃ to 25 ℃ in winter. Li et al. (2012), was the only study to conduct research at cooler temperatures, from 0 ℃ to 15 ℃ from October to December 2008, in Hangzhou China, and acknowledged that the removal efficiencies from days 21 to 35 had declined, possibly due to the lower temperatures, impacting microbial activity and plant growth. Other colder climates experience greater extremes of cold temperature that may have an impact on biodegradation and oil properties. For example, although the rates of biodegradation during the Exxon Valdez oil spill in Prince William Sound, Alaska, were slow due to marine environmental conditions, they were significant (Lee et al., 2015). In arctic marine environments, the success of biodegradation is uncertain due to ice and temperatures (Desmond et al., 2021). Desmond et al. (2021) explored crude oil photodegradation and biodegradation potential in sea ice in a mesocosm experiment. Mesocosm tanks received

artificial sea water and nutrients, and one tank received the addition of indigenous bacteria from Cambridge Bay in the Arctic, previously grown in crude oil contaminated water. The mesocosms were left to freeze until ice formed (25-29 cm) followed by inoculation of 6.6 L of light crude oil below the ice. Ice cores and water samples were collected every three weeks to analyze the microbial community, chemistry, and physical parameters. They observed a shift in microbial community dominance from Bacteroidia to Gammaproteobacteria in both treatments, and genera *Alcanivorax*, an obligate hydrocarbon degrader, was dominant in the melted pond water, but not in the ice. The majority of the oil was not in contact with the brine region of the ice, which supports the highest microbial abundance, indicating that biodegradation in sea ice is minimal until it melts and is released into the water, where biodegradation may be more successful.

Other marine research has explored the response of cold-adapted microbial communities from Labrador Sea sediment to diesel and crude oil in a nutrient stimulated microcosm experiment (Murphy et al., 2021). They found that microorganisms known to degrade aliphatic and aromatic hydrocarbons increased in abundance between day 0, 28, and 71 of exposure to diesel or crude oil at 4 ℃, and that the exposure to contaminants significantly changed the microbial community depending on concentration (0.1% and 1 %) and nutrient stimulation. They observed that some microorganisms in the Labrador Sea are adapted to cold temperatures and have hydrocarbon degradation potential, such as *Cycloclasticus*. This is an important finding for cold marine environments that are used for transport and at risk for potential spill events. Murphy et al. (2021) further noted that the use of nutrients enhanced biodegradation rates. However, biostimulation only enhanced hydrocarbon degradation at 0.1% concentration of diesel and crude oil, and not at 1%.

It is clear that microorganisms are capable of degrading oil compounds at suboptimal temperatures in marine environments, but there is a need to test the effectiveness of EFWs in cold freshwater environments or those that experience fluctuating or extreme cold temperatures and extended ice-on periods during the winter months.

Ten of twelve mesocosm studies note the use of plastic or polyethylene tanks as containment for the remediation study. These types of mesocosms are regularly used for research, however polyethylene is a synthetic plastic polymer and has high sorption capacity for PACs, and thus is often used as a passive sampler (Fries & Zarfl, 2012). None of the studies considered removal of contaminants from the water column by sorption to the mesocosm material. Future research should consider sampling the plastic at the end of the study for extraction to determine how much oil was absorbed into plastic rather than degraded by the EFW treatment. This would allow researchers to understand the total potential of EFWs to degrade contaminants and aid with the design and implementation for oil remediation. It is important to note that this does not discount the findings of the research in Table 2.1 or any future research experiments using plastic containment, as all treatments are conducted in the same containment media and still show differences and trends of degradation between the treatment types.

Although ten of the thirteen studies inoculated their systems with a consortia of bacteria known to degrade contaminants, there is no understanding on how inoculants may survive under variable environmental conditions during real oil spill scenarios, or how they may impact native microorganisms and compete for resources (Ghosal et al., 2016). Historically, bioremediation was studied with microorganisms that are culturable under laboratory conditions, noting that bioremediation performance may differ for the natural environment (Czaplicki & Gunsch, 2016; Malla et al., 2018).

There are many environmental factors influencing oil spill impacts and bioremediation success, such that no spill or remediation strategy is the same (Dupuis & Ucan-Marin, 2015; Lee et al., 2015; Zhu et al., 2001). There is a need to further test EFWs as a bioremediation technique for oil compounds in large scale applications under changing environmental conditions. Because of this, application of inoculants may be more suitable for closed system treatments, such as an effluent treatment facility or oil wastewater pond. For *in-situ* remediation of oil spills in freshwater or marine environments, it may be more appropriate to use plants to stimulate the native microbial community. As discussed in Section 2.3.2.1, oil spill degradation requires a diverse microbial community with various metabolic roles that change over time to transform contaminants to non-harmful end products (Cao et al., 2009; Ghosal et al., 2016; Lee et al., 2015; Zhu et al., 2001). A single or small group of inoculants may not be sufficient for an oil spill in the natural environment, as they may only target a specific oil compound (Rosenberg & Ron, 1996).

Research outlined in Table 2.1 suggested that plants can successfully degrade contaminants without additional inoculation, likely by enhancing the natural rhizosphere microbial community or releasing exudates. However, more time may be required to observe full recovery and research is needed to identify plants that can withstand potential toxicity of oil.

2.5 Conclusion

The use of EFWs for the remediation of oil, hydrocarbons, or related contaminants has been implemented with success in small scale trials and a larger scale oil stabilization pit trial. The greatest success was generally observed in bacterially augmented EFW trials; however, plants alone proved to be more effective than bacteria alone in all cases. Plants may be able to provide surface area to stimulate native microorganisms and release enzymes to degrade

contaminants without the addition of inoculants, suggesting EFWs could be successful for bioremediation of oil spills in natural environments. With the concerns of introducing potentially non-native organisms into an environment, it may be better to solely apply native plants on EFWs to stimulate the existing community when conducting research or treating aquatic contaminants in the natural environment. Further research is required to assess potential of EFWs for oil spill recovery in large-scale field-based trials under variable environmental conditions, especially in colder climates. The use of EFWs for remediating freshwater oil spills is being explored in shoreline enclosure experiments at the International Institute for Sustainable Development Experimental Lakes Area in northwestern Ontario, Canada as part of the FLOating Wetland Treatments to Enhance Remediation (FLOWTER) project, a related project to the Freshwater Oil spill Remediation Study (FOReSt), as described in (Palace et al., 2021). This research (not published) explores changes to the microbial biofilm community on EFW roots upon exposure to model oil spills, and will provide insight into non-invasive oil spill recovery methods.

Chapter 3. Assessing Changes to the Root Biofilm Microbial Community on an Engineered Floating Wetland Upon Exposure to a Modelled Diluted Bitumen Spill

3.1 Introduction

Canada has the third largest crude oil reserve in the world (Dupuis & Ucan-Marin, 2015; Natural Resources Canada, 2020) and is one of the top producers and exporters of oil (Natural Resources Canada, 2020). In the last 30 years, bitumen production in Canada has increased five-fold, from producing 135 thousand barrels per day (8% of crude oil production) in 1990 to 1.8 million barrels per day (~40% of crude oil production) in 2019 (Canada Energy Regulator, 2021a)[3]. Bitumen is a highly viscous product, which must be diluted for some transport mechanisms (e.g., pipelines). Diluted bitumen, hereafter referred to as 'dilbit', is a mixture of 70% bitumen and 30% diluent, such as condensate or naphtha (Canada Energy Regulator, 2021c; Lee et al., 2015). The export of dilbit has increased from 17% to 63% of total Canadian crude oil exports from 1990 to 2019 (Canada Energy Regulator, 2021b)[3]. The increase in production and transport of bitumen or oil products puts nearby ecosystems at risk for accidental spill events, and thus spill responders and industry should have reliable and effective remediation methods in place for when events do occur (Chang et al., 2014; Murray et al., 2018).

Conventional methods, such as mechanical or chemical recovery, can be costly and invasive (Yavari et al., 2015). For example, mechanical recovery in shoreline environments can cause significant damage through excavation and/or removal of vegetation (Hoff, 1995; Lee et al., 2015; Pezeshki et al., 2000; Zhu et al., 2001), and is estimated to regularly recover 10-30% of spilled oil, occasionally greater than 50% (Etkin & Tebeau, 2003). Chemical methods, such as

[3] Data presented from the Canadian Crude Oil Exports: A 30 Year Review (Canada Energy Regulator, 2021a; 2021b) contains information licensed under the Open Government Licence-Canada. https://open.canada.ca/en/open-government-licence-canada

dispersant use, can increase oil exposure to interacting organisms and some have not been approved for use in freshwater (Lee et al., 2015). Biological remediation may be a less-invasive and cost-effective alternative with potential to increase recovery of spilled oil (Rehman et al., 2018). Biodegradation of oil, commonly referred to as monitored natural recovery, occurs when microorganisms metabolize petroleum carbon compounds for energy (Magar et al., 2009). This breakdown can be enhanced by nutrients (biostimulation) or bacterial inoculants (bioaugmentation), and can also be naturally stimulated by plants and their root exudates (Lee et al., 2015). In an oil spill scenario, this may be performed by increasing plant surface area through deploying engineered floating wetlands (EFWs). EFWs, also referred to as floating treatment wetlands, are platforms of emergent vegetation, with roots growing into the water column. This increases surface area interaction with contaminants for phytoremediation and microbial biofilm development for biodegradation (Shahid et al., 2018; Tanner & Headley, 2011). There has been growing interest in the use of EFWs to enhance microbial biodegradation of oil compounds, summarized in Chapter 2, highlighting a need to study this remediation strategy in field-based trials and under variable environmental conditions, such as cold freshwater lakes.

Research at the International Institute for Sustainable Development Experimental Lakes Area (IISD-ELA) in northwestern Ontario, Canada, has explored the use of EFWs for secondary remediation of model oil spills in freshwater shorelines of a boreal lake, as part of the FLOating Wetland Treatments to Enhance Remediation (FLOWTER) project. Canada's boreal zone occupies 28% of land (552 million ha), of which 71 million ha is occupied by lakes, ponds, and rivers (Brandt et al., 2013). Conducting research at the IISD-ELA allows researchers to understand how oil spills may impact and be treated in similar environments, and benefits from

years of baseline data which is often missing to assess recovery following oil spill events (Lee et al., 2015).

The objective of this chapter was to monitor changes to the microbial community on EFW roots upon exposure to a model dilbit spill following primary recovery, and to monitor changes to polycyclic aromatic compound (PAC) chemistry in the water and sediment of the model spill and unoiled reference sites. I hypothesized that the community would shift in the presence of oil to microorganisms known to consume and degrade hydrocarbon compounds. To the best of our knowledge, this was the first freshwater, in-lake experiment to study model oil spills and EFWs.

3.2 Materials and Methods

3.2.1 Research Design and Site Description

A modelled spill was conducted in a wetland shoreline enclosure on Lake 260 (volume= 1,975,969 m^3, surface area= 332,460 m^2, max depth= 15.64 m; IISD-ELA, 2022), a boreal lake at the IISD-ELA, in 2019. Enclosures were constructed with a floating collar (5 m wide x 10 m long) attached to a polypropylene curtain, sealed to the sediment and five meters onto the shore with a double layer of sandbags (>20,000 L) (Curry Industries Ltd., Winnipeg) (Figure A1). Study sites included an experimental enclosure (oiled; EE), a reference enclosure (unoiled; RE), and a lake reference site (unoiled; LR), noting there was no site replication. Due to limited appropriate wetland shoreline area and depth (≤ 2 m), the EE was shortened to approximately 6 m long.

3.2.1.1 Oil Application and Recovery. Cold Lake Blend dilbit, sourced from pipeline stocks as provided by the Canadian Association of Petroleum Producers (CAPP), was weathered in a stainless steel pan with ~220 L of lake water, as described in Palace et al. (2021), for 36

hours on June 19-20, 2019, to simulate oil that would typically reach the shoreline environment. During the weathering process, oil can undergo evaporative loss of lighter compounds (e.g., BTEX), altering the chemical and physical characteristics of oil (Lee et al., 2015). After weathering, the oil was collected into a glass jar and carefully poured (1,444 g) in the EE at the near shore (within 50 cm) environment on June 21, 2019. The EE received primary recovery of shoreline washing for twelve minutes through pumping enclosure water (1,600 L) over the shore and collecting oil on the water surface with polypropylene sorbent media (Spill Ninja, MEP Brothers, Winnipeg) 4 days after oil application on June 25, 2019, to simulate conservative response times in remote locations. Response guidance and support was provided by Dr. Elliott Taylor (Polaris Applied Sciences) to ensure efforts reflected industry standards. Primary recovery removed 49.4 g of dilbit, leaving 1,394 g (97 %) of residual oil in the enclosure. Removal was lower than reported in the literature (Etkin & Tebeau, 2003), however, our efforts were non-invasive and did not include any mechanisms that would alter the shoreline and native vegetation. Residual oil was then treated on June 26, 2019, with secondary remediation of an EFW located in the middle to far shore environment of the enclosures. The RE also received shoreline washing on June 27, 2019, followed by EFW addition. In order to conduct such research, contingency measures were implemented with efforts to have no further impact to the ecosystem than the intended regions (Appendix A- Section A.1.1).

3.2.1.2 Engineered Floating Wetlands. EFWs were BioHaven Floating Islands sourced and produced by Martin Ecosystems (Louisiana, United States), under license by Floating Islands International (Montana, United States). The platform was made of recycled polyethylene terephthalate plastic and coated in polyurea for protection, with holes to transplant emergent vegetation (Floating Islands International, n.d.). EFWs (1.14 m^2; 21 holes of 7.62 cm diameter)

were originally established in 2017 with local emergent wetland plants, Gold Label coconut mulch, and soil, and re-transplanted in June 2019 to replace dead plant material with coconut mulch and *Typha* sp. (cattail) and three *Carex* spp. (sedge); *C. atherodes/utriculata*, *C. lasiocarpa,* and *C. pseudocyperus/hystericina* (identified by Chris Penner, personal communication with Dr. Richard Grosshans, IISD, n.d.). Noting, *Carex* are particularly difficult to identify due to the high number of species, classified by minor changes in plant features (Naczi, 1992, as cited in Starr et al., 2009). EFWs plants were measured for heights and number of live plants, however, due to insect activity, measurements are not discussed herein.

3.2.2 Polycyclic Aromatic Compound Chemistry

3.2.2.1 Water. Water was collected 3 days pre-oil addition and on days 1 to 6, 8, 12, 20, 38, 66, 87, 209, 263, 356, and 411 post-oil addition for PAC chemistry (day 0 is the date of oil application). Total PACs (n = 44) included 16 US Environmental Protection Agency (2014) priority parent PACs and 28 alkylated PACs (aPACs) and heterocyclic PACs, further referred to as aPACs (Table A1). Water was collected in a 1 L amber bottle using a peristaltic pump from the far shore environment in the enclosures, and was transported in a cooler to the Centre for Oil and Gas Research and Development (COGRAD) laboratory at the University of Manitoba, Winnipeg, Manitoba, and 250 mL was vacuum filtered (1.2 μm, Whatman GF/C filter) within 24 hours of collection for liquid-liquid extraction following methods previously described in (Dearnley, 2022). Briefly, the filtrate was transferred into a separatory funnel which received 20 μL of 5 ng/μL recovery internal standard (RIS; suite of d8-naphthalene, d8-acenaphthylene, d10-acenaphthene, d10-fluorene, d10-phenanthrene, d10-pyrene, d12-Benz(a)anthracene, d12-chrysene, d12-benzo(b)fluoranthene, d12-benzo(k)fluoranthene, d12-benzo(a)pyrene, d12-indeno(1,2,3-c,d)pyrene, d14-dibenzo(a,h)anthracene, and d14-benzo(g,h,i)perylene) and 10 g of

sodium chloride (NaCl). The sample was extracted twice with 50 mL dichloromethane (DCM) and gently swirled for 1 minute, and collected into a round bottom flask (total 100 mL DCM) which was reduced using rotary evaporation. Sodium sulphate (Na_2SO_4) was added to remove any water from the extraction process (Dearnley, 2022), and the sample was transferred to a 12 mL round bottle borosilicate glass tube with a Teflon lined screw cap. The remaining sodium sulphate was rinsed three times with Optima ™ hexane, which was transferred into the glass test tube. A solvent exchange from DCM to Optima ™ hexane was conducted using a nitrogen gas evaporator (N-EVAP™111, Organomation Associates Inc., MA, USA and OA-SYS Heating System), until 1 mL of sample remained. Each sample was spiked with 20 µL of an instrument performance internal standard (5 ng/µL d10-anthracene; IPIS) and was transferred into an amber GC vial with a Teflon cap. PACs were detected and quantified on an Agilent 7890 gas chromatograph coupled to a 7000C triple quadrupole mass spectrometer following methods and GC-MS/MS conditions outlined in Idowu et al. (2018).

During sample collection, a field blank was collected by opening an amber bottle containing 200 mL Optima ™ water for the duration of sample collection. PAC extraction for the field blank followed the same procedure as described above for experimental samples. Final concentrations for all samples were corrected for RIS, IPIS, and field blanks by Dr. Lisa Peters.

Water was also regularly monitored for basic quality parameters and was sampled bi-weekly for nutrient chemistry, discussed in Appendix A, Sections A.3 & A.4.

3.2.2.2 Sediment. Sediment was collected with a sediment corer in three random locations (n=3) from each site 3 days pre-oil addition and on days 38, 66, and 91 post-oil addition. Single sediment samples were made on days 249 and 628. The top 5 cm were transferred into a 125 mL amber jar, and refrigerated overnight to remove overlying water once

settled and then frozen at -20℃. Sediment PACs were extracted at the COGRAD laboratory using accelerated solvent extraction methods described in Dearnley (2022) and quantified on GC-MS/MS as described above (Idowu et al., 2018).

3.2.3 Root Microbial Community

Three days before oil addition, single root samples were collected from a random location on each EFW. On days 38 and 91, root samples were collected from three random locations on each EFW (n=3). Collected roots were transferred into a Whirl-pak® bag and placed onto dry ice until transported to a -80 ℃ freezer before shipping to the National Research Council (NRC), Montreal, Quebec, for extraction and sequencing to assess microbial diversity.

3.2.3.1 16S and 18S Gene Amplicon Extraction and Sequencing. Root samples were extracted using the PowerSoil Max DNA extraction kit (cat#12988-10, QIAgen). Between 5 and 10g of roots were weighed and transferred into a PowerMax Bead Tube containing 15 mL of PowerBead Solution. The extraction was done following manufacturer's guidelines. The nucleotide acid elution was done with 3 mL of DNAse-free Ambion water. The extracted gDNA was quantified using the Quant-iT™ PicoGreen™ dsDNA Assay Kit (cat#. P7589, ThermoFisher Scientific).

Taxonomic 16S (prokaryotic) and 18S (eukaryotic) ribosomal ribonucleic acid (rRNA) gene amplifications were done on all the gDNA samples. Bacterial communities, including eubacteria and archaea, were targeted using the primer set 515F-Y (5′-GTGYCAGCMGCCGCGGTAA-3′) / 926R (5′-CCGYCAATTYMTTTRAGTTT-3′). The 18S rRNA gene region of the eukaryotic ribosomal DNA was amplified using the primer set 565F (5′- CCAGCASCYGCGGTAATTCC-3′) / 948R (5′- ACTTTCGTTCTTGATYRA-3′). Primers contained the required Illumina adaptors at the 5′ end of the primer sequences (5′-

TCGTCGGCAGCGTCAGATGTGTATAAGAGACAG-3′ for the forward primer and 5′-GTCTCGTGGGCTCGGAGATGTGTATAAGAGACAG-3′ for the reverse primer).

The V4-V5 region of the bacterial 16S rRNA gene and the V4 region of the eukaryotic rRNA gene were amplified in 25 μL volumes using 12.5 μL of KAPA HiFi HotStart ReadyMixPCR Kit (Roche), 10 μM of each primer, Ambion nuclease-free water, 20 μg of BSA and 1 μL of gDNA. Thermal cycling conditions were as follows: initial denaturation at 95 °C for 3 min; 30 cycles at 95 °C for 30 s, 55 °C (for 16S primers) or 50 °C (for 18S primers) for 30 s, 72 °C for 30 s ; and a final elongation at 72 °C for 7 min. PCRs products were visualized on SyBrSafe-stained 1% agarose gels. PCR amplicons were purified using 0.8X volume of magnetic beads solution (Agencourt AMPure XP, Beckman Coulter Life Science) according to the manufacturer's protocol. Unique codes were added to each sample by amplifying 5 μL of the purified PCR product with 12.5 μL of KAPA HiFi HotStart ReadyMixPCR Kit, 150 nM of each Nextera XT Index Primer (Illumina Inc., San Diego, CA, USA) and Ambion nuclease-free water for a total volume of 25 μL. Thermal cycling conditions were as follows: 3 min at 95 °C, 8 cycles of 30 sec at 95 °C, 30 sec at 55 °C, 30 sec at 72 °C, and a final elongation step of 5 min at 72 °C. Indexed amplicons were purified with the magnetic beads as previously described and quantified using the picogreen fluorescence method and combined in an equimolar ratio. Methods described in this section were provided by Dr. Charles Greer (NRC, Quebec).

Paired-end sequencing (2 × 250 bp) of the 16S and 18S rRNA gene amplicon pools was carried out on an Illumina MiSeq sequencer at the National Research Council in Montreal, using the MiSeq Reagent kit V2, 500 cycles (cat# MS-102-2003, Illumina). The 16S rRNA gene amplicon sequencing data was processed using AmpliconTagger (Tremblay & Yergeau, 2019) and produced a total of 4,052,832 reads, which were further classified into 6,365

clusters/amplicon sequence variants (ASV). The 18S rRNA gene amplicon sequencing produced a total of 4,987,304 reads, which were further grouped into 3,263 ASVs.

3.2.4 Data Analyses

No statistical comparisons were conducted as there was no enclosure replication. Results can be used as a case example to assess whether EFW microbial communities change upon oil exposure, and to inform future replicated research to assess potential of plants and EFWs for secondary oil spill recovery. Trends were analyzed using R (4.2.2) in R Studio (2023.09.1 + 494; Posit Team, 2023; R Core Team, 2022) primarily with tidyverse (v. 2.0.0, Wickham et al., 2019) and ggplot2 (v. 3.4.1, Wickham, 2016) packages. Rarefied ASVs were analyzed for richness (alpha and chao1) and diversity (Shannon and Simpson), as provided from NRC, Quebec, and for Bray-Curtis beta diversity with a principal coordinate analysis (PCoA), and taxonomic profiles using R Studio (2023.09.1 + 494; Posit Team, 2023; R Core Team, 2022), visualized with ggplot2 (v. 3.4.1, Wickham, 2016), using modified R scripts provided by NRC. Additional R packages used for data analyses are included in Appendix D.

Metazoans and class *Embryophyta* (land plants) had high relative abundance, but were removed to analyze the eukaryotic microbial community. Eukaryotic ASVs were inconsistently identified to genus, and often subphyla or clades were inserted into the classification. Edits (such as the removal of subphyla or classes confirmed with the SILVA database (R138.1) (2023) (Glöckner et al., 2017; Quast et al., 2013; Yilmaz et al., 2014), World Register of Marine Species (WoRMS Editorial Board, 2023), and National Center for Biotechnology Information (Schoch et al., 2020) databases, and scientific literature) were made to correct or remove misplacement of taxonomic classifications (e.g., Phragmoplastophyta was misclassified as a phylum), however

missing classifications once corrected (e.g., class/family) were not added. Taxonomic profiles present the lowest level identified.

3.3 Results and Discussion

3.3.1 Polycyclic Aromatic Compound Chemistry

3.3.1.1 Water. Total aqueous PACs before oil addition were 290.21 ng/L, 27.38 ng/L, and 57.90 ng/L in the EE, RE, and LR, respectively (Figure 3.1). After oil addition to the EE, concentrations on day 1 were 1,591.23 ng/L, 95.84 ng/L, and 63.33 ng/L, respectively. The maximum concentration in the EE occurred on day 20, reaching 12,440.83 ng/L, within the chronic (> 96 hour) toxicity range for total polycyclic aromatic hydrocarbons (PAH) causing mortality (LC_{50}) for freshwater biota (Lee et al., 2015; Figure 4.2). Total PACs on day 20 were 1,667.17 ng/L and 795.11 ng/L in the RE and LR, respectively. This peak was estimated to result from a precipitation event on day 19, a record rainfall of 145.6 mm in 24 hours (IISD-ELA meteorological data), causing remobilization and reintroduction of oil from the shoreline and/or sediments. This was supported by the trend in total aqueous PACs declining on days 8 and 12. Concentrations in the EE then declined to 2,336.03 ng/L on day 38, and later to 359.91 ng/L, nearing background conditions on day 66. Total PACs were relatively stable for the remainder of the experiment, where concentrations were last recorded on day 411 at 467.97 ng/L, 202.56 ng/L, and 119.51 ng/L in the in EE, RE, and LR, respectively. However, noting GC-MS/MS runs for two samples (EE and RE) on day 209 failed and are not included. Figure 3.1 presents the first 87 days of exposure, the remaining data are presented in Figure A2.

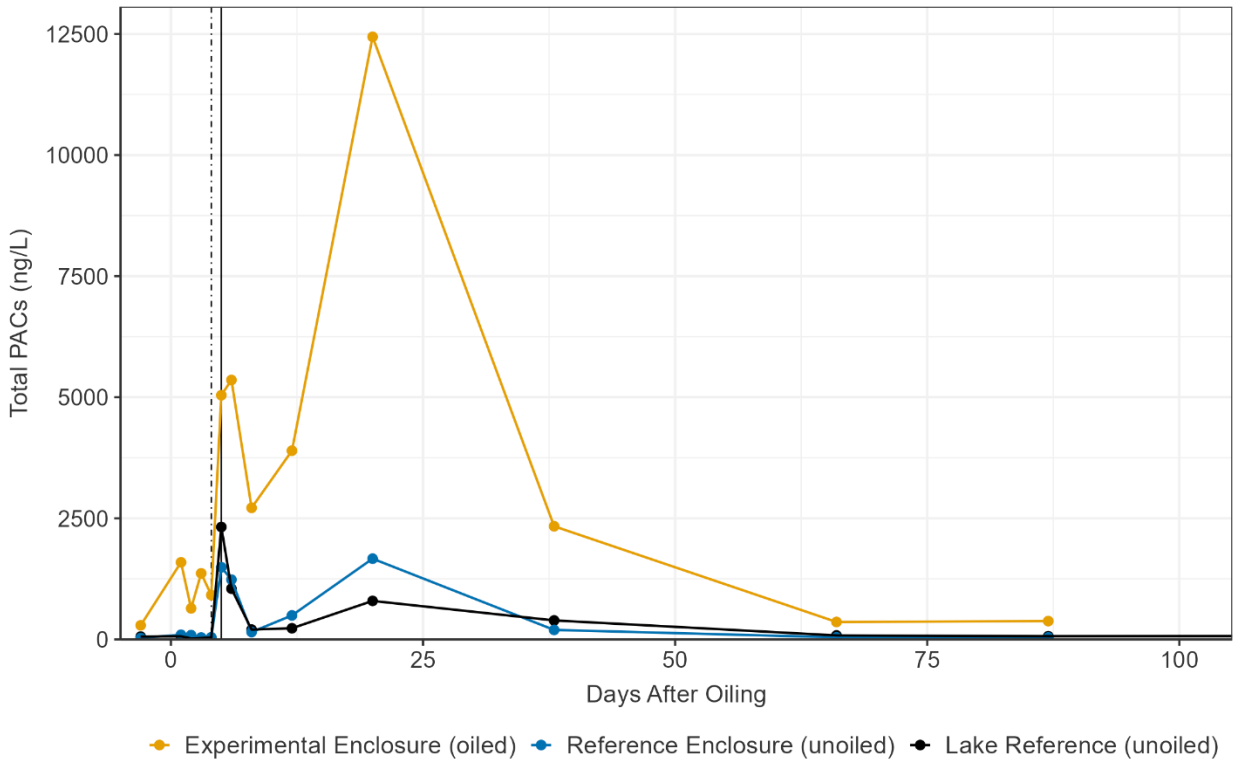

Figure 3.1. Total PACs (n=44) in the water from 3 days pre-oil addition to day 87 post-oil addition during the 2019 dilbit experiment. Vertical lines represent primary (dotted) and secondary (solid) remediation events.

Total PACs in the EE were mostly of 2-, 3- and 4-ring aPACs, with fewer >4-ring compounds (Figure A3 & Figure A4), and with dominance (mean > 100 ng/L) of alkylated naphthalenes (C2, C3, and C4), dibenzothiophenes (C1 and C2), C2-pyrene, and C1-fluorene. Following oil addition, aPACs had a mean (range; n=16) of 90.6% (66.8-99.3%), 70.6% (16.9-98.5%), and 60.1 % (4.28-99.9%) of total PACs in the EE, RE and LR, respectively. aPACs are more persistent compared to parent compounds and have greater chronic toxicity to biota (Lee et al., 2015; Zhu et al., 2001), and increase with continued weathering and evaporative processes (Lee et al., 2015). Total PACs were higher than previous oil spill research at the IISD-ELA (Palace et al., 2021; Rodriguez-Gil et al., 2021), which may be a result of the oil product, PACs

measured, analytical methods (Rodriguez-Gil et al., 2021), remediation efforts, site volume, and environmental conditions. For example, during this study we experienced extreme precipitation which may have caused redistribution and mixing of oil into the water column, where in other studies the oil may have sunk and bound to the sediment. Because of this, there are limitations to comparing studies and past spill events.

3.3.1.2 Sediment. Upon analyzing total sediment PACs, we noted significant variability within site replicates (three samples per site) and high concentrations in unoiled sites, making it difficult to discern differences between sites over the exposure period. This was in part due to a significant contribution from retene, a three-ring PAC, that can be increased during combustion of wood (i.e., forest fires) or diagenic processes (Gabos et al., 2001; Ramdahl, 1983). Forest fires are an essential disturbance for boreal forest rejuvenation (Brandt et al., 2013), and this region is often impacted by nearby fires resulting in ash deposition and smoke, and also has signs of a historic fire in the watershed (1979). In all sampling periods, percent retene of total PACs ranged from 0-92.3%, 22-97%, and 28-98% in the EE, RE, and LR, respectively. In order to assess changes in sediment PACs between sites, we excluded retene from total PACs (n=43) (Figure 3.2), however is included in Figure A5.

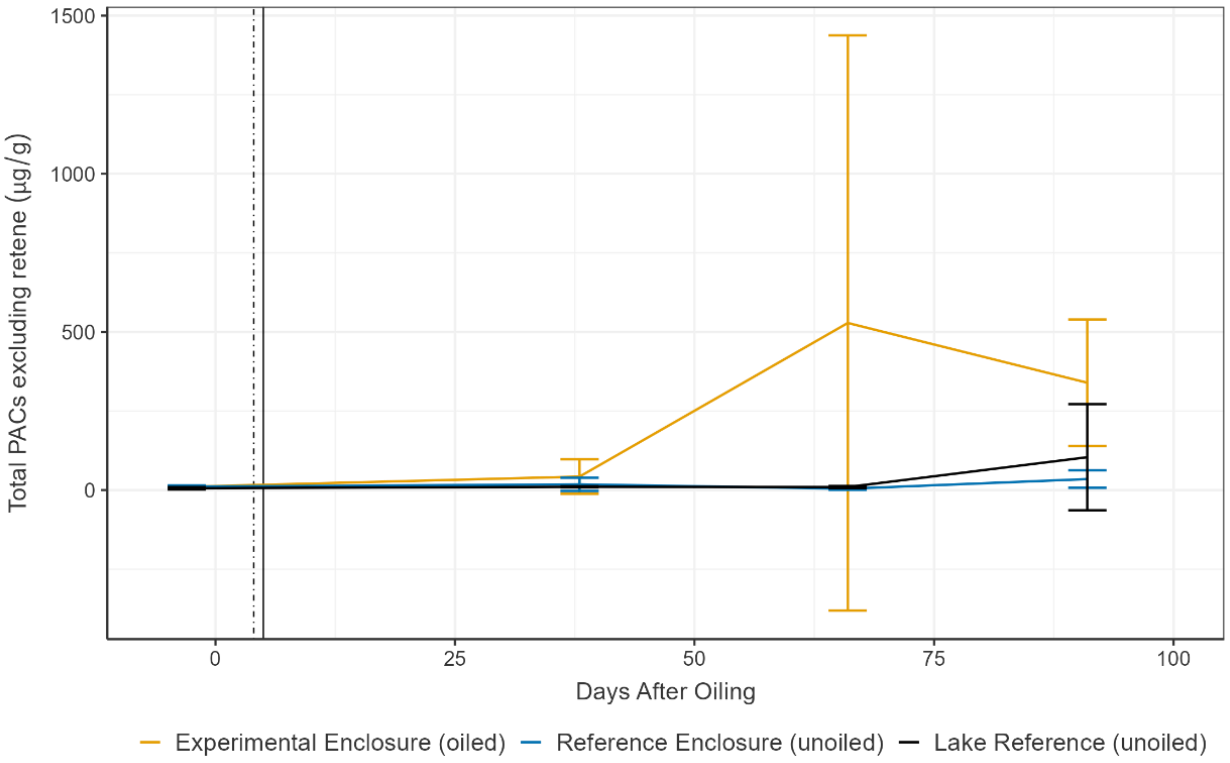

Figure 3.2. Mean (± SD) total sediment PACs (excluding retene; n=43) from 3 days pre-oil addition to day 91 post-oil addition during the 2019 dilbit experiment. Error bars represent standard deviation of triplicate samples at each site. Vertical lines represent primary (dotted) and secondary (solid) remediation events. A sediment sample from the EE on day 91 was lost.

Mean total PACs (± SD; triplicate samples at each site) excluding retene (n=43) during pre-oil conditions were 10.5 ± 1.26 µg/g, 10.9 ± 3.94 µg/g, and 5.78 ± 3.76 µg/g in the EE, RE, and LR, respectively, with contributions from c1-pyrene (14.5-44.0%). Concentrations increased with high variability on day 38 in the EE to 42.6 ± 54.7 µg/g, with large contributions from c3-dibenzothiophene (4.54-20.6%), c2-dibenzothiophene (5.31-19.1%), and c1-pyrene (5.68-15.5%), however the largest change occurred on day 66 at 528.4 ± 909.2 µg/g, mostly of c4-phenanthrene (1.72-87.5 %) and c1-pyrene (6.54-23.6%) in some samples. The variability among replicates indicates potential influence of sample location, similarly observed in Stoyanovich et

al. (2022). Any oil globules contained in the EE sediment samples would have contributed to increased PACs and replicate variability. Sediment PACs in the RE were 18.2 ± 20.6 μg/g and 4.23 ± 3.44 μg/g on day 38 and 66, respectively, and were 10.4 ± 1.50 μg/g and 9.76 ± 3.37 μg/g in the LR, respectively, mostly made of c1-pyrene. Concentrations decreased in the EE on day 91, at 339.4 ± 200.2 μg/g (n=2), almost fully contributed by c1-pyrene (98.9-99%), with little contribution from alkylated dibenzothiophenes or phenanthrene, suggesting potential degradation, loss, or influence of sample location. Concentrations in the RE and LR were 34.8 ± 27.6 μg/g and 103.9 ± 167.7 μg/g, respectively. By day 249, concentrations were similar amongst all sites at 30.3 μg/g, 31.3 μg/g, and 36.6 μg/g, respectively (88.6-93.8 % c1-pyrene), however noting these were a single sediment sample and may reflect sample location (Figure A6). On day 628, sediment PACs remained at 31.8 μg/g in the EE, while the RE and LR had 19.2 μg/g and 1.25 μg/g, respectively. It is clear there is a large contribution of c1-pyrene in the sediment, with and without oil exposure, and it is possible c1-pyrene and other sediment PACs, may have resulted from forest fires (Vergnoux et al., 2011), however the increase on day 38 and 66 in the EE, is likely contributed from dilbit. To assess whether PACs arose from petrogenic or pyrogenic sources, sediment PAC ratios are discussed in Appendix A- Section A.2.2.1.

3.3.2 Root Microbial Community

3.3.2.1 Diversity. Root microbial 16S (prokaryotes) and 18S (eukaryotes) rRNA beta diversity of rarefied ASVs was analyzed using a PCoA to identify differences between EFWs over the experimental period. The PCoA for prokaryotic and eukaryotic beta diversity had 40.13% and 41.28% of explained variation on the first and second axes, respectively (Figure 3.3). All three EFWs on day -3 were clustered together on both PCoAs, indicating similarity before EFW deployment to their respective sites. The greatest differences in the prokaryotic

community were between the LR and enclosures on days 38 and 91, which were clustered together, suggesting there may be an enclosure effect. Differences over the exposure period were observed for the enclosure sites, with greater differences between sites on day 91, indicating a potential seasonal or condition effect. There were no changes in the eukaryotic beta diversity in the LR, while there were changes in the enclosures over the exposure period, with greatest differences between the enclosure sites on day 91, displaying a potential site condition and/or seasonal effect.

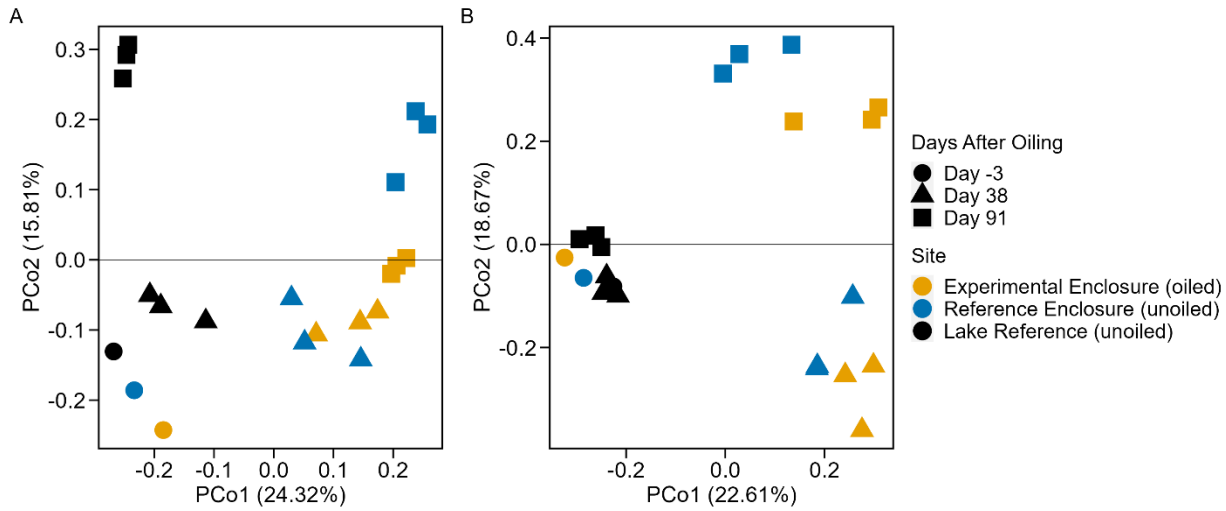

Figure 3.3. Principal Coordinate Analysis of 16S (A) and 18S (B) Bray-Curtis beta diversity in EFW root microbial biofilm during the 2019 dilbit experiment.

Prokaryotes had greater richness, and diversity and evenness than eukaryotes, suggesting there may be no dominating prokaryotic organisms, while certain eukaryotic organisms may be dominant or selected for. While highly variable, the enclosures appear to have greater mean richness than the LR on days 38 and 91, but diversity indices are variable, further suggesting a potential enclosure effect (Table A4).

3.3.2.2 Taxonomic Profiles.

3.3.2.2.1 Prokaryotes. Taxonomic profiles of rarefied ASVs revealed that among all sites and periods, prokaryotes were dominated by phyla *Proteobacteria* (41.5-56.7% relative abundance [RA]), *Bacteroidota* (10.3-20.9%), *Planctomycetota* (5.40-10.9%), *Acidobacteriota* (3.74-8.85 %), and others, of a total of 45 bacteria and archaea phyla identified (Figure A10). The *Proteobacteria* were mostly made of classes *Alphaproteobacteria* (20.3-29.5% of class taxonomic profiles) and *Gammaproteobacteria* (18.9-31.4% of class taxonomic profiles), which are two major groups involved in PAC degradation (Ghosal et al., 2016).

Taxonomic profiles of the top 20 prokaryotic ASVs (genera) represent approximately 40% of community RA, of 704 identified ASVs (Figure 3.4), indicating high community richness. For that reason, the next 21-40 most relatively abundant organisms are presented (Figure 3.5). The highest relative abundance was 7.71% for *Bryobacter*, an aerobic chemoorganotroph found in acidic wetland environments (e.g., sphagnum) (Dedysh, 2019; Kulichevskaya et al., 2010), a common moss in the study lake. Due to high richness and diversity, this section will discuss those with potential roles in oil spill remediation. However acknowledging that other microorganisms may support hydrocarbon degraders, through nitrogen or oxygen production (Radice et al., 2023) for example, and a diverse consortia is important for co-metabolism of complex, or a mixture of, PACs (Cao et al., 2009; Ghosal et al., 2016; Lee et al., 2015; Zhu et al., 2001).

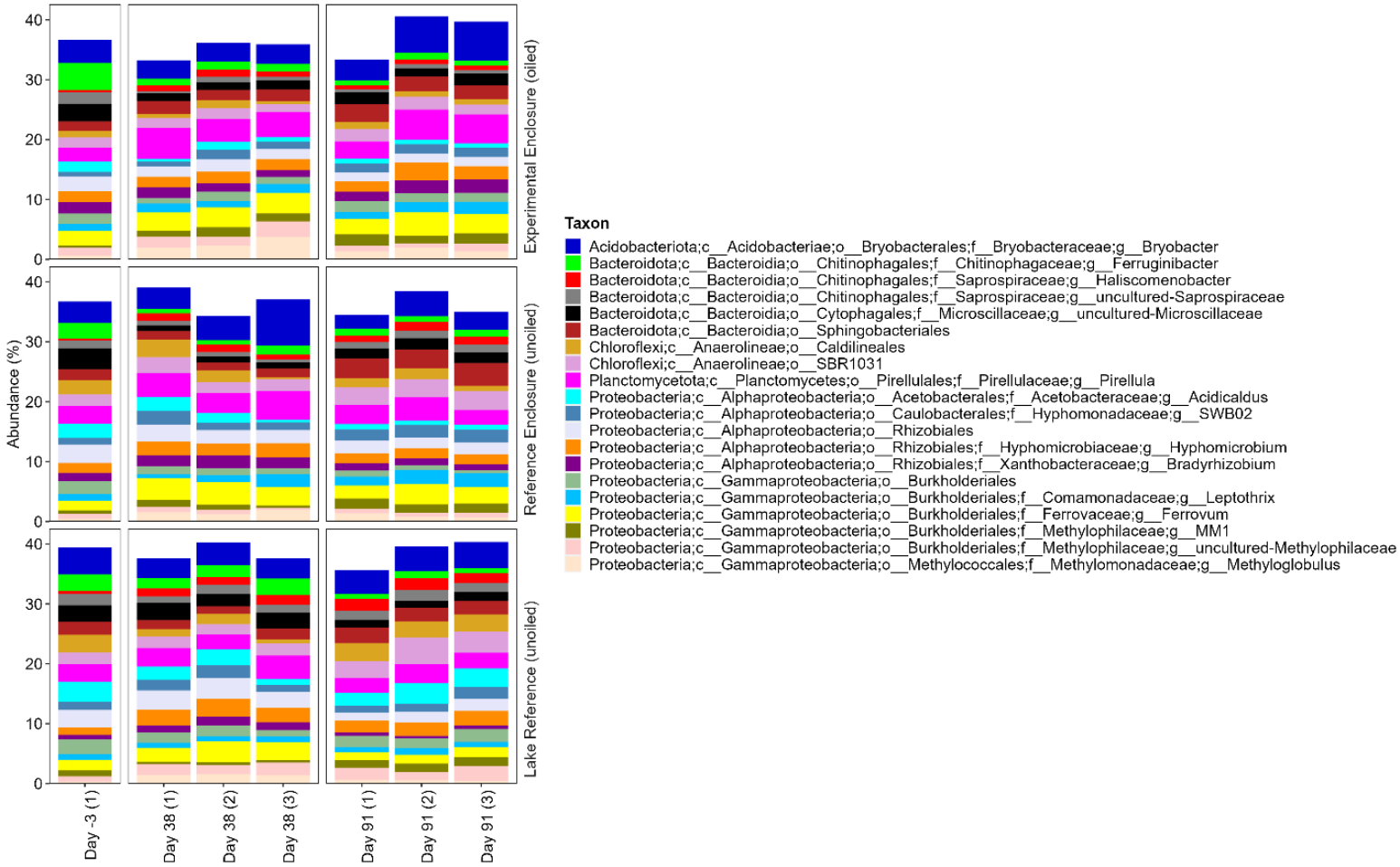

Figure 3.4. Taxonomic profile of the top twenty most relatively abundant 16S ASVs in EFW root biofilm replicates from the EE, RE, and LR 3 days pre-oil addition, and on days 38 and 91 post-oil addition during the 2019 dilbit experiment. Taxon legend includes full taxonomic details to the lowest level identified as available.

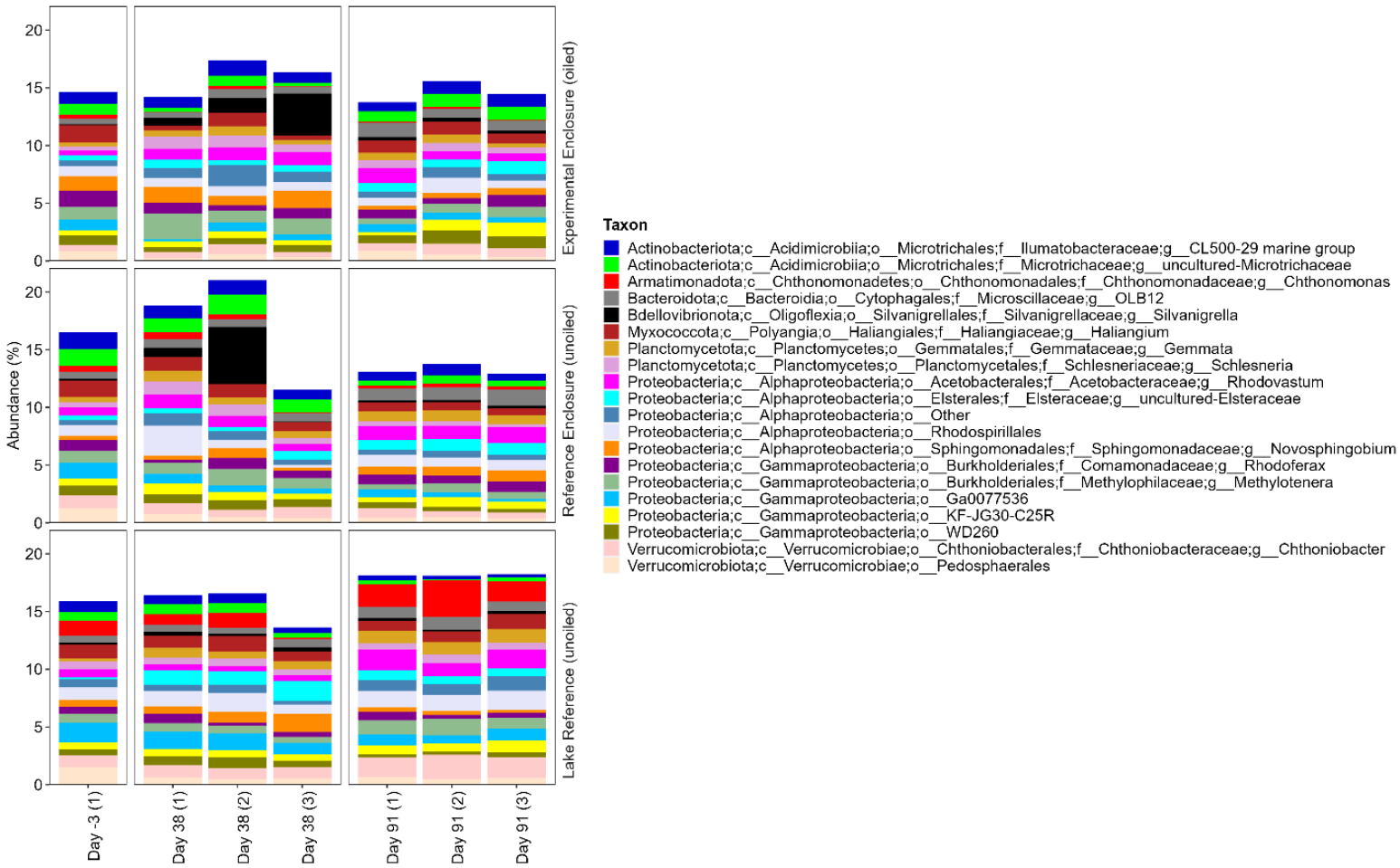

Figure 3.5. Taxonomic profile of the top twenty-one to forty most relatively abundant 16S ASVs in EFW root biofilm replicates from the EE, RE, and LR 3 days pre-oil addition, and on days 38 and 91 post-oil addition during the 2019 dilbit experiment. Taxon legend includes full taxonomic details to the lowest level identified as available.

Three genera belong to order *Rhizobiales*, microorganisms in symbiosis with plants, known for their ability to assist in nitrogen fixation (Fahde et al., 2023; Garrido-Oter et al., 2018; Newton et al., 2011) and plant growth promotion, and can enhance phosphate solubility and accessibility (Fahde et al., 2023). Some have been reported to express various monooxygenase genes for degrading hydrocarbons and the desulfurization of hydrocarbons (e.g., dibenzothiophene) (Abbasian et al., 2016), and various species are known hydrocarbon degraders (Prince et al., 2018). *Bradyrhizobium*, previously found in co-occurrence with hydrocarbon degraders and involved in degradation (Yang et al., 2016), had variable abundance over the exposure period and between sites, peaking in the EE on day 91 (1.55-2.20%), and on day 38 in the RE (1.84-2.11%) and LR (1.24-1.46%). Similarly, *Hyphomicrobium*, found in a consortia capable of degrading aromatic hydrocarbons (*H. facile*, strain Y3; Ozaki et al., 2006), peaked on day 91 in the EE (1.70-2.99%) and on day 38 in the RE (1.96-2.36%) and LR (2.38-2.99%). *Bradyrhizobium* and *Hyphomicrobium* belong to families *Xanthobacteraceae* and *Hyphomicrobiaceae*, known to include hydrocarbon degraders and were detected in salt marsh sediments following the Deepwater Horizon oil spill (Beazley et al., 2012).

Pirellula are aerobic, heterotrophic bacteria, known for their role in biogeochemical processes. Some strains have P450 monooxygenases and epoxide hydrolase for detoxifying pollutants (Glöckner et al., 2003), and while not specific to oil, the expression of these enzymes may have important roles in ring cleavage. *Pirellula* increased in all sites on day 38 (2.47-5.23%), highest in the EE.

Two ASVs belong to *Chloroflexi*, anaerobic bacteria that can degrade petroleum hydrocarbons (Cébron et al., 2022), that have been found in high abundance under oil contamination (Abed et al., 2014; Aburto-Medina et al., 2012; Brown et al., 2013; Cébron et al.,

2022; Peng et al., 2015) and salt marsh sediments following the Deepwater Horizon spill, including class *Anaerolineae* (Engel et al., 2017). ASVs of the order *Caldilineales* had variable abundance among all sites, highest on day 38 in the experimental (0.43-1.34%) and reference (0.29-2.88%) enclosures, and on day 91 in the LR (2.75-3.03%). Presence of the order SBR1031 increased over the exposure period in all three sites, ranging from 1.64-2.16%, 2.91-3.18%, and 2.85-4.35% in the EE, RE, and LR, respectively.

Seven genera from order *Burkholderiales* were in the top forty most abundant prokaryotes. *Burkholderiales* are commonly found in the environment, and some have significant potential for PAC biodegradation (Pérez-Pantoja et al., 2012; Prince et al., 2018). For example, enrichment of *Methylotenera*, a methylotrophic bacterium, has been detected in oil and petroleum contaminated water and is suggested to be a hydrocarbon degrader (Idomeh et al., 2021; Thompson et al., 2017). *Methylotenera*'s abundance was highest in the EE on day 38 (1.06-2.23%). Other methylotrophic *Burkholderiales* included MM1 and an uncultured genus from family *Methylophilaceae. Ferrovum* increased over the exposure period in the EE to a range of 2.56-3.95% on day 91, while RAs were variable in the reference sites, highest on day 38. *Leptothrix*, a noted phenanthrene degrader (Bodour et al., 2003) and *Rhodoferax*, belong to family *Comamonadaceae*, which can express aromatic oxygenase-encoding genes (Pérez-Pantoja et al., 2012), and include hydrocarbon degrading species (Beazley et al., 2012). *Leptothrix* slightly increased in the enclosures over the exposure period, ranging from 1.13-2.01% and 1.49-2.32% on day 91 in the EE and RE, respectively. RA was lower in the LR, highest on day 91 (0.84-1.11%). *Rhodoferax* was variable over time and between sites, highest on day -3 in the EE at 1.42% RA, however days 38 and 91 appeared relatively similar.

Xiao et al. (2013) studied microbial communities in production wells in the Chaoyanggou oil reservoir and found dominance of family *Comamonadaceae* in oil production wells, and family *Hyphomonadaceae*, among others, in formation water from production wells. *Hyphomonadaceae* has previously been correlated with the biodegradation of chemically dispersed Troll and Grane oils at cool temperatures (Ribicic et al., 2018). We observed SWB02 (family *Hyphomonadaceae*) increase in all sites from day -3 to 38, ranging from 0.80-1.58%, 1.25-2.28%, and 1.12-2.12% in the EE, RE, and LR, respectively.

Another methanotroph, *Methyloglobulus* known to degrade methane (Deutzmann et al., 2014), a potential by-product of oil biodegradation (Lee et al., 2015) and/or a potentially major hydrocarbon during spills (King et al., 2015), peaked in all sites on day 38. RA increased from 0.66% on day -3 to 1.99-3.73% on day 38 in the EE, declining to 1.40-1.97% on day 91. While RA ranged from 1.22-1.92% and 1.38-1.55% in the RE and LR on day 38, respectively.

Another well-known PAC degrader is *Novosphingobium,* a metabolically versatile sphingomonad often found in the rhizosphere (Chettri & Singh, 2019; Ghosal et al., 2016; Kertesz & Kawasaki, 2010; Lyu et al., 2014; Rojo, 2021; Sohn et al., 2004; Yang et al., 2016), capable of degrading a suite of PACs (Sohn et al., 2004). *Novosphingobium* was detected in all samples, peaking on day 38, ranging from 0.78-1.53 %, 0.26-0.85 %, and 0.66-1.56% in the EE, RE, and LR, respectively.

An ASV from order *Sphingobacteriales* increased over time in the enclosures, ranging from 2.27-3.00% and 3.15-3.80% in the EE and RE on day 91, respectively, while being more variable in the LR. *Sphingobacteriales* are known to include hydrocarbon degrading species (Beazley et al., 2012; Prince et al., 2018), identified in high abundance under oil contamination (Y. Wang et al., 2021), and some have been identified as late responders to oil contamination

(Franchi et al., 2022; Koo et al., 2015). Family *Flexibacteraceae* from order *Sphingobacteriales* increased in a salt marsh following the Deepwater Horizon spill, as well as families from order *Rhodospirillales* (Beazley et al., 2012), which include genera capable of degrading alkanes, aromatics, and PACs (Prince et al., 2018, and citations within). An ASV from order *Rhodospirillales* peaked on day 91 in the EE (0.68-1.34%) and LR (1.36-1.66%), and on day 38 in the RE (0.26-2.58%).

Other potential hydrocarbon degraders from phylum *Bacteroidota* include *Haliscomenobacter* (Aburto-Medina et al., 2012), and an uncultured *Saprospiraceae* (Taylor et al., 2021), which was a dominant organism after the wells were shut during the Deepwater Horizon spill (Dubinsky et al., 2013), possibly consuming complex carbon sources (McIlroy & Nielsen, 2014). *Haliscomenobacter* increased over time in the reference sites, reaching 1.10-1.56% and 1.67-1.99% in the RE and LR on day 91, respectively, and the EE peaked on day 38 (0.85-1.20%). However, the uncultured *Saprospiraceae* declined in the EE (<1% on days 38 and 91), was variable in the RE (0.46-1.30%), and remained stable in the LR over time (1.00-1.89%).

3.3.2.2.2 Eukaryotes. Eukaryotic phyla were more variable in dominance between sites and over the experimental period than the prokaryotic community, with dominance by *Ciliophora* (16.5-63.9 %), *Diatomea* (3.75-36.6 %), *Charophyta* (0.00-29.4 %), *Cercozoa* (1.96-18.8 %), *Dinoflagellata* (0.91-9.87 %), *Chytridiomycota* (1.85-9.11 %), unidentified phyla (2.48-12.3%), and others, out of 35 phyla identified (Figure A11). *Ciliophora* were dominant on day -3 and on day 91, but slightly decreased in mean RA on day 38 in all sites. While on day 38, other phyla increased, such as *Diatomea* in the LR, and *Charophyta, Dinoflagellata, Cercozoa,* and others in the enclosures.

The top twenty eukaryotic ASVs represented approximately 40-75% of the community and displayed an uneven distribution with some dominant ASVs (Figure 3.6).The RA explained by the top twenty declined in the enclosure sites on day 38, suggesting others may be selected for upon application to the enclosures, as observed in the top 21-40 eukaryotic ASVs (Figure 3.7). The following section will focus on organisms with potential roles in oil spill remediation.

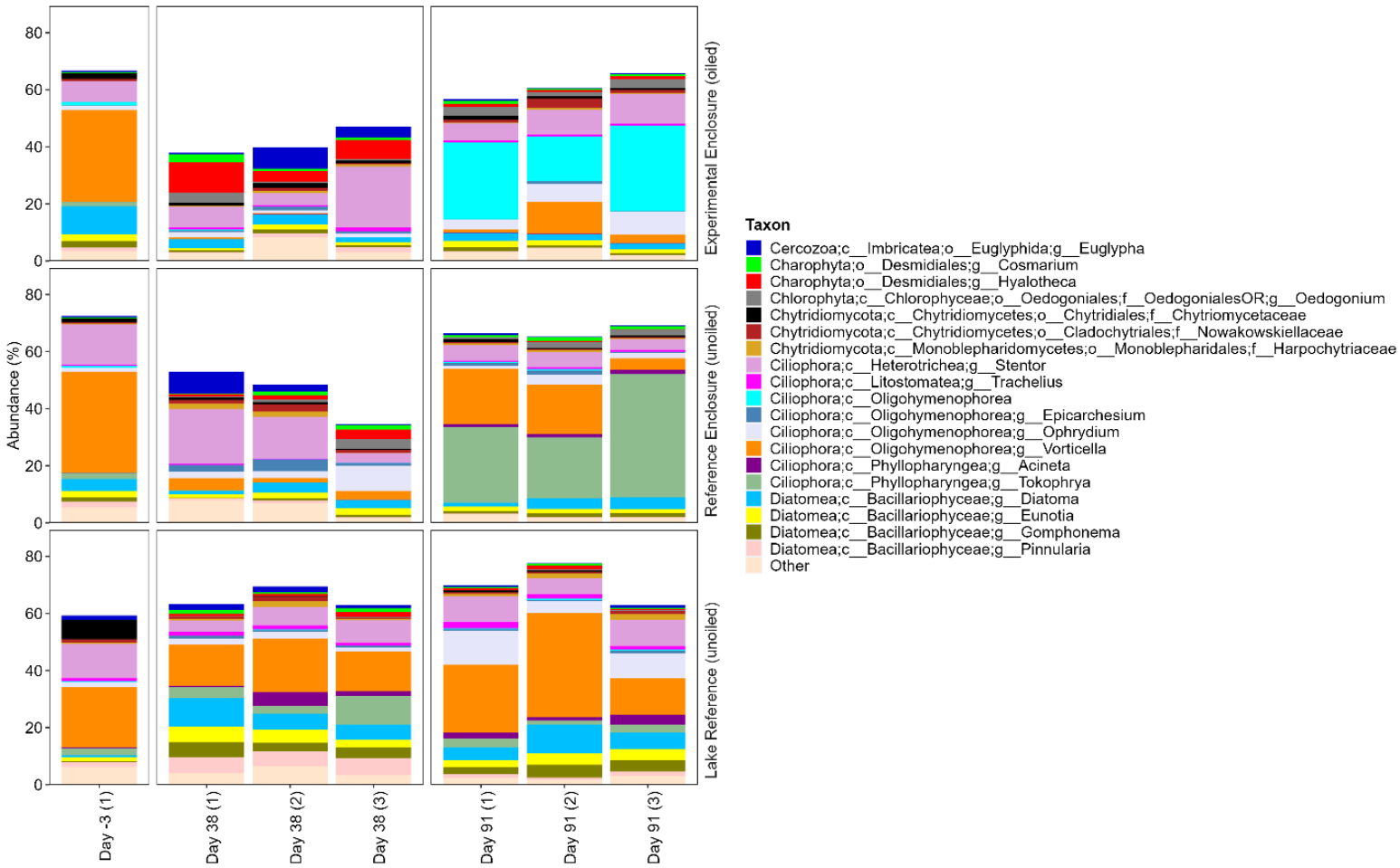

Figure 3.6. Taxonomic profile of the top twenty most relatively abundant 18S ASVs in EFW root biofilm replicates from the EE, RE, and LR 3 days pre-oil addition, and on days 38 and 91 post-oil addition during the 2019 dilbit experiment. Taxon legend includes full taxonomic details to the lowest level identified as available.

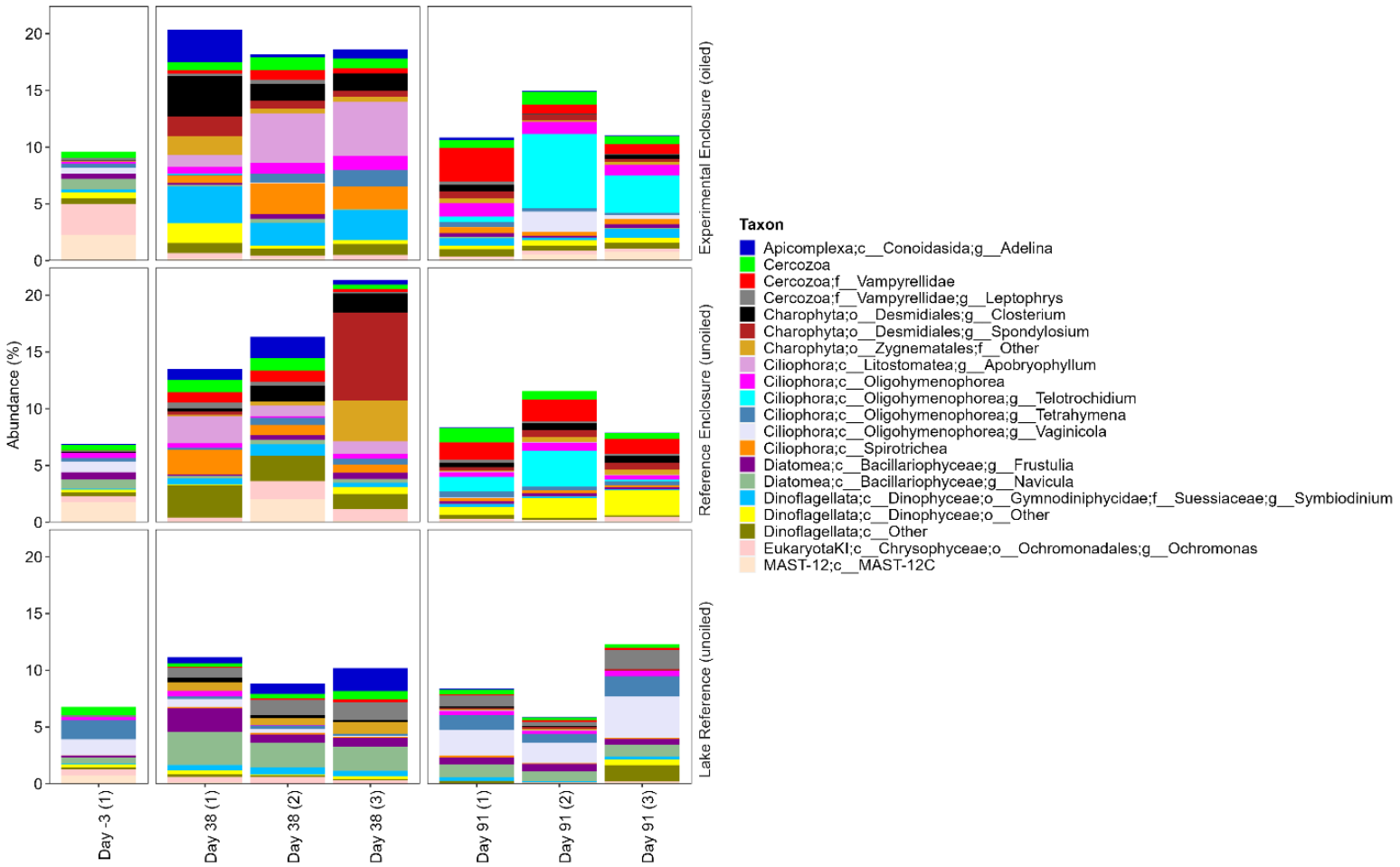

Figure 3.7. Taxonomic profile of the top twenty-one to forty most relatively abundant 18S ASVs in EFW root biofilm replicates from the EE, RE, and LR 3 days pre-oil addition, and on days 38 and 91 post-oil addition during the 2019 dilbit experiment. Taxon legend includes full taxonomic details to the lowest level identified as available.

Some fungi are known hydrocarbon degraders due to their range of substrate specificity and enzyme production (e.g., peroxidases, laccases, monooxygenases) (Haritash & Kaushik, 2009; Kadri et al., 2017). Three unidentified ASVs belonging to phylum *Chytridiomycota* were identified in the top 20 eukaryotic ASVs. *Chytridiomycota*, often referred to as zoosporic fungi are mostly found in aquatic ecosystems (Jobard et al., 2010; Naranjo-Ortiz & Gabaldón, 2019; Prince, 2018), and some are potential aromatic hydrocarbon degraders (Prince, 2018). For example, *Phlyctochytrium reinboldtae* were able to produce some metabolites of naphthalene, though mostly in small trace amounts (Cerniglia et al., 1978). Family *Chytriomycetaceae* were variable in RA among sites and time periods, but highest in the LR on day -3 (6.66%). Family *Nowakowskiellaceae* was also variable over the exposure period in reference locations, however increased in the EE, from 0.75% to 0.92-3.18% on day -3 and 91, respectively. Family *Harpochytriaceae* had low RA in the EE (<1.0%), peaking on day 38 in the RE (0.21-1.80%), while was variable for LR samples, ranging from 0.38-2.08% and 0.96-2.02% on days 38 and 91, respectively.

Algae are essential organisms involved in ecosystem productivity and function, and some are capable of metabolizing PACs (Ghosal et al., 2016; Prince, 2018). The top 40 ASVs had algal representatives from phylas *Chlorophyta, Diatomea, Charophyta,* and *Dinoflagellata. Oedogonium,* a filamentous green algae, had the highest RA on day 38 in the enclosures, increasing from 0.13% to 0.61-3.68% in the EE, and from 0.12% to 0.22-3.36% in the RE, while the LR had <0.5% RA on days 38 and 91. *Oedogonium* has been observed to tolerate vegetable oil spills and has affinity for low oxygen and nutrient rich conditions (Selala et al., 2014), while others found they were unable to adapt to crude oil presence (Oberholster et al., 2014). It has also been targeted for wastewater bioremediation and biofuel production (Adesalu et al., 2016 and

citations within). Another green algae ASV from order *Zygnematales* increased on day 38 in all sites, highest in the RE. RAs ranged from 0.41-1.64%, 0.13-3.61%, and 0.61-1.05% in the EE, RE, and LR, respectively. *Ochromonas*, a chrysophyte algae, was highest on day -3 in the EE (2.76%) and on day 38 in the RE (0.33-1.57%), while had low RA (<1%) in all other sample periods and sites.

There was a clear shift in diatom and desmid abundance between the enclosures and LR, which may result from differing site conditions. Desmid algae increased on day 38, often higher in the EE, while diatoms were often higher in the LR, similar to findings in Kamalanathan et al. (2021). Bruno et al. (1982) found periphyton communities from South Carolina streams dominated by desmid algae had greater uptake of benzo[a]pyrene than those dominated by diatoms, noting desmid cell structure and features (e.g., sheath) may be important for cellular sorption. Desmid *Hyalotheca* increased from 0.06% to 3.77-10.5% in the EE on day 38, while RAs ranged from 0.95-3.41% and 0.75-1.80% in the RE and LR, respectively. Similarly, *Cosmarium* and *Closterium* were highest in the EE on day 38. *Closterium* sp. has previously been studied for degradation of Bonny light crude oil under different light regimes. It was observed that degradation was greater without light, when oil was the only source of carbon (Uzoh et al., 2015). *Spondylosium* increased on day 38 only in the enclosures from 0.00% on day -3 to 0.55-1.73% and 0.00-7.75% in the EE and RE, respectively. *Diatoma* had the largest RA of all diatoms (0.76-10.0%), highest in the LR on day 91, while RA generally declined in the enclosures over the exposure period. Other diatoms peaked in the LR on day 38, including *Eunotia* (2.62-5.50%), *Gomphonema* (2.92-5.31%), *Pinnularia* (5.23-5.86%), *Frustulia* (0.75-2.10%), and *Navicula* (2.13-2.90%), while RA in the enclosures were variable or generally declined over the exposure period. While RA was higher in the LR, some diatoms have been

associated with oil or hydrocarbons. For example, Cerniglia et al. (1982) confirmed *Navicula* sp. could oxidize naphthalene to 1-naphthol at cool temperatures, while others observed temporal shifts to diatom assemblages (*Eunotia, Gomphonema,* and *Pinnularia*) after a vegetable and diesel oil spill in the Negro River, Brazil, based on diatom ecological guild (motile, erect, planktonic, and colonial) (De Faria et al., 2019). The variability of diatoms in our study may be the response of ecological guilds to environmental conditions or disturbance over the experimental period.

Dinoflagellates are common planktonic organisms found in aquatic environments, and include both autotrophic and heterotrophic organisms. Some (e.g., *Symbiodinium pilosum*) are endosymbionts (Levy et al., 2007), and some have been found to tolerate or flourish during oil spill events or experiments (Kamalanathan et al., 2021). *Symbiodinium* and two unidentified dinoflagellates were identified in the top 40 ASVs. *Symbiodinium* had low RA (<1%) excluding samples from the EE on day 38 (2.02-3.26%). One of the unidentified dinoflagellates had low RA (<1%) except day 38 in the EE (0.26-1.74%) and day 91 in the RE (0.70-2.23%). Similarly the other unidentified dinoflagellate had low RA(<1%) except on day 38 in the RE (1.37-2.83%) and on day 91 in the LR (0.04-1.45%). Some researchers found that dinoflagellates can be enhanced by the presence of oil degrading bacteria and growth promoting capabilities (Park et al., 2020), and others found that some marine species can ingest oil droplets under varying conditions (with or without food/chemical dispersants) (Almeda et al., 2014). Research by Almeda et al. (2018) found that oil and chemical dispersants disrupt the grazing pressure by heterotrophic dinoflagellates and ciliates, which allow for more tolerant, bloom forming dinoflagellates to flourish.

Similarly, some ciliates are natural predators to microorganisms and are ubiquitous in freshwater environments (Esteban et al., 2015; Lara et al., 2007; C. V. Robinson et al., 2022), however have also been studied for hydrocarbon degradation potential and tolerance to toxicity. Kachieng'a and Momba (2018, 2017) measured successful co-metabolism of petroleum hydrocarbons with a ciliate consortia, however Prince (2018) questioned whether it was biodegradation by the protozoans or by synergistic bacteria. Others have observed that ciliate grazing can result in bioaccumulation of oil (Rogerson and Berger, 1981) and can enhance bacterial biodegradation (Tso & Taghon, 2006), and their movement may result in oil dispersion in the water column, which could facilitate biodegradation (Gilbert et al., 2014). In fact, Holubar et al. (2000) found that presence of protozoan ciliates enhanced chemical oxygen demand degradation in petroleum contaminated sewage sludge treatment. Some researchers observed correlation between ciliate richness and high molecular weight PAHs (Moss et al., 2015), while others have found sensitivity to crude oil and dispersants (Almeda et al., 2018), indicating variable species tolerance to environmental conditions and pollutants (Jousset et al., 2010; Lara & Acosta-Mercado, 2012; C. V. Robinson et al., 2022).

There were fourteen ciliate genera in the top 40 ASVs that varied in dominance between sites and over time. *Vorticella* dominated the community on day -3 (21.2-35.2%), however declined on day 38 in the enclosures (0.00-4.23%) while remaining dominant in the LR (14.0-18.9%), later increasing in all three sites (1.22-36.5%). There were other dominant ciliates that had variable RA over the exposure period or between sites and replicates, such as *Stentor* (3.27-21.4%) and *Ophrydium* (1.04-11.9%), while some were site specific. *Tokophrya* was highest in the RE on day 91(21.3-43.3%), while was much lower in the EE (0.00%) and LR (1.49-3.21%). An unidentified ASV from class *Oligohymenophorea* increased drastically on day 91 in the EE,

from 1.11% on day -3 to 15.7-30.0%, while the RE and LR were <1%. Palace et al. (2021) previously identified unique operational taxonomic units of *Oligohymenophorea* in water of oil treated sites compared to unoiled sites in a shoreline enclosure study at the IISD-ELA. While research by Lara et al. (2007) found greater presence of *Oligohymenophorea* in non-polluted soil compared to PAH polluted soil. *Telotrochidium* increased from 0.00% on day -3 to 0.51-6.54% and 0.15-3.16% RA on day 91 in the EE and RE, respectively. While none were detected in the LR. *Apobryophyllum* increased from 0.00% to 1.08-4.77% and 0.96-2.38% in the EE and RE on day 38, respectively, and an unknown ASV from class *Spirotrichea* increased from 0.00% to 0.64-2.73% and 0.70-2.17%, respectively. *Aprobryophullum* belongs to class *Litostomatea*, which was previously identified as a dominant representative in an oil sand tailing reclamation site, and has been hypothesized to include species that have a high tolerance to hydrocarbon contamination (Richardson et al., 2020). *Vagnicola* had lower ciliate RA, but increased in the LR on day 91. RA ranged from 0.03-1.80%, 0.00-0.06%, and 1.79-3.66% in the EE, RE, and LR on day 91, respectively. While shifts in our study cannot be attributed to oil, the dominance of ciliates may play a role in biodegradation (directly or by enhancing bacterial biodegradation), and/or other important biogeochemical processes.

Cercozoa, another group of bacterial grazers (Esteban et al., 2015), were in the top 40 ASVs, which similarly have had variable responses to oil. Dalby and Kormas (2008) identified *Cercozoa* as the dominant organism in chronically polluted seawater, but not in oligotrophic or crude oil contaminated microcosms. While Cobanli et al. (2022) found that Novel Clade 2 of Cercozoa increased between day 6 and 10 following dilbit additions to seawater microorganisms during the spring, but not the summer. ASV from family Vampyrellidae increased in the enclosures on day 91, from 0.78-2.96% and 1.34-1.92% in the EE and RE, respectively, and was

<1% in the LR. While *Leptophrys* was highest in the LR on days 38 (0.86-1.55%) and 91 (0.32-1.67%), and were <1% in the enclosures. *Euglypha* increased in all sites on day 38, ranging from 0.58-7.44%, 0.36-7.67%, and 1.15-2.08%, in the EE, RE, and LR, respectively, while remaining samples were <1%, excluding day -3 in the LR (1.51%).

3.4 Conclusions

A model oil spill of diluted bitumen was conducted in a wetland shoreline enclosure on Lake 260 at the IISD-ELA in order to assess how microbial communities change on EFW roots to identify potential as a secondary remediation method following primary shoreline washing. There were greater shifts in diversity of eukaryotes on EFW roots than prokaryotes, but it was difficult to confirm if microbial community changes were attributed to oil exposure, enclosure effects, or seasonal change. However, organisms capable of degrading hydrocarbons or PACs, and those known to support degradation, were identified in this study, and some of these increased in the EE after oil addition.

While microbial results were inconclusive, PACs in the aqueous environment returned to nearing background conditions after ~60 days, and fluctuations were linked to environmental conditions, further supporting the need to test efficiency of remediation efforts in the natural environment. It is possible the PACs were adsorbed to the sediment, underwent biodegradation, or further weathering processes. Sediment PACs were highly influenced by pyrogenic sources, however they increased in the EE after oil addition until day 91, later declining on day 249, where total PACs were similar among oiled and reference sites. This may suggest that aquatic and benthic environments were no longer toxic to interacting biota, however, we noted there was high sediment concentration variability based on sample location.

Chapter 4. Floating Wetland Root Microbial Community Responses to Exposure of a Conventional Heavy Crude Oil Spill in a Freshwater Shoreline

4.1 Introduction

Crude oil is a non-renewable energy source that is extracted and transported around the world by pipelines, trains, trucks, and tanker ships (Crosby et al., 2013; Lee et al., 2015), and although transport technology has advanced (Oliver Wyman, 2019), spills still do occur, and any transport puts nearby ecosystems at risk for accidental release events (Chang et al., 2014; Lee et al., 2015). While oil is naturally occurring, it can cause acute and chronic toxicity to interacting organisms when released at high volumes. Out of the thousands of compounds that can make up crude oil, polycyclic aromatic compounds (PACs) are often of concern due to their toxic, mutagenic, and carcinogenic properties (Cao et al., 2009; Dupuis & Ucan-Marin, 2015; Ghosal et al., 2016; Haritash & Kaushik, 2009; Honda & Suzuki, 2020; Lee et al., 2015; Zhu et al., 2001). PACs often make up a low percent of oil composition, however can range anywhere between 0-60% depending on the product (Fingas, 2015). For example, polycyclic aromatic hydrocarbons made up < 1% of total petroleum hydrocarbons in water, sediment, and biota samples from the Gulf of Mexico following the Macondo crude oil spill in 2010 (Sammarco et al., 2013). PACs are compounds with two or more fused benzene rings, and range in structural complexity and recalcitrance from naphthalene in its simplest form, to more complex structures, like benzo[a]pyrene. The content of PACs and other compounds varies by oil product and their fate and degradation in the environment depends on site and environmental conditions, weather patterns, and local response capacity (Dupuis & Ucan-Marin, 2015; Lee et al., 2015; Raju & Scalvenzi, 2018; Zhu et al., 2001).

After a spill, the typical response is to clean as much oil as possible through deploying mechanical and chemical recovery techniques. Unfortunately some mechanical efforts can cause significant damage to sensitive environments, like freshwater shorelines or wetlands (Lee et al., 2015; Zhu et al., 2001), and leave residual oil in the environment (Das & Chandran, 2011; Etkin & Tebeau, 2003; Lee et al., 2015; Zhu et al., 2001). In addition, some chemical applications can cause dispersion of oil into the water column, increasing exposure to biota (Lee et al., 2015; Zhu et al., 2001). It is sometimes recommended that sensitive environments be left to natural biodegradation processes (Beazley et al., 2012), referred to as monitored natural recovery, where microorganisms metabolize carbon compounds in oil for energy and growth, eventually producing non-harmful by-products (Lee et al., 2015; Magar et al., 2009; Zhu et al., 2001). This process can often be time consuming, but can be enhanced by human intervention through biostimulation or bioaugmentation (Das & Chandran, 2011; Haritash & Kaushik, 2009; Lee et al., 2015; Raju & Scalvenzi, 2018; Zhu et al., 2001).

An alternative is through the addition of vegetation on floating wetlands to stimulate microbial development on plant roots and enhance contaminant interaction and degradation. Floating wetlands are platforms of vegetation that have a dense rhizosphere that are suspended in the water column, and can be deployed in varying depths of water (Shahid et al., 2018; Tanner & Headley, 2011). The use of floating wetlands for successful oil or hydrocarbon remediation has been studied in microcosms, mesocosms, and water stabilization pits, summarized in Chapter 2, and our previous research has explored their use in model diluted bitumen (dilbit) spills in freshwater shoreline enclosures at the International Institute for Sustainable Development Experimental Lakes Area (IISD-ELA) in northwestern Ontario, Canada (Chapter 3).

The objectives of this chapter were to explore changes to the root microbial community on engineered floating wetlands (EFWs) exposed to a modelled conventional heavy crude oil (CHV) spill in order to assess potential of EFWs as a non-invasive, secondary remediation option in freshwater environments. As well as to monitor changes to PAC chemistry in the water and sediment of the oiled and unoiled reference sites. I hypothesized that the rhizosphere microbial community would shift in the presence of oil to microorganisms known to consume and degrade hydrocarbon compounds. Oil products have different chemical and physical characteristics, and such their fate and behaviour in the environment are unique to each spill (Dupuis & Ucan-Marin, 2015; Lee et al., 2015; Zhu et al., 2001). This research allows us to assess EFW microbial community response to different oil products in continental climates that experience fluctuating temperatures, a research need highlighted in Chapter 2.

4.2 Methods

4.2.1 Research Design and Site Description

Modelled CHV spills were conducted in shoreline enclosures on Lake 260 (volume= 1,975,969 m^3, surface area= 332,460 m^2, max depth= 15.64 m; IISD-ELA, 2022), a boreal lake at the IISD-ELA in 2021. Shoreline enclosures included a floating collar (5 m wide x ~6 m long) attached to a polypropylene curtain (Curry Industries Ltd., Winnipeg), sealed to the sediment and five meters onto shore with a double layer of sandbags. FLOWTER sites included an experimental enclosure (oiled; EE), a reference enclosure (unoiled; RE), and a lake reference site (unoiled; LR) (Figure B1), noting there was no site replication. A tritium radioisotope was applied in each enclosure to model exchange rates and to estimate initial volume of the EE (23,447 L) and RE (29,801 L).

4.2.1.1 Oil Application and Recovery. Conventional heavy (CHV) crude oil, sourced from pipeline stocks provided by the Canadian Association of Petroleum Producers, was weathered for 36 hours in a steel weathering pan on 220 L of lake water from May 31 to June 2, 2021. Weathering oil prior to application in the enclosures simulated oil that would typically reach a shoreline environment, described in Palace et al. (2021). Weathering results in chemical and physical changes to oil due to evaporative loss of lighter molecular weight compounds (e.g., BTEX), photooxidation, spreading, dissolution, etc., and is influenced by oil product and environmental conditions (e.g., sunlight and temperature) (Lee et al., 2015). The oil from the weathering pan was collected into glass jars and refrigerated (4 ℃) until application on June 25, 2021, where the oil was poured along the 5 m wide nearshore environment (within 50 cm from shore) of the EE (1,600 g). Four days following application on June 29, 2021, primary recovery of oil from the EE was performed using shoreline washing. This included pumping enclosure water (1,600 L) for twelve minutes over the shore to rinse free oil onto the water's surface so that it could be collected with polypropylene sorbent media (Spill Ninja, MEP Brothers, Winnipeg). A total of 166.3 g of CHV was removed (10%) and leaving 1,433.7 g (~ 90 %) of oil. The residual oil was treated with secondary remediation of an EFW located in the middle to far shore environment of the enclosures on July 1, 2021. The RE also received shoreline washing on June 29, 2021. Contingency measures and personal protective equipment were in place as described in Chapter 3.

4.2.1.2 Engineered Floating Wetlands. EFWs ($\bar{x}$ = 1.26 m^2; 14 holes of 10.16 cm diameter) were BioHaven Floating Islands (polyethylene terephthalate matrix coated in polyurea for protection; Floating Islands International, n.d.) sourced and produced by Martin Ecosystems (Louisiana, United States), under license by Floating Islands International (Montana, United

States), as described in Chapter 3. The EFWs were established in Lake 260 in August 2019 with Gold Label coconut mulch, wetland sediment, and emergent wetland plants; *Typha* sp. (cattail), *Carex utriculata* (common beaked sedge), and *C. lasiocarpa* (wiregrass sedge), and retransplanted on June 12, 2021, to replace plants that did not survive overwinter. Vegetation was planted in densities to reflect those at Lake 260 wetland, including one *Typha* sp., three *C. utriculata*, and ten *C. lasiocarpa* per transplant hole. As discussed in Chapter 3, identification of *Carex* is difficult due to the high number of species worldwide (Naczi, 1992, as cited in Starr et al., 2009).

EFW vegetation were measured monthly for number of live plants by species, and plant heights (mean and max; mm) were recorded for individual cattails and for clusters of sedges. Heights were recorded with a meter stick, carefully stretching the plant or cluster of plants to measure its tallest leaf. Results are included in Appendix B.2.

4.2.2 Polycyclic Aromatic Compound Chemistry

4.2.2.1 Water. Water was collected 3 days pre-oil addition and on days 1, 3, 4, 8, 9, 10, 14, 22, 37, and 73 post-oil addition for total polycyclic aromatic compound (PAC) chemistry. Total PACs (n = 44; Table B1) included 16 US Environmental Protection Agency (2014) priority parent PACs and 28 alkylated PACs (aPACs) and heterocyclic PACs (parent and alkylated dibenzothiophene), and will be further referred to as aPACs. Methods for PAC extraction differed from the 2019 dilbit model spill (Chapter 3) due to restrictions of the COVID-19 pandemic. One litre of water was collected in baked amber bottles from the far shore environment using a peristaltic pump and Teflon tubing, and vacuum filtered at the IISD-ELA laboratory within 4 hours of collection (1.2 μm, Whatman GF/C filter). Eight hundred (800) mL of filtrate was transferred back into the sample bottle and spiked with 20 μL (5 ng/μL) recovery

internal standard (RIS; suite of d8-naphthalene, d8-acenaphthylene, d10-acenaphthene, d10-fluorene, d10-phenanthrene, d10-pyrene, d12-Benz(a)anthracene, d12-chrysene, d12-benzo(b)fluoranthene, d12-benzo(k)fluoranthene, d12-benzo(a)pyrene, d12-indeno(1,2,3-c,d)pyrene, d14-dibenzo(a,h)anthracene, and d14-benzo(g,h,i)perylene). Ten (10) ± 0.1 g of sodium chloride (NaCl) was dissolved in the sample before 150 mL of dichloromethane (DCM) was added for PAC extraction, then placed on a rolling table (Bellco Biotechnology Digital Cell Production Roller Apparatus, Bellco Glass Inc, Vineland, N.J., USA; Cat No. 7621-20115; speed 6.8) for 16 hours of liquid-liquid extraction. The water sample and DCM were transferred into a separatory funnel and the sample bottle was rinsed twice with 20 mL DCM which was added to the separatory funnel. DCM extract was collected into a 250 mL amber jar with a Teflon lid and refrigerated (4 °C) until transported to the Centre for Oil and Gas Research (COGRAD) laboratory at the University of Manitoba, Winnipeg, Manitoba, for further extraction and analysis as described in detail in Guttormson (*in preparation*). Briefly, the sample was transferred into a GeneVac flask, and the sample bottle was rinsed twice with 5 mL Optima ™ hexane and added into the flask. The sample was reduced and solvent exchanged into hexane using the GeneVac Rocket Centrifugal Evaporator (SP Scientific Warminster, PA, USA). Each sample received 1 g of sodium sulphate (Na_2SO_4) to remove any remaining water and the hexane was transferred into a test tube. The flask of sodium sulphate was rinsed twice with 2 mL Optima ™ hexane and added to the test tube. The hexane was then reduced to 1 mL using a nitrogen gas evaporator (N-EVAP™111, Organomation Associates Inc., MA, USA and OA-SYS Heating System). Each sample was spiked with 20 µL of 5 ng/µL instrument performance internal standard (IPIS; d10-anthracene), transferred to an amber GC vial, and refrigerated until GC-MS/MS analyses (Guttormson, *in preparation*).

A field blank was collected during each sampling effort by opening an amber bottle containing 200 mL Optima ™ water during the entire sample collection period. The field blank was extracted in the same process as described above however only 40 mL of DCM was added to the filtrate for extraction.

PACs were detected and quantified using an Agilent 7890 gas chromatograph coupled to a 7000C triple quadrupole mass spectrometer (GC-MS/MS) fitted with an electron ionization source, following methods and conditions outlined in Idowu et al. (2018). Final concentrations were corrected for RIS, IPIS, and field blanks by Dr. Lisa Peters.

Water was also monitored weekly for basic water quality and biweekly for nutrient chemistry. Methods and results are described in Appendix B- Sections B.4 and B.5.

4.2.2.2 Sediment. Using a sediment corer and extruder, the top 5 cm of sediment was collected at three random locations at each site (n=3) 2 days pre-oil addition, and on days 12, 38, and 70 post-oil addition. Collected sediment was placed into 125 mL amber jars, and refrigerated overnight to settle. Once settled, overlying water was removed prior to freezing at -20℃. Sediment PAC extraction occurred at the COGRAD laboratory following accelerated solvent extraction methods described in Xia et al. (2021), and were quantified on GC-MS/MS as described above, following methods in Idowu et al. (2018).

4.2.3 Root Microbial Community

Root biofilm microbial samples were collected from three random locations on each EFW (n=3) 11 days pre-oil addition, and on days 33 and 84 post-oil addition. Roots were collected with sterilized clippers, transferred into a sterile Whirl-pak® bag, and placed onto dry ice until transported to a -80 ℃ freezer. Samples were then shipped to the National Research Council (NRC), Montreal, Quebec, for extraction and 16S (prokaryote) and 18S (eukaryote)

ribosomal ribonucleic acid (rRNA) gene amplicon sequencing to assess microbial community diversity. Methods for gene extraction and sequencing are detailed in Chapter 3- Section 3.2.3.1.

Adenosine triphosphate (ATP) on EFW roots was measured as a metric of microbial energy which equates to microbial quantity/concentrations, using LuminUltra 2nd Generation ATP ® test kits and PhotonMaster Luminometer (LuminUltra, n.d., 2017). This was done to assess whether microbial ATP differed on EFW roots with or without oil exposure. Methods and results are included in Appendix B- Section B.7.

4.2.4 Data Analyses

Due to lack of enclosure replication, no statistical comparisons can be conducted, and as described in Chapter 3, these results should be used to inform potential of EFWs and their microbial communities for the secondary remediation of oil spills and future replicated research. Trends in parameters were visualized in R Studio (2023.09.1 + 494) (Posit Team, 2023; R Core Team, 2022), primarily using tidyverse syntax (v. 2.0.0, Wickham et al., 2019) and plotted with ggplot2 (v. 3.4.1, Wickham, 2016). Rarefied Amplicon Sequence Variant (ASV) data were analyzed for richness (alpha and chao1) and diversity (Shannon and Simpson), Bray-Curtis beta diversity with a Principal Coordinate Analysis (PCoA), and taxonomic profiles using R Studio (2023.09.1 + 494) (Posit Team, 2023; R Core Team, 2022) primarily with ggplot2 (v. 3.4.1, Wickham, 2016), using modified R scripts provided by NRC. Additional R packages used for data analyses are included in Appendix D.

Metazoans and class *Embryophyta* (land plants) were removed as they had a high relative abundance and skewed interpretation for analyzing the microbial eukaryotic community. A replicate from both the RE and LR on day 33 was dominated by Metazoan and *Embryophyta*

ASVs, respectively, and once removed the data no longer passed rarefaction filter requirements and were removed from diversity and taxonomic analyses.

Often, eukaryotic ASVs were misclassified through the insertion of subphyla/clades, for example, and were inconsistently identified to genus. Edits were made to correct taxonomic misclassifications (based on review of taxonomic lineages in the scientific literature and SILVA database (R138.1) (2023) (Glöckner et al., 2017; Quast et al., 2013; Yilmaz et al., 2014), World Register of Marine Species (WoRMS Editorial Board, 2023), and National Center for Biotechnology Information (Schoch et al., 2020) databases), however no classification external to the gene amplicon sequencing results was added. Taxonomic profiles represent the lowest level identified.

4.3 Results and Discussion

4.3.1 Polycyclic Aromatic Compound Chemistry

4.3.1.1 Water. Total aqueous PACs before oil addition were 17.36 ng/L, 14.50 ng/L, and 8.62 ng/L in the EE, RE, and LR, respectively (Figure 4.1). After oil addition, concentrations on day 1 were 771.73 ng/L, 19.99 ng/L, and 24.69 ng/L, respectively, and concentrations remained stable over the exposure period in unoiled sites. Total PACs in the EE peaked at 2,242.13 ng/L on day 14, declining to 342.85 ng/L on day 22. By day 73 concentrations were still higher (114.07 ng/L) but nearing background conditions. Total PAC concentrations were lower and posed less chronic toxicity risk (Lee et al., 2015) than observed in the 2019 dilbit spill (Chapter 3), and peak concentrations observed in our study may be on the low end of chronic (> 96 hr) embryotoxicity for freshwater environments (Lee et al., 2015). Differences between studies may be a result of a different oil product, analytical methods, and annual environmental conditions (e.g., high versus low precipitation years) (Rodriguez-Gil et al., 2021).

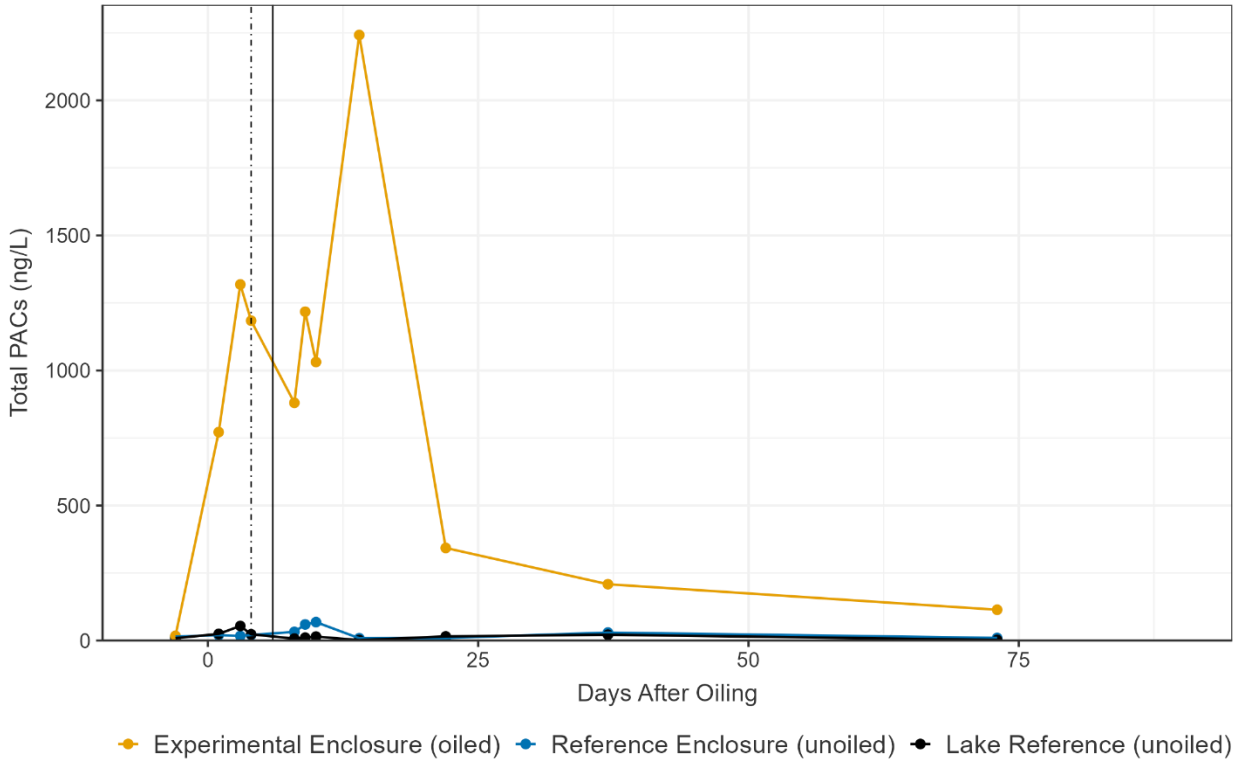

Figure 4.1. Total PACs (n=44) in the water from 3 days pre-oil addition to day 73 post-oil addition during the 2021 CHV experiment. Vertical lines represent primary (dotted) and secondary (solid) recovery events.

Due to the COVID-19 pandemic, analytical methods for PAC extraction from water varied as researchers were isolated on site at the IISD-ELA. In the 2019 dilbit study, raw water samples were transported from site to the COGRAD lab for filtration within 24 hours of collection. This process may have allowed greater dissipation of oil droplets into the aqueous phase increasing PAC concentration in the water (Chapter 3), while in this present study, water was filtered within 4 hours at the IISD-ELA. However, it is also regularly stated that different oil products have varying chemical content, and spills behave differently based on environmental conditions, and such no oil spill is the same (Dupuis & Ucan-Marin, 2015; Lee et al., 2015; Zhu et al., 2001), indicating there may be a number of reasons that the concentrations differed

between model spills. Total PAC concentrations from the CHV spill were similar to results of earlier oil spill remediation studies at the IISD-ELA (Palace et al., 2021; Rodriguez-Gil et al., 2021).

The majority of the total PACs were aPACs (Figure B4), with a mean (range; n=10) of 89.3 % (78.8-97.7%), 91.9 % (88.6-95.6 %), and 75.8 % (37.7-92.0%) of total PACs in the EE, RE, and LR, after oil addition respectively. aPACs in the EE were mostly made of 2- and 3-ring aPACs (Figure B5), including dominance (mean detected at >100 ng/L) of alkylated naphthalenes (C2 and C3). There were less 4- and > 4-ring aPACs compared to the dilbit model spill in 2019 (Chapter 3), which may be due to the oil product chemistry, environmental conditions, analytical methods, or sediment sorption. Of interest, peak total parent PAC concentrations were similar for the dilbit spill and the CHV spill (Figure B4), which may suggest that dilbit has greater content of aPACs, and may be of greater concern for chronic toxicity. Similarly, the dominance of 2- and 3-ring PACs in CHV compared to 2-, 3- and 4-ring in dilbit (Chapter 3) may result in greater biodegradation in CHV, however, noting that each oil spill behaves differently. Results from the 2018 Freshwater Oil Spill Remediation Study (FOReSt) exposure, assessing monitored natural recovery of oil spills also observed greater concentration of 3-, 4-, and >4-ring PACs in dilbit, and 2-ring PACs in CHV (Palace et al., 2021).

4.3.1.2 Sediment. Total sediment PACs in all sites and sample periods had high variability and large contributions from retene (3.08-94.6% of total PACs), a three ring PAC, that is often released into the environment during forest fire events (Gabos et al., 2001; Ramdahl, 1983), a common and important occurrence in the boreal forest (Brandt et al., 2013). In fact, there was a forest fire at a neighbouring lake (Lake 259) during recovery efforts 4 days after oil addition, and the IISD-ELA often experiences impact from nearby fires.

The contribution of retene causes difficulty in comparing total sediment PACs between oiled and unoiled sites, as also observed in the 2019 dilbit study (Chapter 3). Figure 4.2 presents total PACs excluding retene (n = 43), and Figure B6 displays trends of total, parent, and alkylated PACs, and retene alone over the exposure period. Mean (± SD; triplicate samples at each site) total sediment PACs excluding retene during pre-oil conditions were 2.40 ± 1.51 μg/g, 1.03 ± 0.149 μg/g, and 0.56 ± 0.60 μg/g in the EE, RE, and LR, respectively (Figure 4.2). Concentrations peaked in the EE on day 12 to 34.7 ± 13.1 μg/g, with high contributions from c3-dibenzothiophene (11.3-14.2%), c2-dibenzothiophene (10.8-11.3%), c3-phenanthrene (10.0-11.3%), and c2-phenanthrene (9.31-10.8%). Mean concentrations slightly declined on day 38 to 25.5 ± 21.6 μg/g, but had the highest individual sample concentrations, and were dominated by c3-dibenzothiophene (8.92-27.4%), c2-dibenzothiophene (10.4-23.7%), and c1-pyrene (4.71-16.9%). By day 70, concentrations in the EE declined to 8.89 ± 7.58 μg/g, with the largest contributions from c3-phenanthrene (19.6-77.1%), c2-dibenzothiophene (1.51-16.3%), and c3-dibenzothiophene (0.87-12.5%). Replicate variability observed in the EEs may result from heterogeneous deposition or sorption of oil onto sediments, similarly found in previous dilbit model spills at the IISD Experimental Lakes Area (Chapter 3; Stoyanovich et al., 2022). Concentrations remained relatively stable in the reference sites over the exposure period, excluding the RE on day 70 at 12.1 ± 16.8 μg/g, due to large contributions from c3-phenanthrene (27.7-86.0%), while the LR had 2.99 ± 2.24 μg/g, mostly made of c3-phenanthrene (44.7-82.9%).

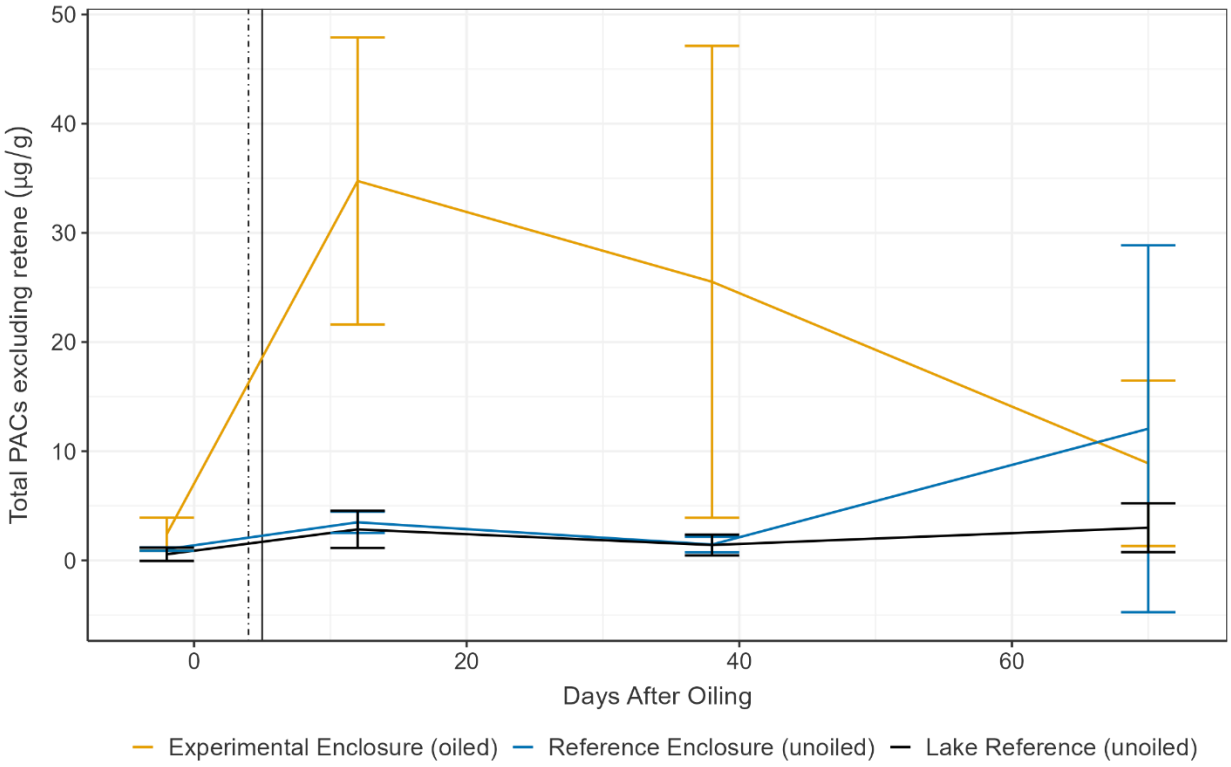

Figure 4.2. Mean (± SD) total PACs (excluding retene; n=43) in sediment from 2 days pre-oil addition to day 70 post-oil addition during the 2021 CHV experiment. Error bars represent standard deviation of triplicate samples at each site. Vertical lines represent primary (dotted) and secondary (solid) remediation events.

Total sediment PACs in this study were a magnitude lower than observed during the dilbit model spill in 2019 (Chapter 3), however, total parent PACs having a similar concentration range (Figure B4). The difference in sediment PACs may be due to differences in oil product or chemistry, environmental conditions, and sorption to the sediment. The retene content in the sediment similarly is a large contributor to total PACs, but concentrations are lower than observed in 2019 sediment samples (Chapter 3), and may reflect sample location. In order to determine if sediment PACs were influenced by petroleum or combustion sources, PAC ratios (Yan et al., 2005; Yunker et al., 2002) are discussed in Appendix B- Section B.3.2.1.

4.3.2 Root Microbial Community

4.3.2.1 Diversity. Differences in the rarefied ASVs for prokaryotic (16S) and eukaryotic (18S) communities over the exposure period were examined for Bray-Curtis beta diversity with a Principal Coordinate Analysis (PCoA). The PCoAs had 51.69 % and 34.71 % explained linear variation on two axes for the prokaryotic and eukaryotic community, respectively (Figure 4.3), indicating greater differences in the eukaryotic community. Beta diversity was similar between all three EFWs on day -11 and changed over the exposure period along the primary axis for the enclosure sites and across both axes for the LR in both communities. The greatest differences were observed between the LR and enclosure sites, and minimal seasonal changes were captured in the PCoA, excluding changes from day -11, which may reflect site conditions.

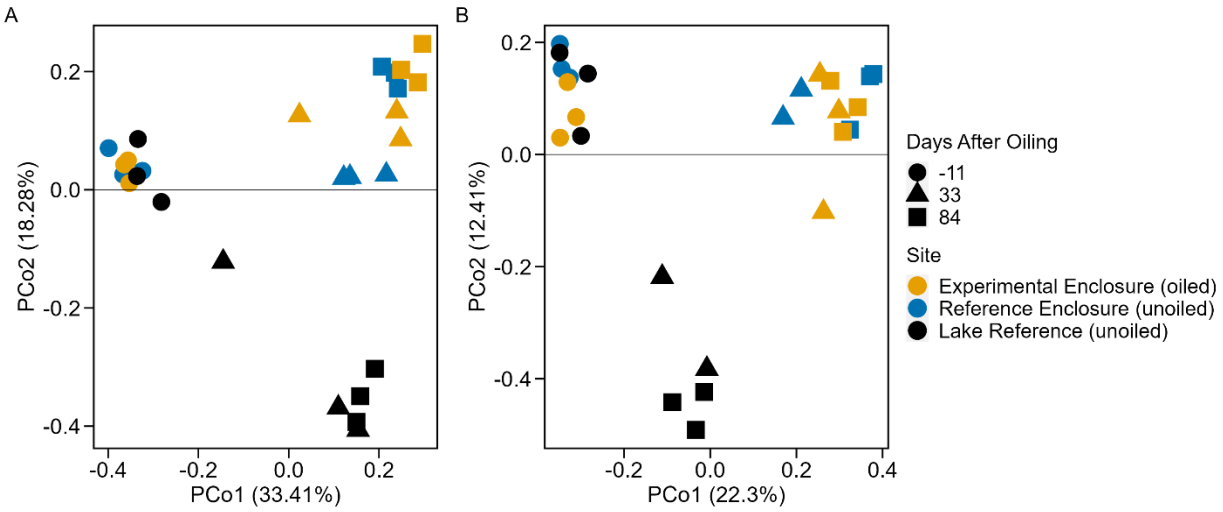

Figure 4.3. Principal Coordinate Analysis of 16S (A) and 18S (B) Bray-Curtis beta diversity in EFW root microbial biofilm during the 2021 CHV experiment.

Prokaryotic organisms had higher ASV richness (alpha and Chao 1) across all sites and sample periods than eukaryotic organisms, and had a more even distribution (Shannon diversity) (Table B4). Prokaryotic richness increased on day 33 in the EE, however, similar trends were not observed for eukaryotes or reference sites. Prokaryotic Shannon diversity increased from day -11

to 33 in the EE, however declined in the LR, indicating a less diverse and even community. While no changes were observed in the RE until day 84. Similarly mean prokaryotic Simpson diversity declined in the LR on day 33, however was relatively stable in the enclosure sites. Mean eukaryotic Shannon diversity was more variable in the reference sites, however generally declined in the EE, and was lowest on day 33 in the LR. Eukaryotic Simpson diversity was relatively stable, excluding samples on day 33 in the LR, displaying high variability. The eukaryotic organisms had more variability among replicates, and it was difficult to identify clear temporal or site differences in richness and diversity indices. Differences among replicates may result from spatial diversity on EFWs, which may be caused by variability in plant species and their exudation patterns, surface area, or active growing sites (Sasse et al., 2018).

4.3.2.2 Taxonomy

4.3.2.2.1 Prokaryotes. Taxonomic profiles of the root microbial prokaryotic community identified 49 phyla of archaea (6) and bacteria (42), dominated by *Proteobacteria* (28.4-57.5% of total community relative abundance [RA]), *Bacteroidota* (9.23-29.5%), *Cyanobacteria* (1.33-17.6%), *Acidobacteriota* (0.84-12.4%), and *Planctomycetota* (4.39-11.9%). The phyla dominance remained relatively stable over the experimental period with some changes, however *Cyanobacteria* increased from day -11 (2.68-3.85%) to day 84 (4.75-17.6%) in the LR site (Figure B16).

The top 20 most abundant prokaryotic ASVs (genera) represent less than 50% of the community (of 945 identified ASVs; Figure 4.4).Total RA explained by these organisms slightly declined in the EE on day 33, likely due to increased richness (Table B4), and so the top 21-40 organisms are presented (Figure 4.5). Due to community diversity, the following section will prioritize discussion on prokaryotes with oil spill degradation potential.

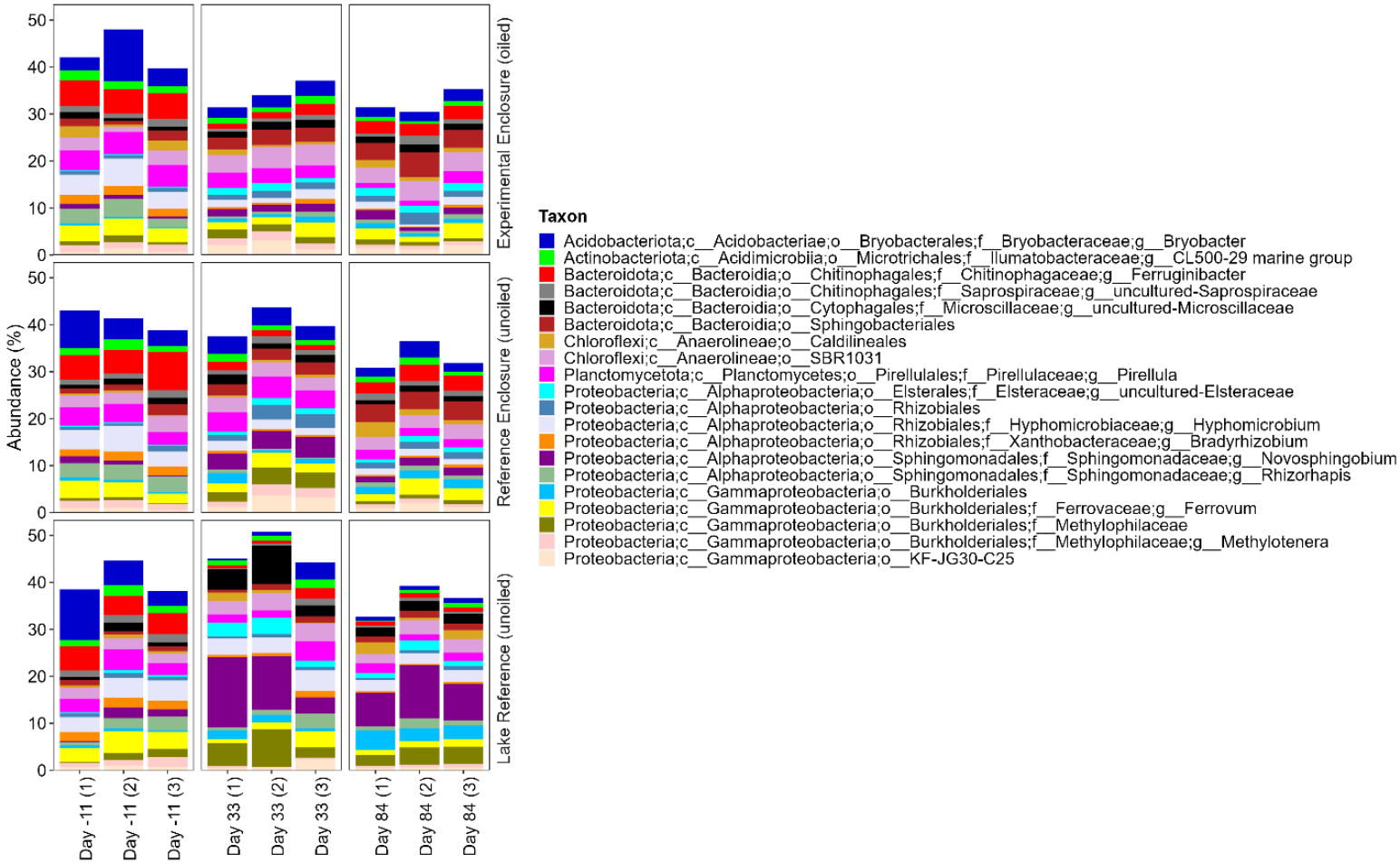

Figure 4.4. Taxonomic profile of the top twenty most relatively abundant 16S ASVs in EFW root biofilm replicates from the EE, RE, and LR 11 days pre-oil addition, and on days 33 and 84 post-oil addition during the 2021 CHV experiment. Taxon legend includes full taxonomic details to the lowest level identified as available.

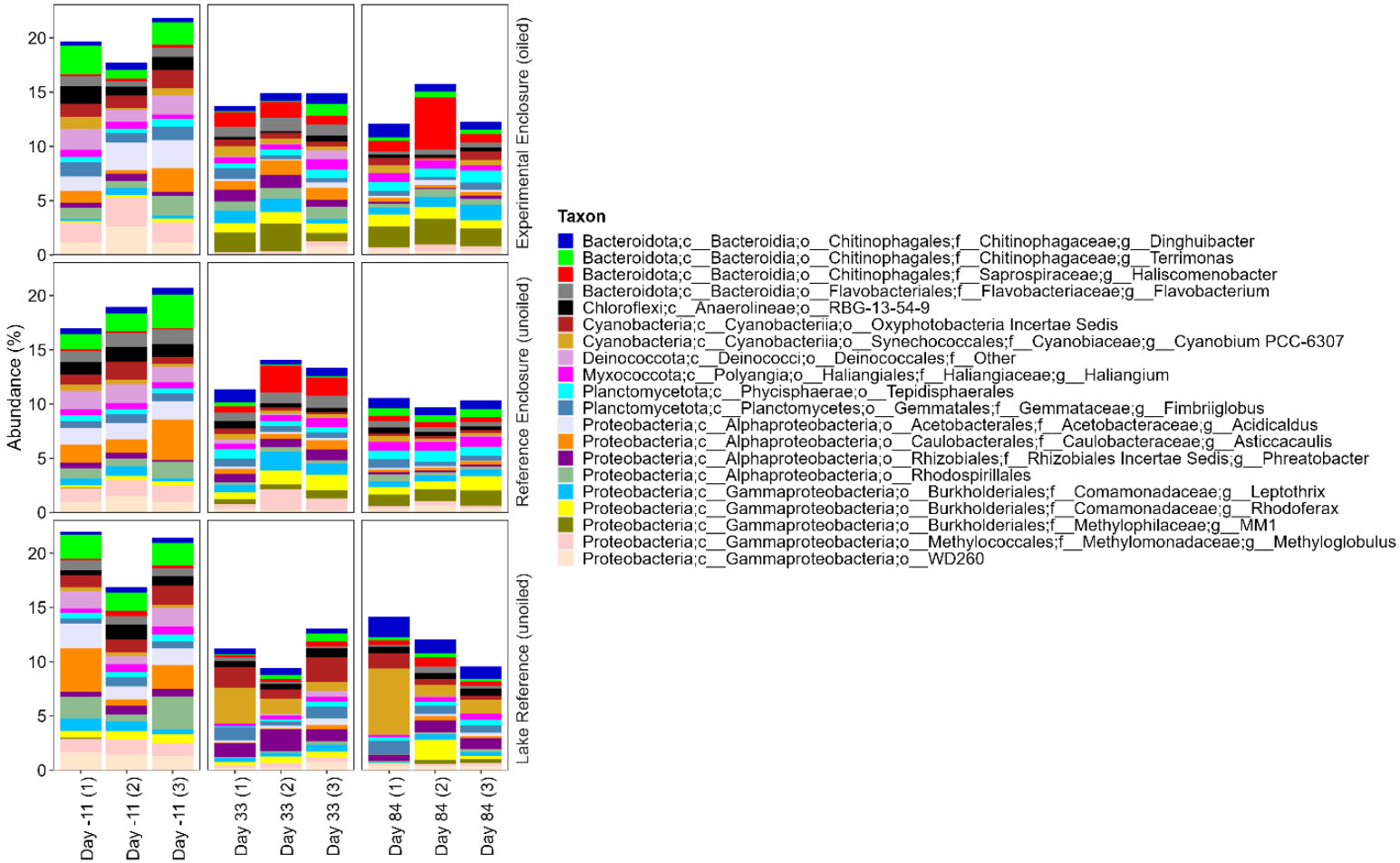

Figure 4.5. Taxonomic profile of the top twenty-one to forty relatively abundant 16S ASVs in EFW root biofilm replicates from the EE, RE, and LR 11 days pre-oil addition, and on days 33 and 84 post-oil addition during the 2021 CHV experiment. Taxon legend includes full taxonomic details to the lowest level identified as available.

The greatest RA was detected for *Novosphingobium* on day 33 in the LR site (3.47-15.0%). This result was surprising, as *Novosphingobium* is a well known hydrocarbon degrader due to their metabolic versatility (Chettri & Singh, 2019; Ghosal et al., 2016; Kertesz & Kawasaki, 2010; Lyu et al., 2014; Rojo, 2021; Sohn et al., 2004; Yang et al., 2016). This may have been caused by proximity to a previous oil spill research site on Lake 260 that may have had residual oil/hydrocarbons present, potentially influencing the microbial community. While not optimal, nor confirmed by chemistry, it does show that the EFW community is capable of drastically shifting to organisms capable of degrading PACs. In addition, *Novosphingobium* was also identified in the enclosure sites but at lower abundances, peaking on day 33 in the EE (1.52-1.75%) and RE (3.48-4.44%).

Rhizorhapis, another genus from family *Sphingomonadaceae*, was identified in the top 20, previously identified as a dominant organism in diesel contaminated soil (Gran-Scheuch et al., 2020). RAs were highest on day -11 in the EE (1.77-3.89%) and RE (3.06-3.35%), while the LR was relatively stable over time, highest on day 33 (0.65-3.16%).

Four top genera belong to order *Rhizobiales*, which are well known for their association with plants and ability to enhance nutrient bioavailability (Fahde et al., 2023; Garrido-Oter et al., 2018; Newton et al., 2011). Some also have hydrocarbon and/or PAC degradation capabilities (Abbasian et al., 2016; Prince et al., 2018), for example *Hyphomicrobium* and *Bradyrhizobium* have previously been identified to have hydrocarbon degradation potential or been present among other hydrocarbon degraders (Ozaki et al., 2006; Yang et al., 2016), however were often highest on day -11, excluding *Hyphomicrobium* which peaked on day 33 in the LR (3.26-4.42%). An unidentified ASV increased over the exposure period in the EE, peaking on day 84 (1.18-2.45%). While RA peaked on day 33 in the RE (1.15-3.12%) and on

day -11 in the LR (0.73-1.04%). *Phreatobacter* was variable over the exposure period among all sites, highest on day 33 ranging from 0.59-1.20%, 0.75-1.00%, and 1.14-2.01% in the EE, RE, and LR, respectively, though no literature supports potential hydrocarbon degradation.

Order *Rhodospirillales,* another *Alphaproteobacteria* detected in the top 40 genera, have genes encoding for monooxygenase enzymes capable of degrading aliphatic hydrocarbons and the desulfurization of hydrocarbons (Abbasian et al., 2016), and include members with hydrocarbon degradation potential (Prince et al., 2018), however declined over the exposure period, highest on day -11, ranging from 0.63-3.03% among all sites.

Order *Burkholderiales* was dominant, with seven genera in the top 40 prokaryotic ASVs. These are common microorganisms, however some are noted to have degradation potential (Pérez-Pantoja et al., 2012; Prince et al., 2018). *Leptothrix* and *Rhodoferax,* from family *Comamonadaceae* have been shown to produce various genes encoding for dioxygenases, hydroxylases, monooxygenases, and demethylases, important for degradation of aromatic compounds (Pérez-Pantoja et al., 2012). *Leptothrix* sp. increased in RA over the exposure period in the EE, ranging from 0.57-1.39 % on day 84. While RA peaked on day 33 in the RE (0.71-1.75 %), and declined in the LR over time. *Rhodoferax* also increased over the exposure period in the EE, ranging from 0.75-1.10% on day 84. The RA peaked on day 33 in the RE at 0.64-1.41%, on day 84 in the LR at 0.12-1.88%. Mean RA of *Ferrovum* remained relatively stable over the exposure period in the EE and RE, highest on day -11 (2.11-3.63%), but declined in the LR site over time, reaching 1.13-1.58% on day 84. An unidentified ASV declined in the enclosure sites over the exposure period, however peaked on day 84 in the LR (2.67-4.05%). *Methylotenera* sp., has been identified as a potential hydrocarbon degrader (Idomeh et al., 2021; Thompson et al., 2017), and peaked in the enclosure sites on day 33 (1.20-1.92% and 1.08-2.31%

in the EE and REs, respectively), while it declined in the LR on day 33 (<1%). Other *Methylophilaceae* including MM1 and an unidentified genus was dominant in the top 40 ASVs. The unidentified genus was highest on day 33 in all sites, ranging from 1.41-1.90%, 1.96-3.66%, and 2.15-8.05% in the EE, RE, and LR, respectively. MM1 was highest in the EE on day 33, ranging from 0.78-2.54%, and on day 84 in the RE (1.06-1.37%), while RA was low in the LR.

Methylotrophic bacteria have roles in consuming methane or C1 substrates (Rojas-Gätjens et al., 2022), which can be a by-product of oil biodegradation, found in oil (Lee et al., 2015), or released during spill events, as observed during the Deepwater Horizon spill (Kessler et al., 2011), where methylotrophs and methanotrophs increased months after the spill (Redmond & Valentine, 2012). Kessler et al. (2011) stated that methane consumption likely occurred prior to sampling and the remaining organisms were likely inactive by the fall. However, later hypotheses by Gutierrez and Aitken (2014) stated that some members of *Methylophaga* may in fact have had hydrocarbon degradation capabilities during Deepwater Horizon event. Another methylotrophic bacterium in our study, *Methyloglobulus*, was detected in the top 40, but its abundance declined over time, with RAs < 1% among all sites on days 33 and 84.

Unidentified genera from order *Sphingobacteriales,* which include known hydrocarbon degrading species (Beazley et al., 2012; Prince et al., 2018), increased over the exposure period in all three sites, and were more numerous in the enclosures. The highest RA was detected in the EE on day 84, ranging from 3.61-5.25%, which had one of the highest RAs (top 4) detected for all prokaryotes in the EE. While RAs ranged from 3.66-3.92% and 1.27-1.52% in the RE and LR, respectively. *Sphingobacteriales* are known to be late responders to oil (Franchi et al., 2022; Koo et al., 2015), which may confirm why they dominated the EE community on day 84. Other *Bacteroidota* in our samples with potential roles in oil spill degradation include *Flavobacterium*

(Bôto et al., 2021; Z. Liu & Liu, 2013; W. F. Song et al., 2018), *Haliscomenobacter* (Aburto-Medina et al., 2012), *Dinghuibacter* (M. Wang et al., 2021), *Terrimonas* (Adrion et al., 2016; M. Song et al., 2015; Zhang et al., 2011), *Ferruginibacter,* and uncultured *Saprospiraceae* (Taylor et al., 2021) and *Microscillaceae*. *Flavobacterium* was <1% in the LR, and declined over time in the RE, highest on day -11 (1.02-1.35%), while RA in the EE peaked on day 33 (0.97-1.23%) and were <1% during other sampling rounds. *Haliscomenobacter* increased over time in the EE, peaking on day 84 (0.75-4.81%), which included a replicate in the top 5 highest RAs for this site. While RA peaked on day 33 in the RE (0.57-2.47%) and was <1% in the LR. *Dinghuibacter* were generally low in RA (<1%) excluding day 84 in the EE (0.70-1.25%) and LR (1.11-1.84%) and on day 33 in the RE (0.42-1.19%). *Terrimonas* generally declined over time with some variability, but was highest on day -11 among all sites, ranging from 0.83-2.66%, 1.42-3.14%, and 1.70-2.21% in the EE, RE, and LR, respectively. *Ferruginibacter* generally declined over the exposure period, with highest dominance on day -11, ranging from 5.22-5.46%, 5.02-8.06%, and 4.08-5.22%, respectively. However, RA was still dominant by day 84, ranging from 2.49-2.83%, 2.45-3.50%, and 0.97-1.02%, respectively. Uncultured *Saprospiraceae* was variable in the EE with the highest RA detected on day 84 (0.64-1.88%), while RA generally declined in the reference sites over time. Uncultured *Microscillaceae* increased over time in the EE with an RA ranging from 1.36-1.68% on day 84, while RA peaked on day 33 in the RE (1.07-2.12%) and LR (2.32-8.16%).

Some species of cyanobacteria have been found to oxidise PACs, including naphthalene and phenanthrene, as summarized in Juhasz and Naidu (2000) and Ichor et al. (2016), and a number of researchers have found successful growth on alkanes, PACs, and oil as summarized in Prince et al. (2018). ASV of order *Oxyphotobacteria* declined over the exposure period in the

enclosure sites, however peaked in the LR on day 33 (0.88-2.25%). *Oxyphotobacteria* had previously been observed to increase during early exposure to water accommodated fraction of crude oil, however later exhibited intolerance in a seawater microcosm study (Zhou et al., 2022). *Cyanobium* PCC-6307, similarly declined over the exposure period in the EE, and was <1% in all samples in the RE. RA increased in the LR, peaking on day 84 (1.05-6.11%). Hancock et al. (2021) found some cyanobacteria phylotypes, including some from family *Synechococcacceae,* are resilient to crude oil exposure.

Chloroflexi are able to anaerobically degrade hydrocarbons (Cébron et al., 2022), and have been detected as a dominant organism in oil contaminated environments (Brown et al., 2013; Cébron et al., 2022; Engel et al., 2017; Peng et al., 2015). Order *Caldilineales* was highly variable, but typically increased in the reference locations, peaking on day 84 in the RE (0.92-3.09%) and LR (0.48-2.48%), while the EE was highest before oil addition (0.51-2.37%). Order SBR1031 was stable over the exposure period in the reference sites (2.06-3.75%), while it peaked on day 33 in the EE (3.77-4.56%). ASV from order RBG-13-54-9 declined over the exposure period in all sites, highest on day -11, ranging from 0.81-1.61%, 1.12-1.34%, and 0.46-1.39%, in the EE, RE, and LR, respectively.

4.3.2.2.2 Eukaryotes. Taxonomic profiles of the root microbial eukaryotic community identified 41 phyla, with more variable dominance between sites and sample periods than the prokaryotic community, including variability among replicates, which may reflect EFW sample location (Figure B17). The community was dominated by phyla *Ciliophora* (0.49-57.1%), *Dinoflagellata* (2.65-46.5%), *Chytridiomycota* (1.96-25.2%), *Cercozoa* (0.81-23.7%), *Basidiomycota* (0.10-61.1%), *Cryptomycota* (0.08-34.5%), *Peronosporomycetes* (0.72-36.2%), *Apicomplexa* (0.51-15.8%), *Chlorophyta* (0.41-12.7%), *Aphelidea* (0.00-10.4%), and two

unknown eukaryotic phyla (1.80-17.1% and 2.61-12.0%). The LR had greater dominance by *Basidiomycota* on day 33 and *Dinoflagellata* on days 33 and 84, while the EE had dominance by *Cryptomycota* on day 33. *Ciliophora* was variable among sites over time, highest on day 84 in the EE.

The top 20 eukaryotic ASVs represented approximately 30-60% of total community RA, with variability between sites, sample periods, and within replicates (Figure 4.6). The total RA explained by these organisms increased on day 33 in the EE and in a sample in the LR, indicating the most dominant ASVs were likely a result of site conditions after deployments. The top 21-40 ASVs similarly had variable abundances between sites, but displayed clear selection of certain organisms over time and between sites (Figure 4.7).

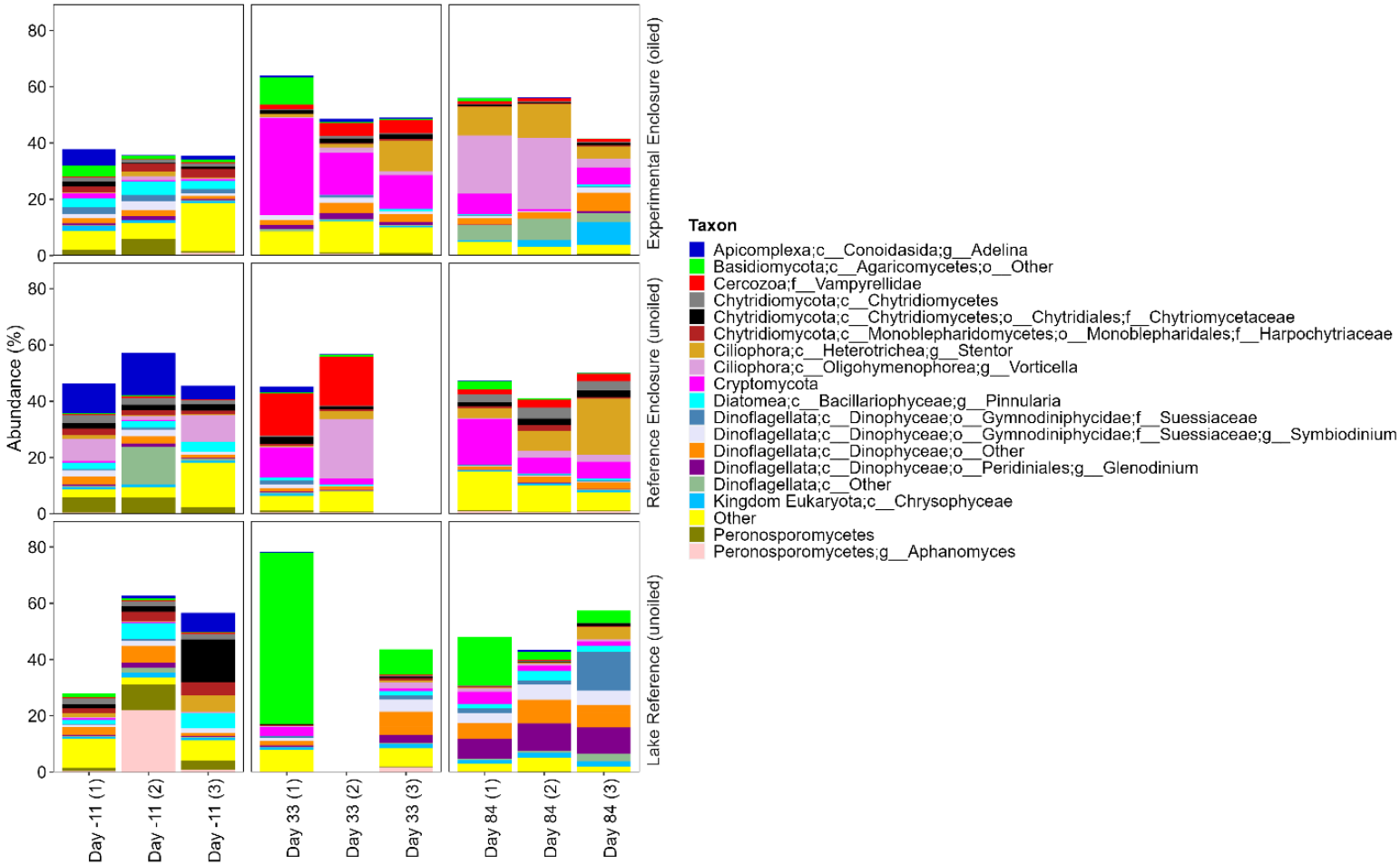

Figure 4.6. Taxonomic profile of the top twenty most relatively abundant 18S ASVs in EFW root biofilm replicates from the EE, RE, and LR 11 days pre-oil addition, and on days 33 and 84 post-oil addition during the 2021 CHV experiment. Taxon legend includes full taxonomic details to the lowest level identified as available.

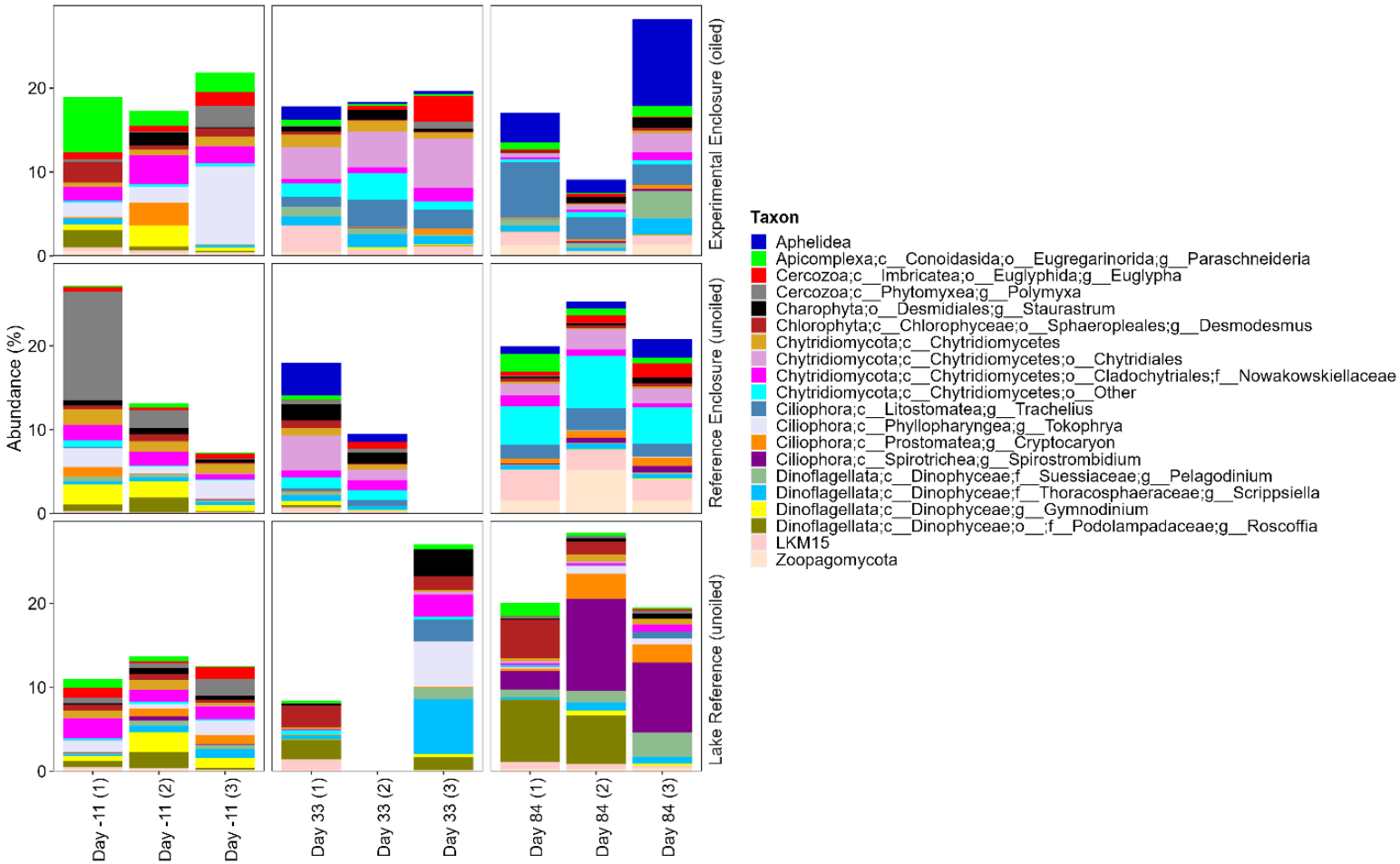

Figure 4.7. Taxonomic profile of the top twenty-one to forty most relatively abundant 18S ASVs in EFW root biofilm replicates from the EE, RE, and LR 11 days pre-oil addition, and on days 33 and 84 post-oil addition during the 2021 CHV experiment. Taxon legend includes full taxonomic details to the lowest level identified as available.

The most dominant organisms were fungal representatives, which may have important roles in PAC degradation. Some fungi are capable of releasing ligninolytic and non-ligninolytic enzymes to facilitate PAC degradation (Haritash & Kaushik, 2009; Kadri et al., 2017). The highest RA was ASV of class *Agaricomycetes* from phylum *Basidiomycota,* known to include a series of genera with PAC degradation potential (Prince, 2018), ranging from 9.05-61.0% on day 33 in the LR. It also increased in the EE on day 33, but in lower abundance (0.41-9.75%), while the RE peaked on day 84 (0.35-2.98%). While ASV from phylum *Cryptomycota* was highest on day 33 in the EE (12.0-34.5%), and on day 84 in the RE (5.73-16.2%) and LR (1.70-4.31%). Seven unidentified ASVs from phylum *Chytridiomycota,* known to include PAC degrading genera (Prince, 2018), were in the top 40 at variable abundances, some peaked in the EE (for example, an ASV from order *Chytridiales* was highest on day 33 at 3.82-5.84%), while others declined over time. Lemmel et al. (2021) assessed fungal communities in industrial brownfield contaminated soils and found *Basidiomycota* (including class *Agariomycetes*) and *Chytridiomycota* were higher in uncontaminated sites compared to PAH and heavy metal contaminated sites, while *Cryptomycota* were higher in contaminated soils, likely due to metals. However, others have found Operational Taxonomic Units of phyla *Basidiomycota* and *Cryptomycota* in higher abundance in soil near an oil seep, noting potential role of *Lactarius* sp. (*Basidiomycota*) in hydrocarbon biodegradation (Cébron et al., 2022). Similarly, Aguilar et al. (2016) found *Cryptomycota* dominance in anoxic sediment of an oil sands tailing pond, and Mahmoudi et al. (2013) detected dominance of classes *Agariomycetes* (*Basidiomycota)* and *Chytridiomycetes* in saltmarsh sediments 18 months following Deepwater Horizon spill. The dominance in fungal ASVs on EFW roots likely plays an important role in biodegradation.

Some algae are also known to have hydrocarbon degradation potential (Ghosal et al., 2016; Prince, 2018). ASV from class *Chrysophyceae* increased from day -11 (0.73-1.72%) to day 84 (0.57-8.06%) in the EE, while RA was <1% in the RE, and ranged from 0.60-1.98% in the LR during all sample periods. Research by Finkel et al. (2020) observed that chrysophytes positively responded to Macondo surrogate crude oil water accommodated fraction treatments and dispersants, while green algae were generally insensitive to oil and dispersants, and dinoflagellates and diatoms were sensitive, with some mixed responses. In addition, research by Cederwall et al. (2020) found no impact to chrysophyte, *Dinobryo sertularia*, in mesocosms treated with dilbit.

In our study, diatom, *Pinnularia* declined over the exposure period in the enclosure sites, however, was variable in the LR, likely a reflection of differing site conditions or seasons. De Faria et al. (2019) identified that diatom assemblages/guilds respond to environmental conditions. The highest RA for *Pinnularia* was detected on day -11 for all sites, ranging from 2.86-4.75%, 2.22-3.52%, and 1.47-5.53% in the EE, RE, and LR, respectively. Desmid algae, *Staurastrum*, was relatively stable over the exposure period in the EE, ranging from 0.00-1.56%. RA was <1% in the RE and LR, excluding samples on day 33 ranging from 1.29-1.91% and 0.21-3.27%, respectively. Green algae, *Desmodesmus,* was highest in the EE before oil addition (0.50-2.47%) while days 33 and 84 had low RA (< 1%), while the LR increased over the exposure period, peaking on day 84 (0.00-4.59%) and the RE had low RA (<1%) in all samples.

Dinoflagellates can include auto-, mixo-, or heterotrophic organisms (Siano et al., 2010), with some capable at toxin production (Deng et al., 2023), and others observed to flourish after an oil spill event (Almeda et al., 2018). Some species can ingest oil droplets (Almeda, Connelly, et al., 2014) and others are enhanced by oil degrading bacteria (Park et al., 2020). Almeda et al.

(2018) observed a grazing pressure shift from heterotrophic dinoflagellates and ciliates to bloom forming dinoflagellates when exposed to oil and dispersants, however, Finkel et al. (2020) observed a negative response to oil and dispersants. There were 10 dinoflagellates in the top 40 ASVs, often with large increase in abundance on day 84 in the LR. An endosymbiont, *Symbiodinium* (Levy et al., 2007; Siano et al., 2010), increased over the exposure period in the LR site, reaching 3.51-5.53% on day 84, while abundance was highest on day -11 for the EE (0.85-3.24%) and RE (1.02-2.45%), declining over time. Similarly, bloom forming *Glenodinium* (Ulloa et al., 2017) and an unidentified ASV from family *Suessiaceae* peaked in the LR on day 84, at 7.09-9.78% and 1.39-13.9%, respectively, while they declined or were variable in the enclosure sites. Another bloom former, *Scrippsiella*, previously identified to increase upon exposure to oil and dispersant (*S. trochoidea*; Almeda et al., 2018), increased over the exposure period in the EE, ranging from 0.36-1.85% on day 84, however was highest on day 33 in the LR (0.49-6.56%), and had low RA (<1%) in the RE. *Gymnodinium*, known to include toxin producing species (Deng et al., 2023), had the highest RA in all sites on day -11 ranging from 0.36-2.52%, declining to <1% on days 33 and 84. This genus was previously noted as sensitive to dilbit exposure, as identified in a mesocosm experiment (Cederwall et al., 2020). Our results, however, may reflect responses to seasonal and/or site conditions. Similar trends were observed in the EE and RE for *Roscoffia*. While the RA of *Roscoffia* increased over the exposure period in the LR, reaching 0.00-7.38% on day 84. Another endosymbiont, *Pelagodinium* (Siano et al., 2010), increased over the exposure period in the EE and LR, ranging from 0.59-3.27% and 0.92-2.91% on day 84, respectively, but had a low RA (< 1%) in the RE. While most dinoflagellates increased in the LR, an unidentified dinoflagellate had the largest increase in the EE on day 84 (3.21-7.66%), while RA in the RE declined over time and the LR was variable. While

dinoflagellate response to oil in the literature is variable, the increase in the LR may be a response to shift in grazing pressure or environmental conditions, such as potential residual PACs or oil near previous experiments, however not confirmed.

Six ciliates were in the top 40 ASV, and similar to dinoflagellates, can shift as a response to environmental conditions. Ciliate tolerance to conditions and pollutants can vary by species (Jousset et al., 2010; Lara & Acosta-Mercado, 2012; C. V. Robinson et al., 2022), for example some are sensitive to oil and dispersants (Almeda et al., 2018; Almeda, Hyatt, et al., 2014), while others flourish under PAC exposure (Moss et al., 2015). Others have identified that grazing activity can enhance biodegradation (Tso & Taghon, 2006) or result in direct bioaccumulation (Rogerson & Berger, 1981), and some have reported successful petroleum hydrocarbon co-metabolism by a consortia (Kachieng'a & Momba, 2017, 2018), though questioned by Prince (2018).

No genera dominated all sites at a given time, but rather shifted over the exposure period between sites, likely due to changing conditions. *Stentor* increased in dominance over the exposure period in the enclosure sites, peaking on day 84 in the EE (4.31-12.1%) and RE (3.44-19.9%), while RA was variable in the LR, highest on day -11 (0.13-5.82%). *Vorticella* drastically increased in the EE, from day 11 (0.16-1.40%) to day 84 (2.35-25.4%). While RA peaked on day 33 in the RE (0.28-21.1%) and LR (0.36-2.22%), however noting the RA on day -11 was high in the RE (1.47-9.40%). *Tokophrya* had low RA (< 1%) in the EE and RE on days 33 and 84, except day -11, ranging from 1.69-9.31% and 0.85-2.25%, respectively, while some replicates in the LR peaked on day 33 (0.08-5.47%). *Trachelius* often had low RA (<1%), but increased over the exposure period, peaking on day 84 in the EE (2.42-6.61%) and RE (1.61-2.68%), while RA peaked on day 33 in the LR (0.00-2.62%). This genus is from class *Litostomatea*, which has been

previously found to include Operational Taxonomic Units with potential high tolerance to hydrocarbon contamination (Richardson et al., 2020). *Cryptocaryon* declined in the EE over the exposure period, highest on day -11 (0.3-2.69%), while the RE and LR were variable, with the greatest detected RA on day -11 (0.04-1.12%) and day 84 (0.27-2.98%), respectively. *Spirostrombidium*, previously noted as sensitive to oil and dispersant (Almeda, Hyatt, et al., 2014), had low RA (<1%) in all sites and sample periods, except for a drastic increase on day 84 in the LR (2.23-11.0%). While the literature is variable, ciliates may facilitate oil degradation (Kachieng'a & Momba, 2017, 2018) or indirectly through grazing activities (Tso & Taghon, 2006), and have displayed species tolerance/selection to differing conditions among sites.

Cercozoa are also known eukaryotic grazers that have been previously observed to have variable responses upon crude oil contamination (Cobanli et al., 2022; Dalby & Kormas, 2008), which may indicate different species tolerance. *Cercozoa*, mostly of Glissomonads, was a dominant eukaryotic group identified in oil sands tailing ponds, and authors noted their potential role on grazing hydrocarbon degraders (Richardson et al., 2020). ASV from family *Vampyrellidae* peaked on day 33 in the EE (1.69-4.75%) and RE (14.9-17.5%), while RA was <1% in the LR in all sample periods. *Euglypha* was variable among all sites and sample periods, with the highest RA on day 33 in the EE (0.00-3.09%), on day 84 in the RE (0.49-1.67%), and day -11 in the LR (0.21-1.43%), with many sample periods having low RA (<1%). Plant root parasite (Niehl et al., 2020), *Polymyxa* was <1% RA in all sites, excluding samples on day -11 among all sites with high variability (0.08-13.0%).

4.4 Conclusions

To understand how microorganisms shift on EFWs upon oil exposure, we conducted modelled conventional heavy crude oil spills in shoreline enclosures on Lake 260 at the IISD-

ELA in 2021. The eukaryotic community had lower richness and evenness, displaying greater selection for specific microorganisms over the exposure period, in both oiled and unoiled sites. However, there were shifts observed in both prokaryotic and eukaryotic communities over the exposure period, mostly due to dominance of *Novosphingobium*, *Cyanobacteria*, *Basidiomycota*, and *Dinoflagellata* in the LR site, *Cryptomycota* in the EE, and *Ciliophora* among all sites. Shifts in microbial composition couldn't be attributed specifically to oil exposure, seasonal effects, or site conditions, however there were a number of organisms capable at degrading PACs, and major changes in the LR may have been impacted by previous oil spill research, however chemistry data was not available to confirm this speculation. While not optimal, results show the capacity of EFWs to drastically shift to dominating organisms under changing site conditions.

PACs in the aqueous environment, mostly dominated by 2- and 3-ring aPACs, peaked on day 14, and returned to nearing background conditions by day 73. Sediment PACs were strongly influenced by pyrogenic sources, however, were increased in the EE on days 12 and 38, likely where oil settled or sorbed into the sediment, appearing to decline by day 70. These findings indicate potential of EFWs for secondary remediation of oil spills; however it is suggested that further replicated research be conducted to confirm findings.

Chapter 5. Removal of Phenanthrene From Freshwater by three Emergent Wetland Plants

5.1 Introduction

Polycyclic aromatic compounds (PACs) pose significant concerns to the environment and interacting biota when released in high concentrations (e.g., oil spills) due to their potential toxic, carcinogenic, and mutagenic properties (Cao et al., 2009; Dupuis & Ucan-Marin, 2015; Ghosal et al., 2016; Haritash & Kaushik, 2009; Honda & Suzuki, 2020; Lee et al., 2015; Zhu et al., 2001). PACs are aromatic compounds with two or more fused aromatic rings, and their complexity and recalcitrance increases with the number of rings (Lee et al., 2015; Zhu et al., 2001). After an oil spill, the typical response is to recover as much oil as possible using mechanical and chemical recovery methods. Unfortunately, some methods can be damaging to sensitive environments (such as dredging sediment or excavating oiled material from freshwater shorelines) (Hoff, 1995; Lee et al., 2015; Pezeshki et al., 2000; Zhu et al., 2001), may increase contaminant-biota interactions (Lee et al., 2015), and can leave residual oil in the environment (Das & Chandran, 2011; Etkin & Tebeau, 2003; Lee et al., 2015; Zhu et al., 2001).

There is a need for improved remediation methods that are less damaging to sensitive environments and increase oil removal (Lee et al., 2015). Research at the International Institute for Sustainable Development Experimental Lakes Area (IISD-ELA) has explored non-invasive methods for oil spill recovery by conducting model oil spills of diluted bitumen (Chapter 3) and conventional heavy crude oil (Chapter 4) in shoreline enclosures of an experimental boreal lake, and exploring impacts and toxicity to biota. The FLOating Wetland Treatments to Enhance Remediation (FLOWTER) project was established to determine the effectiveness of engineered floating wetlands (EFWs) as a minimally invasive remediation method, where plants stimulate microbial colonization in the rhizosphere to enhance biodegradation of oil contaminants.

Biodegradation is a natural and cost-effective method for oil spill remediation (Rehman et al., 2018), but often needs human intervention to enhance the degradation rate, such as biostimulation or bioaugmentation using the addition of nutrients or bacterial inoculants, respectively (Das & Chandran, 2011; Haritash & Kaushik, 2009; Lee et al., 2015; Raju & Scalvenzi, 2018; Zhu et al., 2001). Plants may also be an effective method to enhance microbial biodegradation, owing to their extensive root surface area and release of exudates into the rhizosphere to support the microbial community (Bisht et al., 2015; Dhir, 2013; He & Chi, 2016; Lee et al., 2015; Macek et al., 2000; Martin et al., 2014; Muratova et al., 2009; Pilon-Smits, 2005; Shahzad et al., 2016), while some microorganisms can also benefit plants by reducing contaminant toxicity (e.g., contaminant catabolism) and providing plant growth enzymes (e.g., indole-3-acetic acid) (Afzal et al., 2019; Golubev et al., 2009; Hussain et al., 2019; J. Liu et al., 2018; Rehman et al., 2018, 2021). This synergistic relationship is an effective method for the bioremediation of contaminated sites, and recent research has confirmed the successful use of EFWs to remediate oil or hydrocarbon contaminants, summarized in Chapter 2.

To further assess whether EFWs can enhance oil spill recovery, we conducted an experiment to determine the removal of phenanthrene ($C_{14}H_{10}$) from contaminated freshwater microcosms by three emergent plants. Phenanthrene is a three ring PAC and a priority pollutant listed by the United States Environmental Protection Agency (US EPA, 2014). Due to its potential toxicity, the Canadian Council of Ministers of the Environment (CCME, 1999a) guideline for the protection of aquatic life suggest phenanthrene should not exceed 0.4 μg/L for long-term exposure in freshwater. The presence of phenanthrene in the environment is often used as an indication of oil contamination (Ghosal et al., 2016; Waigi et al., 2015), and was a

prevalent compound detected in previous in-lake, model oil spill research at the IISD-ELA (Stoyanovich et al., 2022; and Chapters 3 & 4).

The objective of this chapter was to assess the efficacy of different wetland plants (*Typha* sp., *Carex utriculata*, and *C. lasiocarpa*) to enhance removal of phenanthrene from freshwater, and to compare removal rates among plant treatments. I hypothesized that plants would contribute to the removal of phenanthrene, and that removal rates would vary by plant type.

5.2 Methods

5.2.1 Chemicals

Phenanthrene ($C_{14}H_{10}$; molecular weight: 178.23 g/mol) in methanol (5000 µg/mL; CAS: 85-01-8) and phenanthrene d-10 ($C_{14}D_{10}$; molecular weight = 188.29) in methanol (2000 µg/mL; CAS: 1517-22-2) were obtained from Sigma Aldrich (St. Louis, Missouri, USA). Phenanthrene d-10 was diluted in Optima ™ methanol to form a stock solution of 5 ng/µL as the recovery internal standard (RIS) for assessing extraction efficiency and phenanthrene concentration using isotope dilution calculations.

Microcosms of lake water, described in Section 5.2.2 below, were initially amended with 10% strength modified Hoagland nutrient solution, using stock solutions of macronutrients; KNO_3, $Ca(NO_3)_2•4H_2O$, $MgSO_4•7H_2O$, KH_2PO_4, micronutrients; H_3BO_3, $MnCl_2•4H_2O$, $ZnSO_4•7H_2O$, $CuSO_4•5H_2O$, and $H_2MoO_4•2H_2O$, and an iron solution of $C_{12}H_{12}Fe_2O_{18}$ (Hoagland & Arnon, 1938). A 5% strength modified Hoagland nutrient solution in lake water was used to replace water lost to evapotranspiration. Final nutrient concentrations in one litre of media are indicated in Table C1, and were selected to ensure that nutrient availability was not a limitation of the study, but that it was not representative of completely unrealistic conditions, as

boreal lakes at the IISD-ELA are oligotrophic and have poor nutrient availability. However, noting that concentrations in 5% media are considered hypereutrophic based on Wetzel (1983) trophic classifications in Spalinger and Bouwens (2016).

5.2.2 Experimental Design

Glass microcosms (4 L capacity jar; height: ~ 25.5 cm; diameter: ~ 15.25 cm; jar mouth diameter: ~10 cm) of lake water (3 L filtered with 52 μm nitex mesh to remove zooplankton) from Lake 260 at the IISD-ELA were established with and without emergent vegetation in triplicate for each treatment (**Error! Reference source not found.**). Plants, *Typha* sp. (cattail), *Carex utriculata* (common beaked sedge, here-after referred to as Sedge A), and *C. lasiocarpa* (wiregrass sedge, here-after referred to as Sedge B), were collected from the Lake 260 wetland on June 6, 2022, and were thoroughly rinsed in the lake and with a hose to remove sediment or soil that could sorb phenanthrene. As discussed in Chapters 3 and 4, identification of *Carex* species is difficult due to the large number of species characterized by minor differences (Naczi, 1992, as cited in Starr et al., 2009), and species names should be compared with caution.

Experimental Treatments (in triplicate)

(A) Lake Water (no phenanthrene or plants)
(B) Phenanthrene (no plants)
(C) Cattail
(D) Sedge A
(E) Sedge B
(F) Phenanthrene + Cattail
(G) Phenanthrene + Sedge A
(H) Phenanthrene + Sedge B

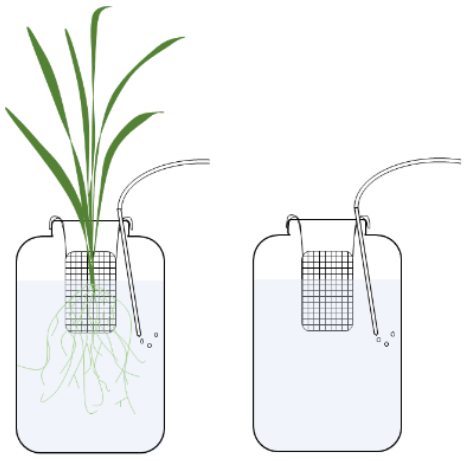

Figure 5.1. List of experimental treatments (in triplicate) and microcosm diagram (excluding foil cover and sample port; not to scale). Images of the entire experimental set up are included in Figure C1.

Plants were placed into uncoated stainless steel perforated pots (7.6 cm diameter and 10.16 cm long) to support hydroponic growth and placed into experimental microcosms of 3 L lake water amended with 10% strength Hoagland nutrient solution. It was particularly important to create these hydroponic pots with stainless steel, as PACs and oil compounds can adsorb to the surface of some plastic material, such as polyethylene (Fries & Zarfl, 2012), and coated or galvanized stainless steel can include Zn and other elements that may leach into the water.

Hydroponic pots initially received either one Cattail, two Sedge A, or five Sedge B, and microcosms without plants received an unplanted hydroponic pot. Microcosm jars were covered with foil to reduce sunlight penetration into the water with efforts to eliminate photodegradation or photooxidation of phenanthrene, which can form more toxic photoproducts (McConkey et al., 1997). Microcosms were then randomly placed in a larger pool of water to maintain similar temperature between microcosms, gently aerated, and left for five weeks at ambient environmental conditions to establish. Because there was no wind or wave aeration as would be observed in a lake, aerators were connected to each microcosm with aquarium tubing and a glass pipette (**Error! Reference source not found.**), providing gentle aeration to ensure mixing and reduce chance of anoxia from root respiration or metabolism. Water added to the microcosms to make up for evaporative loss or transpiration was amended with 5% strength Hoagland solution in lake water. Plants that died were removed and replaced during the establishment period. During establishment this only included one Sedge B plant, replaced in microcosm 20 (Phenanthrene + Sedge B).

The experiment was established in a fenced region covered with greenhouse plastic to eliminate dilution from precipitation events while maintaining natural light availability and air flow. The amount of photosynthetic active radiation (PAR) reduced by the greenhouse plastic

was ~20%, determined using a LI COR data logger (Model LI-1400, Serial No. DLA-1921, U.S.A.) over five-minute intervals for one hour on June 27, 2022. Onset HOBO Pendant MX Temperature/Light loggers were deployed in a non-experimental microcosm (without plants), in the pool, and above the pool to record temperature (℃) and light (lux) every five minutes.

Once established, the experimental microcosms received an injection of 0.6 mL of phenanthrene standard (5000 μg/mL in methanol) to reach an initial nominal concentration of 1 mg/L (day 0), and were monitored for basic water quality, phenanthrene chemistry, plant growth metrics, and microbial biofilm metrics over three weeks.

5.2.3 Basic Water Quality

Microcosm water was monitored for temperature (℃), dissolved oxygen (DO; mg/L), specific conductivity (μS/cm), and pH every 3 days using a Yellow Springs Instrument (YSI) Professional Series Plus multiparameter meter (YSI QUATRO, 18C100206. Xylem, Yellow Springs, Ohio). During monitoring, all non-contaminated microcosms were measured first with efforts to reduce risk of phenanthrene contamination between microcosms and the probe was rinsed thoroughly with lake water after each measurement.

5.2.4 Phenanthrene

5.2.4.1 Extraction. Water was sampled from microcosm treatments A, B, F, G, and H for phenanthrene analyses on days 0 (taken 4-7 hours after application to ensure mixing post injection), 2, 5, 10, and 21, using a 30 mL gas tight glass syringe attached to a stainless steel luer lock and glass borosilicate filter (GF/C, 1.2 μm pore size) to remove any suspended solids (e.g., roots/ biofilm). Prior to sample collection, water with 5% strength Hoagland solution was added to the microcosms to replace water loss from evapotranspiration and bring microcosms back to 3 L. Using an empty syringe, air was sparged through the sample port (stainless steel straw and

Teflon tubing) to mix the microcosm water prior to sample collection. Initially, 5 mL of water was collected to rinse the syringe and luer lock/filter system and disposed into waste. Then 25 mL of water was collected, and 20 mL was filtered into a 40 mL amber vial with a Teflon cap for phenanthrene extraction. The remaining 5 mL of water was sampled for photoelectrochemical oxygen demand analyses, however methanol in the phenanthrene standard skewed interpretation and is discussed further in Appendix C- Section C.2. During each sample period, a method blank was collected following methods described above with Optima ™ water.

For extractions, each sample vial received 20 μL of 5 ng/μL of phenanthrene d-10 Recovery Internal Standard (RIS; in methanol), 0.5 g of sodium chloride (NaCl; salt) and was gently mixed until dissolved, followed by the addition of 10 mL of dichloromethane (DCM). The vial was vortexed using an S/P Deluxe Mixer (S8220; McGaw Park Illinois) for 20 seconds, pressure in the vial was released in a fume hood, followed by another 20 second vortex. Using glass borosilicate Pasteur pipettes, the DCM was carefully removed and placed into a 30 mL glass vial with a Teflon cap. Another 10 mL of DCM was added to the vial to repeat the extraction process. Upon completion, the vial was sealed and refrigerated until further extraction and analyses.

At the Centre for Oil and Gas Research and Development (COGRAD) laboratory (University of Manitoba, Winnipeg, MB), sodium sulphate (Na_2SO_4) was added to each sample vial and vortexed to remove any water contamination remaining from the extraction process. The solvent was transferred to a clean glass vial, and the sample vial was rinsed twice with Optima ™ hexane to ensure all extracts were removed from solids, and the solvent was transferred into the corresponding vial. A solvent exchange was performed with liquid-liquid extraction using Optima ™ hexane and the DCM was evaporated using a nitrogen gas evaporator (N-

EVAP™111, Organomation Associates Inc., MA, USA and OA-SYS Heating System) until 1 mL of hexane remained. To each sample, an instrument performance internal standard (20 µL of 5 ng/µL d10-anthracene) was added and the sample was transferred to an amber vial.

5.2.4.2 Quantification. Phenanthrene and phenanthrene-d10 were detected and quantified in extracts on an Agilent 7890 gas chromatograph coupled to a 7000C triple quadrupole mass spectrometer, following methods and conditions outlined in Idowu et al. (2018). Using isotopic dilution methods, previously described in Heumann (1992, 1986), the peak area of deuterated phenanthrene RIS (representing 100 ng) was used to calculate concentration of phenanthrene in each sample (Equation 1). Mean (±SD) extraction efficiency over the duration of all sample periods was 84 ± 16 %.

$$Equation\ 1.\ Phenanthrene\ Concentration\ (mg/L) = \left(\frac{\left(\frac{phenanthrene\ peak\ area}{phenanthrene\ d10\ peak\ area} \right) * 100\ (ng)}{sample\ volume} \right) \Big/ 1000$$

5.2.5 Plant Growth

In order to determine if plants were impacted by potential phenanthrene toxicity, microcosms were monitored for plant counts (number of live plants), maximum height (mm; gently measured the stretched leaf with a meter stick) and any notable changes (e.g., browning leaves) every 3 days, and for biomass (g) at the end of the study. Plants were divided into above and belowground material and weighed to determine wet biomass (g). Dry biomass was measured (g) after drying in an oven at 60 ℃ for 48 hours.

5.2.6 Microbial Biofilm

Adenosine triphosphate (ATP) and oxygen consumption (respirometry trials) were monitored three times (days 1, 8, and 15) over the duration of the experiment in root and microbial biofilm samples.

5.2.6.1 Adenosine Triphosphate. LuminUltra 2nd Generation ATP ® Testing kits and PhotonMaster Luminometer were used to measure total ATP (pg) of the root biofilm, that directly corresponds to microbial biomass (LuminUltra, n.d., 2017). Following manufacturers guidelines for measured deposit, small root samples were collected weekly (days 1, 8, and 15) from each microcosm containing plant material. In order to standardize to root metrics, the roots were removed from the lysing agent following the assay and rinsed three times in deionized reverse osmosis water and gently dried using a kimwipe. Root samples were weighed for wet biomass (g) and photographed for surface area (cm^2) determined using Fiji software (v. 1.53c; Schindelin et al., 2012). Roots were then dried for 24 hours at 60 ℃, and weighed for dry biomass (g). ATP in each root sample was calculated by manufacturers calculations and standardized to dry root weight, which had the best linear relationship compared to wet weight and area.

5.2.6.2 Respirometry. Respirometry trials were conducted to measure the rate of oxygen consumption by roots and associated microbial biofilm in weekly experiments. Lake water was aerated to saturation for at least 30 minutes, filtered through a 0.2 μm filter, and pipetted into PreSens glass SensorVials SV-PSt5-20 mL. Vials were then placed into a dark, temperature-controlled environment (21 ℃) for thirty minutes. The vials were removed and microbubbles forming on the sensor were removed. Five centimeter root clippings collected from each microcosm containing plant material were placed into designated vials, filled with the filtered lake water and sealed with a lid to ensure no gas filled headspace. Vials were placed into PreSens SDR Sensor Dish Reader, in a dark, temperature-controlled environment set for 21 ℃. Each SDR Sensor Dish Reader included a triplicate control of filtered lake water with no root clippings to measure background noise or potential oxygen consumption. Oxygen concentration

(mg/L) was recorded every two minutes until the end of the trial using PreSens software (SDR v4.0.0). Upon completion, roots were extracted and analyzed for biomass (g) and surface area (cm^2) as described in Section 5.2.6.1, which were then used to correct rate of oxygen consumption per root metric (e.g., mg O_2/L/minute/mg).

5.2.7 Statistical Analyses

Statistical analyses were performed using R (4.2.2) in R Studio (2023.09.1 + 494) (Posit Team, 2023; R Core Team, 2022) primarily using tidyverse (v. 2.0.0, Wickham et al., 2019), and visualized using ggplot2 (v. 3.4.1, Wickham, 2016). Primary R packages used for data analyses are described below for each metric, and additional packages are included in Appendix D.

5.2.7.1 Basic Water Quality. Basic water quality was analyzed for significant differences with an analysis of variance (ANOVA) or Kruskal Wallace test, based on normality and homoscedasticity of the dataset, followed by pairwise comparisons of treatments using Tukey Kramer Honest Significant Differences (HSD) or Dunn Test (with holm *p*-value adjustment methods), using the *stats* (v.4.2.2; R Core Team, 2022) and *FSA* packages (v. 0.9.4; Ogle et al., 2023). This was conducted by using the parameter mean for each microcosm (day 1-19) as a treatment replicate for the ANOVA or Kruskal Wallace. Significant differences were identified with a p-value < 0.05. In addition, Generalized Additive Mixed Models (GAMM) were prepared to assess water quality response as a result of the interaction between time and treatment. GAMMs were prepared following modified script from Pedersen et al. (2020, 2019) and Wood (2017) using the *mgcv* package (v 1.9-0; Wood, 2023, 2017, 2004). Models included the overall effect of treatment, a group level smoother of exposure day by treatment using thin plate regression splines (Wood, 2003), and a random effect smoother for microcosm replicates by treatment, using the restricted maximum likelihood method (Wood, 2011). Global smoothers

for time were not included to allow trends of each treatment type to vary without penalty for specific conductivity and pH GAMMS. However a global smoother for time was included in the DO GAMM due to similar trends between treatments over the exposure period. GAMMs were plotted in ggplot2 (v. 3.4.1, Wickham, 2016) by predicting the model daily for 21 days for each microcosm replicate and wrapped by treatment. It should be stated that GAMM outputs are approximate, and have been conducted to support interpretation of data. Details on limitations and results are included in Appendix C- Section C.3.

5.2.7.2 Phenanthrene. Phenanthrene removal rates (mg/hour) were calculated for each treatment using mixed effect, first order exponential decay model (Equation 2). The SSasymp function in nls (*stats* package; v.4.2.2; R Core Team, 2022) was used to identify initial values to develop the exponential decay model using the *nlme* package (v. 3.1-160; Pinheiro, Bates, & R Core Team, 2022; Pinheiro & Bates, 2000). Microcosm replicates served as the random effect for the y-intercept, and fixed effects were the y-intercept and rate. Visualization of exponential decay models were based on hourly predictions over 600 hours. The model was used to identify differences between rates (k) of phenanthrene removal with a 95% confidence interval and the DT_{50} for each treatment (Equation 3), which is the time to get to half of the initial concentration (United States Environmental Protection Agency, 2023a, 2023b).

$Equation\ 2. First\ Order\ Exponential\ Decay$	$y_t = y_0 e^{-kt}$
$Equation\ 3. DT50$	$DT50 = ln2/k$

y_0= intercept (initial phenanthrene concentration), k=slope/rate of removal, t=study time (hour); Model sourced from United States Environmental Protection Agency (2023a, 2023b).

5.2.7.3 Plant Growth. Plants, initially planted with one Cattail, two Sedge A, and five Sedge B per microcosm, were established for 5 weeks, which resulted in new shoots in some microcosms prior to the start of the experiment. Over the experimental period, the number of Cattail in each microcosm did not change, however numbers of Sedge A and Sedge B varied due to new shoot growth. No statistical analyses were conducted for plant counts, however relationships to final biomass were analyzed for some water quality parameters with a linear model using the *stats* package (v.4.2.2; R Core Team, 2022). In addition, biomass was not statistically analyzed to determine potential impact of phenanthrene as they were collected from a donor wetland and may have had different initial biomass. Table C5 includes summary of final dry biomass by treatment.

Plant growth rates (height) were analyzed using mixed effect growth models to assess whether phenanthrene impacted the plant. Due to insect consumption on leaves in some Sedge A treatments, they could not be modelled for growth rates and were excluded from analyses. A logistic growth model was used to measure height growth rates for Cattail treatments, however not all Sedge B reached a carrying capacity/stationary phase and did not follow logistic growth. Growth rates for Sedge B were estimated using exponential growth models. It is acknowledged that plants will not grow indefinitely, but as plants did not reach the stationary phase in all microcosms, this model allowed for identification of rates during the experimental period.

Logistic growth was modelled using the SSlogis self-starting function from nls (*stats* package v.4.2.2; R Core Team, 2022) to identify starting values for a mixed effect logistic growth model (Equation 4), modified from Paine et al. (2012), using the *nlme* package (v. 3.1-160; Pinheiro et al., 2022; Pinheiro & Bates, 2000). Each microcosm replicate served as the random effect for carrying capacity, and fixed effects were carrying capacity, b, and rate.

Exponential growth was modelled using nls (*stats* package v.4.2.2; R Core Team, 2022) and SSexpf self-starting function from the *nlraa* package (v.1.9.3; Miguez, 2023) to identify starting values for a mixed effect exponential growth model (Equation 6) using the *nlme* package (v. 3.1-160; Pinheiro et al., 2022; Pinheiro & Bates, 2000). Each microcosm replicate served as the random effect for the intercept, and fixed effects included intercept and rate. Visualization of growth models were based on daily predictions for 25 days.

Differences in intrinsic growth rate (*r*) between phenanthrene exposed and unexposed plants were confirmed if the 95% confidence intervals did not overlap. The estimated intrinsic growth rate (est. r) can be used to calculate approximate finite growth rate (dH/dt; mm/day; Equation 5 & 7) for each microcosm (Paine et al., 2012; Vandermeer, 2010), noting there are limitations to this calculation with using the estimated rate for all replicates.

$Equation\ 4. Logistic\ Growth\ Model$	$H = k/(1 + be^{-rt})$
$Equation\ 5. Logistic\ Finite\ Growth\ Rate$	$dH/dt = (H * est.r) * \left(1 - \frac{H}{est.k}\right)$
$Equation\ 6. Exponential\ Growth\ Model$	$H = y_0 e^{rt}$
$Equation\ 7. Exponential\ Finite\ Growth\ Rate$	$dH/dt = H * est.r$

H = height; k =carrying capacity; est.k = estimated model carrying capacity; b=(k-N_0)/N_0 [N_0 = initial height, set to 20 mm]; r = intrinsic rate of growth; est.r = estimated intrinsic model rate; t = time (exposure day); y_0 = intercept; dH/dt = finite growth rate [change in height over time; mm/day]; Model equations sourced or modified from (Paine et al., 2012).

5.2.7.4 Microbial Biofilm. Root biofilm ATP concentrations were compared for significant differences (p<0.05) during each sample period using a Kruskal Wallace test,

followed by multiple pairwise comparisons using a Dunn Test (holm *p*-value adjustment) with the *stats* (v.4.2.2; R Core Team, 2022) and *FSA* packages (v. 0.9.4; Ogle et al., 2023). Rates of oxygen consumption were calculated with a linear model for each individual vial over 1.5 hours from minute 300 to 390 to ensure temperature acclimatization and that not all oxygen had been consumed. On each PreSens SDR Sensor Dish Reader, triplicate controls of filtered lake water with no root clippings were used to correct for background noise in the experimental vials prior to rate calculations using a linear model in the *stats* package (v.4.2.2; R Core Team, 2022). The slopes were then corrected for dry biomass and were compared for significant differences ($p < 0.05$) between microcosm treatments using an ANOVA and Tukey HSD for each sample period using the *stats* package (v.4.2.2; R Core Team, 2022). The relationship between oxygen consumption (mg/L/min) and dry root biomass (mg) were analyzed with a linear model using the *stats* package (v.4.2.2; R Core Team, 2022).

5.3 Results

5.3.1 Basic Water Quality

Temperatures were recorded every 5 minutes during the experimental period with the use of Onset HOBO Pendant MX temperature and light loggers in a microcosm, the containment pool, and outside the pool. Mean temperature(± standard deviation [SD]) in the microcosm was 20.79 ± 3.111 ℃ (range: 14.50 to 28.65 ℃; n=6,087), similar to pool conditions of 20.88 ± 3.127 ℃ (range: 14.45 to 29.43 ℃; n=6,092). Temperatures outside were more variable, likely due to greater sun exposure, at 22.26 ± 8.320 ℃ (range: 10.38 to 55.08 ℃; n=6,089) (data not shown). Temperature was also monitored with a multimeter probe every 3 days. A Kruskal Wallace test indicated significant difference between treatments (χ^2=18.90, p=0.008, df=7). However, a multiple pairwise Dunn Test revealed no significant differences between treatments

with holm adjusted *p*-values (Figure C2). It is important to note that multimeter probe measurements were a snapshot of the conditions at the time of measurement, and do not reflect potential diurnal patterns. Light exposure was also recorded with the HOBO Pendant MX loggers and was lowest in the microcosm at 82.85 ± 341.1 lux (range: 0.00 to 12,180.48 lux; n=6,087), followed by pool conditions of 7,083.90 ± 12,736.4 lux (range: 0.00 to 61,829.12 lux; n=6,092), and outside the pool at 8,843.71 ± 14,707.9 lux (range: 0.00 to 80,138.24 lux; n=6,089) (data not shown), demonstrating that the foiled microcosms had reduced light exposure. This is particularly important in order to confirm whether loss of phenanthrene in the microcosms was due to plant presence or other external factors, like photodegradation caused by sunlight penetration.

Trends in microcosm conductivity displayed clear differences among treatment types, which appeared to increase in microcosms with decreasing plant biomass (Figure 5.2A). The lowest mean (± SD) conductivity was in Phenanthrene + Cattail (148.1 ± 34.16 μS/cm; n=21) and Cattail (166.4 ± 36.07 μS/cm; n=20) microcosms, while the highest conductivity was recorded in Phenanthrene (373.1 ± 67.33 μS/cm; n=21) and Lake Water (418.1 ± 98.73 μS/cm; n=21) microcosms. An ANOVA confirmed a significant difference among treatments ($F = 82.1$, $p = 2.42e^{-11}$, Df = 7), and trends by plant type (Figure 5.2B). A linear model assessing the relationship between total dry biomass and mean conductivity revealed a significant, moderate negative relationship ($y = -8.534x + 331.457$, $p = 0.0004$, $R^2 = 0.55$) (Figure C3). The results of a GAMM indicated a significant effect of interactions between exposure day and treatments of Lake Water ($p < 2e^{-16}$), Phenanthrene ($p = 5.68e^{-04}$), Phenanthrene + Cattail ($p = 6.87e^{-03}$), Sedge A ($p = 8.72e^{-03}$), Phenanthrene + Sedge A ($p = 7.19e^{-03}$) and Phenanthrene + Sedge B ($p = 1.04e^{-03}$) on conductivity with 89.3% deviation explained ($R^2 = 0.869$, n = 167, -REML = 805.75)

(Figure C4;Table C2). As well, there was only one significant random effect of microcosm replicate for the Lake Water treatment ($p = 0.0483$) on conductivity.

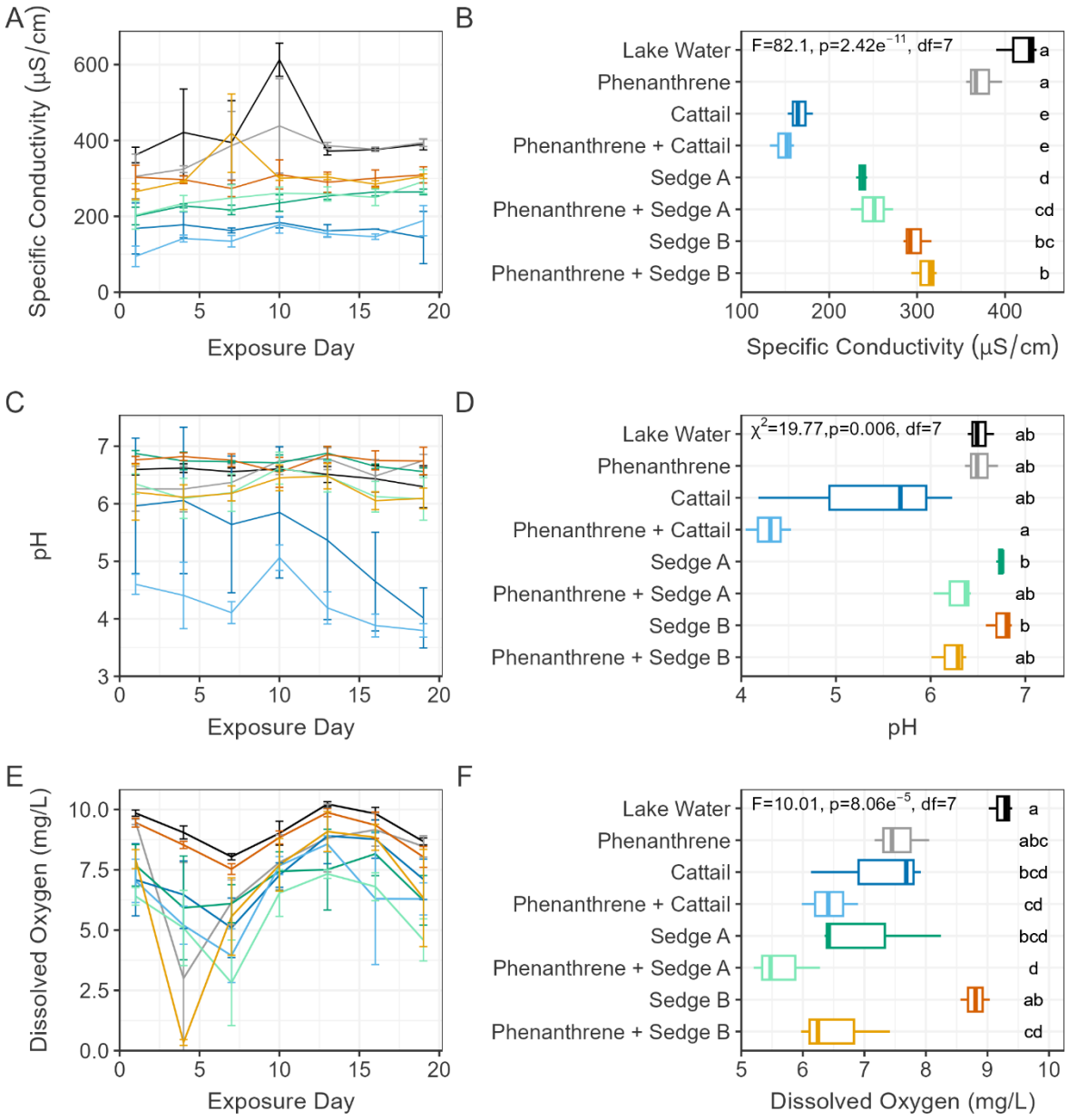

Figure 5.2. Mean trends and boxplots of specific conductivity (A&B), pH (C&D) and dissolved oxygen (E&F) in freshwater microcosms over the experimental period. Error bars in trend figures represent standard deviation of microcosm replicates (n=3). Letters in boxplot figures represent significant differences ($p<0.05$) identified from parametric (ANOVA and Tukey Kramer HSD) or non-parametric (Kruskal Wallace and Dunn Test) multiple pairwise comparisons. Note: One Cattail microcosm replicate had a conductivity under range on day 16.

Trends in pH suggest some differences between treatments, specifically in microcosms containing Cattail, which appeared to have lower pH than other treatments that were more clustered together over the experimental period (Figure 5.2C). A Kruskal Wallace test identified a significant difference in microcosm pH between treatments ($\chi^2 = 19.77$, $p = 0.006$, Df = 7), and a Dunn Test confirmed significant differences between Phenanthrene + Cattail to Sedge A ($p_{holm\text{-}adj} = 0.05$) and Sedge B ($p_{holm\text{-}adj} = 0.03$) treatments, but no other significant differences were identified (Figure 5.2D). Pairwise comparisons, however, do not consider the slope or trend of pH over the exposure period. For example, the pH in Cattail microcosms declined over the exposure period resulting in a wide distribution, as observed in the boxplots (Figure 5.2D). A GAMM indicated there were significant effects between the interaction of exposure day and Lake Water ($p = 0.0370$), Phenanthrene ($p = 1.26e^{-03}$), Cattail ($p < 2e^{-16}$), Phenanthrene + Cattail ($p < 2e^{-16}$), and Phenanthrene + Sedge A ($p = 0.0161$) treatments on pH, with 96.3% deviance explained ($R^2 = 0.952$, n = 168, -REML = 31.704), however acknowledging there may be limitations and approximations to these modelled values (Figure C5; Table C3). All microcosm replicates/random effects had a significant effect on pH ($p<0.05$), except Sedge A, and the greatest random effect was observed for Cattail microcosms, with larger variability of pH readings between replicates.

Dissolved oxygen varied over the exposure period for all treatments, but trends plummeted to near 0 mg/L on day 4 of exposure for some Phenanthrene and Phenanthrene + Sedge B microcosms (Figure 5.2E). These treatments also experienced visual changes to water conditions, where the water became slightly opaque and turbid, with a white appearance. The turbidity improved in the Phenanthrene + Sedge B treatments by day 7 where no cloudiness was noted. However, the water remained opaque and cloudy in the Phenanthrene treated microcosms

until exposure day 13, despite oxygen returning by day 7. Trends in DO also declined on day 7 in other microcosms, but were not as pronounced as Phenanthrene + Sedge B (Figure 5.2E; Figure C6). An ANOVA indicated significant differences of DO between treatments ($F = 10.01$, $p = 8.06e^{-05}$, $Df = 7$), and a Tukey HSD test identified some significant pairwise differences ($p < 0.05$) (Figure 5.2F).

Treatments that included vegetation typically had lower DO, excluding Sedge B microcosms, which was more similar to Lake Water treatment (Figure 5.2F). However, Phenanthrene + Sedge B had significantly lower DO than Sedge B (p=0.01). Generally, treatments containing phenanthrene had lower DO than their unexposed counterpart, however, these differences were not always statistically significant, and not as defined for Sedge A and Cattail treatments. A GAMM indicated there was a significant effect of exposure day ($p < 2e^{-16}$), and interactions between exposure day and treatments of Phenanthrene ($p < 2e^{-16}$) and Phenanthrene + Sedge B ($p < 2e^{-16}$) on DO concentrations, with 82.8% deviance explained ($R^2 = 0.784$, n = 168, -REML = 275.37) (Figure C6; Table C4). All treatment displayed a similar trend shape over time, however with more pronounced decline on day 4 in Phenanthrene and Phenanthrene + Sedge B microcosms as discussed. There were also some significant effects of microcosm replicates as the random effect for Cattail ($p = 2.02e^{-03}$), Sedge A ($p = 5.59e^{-04}$), and Phenanthrene + Sedge B ($p = 0.0194$) treatments on DO. Similar to pH, we acknowledge there are limitations and approximations to these modelled values, and should be interpreted with caution.

5.3.2 Phenanthrene

Concentrations rapidly declined in all treatments containing vegetation by the first sample event (hours 4-7), and concentrations remained elevated in Phenanthrene microcosms

without vegetation, with high variability (Figure 5.3). While an ANOVA revealed concentrations during the first sampling were not significantly different ($F = 3.784$, $p = 0.059$, $df = 3$), initial removal may occur quickly with plant treatment. By day 2 of exposure, concentrations continued to decline in both Phenanthrene + Cattail and Phenanthrene + Sedge A microcosms, remained stable in Phenanthrene + Sedge B microcosms, and increased slightly in Phenanthrene microcosms. By day 5, phenanthrene concentrations began to decline in Phenanthrene microcosms without vegetation, as well as in the Phenanthrene + Sedge B microcosms. After 21 days, all microcosms had over 94% removal of phenanthrene from the initial nominal concentration of 1 mg/L and over 89% from initial measured concentrations. Concentrations in experimental microcosms and method blanks are summarized in Table C6.

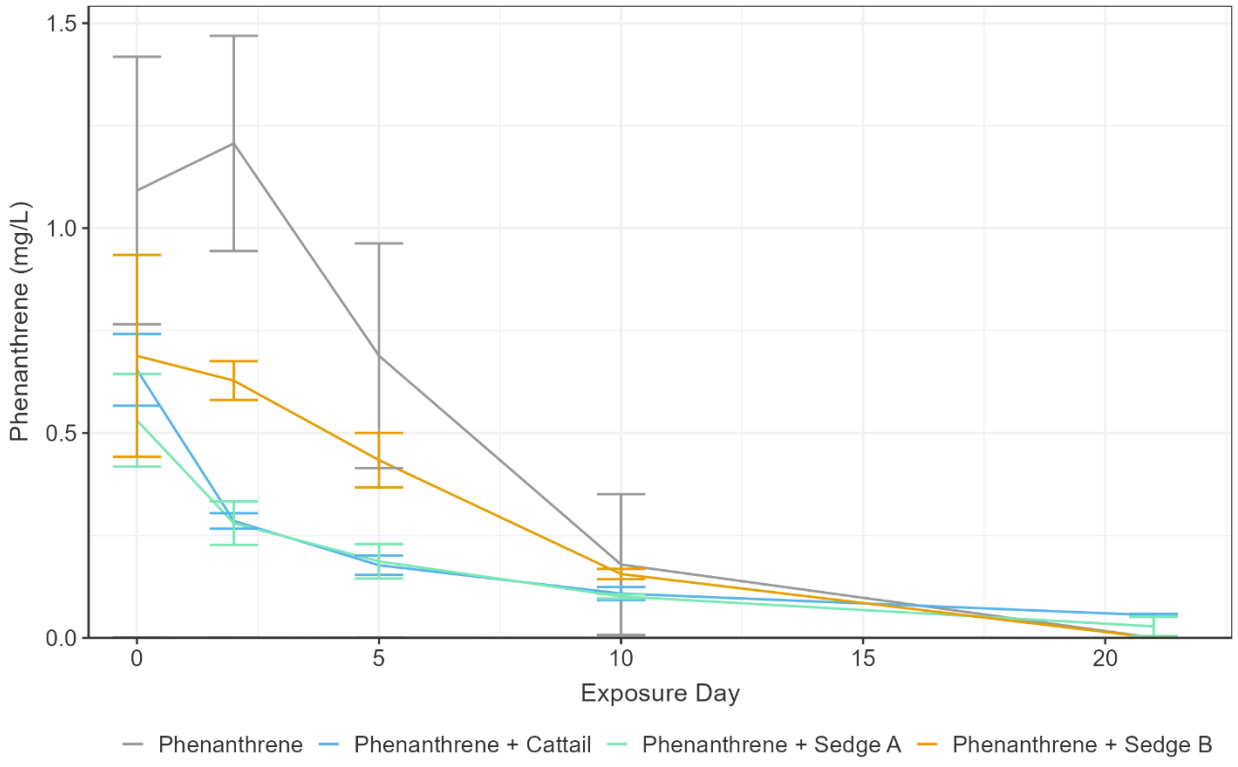

Figure 5.3. Mean concentration (± SD) of phenanthrene (mg/L) in microcosm water over 21 days of exposure. Error bars represent standard deviation of microcosm replicates (n=3).

Figure 5.4 displays models and the estimated removal rate (k) with 95% confidence interval range (overlap indicates no significant difference). Phenanthrene + Cattail treatments had higher removal rates than Phenanthrene + Sedge B treatments, however there were no differences between Phenanthrene + Sedge A and any other treatment. There was a small overlap between Phenanthrene and Phenanthrene + Cattail treatments, indicating no differences, but rates of phenanthrene removal by Phenanthrene + Cattail were generally higher. This was supported by the estimated DT_{50} generated from the model (Table 5.1), which was 55 hours, 78 hours, 120 hours, and 127 hours for Phenanthrene + Cattail, Phenanthrene + Sedge A, Phenanthrene, and Phenanthrene + Sedge B microcosms, respectively (acknowledging the rates are calculated based on initial concentrations (y_0), which were slightly lower for microcosms containing plants).

While an ANOVA indicated no significant differences for concentrations on day 0, the y_0 intercept generated from the model indicated that Phenanthrene microcosms had a greater initial concentration than the plant treated microcosms, supporting that treatments with vegetation may have rapid treatment of phenanthrene (Table 5.1). The relationship between removal rates and mean final plant dry biomass (g) of each plant treatment was analyzed with a linear model ($y = 0.0005x+0.0024$), revealing a strong positive correlation ($R^2 = 0.94$). However, this was not statistically significant ($p = 0.16$) (Figure C7).

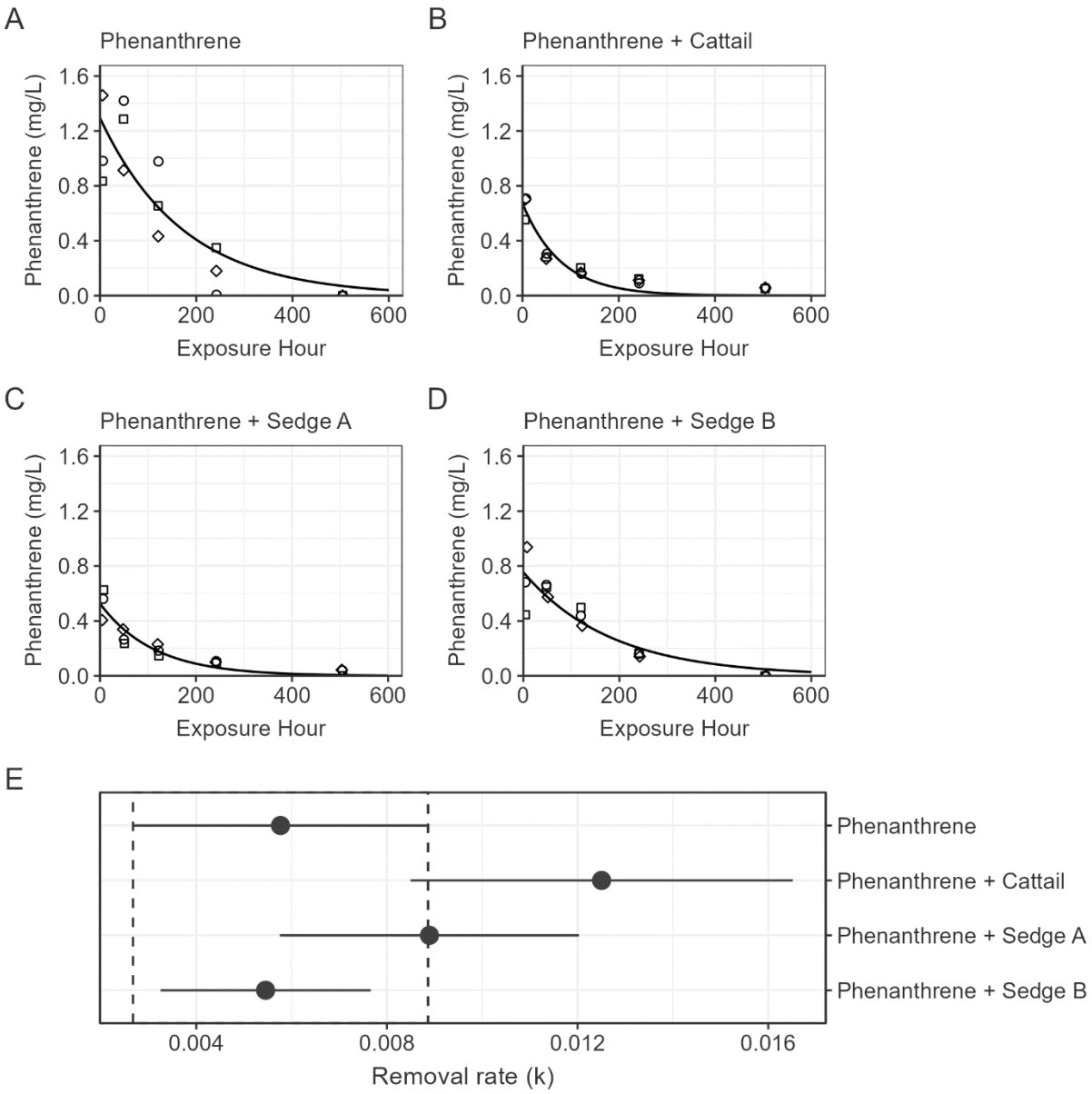

Figure 5.4. Non-linear, first order exponential decay models (lines) and microcosm replicate concentrations (points) (A-D), estimated removal rate (E) for each treatment. Model trends were based on hourly predictions over 600 hours. Whiskers in E represent 95% confidence interval, and dotted vertical lines are the 95% confidence interval range for Phenanthrene.

Table 5.1. First order exponential decay model output estimates (95% confidence interval).

Treatment	y0 (mg/L)	k	DT_{50} (hours)
Phenanthrene	1.29 (1.01- 1.58)	0.0058 (0.0027-0.0089)	120 (78-259)
Phenanthrene + Cattail	0.67 (0.57-0.77)	0.013 (0.0085-0.0165)	55 (42-82)
Phenanthrene + Sedge A	0.53 (0.44-0.61)	0.0089 (0.0058-0.0120)	78 (58-120)
Phenanthrene + Sedge B	0.76 (0.63-0.88)	0.0055 (0.0032-0.0077)	127 (90-213)

y0: Y intercept, k: removal rate, DT_{50}: Hours to reduce concentration to half of the initial concentration

5.3.3 Plant Growth

There were no differences in intrinsic growth rate (r) between Cattail (estimated rate: 0.186) and Phenanthrene + Cattail (estimated rate: 0.215), as identified with overlapping 95% confidence intervals from a logistic model of plant height (Figure 5.5). The finite growth rate (mm/day) varies daily with a logistic growth model, and the estimated growth on day 1 of exposure ranged from 6.90-41.5 mm/day and 10.7-13.5 mm/day for Cattail and Phenanthrene + Cattail microcosms. Of note, there was more variability in growth and carrying capacity of Cattail treatments compared to Phenanthrene + Cattail treatments, which may reflect growth stage when experiment started, as plants were not grown by seed. Similarly, there were no differences in intrinsic growth rates between Sedge B (estimated rate: 0.009) and Phenanthrene + Sedge B (estimated rate: 0.010) from the exponential growth model (Figure 5.6). Finite growth rate (mm/day) calculated on day 19 ranged from 8.72-10.10 mm/day and 9.79-10.50 mm/day for Sedge B and Phenanthrene + Sedge B microcosms. Some physical changes to the plants were observed with some leaves yellowing or browning, mostly occurring after 13 days of exposure, however this occurred in treatments with and without phenanthrene.

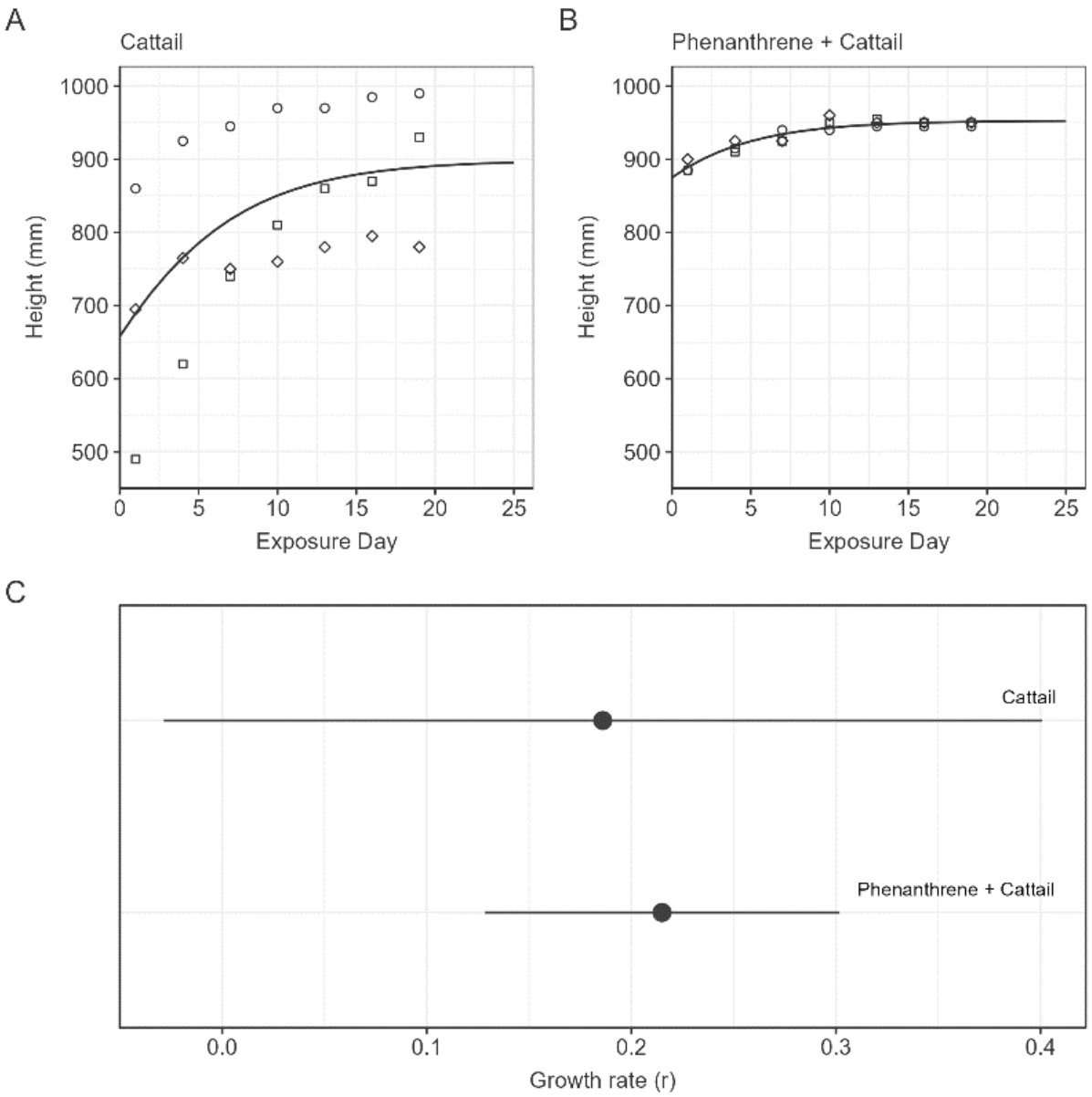

Figure 5.5. Logistic growth model (height) for Cattail (A) and Phenanthrene + Cattail (B) microcosms. Estimated intrinsic growth rate (r) and 95% confidence interval whiskers are presented in C. Model trends (A & B) were based on daily predictions for 25 days.

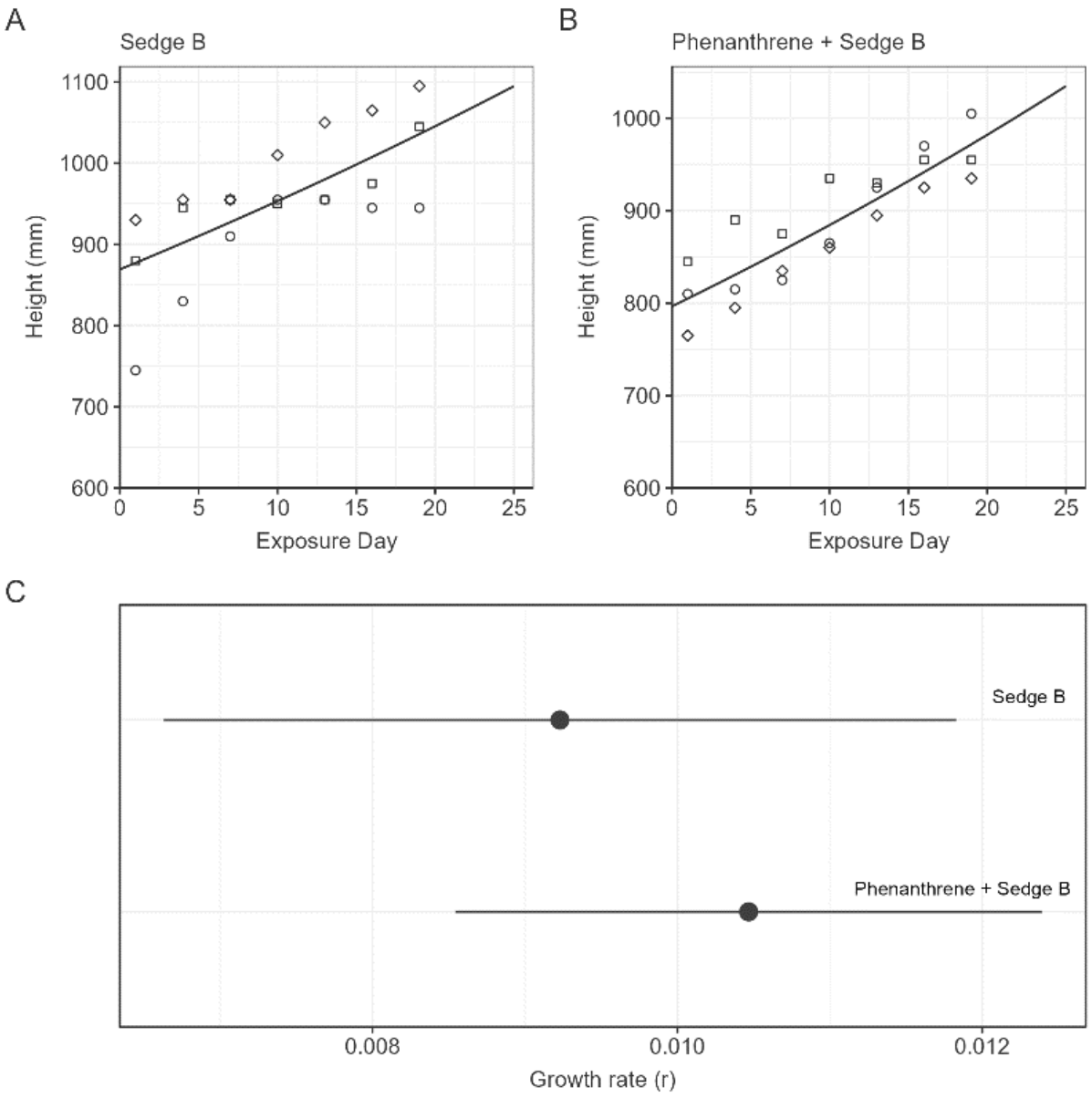

Figure 5.6. Exponential growth model (height) for Sedge B (A) and Phenanthrene + Sedge B (B) microcosms. Estimated intrinsic growth rate (r) and 95% confidence interval whiskers are presented in C. Model trends (A & B) were based on daily predictions for 25 days.

5.3.4 Microbial Biofilm

5.3.4.1 Adenosine Triphosphate. A Kruskal Wallace test on day 1 indicated significant differences of root and biofilm adenosine triphosphate (ATP) between treatments, and a Dunn Test further confirmed that Cattail had greater ATP/microbial colonization than Phenanthrene + Sedge B ($p_{holm} = 0.046$), however, no other differences were identified (Table 5.2). Further, there were no differences in ATP concentrations between treatments on days 8 and 15, however mean ATP concentration appeared higher for Cattail microcosms. Ultimately there were no statistical differences in ATP concentrations of individual plant types with or without phenanthrene exposure.

Table 5.2. Mean (± standard deviation of microcosm replicates [n=3]) root biofilm ATP (ng ATP/mg dry root) on days 1, 8, and 15 of exposure.

Treatments	**Day 1**	**Day 8**	**Day 15**
Cattail	680.7 ± 206.9 [a]	268.9 ± 202.5 [a]	332.3 ± 442.0 [a]
Phenanthrene + Cattail	152.3 ± 29.92 [ab]	93.87 ± 48.79 [a]	59.29 ± 27.09 [a]
Sedge A	218.3 ± 71.84 [ab] (n = 2)	119.0 ± 78.28 [a]	103.4 ± 102.5 [a]
Phenanthrene + Sedge A	99.57 ± 33.84 [ab]	112.0 ± 96.66 [a]	88.61 ± 26.73 [a]
Sedge B	295.2 [NA *](n = 1)	102.5 ± 112.6 [a]	43.22 ± 49.25 [a]
Phenanthrene + Sedge B	53.87 ± 65.47 [b]	113.2 ± 55.00 [a]	65.69 ± 37.74 [a]
Kruskal Wallace Test	$\chi^{2=}$ 11.02, $p = 0.03$, df = 4	$\chi^2 = 1.42$, $p = 0.92$, df = 5	$\chi^2 = 3.01$, $p = 0.70$, df = 5

Letters indicate significant differences ($p<0.05$) based on a Kruskal-Wallace test and Dunn Test with p-value holm adjustment; * Sedge B was not included in the Kruskal Wallace on day 1 of exposure due to an n of 1 (as final dry weights were negative or 0 due to housing weight).

5.3.4.2 Respirometry. When corrected for plant biomass, there were no significant differences in oxygen consumption by plant roots and biofilm between treatments on days 8 and 15. However, there were differences between some treatments on day 1 of exposure ($F = 6.198$, $p = 0.005$, df = 5) (Figure 5.7). Cattail treatments had greater oxygen consumption than Phenanthrene + Sedge B ($p = 0.007$) and Sedge B ($p = 0.006$) treatments. Of note, negative values represent slope of oxygen consumption/removal.

A linear model of dry biomass (mg) and uncorrected rate of oxygen consumption (mg O_2/L/min) revealed a moderate to strong, negative correlation on day 1 of exposure ($r^2 = 0.76$, $p = 2.61e^{-06}$, y = -0.001x-0.0002), indicating that larger roots had greater oxygen consumption. While there was no correlation on day 8 ($r^2 = 0.23$, $p = 0.04$, y = -0.0006x-0.002) and a minor correlation on day 15 ($r^2 = 0.50$, $p = 0.001$, y = -0.0006x-0.0008) (Figure C8), with significant relationships in all analyses. Due to the variation, there may be other plant or microbial functions influencing oxygen consumption during different time points. However, ultimately there were no significant differences in oxygen consumption of individual plant types previously exposed or unexposed to phenanthrene.

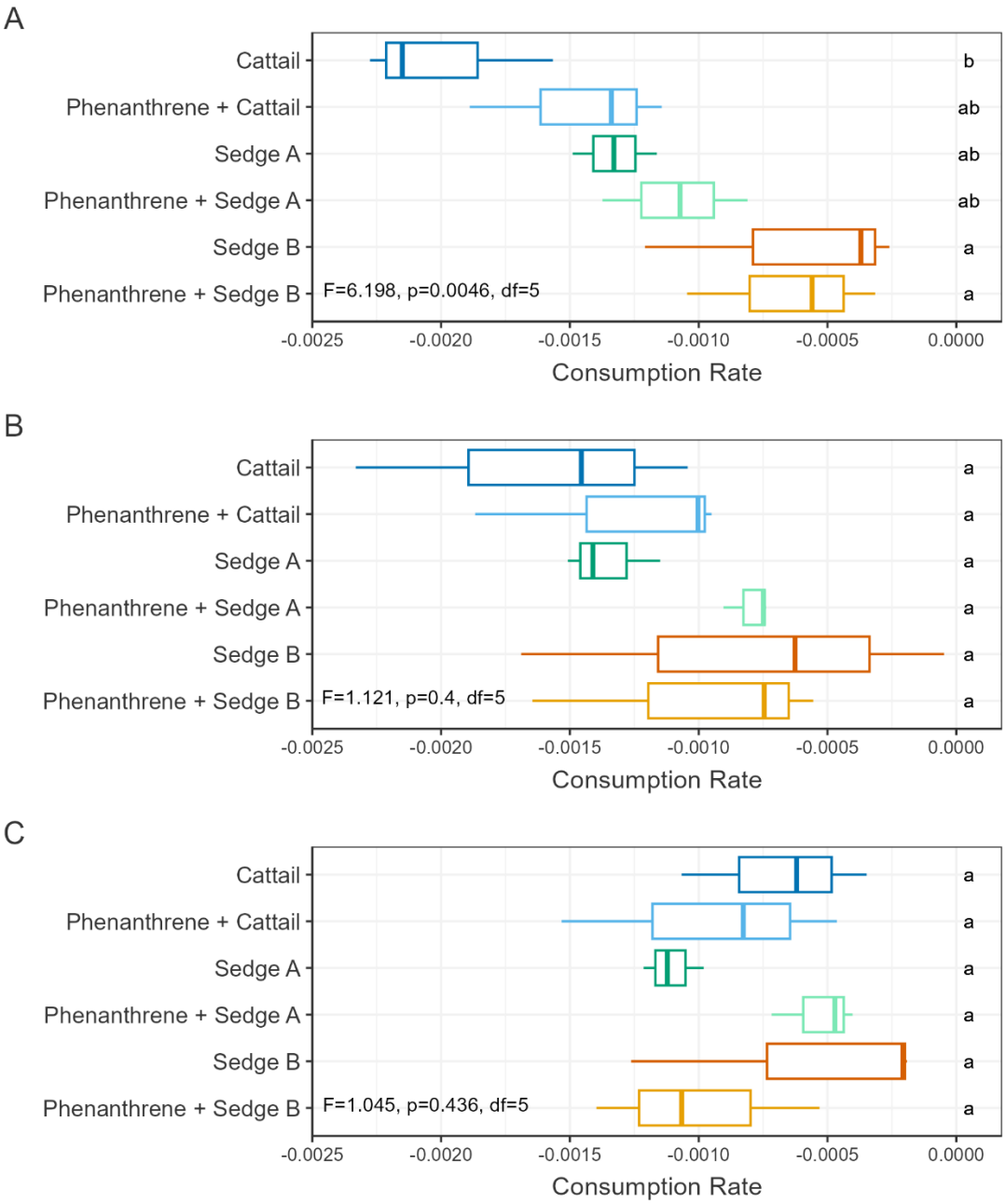

Figure 5.7. Rate of oxygen consumption (mg O2/L/min/mg dry weight) from minute 300 to 390 during respirometry trials on (A) day 1, (B) day 8, and (C) day 15 of the experiment (negative values indicate oxygen removal). Letters represent significant difference ($p < 0.05$) as identified with an ANOVA and Tukey Kramer pair-wise comparison during each sample period.

5.4 Discussion

Mean microcosm temperatures were often within optimal conditions for biodegradation of petroleum hydrocarbons (HOBO Pendant MX logger data; Section 5.3.1), which ranges from 20-30 ℃ for freshwater environments (Atlas, 1985, as cited in Al-Hawash et al., 2018; Bartha & Bossert, 1984, and Cooney, 1984, as cited in Das and Chandran, 2011). Water quality monitoring that occurred every 3 days had slightly lower temperatures, but these data represent a snapshot of microcosm conditions and may have been influenced by cooler overnight temperatures, which in-turn, may influence biodegradation. There were no pairwise differences in microcosm treatments on temperature (Figure C2), however, the order and length of time required to measure each microcosm may have had an influence on multimeter probe readings (see Section 5.2.3 & 5.3.1). While not significantly different, the boxplots indicate that uncontaminated microcosms generally had lower temperatures than microcosms containing phenanthrene, which may result from lower temperatures overnight. This may have an influence on other measurements such as pH and DO (Barron et al., 2005; Jones et al., 2017) that also exhibit diurnal patterns (CCME, 1999b; Dodds, 2002; Pokorný & Květ, 2004), and should be considered in further interpretation of data.

Trends and relationships of other water quality parameters displayed some significant differences between treatments. For example, there was a clear relationship between plant type and conductivity (Figure 5.2B). It was hypothesized that plants with larger biomass would have greater nutrient uptake, resulting in decreased salt content in microcosms from Hoagland media and hence lower conductivity. Although the data revealed a negative correlation in this relationship (Figure C3), there may also be a plant-specific effect on uptake (e.g., surface area, transpiration). Table C5 includes a summary of final dry biomass by treatment. The GAMM

(Figure C4; Table C2) indicated significant interactions between exposure day and some treatments, which may be caused by peaks in data as observed for Lake Water microcosms, or increasing trends over the exposure period. While inconclusive, as plant growth and metabolism slow, there may be a reduced requirement for nutrients causing nutrient salt content to slowly increase over time.

A plant effect was also observed for pH, where Phenanthrene + Cattail microcosms generally had lower pH than other treatments, though not always statistically significant. Differences in pH may have been caused by root respiration, plant exudation, and/or metabolism (Das & Chandran, 2011; Hinsinger et al., 2003; Lee et al., 2015), though metabolism was not likely the driver, as pH declined prior to the start of the experiment (data not shown). Stottmeister et al. (2003) summarized that organic acids and other exudates can be released under nutrient limitation. In our study, the rapid uptake of nutrient salts by cattail may have resulted in lower nutrient availability in the microcosm, potentially causing the plants to release acids. It is also possible that cattails have different exudation products than the two sedge species, or greater respiration. Although significant differences were not observed for Cattail microcosms, trends indicate declining pH over the experimental period (Figure 5.2D; Figure C5; Table C3), perhaps a result of increasing acidic exudates. However, noting there was a strong influence of microcosm replicate on the Cattail model, indicating variability of readings between microcosms. While it did not appear to impact degradation, low pH can influence biodegradation potential as optimal conditions range from 6.5 to 8, and may further influence microbial composition (Lee et al., 2015). It is clear there were effects of plant type on microcosm water quality, however no impact of phenanthrene on conductivity or pH were identified.

Differences in DO, while not always statistically significant, revealed a potential effect of both plant type/biomass and phenanthrene. An important note is that plants can both release oxygen into the rhizosphere, allowing them to grow under harsh anoxic conditions, and also consume oxygen through root respiration (Pokorný & Květ, 2004; Stottmeister et al., 2003). It is likely that both factors are observed in our measurements, while noting that these represent a snapshot of microcosm conditions, and oxygen in aquatic ecosystems often follow diurnal patterns (CCME, 1999b). Generally, microcosms containing larger plants (Cattail and Sedge A), with or without phenanthrene, had lower DO than Sedge B and Lake Water (Figure 5.2F), which may be a result of greater root respiration. Interestingly, microcosms of Phenanthrene + Sedge B had significantly lower DO than Sedge B microcosms, indicating an effect of phenanthrene. This was also observed in treatments without vegetation, where Phenanthrene microcosms typically had lower DO than Lake Water, though not statistically different. This may have resulted by a rapid decline in DO on day 4 in Phenanthrene and Phenanthrene + Sedge B microcosms (Figure 5.2E & Figure C6).

It was hypothesized that available oxygen was consumed for aerobic metabolism of phenanthrene and the lack of vegetation or small root system associated with Sedge B was not able to produce sufficient oxygen release into the rhizosphere, causing oxygen to decline. During this sample period, these microcosms were visibly cloudy which may indicate a microbial bloom. While this cannot be confirmed, the DT_{50} values identified from the phenanthrene exponential decay models were approximately 5 days for these two treatments (Table 5.1), so it is clear there was phenanthrene removal occurring, which may have included microbial aerobic metabolism.

Stottmeister et al. (2003) and Wieβner et al. (2002) note the importance of above ground biomass, including surface area and stomata in oxygen release, in addition to other internal processes and drivers. While others also note the role of root biomass (Randerson et al., 2011), suggesting it may be species dependent. In fact, Moorhead and Reddy (1988) found evidence of greater oxygen release of select macrophytes with smaller root systems, and while not strongly correlated suggest it may be related to greater root respiration in older and larger roots. Sedge B, whose common name is Wiregrass sedge, has a very small and thin leaf area which may not support sufficient oxygen release into the rhizosphere for metabolism, as potentially observed on day 4 for Phenanthrene + Sedge B (Figure 5.2E). In addition, the smaller root area may have led to lower root respiration (Moorhead & Reddy, 1988), increasing microcosm DO (Figure 5.2F). Trends in other microcosms also slightly declined on day 7, but were not as pronounced as Phenanthrene + Sedge B and Phenanthrene microcosms on day 4, and no significant relationship to exposure day was observed for other microcosms treatments as observed in the GAMM (Table C4). It is possible other plant treatments also exhibited aerobic metabolism but were able to release oxygen more readily. Specifically, Phenanthrene + Cattail had less of a decline, and are well known for their ability to transfer oxygen to the rhizosphere (Wieβner et al., 2002). Selection of plants that can support aerobic degradation may be an important criterium for phenanthrene removal. However, it is important to acknowledge that differences in oxygen may also arise from the time of measurement, as oxygen solubility changes with temperature (CCME, 1999b), and the decline may be a result of this. Of note, trends in temperature recorded with the multimeter probe were highest on day 7 (Figure C2-A), which may have influenced the slight decline in DO.

All treatments had successful phenanthrene removal after 21 days of exposure (≥ 89% from initial measured concentrations; Table C6). It was initially surprising that the Phenanthrene microcosms without vegetation had successful removal. However, we hypothesized that the addition of nutrients through the Hoagland media stimulated the native microorganisms in the lake water, enhancing phenanthrene removal. This is a common practice implemented during oil spills to facilitate biodegradation (Das & Chandran, 2011; Haritash & Kaushik, 2009; Lee et al., 2015; Raju & Scalvenzi, 2018; Zhu et al., 2001). While inconclusive, this may be supported by the observed decline in DO on day 4 of exposure as discussed above. Unfortunately, because of this, there was a slight overlap in the 95% confidence interval of removal rates between Phenanthrene and Phenanthrene + Cattail microcosms (Figure 5.4E). It is suggested that future research have a control treatment with no supplemented nutrients and/or an autoclaved water treatment (abiotic control).

Moreover, while we could not confirm that plants enhanced removal of phenanthrene compared to the control, it is clear that cattail treatments generally have faster removal rates, further supported by the DT_{50} (noting all models had a different y_0). In fact, all plant treatments had lower estimated y_0 for the exponential decay model than Phenanthrene microcosms during the first round of sampling, suggesting plant treatments may have had fast removal of phenanthrene during the first ~4-7 hours of exposure (Table 5.1). However, the ANOVA analysis on day 0, indicated no statistically significant differences ($p = 0.059$), however was close to significant. The decline in phenanthrene concentrations may have been caused by rapid metabolism, incomplete mixing, or the adsorption of phenanthrene onto plant roots.

Flocco et al. (2002) studied the removal and toxic effects of phenanthrene (50 mg/L) on *Medicago sativa* L. (alfalfa) in a 30 day hydroponic experiment, and similarly noted a faster

removal in the presence of vegetation (half life: 11.3 days with alfalfa and 31 days without). They discussed that phenanthrene would likely be quickly adsorbed to the roots due to compound lipophilicity and hydrophobicity, and unlikely to be taken up into plant tissue. The ability for plants to uptake chemicals is influenced by hydrophobicity of the compound, represented by their octanol water partition coefficient (log K_{ow}). Compounds with a log K_{ow} ranging between 0.5 and 3 are within hydrophobic and solubility properties to allow for plant uptake (Pilon-Smits, 2005; Trapp & Karlson, 2001). Phenanthrene has a log K_{ow} of 4.46 (Hansch et al., 1995, as cited in National Center for Biotechnology Information, 2023), suggesting that it may pass into cell membranes and adsorb to the root, but unlikely to be translocated into shoot tissue (Flocco et al., 2002; Jatav & Singh, 2015; Pilon-Smits, 2005; Trapp & Karlson, 2001). It is possible in this study that the phenanthrene quickly adsorbed to plant roots when introduced.

While higher concentrations will often be found in the roots, others have detected phenanthrene in shoot tissue (Chen et al., 2019; Pérez-Hernández et al., 2020; Sun et al., 2014; Zhou & Gao, 2019), and although this may pose potential concerns of phytotoxicity, some plants can internally metabolize phenanthrene with enzymes or endophytic microorganisms. Jia-hua et al. (2009) measured phenanthrene uptake into root tissue of four submerged macrophytes upon exposure to 0.5 mg/L and 1 mg/L phenanthrene. Concentrations initially increased, but later declined in tissues until 40 days of exposure. Similar trends have been observed in shoot tissue, which may be a result of internal metabolism (Chen et al., 2019; Pérez-Hernández et al., 2020; Sun et al., 2014). This has previously been suggested by Zazouli et al. (2023, 2022), who monitored uptake and metabolites of pyrene and phenanthrene in tissue of *Azolla filiculoides* and *Lemna gibba*. While they found metabolites of both compounds, they observed greater accumulation of pyrene, suggesting more effective internal metabolism of phenanthrene. Future

research should explore adsorption and absorption of phenanthrene to roots, and while minimal, measure phenanthrene and metabolites in shoot tissue to confirm translocation potential.

Between plant treatments, Phenanthrene + Cattail had greater removal rates than Phenanthrene + Sedge B, but not Phenanthrene + Sedge A. This may result from differences in plant biomass, however, while the results from the linear model indicated a strong correlation, they were not significant. Other plant specific properties may be important to study their roles in removal of phenanthrene, such as enzymes (Muratova et al., 2009), exudation products (He & Chi, 2016; Louvel et al., 2011; Phillips et al., 2012), or potential uptake as discussed above. While exudation products may support microbial colonization and PAC degradation, on occasion can repress degradation (Phillips et al., 2012) or act as a competitive, readily available carbon source (Louvel et al., 2011). In our study, all treatments showed successful degradation potential, however the lowest concentrations on day 21 were in Phenanthrene and Phenanthrene + Sedge B microcosms (Table C6), with most replicate samples near the CCME (1999a) guidelines for the protection of aquatic life (0.4 μg/L). It is possible there may have been competing carbon sources in Phenanthrene + Cattail and Phenanthrene + Sedge A treatments, but this has not been confirmed and no lag phase was observed. Ultimately, these treatments still had a lower estimated DT_{50}, and may offer reduced periods of high contaminant exposure, which may be important when considering interacting biota in the natural environment. Future research to explore exudation products and microbial community composition on plant roots with and without phenanthrene exposure could inform the potential for plant species in enhancing phenanthrene removal.

It is clear in our study that there are plant-specific factors controlling phenanthrene removal and water quality parameters, which has been observed in other research. Jia-hua et al.

(2009) assessed plant-promoted phenanthrene dissipation by four submerged macrophytes and found phenanthrene removal was not often related to accumulation, but to a combination of plant enhanced biodegradation and sedimentation, and their importance varied by species. For example, removal success by *Potamogeton maackianu* and *Ceratophyllum demersum* was related to enhanced sedimentation and biodegradation, while *Elodea canadensi* was related to mostly to biodegradation and exhibited the highest uptake, and *Potamogeton crispu* had the greatest phenanthrene dissipation attributed to enhance biodegradation.

Similarly, He and Chi (2016) found differences in sediment phenanthrene and pyrene dissipation potential of four submerged macrophytes, and found a strong correlation between sediment redox potential and phenanthrene ($r = 0.76$, $p < 0.01$) and pyrene ($r = 0.34$, $p < 0.01$) dissipation. They also noted that plant uptake and accumulation only accounted for 0.2-1.0% and 0.4-6.9% of phenanthrene and pyrene dissipation, respectively, and that the ability of submerged plants to enhance removal of PAHs may be attributed to oxygen release supporting biodegradation. In their study, *Vallisneria spiralis* had highest phenanthrene and pyrene dissipation, as well as the most extensive root system, fastest growth, and largest sediment redox potential. The ability of plants to release oxygen into the rhizosphere may be an important driver of aerobic biodegradation of PACs in aquatic environments. While we did not measure oxygen release by different plants in our study, we did observe differences in oxygen concentrations between microcosms (Figure 5.2F), which may result from oxygen release, root respiration, and aerobic metabolism.

At an initial exposure of 1 mg/L, there were no negative impacts of phenanthrene on Cattail and Sedge B growth rates for height, as well as no clear impacts of phenanthrene on root microbial colonization as measured through ATP or oxygen consumption in plant treated

microcosms. There were some signs of leaf browning/yellowing, however this occurred among plants with and without phenanthrene exposure. Others have observed negative impacts on vegetation at higher phenanthrene concentrations (various effects of concentrations ranging from 1-50 mg/L; 10-100 mg/kg), such as survival, decreased growth index and biomass, low nutrient consumption, acute effects on leaves (e.g., yellowing, drying, burning), and reduced pigment, frond number, exudation, and enzyme activity (Flocco et al., 2002; Kösesakal & Seyhan, 2023; Muratova et al., 2009; Zazouli et al., 2022, 2023). Flocco et al. (2002) further note that these impacts may be greater in hydroponic studies where plants are in direct contact with the contaminant, compared with natural soil environments where plants may be further protected by soil interaction. Kösesakal & Seyhan (2023) monitored stress tolerance of a freshwater fern, *Azolla filiculoides* Lam, at varying concentrations of phenanthrene, and found no toxicity to concentrations ≤ 5 mg/L, but their tolerance limit was < 10 mg/L. They also noted an increase in production of flavonoids and phenolics by the plant when exposed to 10 mg/L phenanthrene, which are produced as antioxidants to deal with stress.

Generally, increasing concentration results in greater toxic effects and ultimately the capacity to remediate contaminants (Zazouli et al., 2014, as cited in Zazouli et al., 2023). Selection of plants with these capabilities may be important when treating high concentrations of contaminants in the natural environment. Wetland plants, including *Typha* and *Carex* spp., are commonly selected and used to treat contaminated wastewater due to their ability to survive under harsh conditions (Stottmeister et al., 2003). However, species specific traits may be important to consider when selecting plants to treat phenanthrene contamination, as well as understanding potential toxic effects at different growth stages (e.g., from seed). Although our study did not prioritize monitoring all potential phytotoxic effects of phenanthrene on plant

development, it may have been beneficial to monitor initial biomass, to have started plants from seed, or to monitor changes to pigment. Future researchers may want to integrate these considerations into their studies.

While some studies note negative impacts, it is important to consider the environmental relevance of tested concentrations. In this study, we monitored removal of 1 mg/L phenanthrene, which is higher than total PACs (N = 44) in our previous in lake oil experiments (Chapter 3 & 4), which had a maximum detected concentration of 0.012 mg/L (Chapter 3). It is also higher than maximum total PAC concentrations (0.0029 mg/L, N = 46) measured in a low-energy in-lake limnocorral study at the IISD-ELA, which was designed to represent the highest untreated on shore/surface water impacting oil spill (diluted bitumen) volumes in North America (Rodriguez-Gil et al., 2021). Following the 2010 Deepwater Horizon Spill in the Gulf of Mexico, C1-phenanthrenes/anthracenes had a mean (± SD) detection of 1.17 ± 8.00 mg/L in seawater (N = 48), while C2- and C4-phenanthrenes/anthracenes were present at much lower concentrations. Further, authors noted concentrations of compounds measured in seawater were higher than reported in other studies, which may reflect differences in sample location and time, and sampling methods (Sammarco et al., 2013). While understanding toxic thresholds is valuable for plant selection, it is suggested to study their potential and functional roles at concentrations relevant to events in the natural environment.

5.5 Conclusions

All treatments had successful removal of phenanthrene after 21 days of exposure, with Cattail having greater removal rates than Sedge B, but not Sedge A, supporting our second hypothesis that removal rates of phenanthrene will vary by plant type. However, microcosms without vegetation also had successful removal, rejecting our first hypothesis that plants would

enhance removal compared to the control. We further hypothesized that this may be a result of biostimulation from Hoagland nutrient solution, but we could not make any definitive conclusions from these experiments. Microcosm conductivity and pH were related to plant type but not phenanthrene exposure, while dissolved oxygen was influenced by both plant type and phenanthrene, likely resulting from root respiration, root oxygen release, and/or aerobic metabolism. These differences may indicate plant specific factors controlling their success in phenanthrene removal that should be explored.

Chapter 6. Significance, Recommendations, and Future Directions

6.1 Significance and Contributions to Knowledge Related to Oil Spill Response

In 2015, the Royal Society of Canada published an influential report on the behaviour and impacts of crude oil and spill responses on aquatic ecosystems, and highlighted a series of high priority research needs (Lee et al., 2015). Those relevant to the development of this PhD research at the International Institute for Sustainable Development Experimental Lakes Area (IISD-ELA) included a need for baseline research/knowledge of regions potentially at risk of future spills, and to investigate efficacy of oil spill response, specifically, *"Research is needed to develop and improve methods for remediation, reclamation or restoration of damaged marine and freshwater habitats following oil spills"* (Lee et al., 2015, p. 34). Additional recommendations in relation to this research include, "*More data are required for natural and chemically-enhanced dispersion of unconventional oils and diluted bitumen blends, especially in fresh water"* (Lee et al., 2015, p. 87)*, "Conduct Experiments on Efficacy of Current and Emerging Oil Spill Countermeasures (Short-Term to Medium-Term)"* (Lee et al., 2015, p. 361), as well as,

> *The interaction between residual oil in the water with suspended particulate matter of organic origin (e.g., phytoplankton, detritus, extracellular released products) and inorganic origin (e.g., mineral fines) (OMA and clay flocs) on the environmental persistence of spilled oil (sinking, oil biodegradation rates, etc) requires further study.* (Lee et al., 2015, p. 113)
>
> *Field studies are needed to determine the comparative fate, behaviour and effects of oil in wetlands with varied hydraulic regimes (bogs, fens, marshes, swamps), including areas of permafrost. Habitat restoration methods for shoreline*

> *vegetation need to be developed to ensure the rapid recovery of shoreline ecosystems and the optimum balance between oil clean up and habitat protection.* (Lee et al., 2015, p. 134)

The IISD-ELA is located within the boreal shield, the largest ecozone in Canada (Brandt et al., 2013; Natural Resources Canada, 2022), and has over 50 years of baseline data on boreal freshwater lakes. As stated throughout this thesis, conducting research at this facility may inform how oil spills should be treated in similar environments across Canada, and the historic baseline data supports monitoring effectiveness of ecosystem recovery (Lee et al., 2015). In addition, Lee et al. (2015) stated "*Most of what we know about the oil spill response technologies has been developed through results from studies in the laboratory, mesocosm test systems and case studies (with limited controls and treatment replication).*" (p. 218), and recommended controlled field trials in freshwater shorelines to advance response methods. This is also an important recommendation for bioremediation approaches, as often plants and microorganisms in the natural environment do not respond similarly to laboratory scale experiments where conditions are optimal (Czaplicki & Gunsch, 2016; Malla et al., 2018). Being able to conduct intentional oil spills at this facility has also allowed our research team to closely monitor impacts of oil on all levels of an ecosystem (included in other theses and publications), including how oil disperses naturally. For example, we observed a peak of polycyclic aromatic compound (PAC) concentration following a large precipitation event, causing reintroduction and remobilization of diluted bitumen into the water column (see Chapter 3- Section 3.3.1). These events show the importance of field based experiments.

This PhD research specifically explored the use of EFWs as a non-invasive, secondary remediation method for oil spills following primary recovery in freshwater shoreline

environments, responding to the research needs described above to protect shoreline habitat, study residual oil in the water and sediment of a wetland/organic shoreline environment, and test spill response methods in field experiments (Lee et al., 2015). Current conventional oil spill practices can cause significant, long-term damage to sensitive environments through physical removal practices (Hoff, 1995; Lee et al., 2015; Pezeshki et al., 2000; Zhu et al., 2001), and can leave a substantial volume of oil in the environment (Das & Chandran, 2011; Etkin & Tebeau, 2003; Lee et al., 2015; Zhu et al., 2001). The use of EFWs is a common practice around the world, but their use for remediating oil and hydrocarbons is relatively new. In Chapter 2, thirteen articles that study the use of EFWs for the remediation of oil, diesel, and oil degradation by-products were synthesized to inform potential for oil spill response. We also highlighted a series of research needs including understanding efficacy of EFWs for oil spill response in larger scale, uncontrolled environments with variable conditions, such as fluctuating temperatures. As described above, it is important to study bioremediation under non-optimal, environmental conditions.

In this PhD, I specifically monitored changes to the microbial community in the EFW rhizosphere after simulated oil spills in shoreline enclosures to determine potential for secondary oil spill recovery of diluted bitumen (Chapter 3) and conventional heavy crude oil (Chapter 4). This responded to both industrial and scientific research needs, and to our knowledge, was the first experiment to study EFWs and model oil spills in freshwater lakes. Results from this research indicated that EFWs can support a large diversity of microorganisms, and while changes could not be attributed specifically to oil exposure, EFWs were able to naturally support some microorganisms capable at degrading hydrocarbons and/or oil. This was a particularly important result, as previous research has studied the addition/combination of bacterial inoculants with

plants (Afzal et al., 2019; Fahid, Ali, et al., 2020; Fahid, Arslan, et al., 2020; Hussain et al., 2019; Ijaz et al., 2015; Rehman et al., 2018, 2019, 2021; Saleem et al., 2018, 2019), which may not perform or survive in natural, non-optimal conditions. In addition, as discussed in Chapter 2, bacterial inoculants could have potential impact to native microorganisms by outcompeting for resources (Ghosal et al., 2016).

In environmental scale research there are complex interactions that may restrict knowledge of specific processes and roles of plants in enhancing remediation. In efforts to respond to this, I conducted a microcosm scale experiment to assess the efficacy of plants in removing phenanthrene from freshwater and further to compare removal rates between three emergent wetland plants to provide guidance on EFW design. This study supported additional research on the FLOWTER project by Master's student Aidan Guttormson, optimizing EFW design with plant species composition and nutrient addition (biostimulation) for PAC removal from model oil spills, produced by adding CHV water accommodated fractions to lake water mesocosms (Guttormson, *in preparation*). Data presented in this PhD thesis confirmed all treatments of emergent plants, *Typha* sp., *Carex utriculata,* and *C. lasiocarpa* can successfully reduce over 94% of phenanthrene from an initial nominal concentration of 1 mg/L (Chapter 5; ≥89% from initial measured concentrations). The rate of removal was faster in microcosms containing *Typha* sp. than those with *C. lasiocarpa,* but not *C. utriculata*. In addition, rate of removal of plant treated microcosms were not different from the control, likely due to incidental biostimulation. However, despite minor overlaps of 95 % confidence intervals, it is clear that *Typha* sp. generally have faster removal than the control, supported by the DT_{50}s discussed in Chapter 5. Our data suggest that there are other, unexplored, plant specific functions of *Typha* and *Carex* that may be driving phenanthrene removal. This work has provided suggestions for

new avenues of research for these three emergent wetland plants, discussed in Chapter 5 and Section 6.3.

Ultimately, results from this PhD research advance our collective knowledge on EFWs and suggests they may be successful in enhancing removal of PACs without the need for bacterial inoculants. However, further research is encouraged to assess the reduction of complex/recalcitrant PACs (e.g., benzo[a]pyrene) and to confirm the active roles of microorganisms on oil exposed EFWs. This provides an opportunity to communicate results with spill responders and the oil industry to encourage adoption of non-invasive practices for the recovery of residual oil following spills, in efforts to enhance recovery without long term damage. Deployments in active spill sites will provide further opportunities for research and knowledge to advance this field.

6.2 Recommendations

There are a few guiding points that may enable oil spill responders with the effective deployment of EFWs following primary recovery of oil spills, which are primarily focused on the selection of the plant species. It is recommended to select native plants from the designated region if introducing as an in-situ remediation method, to ensure that the deployed plants can withstand the environmental conditions and resources in the designated site (Pilon-Smits, 2005). As well, some may want to consider the potential risk of introducing a non-native plant species. Moreover, a nutrient source may be required to support growth of the plants, depending on site conditions, nutrient availability, and plant requirements. For example, lakes at the IISD-ELA are nutrient poor, and without the support of sediment or soil environments, plants may require additional support for successful hydroponic growth. This may include nutrient amended soil in EFW media.

Ensuring the variety of plant species can withstand contaminant concentrations will be important for the ability to remediate the environment (Pilon-Smits, 2005). For example, it was synthesized in Zazouli et al. (2023) that increasing contaminant concentration and toxicity ultimately reduces the capacity of plants to remediate the environment. As discussed in Chapter 5, *Typha* and *Carex* are commonly used to remediate wastewater contaminants and are known to survive in harsh environments (Stottmeister et al., 2003). In this study, these genera have shown potential for removing phenanthrene when planted alone and were able to withstand 1 mg/L initial nominal concentrations (see Chapter 5 growth rate comparisons for *Typha* sp., and *C. lasiocarpa* heights).

Finally, selecting plants that have rapid development and a large root system to support microbial colonization may be beneficial (Pilon-Smits, 2005), as it may increase interaction with contaminants in the aqueous environment. While this wasn't specifically targeted in my PhD research, results from the phenanthrene experiment (Chapter 5) revealed a strong, but not significant, relationship between final dry biomass and phenanthrene removal rates. Understanding surface area requirements for successful remediation would be a useful future research question.

6.3 Future Directions

Over the duration of this PhD research on the FLOWTER project, I acknowledged a few limitations and gaps in research that may help to further support decision making and EFW design for successful deployment. In Chapters 3 and 4 of this thesis I demonstrated how EFWs can support a naturally diverse microbial community in the rhizosphere with the potential to remediate crude oil at contaminated sites. This was supported by previous research. However, due to lack of enclosure replication, results were inconclusive as to whether changes were

attributed specifically to oil exposure. While there were limitations on enclosure replication, there were organisms capable of degrading PACs present on EFW roots, and we were able to show potential of EFWs as a non-invasive strategy for oil spill remediation. Future research should include replication of treatments to statistically conclude whether presence of crude oil shifts the microbial community to hydrocarbon degraders. This recommendation was made by Lee et al. (2015) in order to calculate experimental error. In addition, future research may want to explore which microorganisms on EFWs are actively contributing to the removal of PACs or other oil compounds through monitoring activity and gene expression with metatranscriptomics and/or proteomics. This may inform which organisms are involved in the cleavage of aromatic rings or those metabolizing linear alkanes or alkyl structures, and may show value of a diverse consortia for co-metabolism of oil.

An important contribution to the success of EFW deployments for oil spill response will be to assess surface area requirements for successful aqueous removal. It is understood that microbial and plant interaction with contaminants will facilitate the breakdown of products, and future research should explore EFW coverage requirements to remove a desired percentage of PACs from aqueous media without having negative impacts on freshwater biotic processes, including limiting light from shading or oxygen availability from root respiration.

In Chapter 5 of this thesis, I demonstrated the successful removal of phenanthrene from freshwater microcosms with and without vegetation, however, we did not explore specific roles of removal by plants and/or microorganisms (e.g., uptake or biodegradation). These factors may be important for selection of plants for bioremediation in the natural environment and should be

well understood. As described in Chapter 5, those specific to *Typha* and *Carex* species may include[4]:

- Assessing phenanthrene or other PAC uptake and adsorption, as well as monitoring internal metabolism by plant enzymes or endophytic microorganisms (Chen et al., 2019; He & Chi, 2016; Jia-hua et al., 2009; Kösesakal & Seyhan, 2023; Pérez-Hernández et al., 2020; Sun et al., 2014; Zazouli et al., 2022, 2023; Zhou & Gao, 2019).
- Refine quantification of phenanthrene removal by determining phenanthrene metabolites or by-products in aqueous media and in plant tissue (Zazouli et al., 2022, 2023).
- Identify specific plant exudates that may stimulate or repress degradation with and without phenanthrene exposure (He & Chi, 2016; Louvel et al., 2011; Muratova et al., 2009; Phillips et al., 2012).
- Quantify and identify roles of epiphytic and endophytic microbial communities associated with different plant species with and without phenanthrene exposure (Chen et al., 2019; Muratova et al., 2009; Sun et al., 2014; Zhou & Gao, 2019).
- Assess relationship of plant biomass, surface area, and morphology on remediation potential (He & Chi, 2016; Zhou & Gao, 2019).
- Identify plant toxicity thresholds within environmentally relevant concentrations (Flocco et al., 2002; Kösesakal & Seyhan, 2023; Muratova et al., 2009; Zazouli et al., 2022, 2023).

[4] References associated with recommendations are included for future research methods, these articles were not specific to *Typha* or *Carex* species discussed in this thesis.

In addition, due to the successful removal in the control, hypothesized to result from biostimulation, I encourage future research to include an additional abiotic control or a control without nutrient addition to confirm if removal was a result of biotic or abiotic processes.

This PhD research has successfully responded to research needs by assessing the potential of plants and microorganisms on EFWs as a non-invasive oil spill response method. Specifically, I identified that EFWs support a naturally diverse microbial community, including organisms capable of degrading oil compounds without the need for bacterial inoculation. In addition, I measured successful removal of phenanthrene, a three ring PAC and US EPA priority pollutant (2014), from freshwater microcosms with different treatments, and made a series of recommendations as described above to advance collective knowledge in this field. The next steps in the evolution of this process would be to deploy and test the efficacy of EFWs at real spill or contaminated sites to examine how the microbial community contributes to biodegradation processes. This will advance the knowledge on whether EFWs can be actively deployed to remove residual oil compounds without damaging sensitive environments.

6.4 Conclusions

My PhD thesis has demonstrated that EFWs have potential as a non-invasive oil spill remediation strategy, ideal for sensitive environments where conventional recovery may be contraindicated. In lake, model oil spill experiments confirmed that EFWs support a diverse microbial community in the rhizosphere, with higher richness and evenness of prokaryotes than eukaryotes. While I was unable to confirm whether community shifts were specifically attributed to oil exposure, I did identify the presence of organisms capable at degrading hydrocarbons and oil. Moreover, in some cases, we observed drastic shifts in the microbial community on EFWs (including some hydrocarbon degraders; Chapter 4). This shows that communities can drastically

shift, which may be important for oil spill remediation applications. Due to the high diversity of microorganisms and lack of enclosure replication, it was difficult to confirm or reject the hypothesis that the rhizosphere microbial community would shift in the presence of oil to microorganisms known to consume and degrade hydrocarbon compounds, however, I did observe a decline in total PACs over the experimental period and site specific selection of some microorganisms. During both experiments (Chapter 3 & 4), total PACs declined in aqueous media after approximately 60-70 days of exposure, however due to complex nature of ecosystems, it is likely that removal was attributed to a series of processes (e.g., sorption to sediment, photodegradation, volatilization, biodegradation, etc.).

In order to identify whether plants on EFWs can enhance removal of PACs, I conducted a hydroponic experiment to assess the efficacy of different emergent wetland plants in removing 1 mg/L phenanthrene, a three ring PAC, from freshwater microcosms. After 21 days of exposure, all treatments exhibited successful removal, including the control (≥ 94% from 1 mg/L initial nominal concentration; ≥ 89% from initial measured concentration). Treatment of *Typha* sp. had greater removal rates than *Carex lasiocarpa*, but not *C. utriculata*, supporting the hypothesis that rates of removal would vary by plant type. However, due to the control exhibiting successful removal, there were no differences between plant treatments and the control, rejecting the hypothesis that plants would enhance removal compared to untreated microcosms. However, I expect this was the result of nutrient addition causing biostimulation, and make the recommendation that future research include an abiotic control or a treatment without nutrient amendment to re-assess this research question. This research indicated successful removal of phenanthrene in freshwater microcosms, however it was clear there may be plant specific

functions controlling the success of removal and water quality conditions, and it is suggested that these be explored to further understand roles in removal success.

While this thesis has demonstrated potential for oil spill response, future research directions will help to further knowledge in this field and advance the uptake of less invasive methods for remediating and protecting sensitive freshwater environments. The collective knowledge of this research and related fields is significant to Canada, who has one of the largest crude oil reserves (Dupuis & Ucan-Marin, 2015; Natural Resources Canada, 2020), 20% of the world's freshwater and 7% of its renewable freshwater supply (Environment and Climate Change Canada, 2022; Environment and Natural Resources, 2020; Statistics Canada, 2011).

References

Abbasian, F., Palanisami, T., Megharaj, M., Naidu, R., Lockington, R., & Ramadass, K. (2016). Microbial diversity and hydrocarbon degrading gene capacity of a crude oil field soil as determined by metagenomics analysis. *Biotechnology Progress*, *32*(3), 638–648. https://doi.org/10.1002/btpr.2249

Abed, R. M. M., Al-Kharusi, S., Prigent, S., & Headley, T. (2014). Diversity, distribution and hydrocarbon biodegradation capabilities of microbial communities in oil-contaminated cyanobacterial mats from a constructed wetland. *PLoS ONE*, *9*(12), 1–22. https://doi.org/10.1371/journal.pone.0114570

Aburto-Medina, A., Adetutu, E. M., Aleer, S., Weber, J., Patil, S. S., Sheppard, P. J., Ball, A. S., & Juhasz, A. L. (2012). Comparison of indigenous and exogenous microbial populations during slurry phase biodegradation of long-term hydrocarbon-contaminated soil. *Biodegradation*, *23*(6), 813–822. https://doi.org/10.1007/s10532-012-9563-8

Adesalu, T. A., Julius, M. L., & Temenu, T. O. (2016). Molecular characterization, lipid analysis and GC-MS determination of bioactive compounds identified in a West African strain of the green alga Oedogonium (Chlorophyta). *Journal of Pharmacognosy and Phytochemistry*, *5*(6), 01–06.

Adrion, A. C., Singleton, D. R., Nakamura, J., Shea, D., & Aitken, M. D. (2016). Improving polycyclic aromatic hydrocarbon biodegradation in contaminated soil through low-level surfactant addition after conventional bioremediation. *Environmental Engineering Science*, *33*(9), 659–670. https://doi.org/10.1089/ees.2016.0128

Afzal, M., Rehman, K., Shabir, G., Tahseen, R., Ijaz, A., Hashmat, A. J., & Brix, H. (2019). Large-scale remediation of oil-contaminated water using floating treatment wetlands. *Npj*

Clean Water, *2*(3), 10. https://doi.org/10.1038/s41545-018-0025-7

Aguilar, M., Richardson, E., Tan, B. F., Walker, G., Dunfield, P. F., Bass, D., Nesbø, C., Foght, J., & Dacks, J. B. (2016). Next-generation sequencing assessment of eukaryotic diversity in oil sands tailings ponds sediments and surface water. *Journal of Eukaryotic Microbiology*, *63*(6), 732–743. https://doi.org/10.1111/jeu.12320

Al-Hawash, A. B., Dragh, M. A., Li, S., Alhujaily, A., Abbood, H. A., Zhang, X., & Ma, F. (2018). Principles of microbial degradation of petroleum hydrocarbons in the environment. *Egyptian Journal of Aquatic Research*, *44*(2), 71–76. https://doi.org/10.1016/j.ejar.2018.06.001

Almeda, R., Connelly, T. L., & Buskey, E. J. (2014). Novel insight into the role of heterotrophic dinoflagellates in the fate of crude oil in the sea. *Scientific Reports*, *4*, 1–9. https://doi.org/10.1038/srep07560

Almeda, R., Cosgrove, S., & Buskey, E. J. (2018). Oil spills and dispersants can cause the initiation of potentially harmful dinoflagellate blooms (“Red Tides”). *Environmental Science and Technology*, *52*(10), 5718–5724. https://doi.org/10.1021/acs.est.8b00335

Almeda, R., Hyatt, C., & Buskey, E. J. (2014). Toxicity of dispersant Corexit 9500A and crude oil to marine microzooplankton. *Ecotoxicology and Environmental Safety*, *106*, 76–85. https://doi.org/10.1016/j.ecoenv.2014.04.028

Atlas, R. M. (1995). Petroleum biodegradation and oil spill bioremediation. *Marine Pollution Bulletin*, *31*(4–12), 178–182. https://doi.org/10.1016/0025-326X(95)00113-2

Barron, J., & Ashton, C. (2005). The effect of temperature on conductivity measurement. In *Technical Services Department, Reagecon Diagnostics Ltd.* (Vol. 7, Issue 3). https://doi.org/10.11648/j.ajpa.20170501.11

Barron, J., Ashton, C., & Geary, L. (2005). The effects of temperature on pH measurement. In *Technical Services Department, Reagecon Diagnostics Ltd.: Vol. TSP-01* (Issue 2).

Beazley, M. J., Martinez, R. J., Rajan, S., Powell, J., Piceno, Y. M., Tom, L. M., Andersen, G. L., Hazen, T. C., van Nostrand, J. D., Zhou, J., Mortazavi, B., & Sobecky, P. A. (2012). Microbial community analysis of a coastal salt marsh affected by the Deepwater Horizon oil spill. *PLoS ONE, 7*(7), e41305. https://doi.org/10.1371/journal.pone.0041305

Bennett, D. M., Fritz, S. C., Holz, J. C., Holz, A. A., & Zlotnik, V. A. (2007). Evaluating climatic and non-climatic influences on ion chemistry in natural and man-made lakes of Nebraska, USA. *Hydrobiologia*, *591*(1), 103–115. https://doi.org/10.1007/s10750-007-0798-z

Bisht, S., Pandey, P., Bhargava, B., Sharma, S., Kumar, V., & Krishan, D. (2015). Bioremediation of polyaromatic hydrocarbons (PAHs) using rhizosphere technology. *Brazilian Journal of Microbiology*, *46*(1), 7–21. https://doi.org/10.1590/S1517-838246120131354

Bodour, A. A., Wang, J. M., Brusseau, M. L., & Maier, R. M. (2003). Temporal change in culturable phenanthrene degraders in response to long-term exposure to phenanthrene in a soil column system. *Environmental Microbiology*, *5*(10), 888–895. https://doi.org/10.1046/j.1462-2920.2003.00481.x

Bôto, M. L., Magalhães, C., Perdigão, R., Alexandrino, D. A. M., Fernandes, J. P., Bernabeu, A. M., Ramos, S., Carvalho, M. F., Semedo, M., LaRoche, J., Almeida, C. M. R., & Mucha, A. P. (2021). Harnessing the potential of native microbial communities for bioremediation of oil spills in the Iberian Peninsula NW coast. *Frontiers in Microbiology*, *12*, 633659. https://doi.org/10.3389/fmicb.2021.633659

Brandt, J. P., Flannigan, M. D., Maynard, D. G., Thompson, I. D., & Volney, W. J. A. (2013). An introduction to Canada's boreal zone: Ecosystem processes, health, sustainability, and environmental issues. *Environmental Reviews*, *21*(4), 207–226. https://doi.org/10.1139/er-2013-0040

Brown, D., Wilson, S., Caffrey, S. M., Bordenave, S., Gieg, L. M., Ramos-Padron, E., Voordouw, G., Chatterjee, I., Sensen, C. W., Dong, X., & An, D. (2013). Microbial community and potential functional gene diversity involved in anaerobic hydrocarbon degradation and methanogenesis in an oil sands tailings pond. *Genome*, *56*(10), 612–618. https://doi.org/10.1139/gen-2013-0083

Bruno, M. G., Fannin, T. E., & Leversee, G. J. (1982). The disposition of benzo(a)pyrene in the periphyton communities of two South Carolina streams: Uptake and biotransformation. *Canadian Journal of Botany*, *60*(10), 2084–2091. https://doi.org/10.1139/b82-255

Canada Energy Regulator. (2021a). *Annual Canadian crude oil production by type. Data from Canadian crude oil exports: A 30 year review.* https://doi.org/10.35002/zd9v-jj06 [5]

Canada Energy Regulator. (2021b). *Annual crude oil exports volume by type. Data from Canadian crude oil exports: A 30 year review*. https://doi.org/10.35002/zd9v-jj06 [5]

Canada Energy Regulator. (2021c). *Canadian Crude Oil Exports: A 30 Year Review*. https://www.cer-rec.gc.ca/en/data-analysis/energy-commodities/crude-oil-petroleum-products/report/canadian-crude-oil-exports-30-year-review/index.html

Canada Energy Regulator. (2023). *Crude oil pipeline transportation system*. https://www.cer-rec.gc.ca/en/data-analysis/facilities-we-regulate/canadas-pipeline-system/2021/crude-oil-

[5] Data presented from the Canadian Crude Oil Exports: A 30 Year Review (Canada Energy Regulator, 2021a; 2021b) contains information licensed under the Open Government Licence-Canada. https://open.canada.ca/en/open-government-licence-canada

pipeline-transportation-system.html#:~:text=In Canada%2C crude oil is,U.S. PADDs I and III.

Cao, B., Nagarajan, K., & Loh, K. C. (2009). Biodegradation of aromatic compounds: Current status and opportunities for biomolecular approaches. *Applied Microbiology and Biotechnology*, *85*(2), 207–228. https://doi.org/10.1007/s00253-009-2192-4

CCME. (1999a). *Canadian water quality guidelines for the protection of aquatic life- Polycyclic aromatic hydrocarbons (PAHs)*. https://ccme.ca/en/res/polycyclic-aromatic-hydrocarbons-pahs-en-canadian-water-quality-guidelines-for-the-protection-of-aquatic-life.pdf

CCME. (1999b). *Canadian water quality guidelines for the protection of aquatic life - Dissolved oxygen (freshwater)*. https://ccme.ca/en/res/dissolved-oxygen-freshwater-en-canadian-water-quality-guidelines-for-the-protection-of-aquatic-life.pdf

Cébron, A., Borreca, A., Beguiristain, T., Biache, C., & Faure, P. (2022). Taxonomic and functional trait-based approaches suggest that aerobic and anaerobic soil microorganisms allow the natural attenuation of oil from natural seeps. *Scientific Reports*, *12*(1), 1–16. https://doi.org/10.1038/s41598-022-10850-4

Cederwall, J., Black, T. A., Blais, J. M., Hanson, M. L., Hollebone, B. P., Palace, V. P., Rodríguez-Gil, J. L., Greer, C. W., Maynard, C., Ortmann, A. C., Rooney, R. C., & Orihel, D. M. (2020). Life under an oil slick: Response of a freshwater food web to simulated spills of diluted bitumen in field mesocosms. *Canadian Journal of Fisheries and Aquatic Sciences*, *77*(5), 779–788. https://doi.org/10.1139/cjfas-2019-0224

Cerniglia, C. E., Gibson, D. T., & Van Baalen, C. (1982). Naphthalene metabolism by diatoms isolated from the Kachemak Bay region of Alaska. *Journal of General Microbiology*,

128(5), 987–990. https://doi.org/10.1099/00221287-128-5-987

Cerniglia, C. E., Hebert, R. L., Szaniszlo, P. J., & Gibson, D. T. (1978). Fungal transformation of naphthalene. *Archives of Microbiology*, *117*(2), 135–143. https://doi.org/10.1007/BF00402301

Chakraborty, R., Wu, C. H., & Hazen, T. C. (2012). Systems biology approach to bioremediation. *Current Opinion in Biotechnology*, *23*(3), 483–490. https://doi.org/10.1016/j.copbio.2012.01.015

Chang, S. E., Stone, J., Demes, K., & Piscitelli, M. (2014). Consequences of oil spills: A review and framework for informing planning. *Ecology and Society*, *19*(2), 26. https://doi.org/10.5751/ES-06406-190226

Chen, S. (2018). *A comparison of response technologies for offshore oil spills*. *Exxon Valdez and BP Gulf of Mexico Oil Spills.* [Master's Thesis, North Carolina State University]. NC State Repository https://repository.lib.ncsu.edu/items/4c9e3485-6675-4441-bb79-cbe4b1d92f4d

Chen, S., Ma, Z., Li, S., Waigi, M. G., Jiang, J., Liu, J., & Ling, W. (2019). Colonization of polycyclic aromatic hydrocarbon-degrading bacteria on roots reduces the risk of PAH contamination in vegetables. *Environment International*, *132,* 105081. https://doi.org/10.1016/j.envint.2019.105081

Chettri, B., & Singh, A. K. (2019). Kinetics of hydrocarbon degradation by a newly isolated heavy metal tolerant bacterium Novosphingobium panipatense P5:ABC. *Bioresource Technology, 294,* 122190. https://doi.org/10.1016/j.biortech.2019.122190

Cobanli, S. E., Wohlgeschaffen, G., Ryther, C., Macdonald, J., Gladwell, A., Watts, T., Greer, C. W., Elias, M., Wasserscheid, J., Robinson, B., King, T. L., & Ortmann, A. C. (2022).

Microbial community response to simulated diluted bitumen spills in coastal seawater and implications for oil spill response. *FEMS Microbiology Ecology*, *98*(5), 1–13. https://doi.org/10.1093/femsec/fiac033

Crosby, S., Fay, R., Groark, C., Kani, A., Smith, J. R., Sullivan, T., & Pavia, R. (2013). *Transporting Alberta oil sands products : Defining the issues and assessing the risks. U.S. Dept. of Commerce, NOAA Technical Memorandum NOS OR&R 43.* Emergent Response Division, NOAA. https://repository.library.noaa.gov/view/noaa/2670

Czaplicki, L. M., & Gunsch, C. K. (2016). Reflection on molecular approaches influencing state-of-the-art bioremediation design: Culturing to microbial community fingerprinting to omics. *Journal of Environmental Engineering*, *142*(10), 31. https://doi.org/10.1061/(asce)ee.1943-7870.0001141

Dalby, A. P., & Kormas, K. A. (2008). Cosmopolitan heterotrophic microeukaryotes are active bacterial grazers in experimental oil-polluted systems. *Environmental Microbiology*, *10*(1), 47–56. https://doi.org/10.1111/j.1462-2920.2007.01428.x

Das, N., & Chandran, P. (2011). Microbial degradation of petroleum hydrocarbon contaminants: An overview. *Biotechnology Research International*, *2011*, 941810. https://doi.org/10.4061/2011/941810

DataStream Initiative. (2021). *A Monitor's Guide to Water Quality*. https://datastreamorg.sharepoint.com/sites/Datastream/Shared%20Documents/Forms/AllItems.aspx?id=%2Fsites%2FDatastream%2FShared%20Documents%2FFiles%2F6%20%2D%20Outreach%20and%20User%20Related%2FScience%20Explainers%2F5%20%2D%20Printable%20PDF%2FEnglish%2F2021%2FEN%5FPrintable%5FSciExp%5F220612%5FFull%2Epdf&parent=%2Fsites%2FDatastream%2FShared%20Documents%2FFile

s%2F6%20%2D%20Outreach%20and%20User%20Related%2FScience%20Explainers%2F5%20%2D%20Printable%20PDF%2FEnglish%2F2021&p=true&ga=1

De Faria, D. M., Costin, J. C., Tremarin, P. I., & Ludwig, T. A. V. (2019). Temporal changes in biological traits of diatom communities in response to an oil spill in a subtropical river. *Anais Da Academia Brasileira de Ciencias*, *91*(2), 1–17. https://doi.org/10.1590/0001-3765201920170863

Dearnley, J. (2022). *Assessing exposure of small-bodied fish to experimental crude oil spills in contained shoreline environments using biliary polycyclic aromatic compound metabolites* [Master's Thesis, University of Manitoba]. University of Manitoba MSpace https://mspace.lib.umanitoba.ca/items/0358eda5-7e1b-4b9c-8d24-531266255a50

Dedysh, S. N. (2019). Bryobacter. In *Bergey's Manual of Systematics of Archaea and Bacteria.* (pp. 1–5). John Wiley & Sons, Inc., in association with Bergey's Manual Trust. https://doi.org/10.1002/9781118960608.gbm01667

Deng, Y., Wang, K., Hu, Z., Hu, Q., & Tang, Y. Z. (2023). Toxic and non-toxic dinoflagellates host distinct bacterial communities in their phycospheres. *Communications Earth and Environment*, *4*(1), 1–10. https://doi.org/10.1038/s43247-023-00925-z

Desmond, D. S., Saltymakova, D., Smith, A., Wolfe, T., Snyder, N., Polcwiartek, K., Bautista, M., Lemes, M., Hubert, C. R. J., Barber, D. G., Isleifson, D., & Stern, G. A. (2021). Photooxidation and biodegradation potential of a light crude oil in first-year sea ice. *Marine Pollution Bulletin*, *165*, 112154. https://doi.org/10.1016/j.marpolbul.2021.112154

Deutzmann, J. S., Hoppert, M., & Schink, B. (2014). Characterization and phylogeny of a novel methanotroph, Methyloglobulus morosus gen. nov., spec. nov. *Systematic and Applied Microbiology*, *37*(3), 165–169. https://doi.org/10.1016/j.syapm.2014.02.001

Devlin, S. P., Vander Zanden, M. J., & Vadeboncoeur, Y. (2016). Littoral-benthic primary production estimates: Sensitivity to simplifications with respect to periphyton productivity and basin morphometry. *Limnology and Oceanography: Methods*, *14*(2), 138–149. https://doi.org/10.1002/lom3.10080

Dhir, B. (2013). *Phytoremediation: Role of aquatic plants in environmental clean-up*. Springer India. https://doi.org/10.1007/978-81-322-1307-9

Dodds, W. K. (2002). *Freshwater ecology: Concepts and environmental applications*. Elsevier Science.

Dowle, M., & Srinivasan, A. (2023). *_data.table: Extension of 'data.frame'_. R package version 1.14.8.* https://cran.r-project.org/package=data.table

Dubinsky, E. A., Conrad, M. E., Chakraborty, R., Bill, M., Borglin, S. E., Hollibaugh, J. T., Mason, O. U., M. Piceno, Y., Reid, F. C., Stringfellow, W. T., Tom, L. M., Hazen, T. C., & Andersen, G. L. (2013). Succession of hydrocarbon-degrading bacteria in the aftermath of the deepwater horizon oil spill in the Gulf of Mexico. *Environmental Science and Technology*, *47*(19), 10860–10867. https://doi.org/10.1021/es401676y

Dupuis, A., & Ucan-Marin, F. (2015). A literature review on the aquatic toxicology of petroleum oil: An overview of oil properties and effects to aquatic biota. *DFO Canadian Science Advisory Secretariat Research Document 2015/007*. vi + 52 p. https://publications.gc.ca/collections/collection_2015/mpo-dfo/Fs70-5-2015-007-eng.pdf

Effendi, H., Munawaroh, A., & Puspa Ayu, I. (2017). Crude oil spilled water treatment with Vetiveria zizanioides in floating wetland. *Egyptian Journal of Aquatic Research*, *43*, 185–193. https://doi.org/10.1016/j.ejar.2017.08.003

Engel, A. S., Liu, C., Paterson, A. T., Anderson, L. C., Eugene Turner, R., & Overton, E. B.

(2017). Salt marsh bacterial communities before and after the Deepwater Horizon oil spill. *Applied and Environmental Microbiology*, *83*(20), 1–22. https://doi.org/10.1128/AEM.00784-17

Environment and Climate Change Canada. (2022). *Federal Sustainable Development Strategy 2022 to 2026*. https://www.canada.ca/content/dam/eccc/documents/pdf/federal-sustainable-development-strategy/2022%20to%202026%20Federal%20Sustainable%20Development%20Strategy-2.pdf

Environment and Natural Resources. (2020). *Hydrology of Canada*. https://www.canada.ca/en/environment-climate-change/services/water-overview/quantity/monitoring/survey/hydrology.html

Esteban, G. F., Finlay, B. J., & Warran, A. (2015). Free-living protozoa. In J. H. Thorp & D. C. Rogers (Eds.), *Thorp and Covinch's Freshwater Invertebrates: Ecology and General Biology* (4th ed., pp. 113–132). Elsevier Inc.

Etkin, D. S., & Tebeau, P. (2003). Assessing progress and benefits of oil spill response technology development since Exxon Valdez. *2003 International Oil Spill Conference*, 843–850. https://doi.org/10.7901/2169-3358-2003-1-843

Fahde, S., Boughribil, S., & Sijilmassi, B. (2023). Rhizobia : A promising source of plant growth-promoting molecules and their non-legume interactions : Examining applications and mechanisms. *Agriculture*, *13*(1279), 21. https://doi.org/10.3390/agriculture13071279

Fahid, M., Ali, S., Shabir, G., Ahmad, S. R., Yasmeen, T., Afzal, M., Arslan, M., Hussain, A., Hashem, A., Allah, E. F. A., Alyemeni, M. N., & Ahmad, P. (2020). Cyperus laevigatus L. enhances diesel oil remediation in synergism with bacterial inoculation in floating

treatment wetlands. *Sustainability*, *12*(6), 15. https://doi.org/10.3390/su12062353

Fahid, M., Arslan, M., Shabir, G., Younus, S., Yasmeen, T., Rizwan, M., Siddique, K., Ahmad, S. R., Tahseen, R., Iqbal, S., Ali, S., & Afzal, M. (2020). Phragmites australis in combination with hydrocarbons degrading bacteria is a suitable option for remediation of diesel-contaminated water in floating wetlands. *Chemosphere*, *240*, 124890. https://doi.org/10.1016/j.chemosphere.2019.124890

Fatima, K., Imran, A., Amin, I., Khan, Q. M., & Afzal, M. (2016). Plant species affect colonization patterns and metabolic activity of associated endophytes during phytoremediation of crude oil-contaminated soil. *Environmental Science and Pollution Research*, *23*(7), 6188–6196. https://doi.org/10.1007/s11356-015-5845-0

Fatima, K., Imran, A., Amin, I., Khan, Q. M., & Afzal, M. (2018). Successful phytoremediation of crude-oil contaminated soil at an oil exploration and production company by plants-bacterial synergism. *International Journal of Phytoremediation*, *20*(7), 675–681. https://doi.org/10.1080/15226514.2017.1413331

Ferrera-Rodríguez, O., Greer, C. W., Juck, D., Consaul, L. L., Martínez-Romero, E., & Whyte, L. G. (2013). Hydrocarbon-degrading potential of microbial communities from Arctic plants. *Journal of Applied Microbiology*, *114*(1), 71–83. https://doi.org/10.1111/jam.12020

Fingas, M. (2015). Introduction to oil chemistry and properties. In M. Fingas (Ed.), *Handbook of Oil Spill Science and Technology* (pp. 53–77). John Wiley & Sons, Inc. https://doi.org/10.1002/9781118989982

Finkel, Z. V., Liang, Y., Nanjappa, D., Bretherton, L., Brown, C. M., Quigg, A., & Irwin, A. J. (2020). A ribosomal sequence-based oil sensitivity index for phytoplankton groups.

Marine Pollution Bulletin, *151*, 110798. https://doi.org/10.1016/j.marpolbul.2019.110798

Firke, S. (2023). *_janitor: Simple tools for examining and cleaning dirty data_. R package version 2.2.0*. https://cran.r-project.org/package=janitor

Floating Islands International. (n.d.). *Products*. Retrieved October 11, 2022, from https://www.floatingislandinternational.com/products.html#biohavens

Flocco, C. G., Lobalbo, A., Carranza, M. P., Bassi, M., Giulietti, A. M., & Cormack, W. Mac. (2002). Some physiological, microbial, and toxicological aspects of the removal of phenanthrene by hydroponic cultures of alfalfa (Medicago sativa L.). *International Journal of Phytoremediation*, *4*(3), 169–186. https://doi.org/10.1080/15226510208500081

Franchi, E., Cardaci, A., Pietrini, I., Fusini, D., Conte, A., De Folly D'Auris, A., Grifoni, M., Pedron, F., Barbafieri, M., Petruzzelli, G., & Vocciante, M. (2022). Nature-based solutions for restoring an agricultural area contaminated by an oil spill. *Plants*, *11*(17), 18. https://doi.org/10.3390/plants11172250

Freitas, B. G., Brito, J. G. M., Brasileiro, P. P. F., Rufino, R. D., Luna, J. M., Santos, V. A., & Sarubbo, L. A. (2016). Formulation of a commercial biosurfactant for application as a dispersant of petroleum and by-products spilled in oceans. *Frontiers in Microbiology*, *7*(1646), 1–9. https://doi.org/10.3389/fmicb.2016.01646

Fries, E., & Zarfl, C. (2012). Sorption of polycyclic aromatic hydrocarbons (PAHs) to low and high density polyethylene (PE). *Environmental Science and Pollution Research*, *19*(4), 1296–1304. https://doi.org/10.1007/s11356-011-0655-5

Gabos, S., Ikonomou, M. G., Schopflocher, D., Fowler, B. R., White, J., Prepas, E., Prince, D., & Chen, W. (2001). Characteristics of PAHs, PCDD/Fs and PCBs in sediment following

forest fires in northern Alberta. *Chemosphere*, *43*(4–7), 709–719. https://doi.org/10.1016/S0045-6535(00)00424-0

Garrido-Oter, R., Nakano, R. T., Dombrowski, N., Ma, K. W., McHardy, A. C., & Schulze-Lefert, P. (2018). Modular traits of the Rhizobiales root microbiota and their evolutionary relationship with symbiotic Rhizobia. *Cell Host and Microbe*, *24*(1), 155–167. https://doi.org/10.1016/j.chom.2018.06.006

Ghosal, D., Ghosh, S., Dutta, T. K., & Ahn, Y. (2016). Current state of knowledge in microbial degradation of polycyclic aromatic hydrocarbons (PAHs): A review. *Frontiers in Microbiology*, *7*, 1369. https://doi.org/10.3389/fmicb.2016.01369

Gilbert, D., Jakobsen, H. H., Winding, A., & Mayer, P. (2014). Co-transport of polycyclic aromatic hydrocarbons by motile microorganisms leads to enhanced mass transfer under diffusive conditions. *Environmental Science and Technology*, *48*(8), 4368–4375. https://doi.org/10.1021/es404793u

Gilfillan, E. S., Maher, N. P., Krejsa, C. M., Lanphear, M. E., Ball, C. D., Meltzer, J. B., & Page, D. S. (1995). Use of remote sensing to document changes in marsh vegetation following the Amoco Cadiz oil spill (Brittany, France, 1978). *Marine Pollution Bulletin*, *30*(12), 780–787. https://doi.org/10.1016/0025-326X(95)00069-Y

Glöckner, F. O., Kube, M., Bauer, M., Teeling, H., Lombardot, T., Ludwig, W., Gade, D., Beck, A., Borzym, K., Heitmann, K., Rabus, R., Schlesner, H., Amann, R., & Reinhardt, R. (2003). Complete genome sequence of the marine planctomycete Pirellula sp. strain 1. *Proceedings of the National Academy of Sciences of the United States of America*, *100*(14), 8298–8303. https://doi.org/10.1073/pnas.1431443100

Glöckner, F. O., Yilmaz, P., Quast, C., Gerken, J., Beccati, A., Ciuprina, A., Bruns, G., Yarza,

P., Peplies, J., Westram, R., & Ludwig, W. (2017). 25 years of serving the community with ribosomal RNA gene reference databases and tools. *Journal of Biotechnology*, *261*, 169–176. https://doi.org/10.1016/j.jbiotec.2017.06.1198

Golubev, S. N., Schelud'Ko, A. V., Muratova, A. Y., Makarov, O. E., & Turkovskaya, O. V. (2009). Assessing the potential of rhizobacteria to survive under phenanthrene pollution. *Water, Air, and Soil Pollution*, *198*(1–4), 5–16. https://doi.org/10.1007/s11270-008-9821-x

Gran-Scheuch, A., Ramos-Zuñiga, J., Fuentes, E., Bravo, D., & Pérez-Donoso, J. M. (2020). Effect of co-contamination by pahs and heavy metals on bacterial communities of diesel contaminated soils of south Shetland islands, Sntarctica. *Microorganisms*, *8*(11), 1–17. https://doi.org/10.3390/microorganisms8111749

Graves, S., Piepho, H., & Dorai-Raj, S. (2019). *_multcompView: Visualization of paired comparisons_. R package version 0.1-8*. https://cran.r-project.org/package=multcompView

Grolemund, G., & Wickham, H. (2011). Dates and Time Made Easy with lubridate. *Journal of Statistical Software*, *40*(3), 1–25. https://doi.org/10.18637/jss.v040.i03

Gutierrez, T., & Aitken, M. D. (2014). Role of methylotrophs in the degradation of hydrocarbons during the Deepwater Horizon oil spill. *The ISME Journal*, *8*(12), 2543–2545. https://doi.org/10.1038/ismej.2014.88

Guttormson, A. (in preparation). Effects of plant species composition and nutrient addition ratio on the efficacy of bioremediation of simulated freshwater oil spills by engineered floating wetlands. [Unpublished Master's Thesis]. University of Manitoba.

Hancock, T. L., Blonder, S. L., Bury, A. A., Smolinski, R. A., Parsons, M. L., Robertson, A., &

Urakawa, H. (2021). Succession pattern and phylotype analysis of microphytobenthic communities in a simulated oil spill seagrass mesocosm experiment. *Science of the Total Environment*, *784*, 147053. https://doi.org/10.1016/j.scitotenv.2021.147053

Haritash, A. K., & Kaushik, C. P. (2009). Biodegradation aspects of polycyclic aromatic hydrocarbons (PAHs): A review. *Journal of Hazardous Materials*, *169*, 1–15. https://doi.org/10.1016/j.jhazmat.2009.03.137

He, Y., & Chi, J. (2016). Phytoremediation of sediments polluted with phenanthrene and pyrene by four submerged aquatic plants. *Journal of Soils and Sediments*, *16*(1), 309–317. https://doi.org/10.1007/s11368-015-1221-4

Heumann, K. G. (1986). Isotope dilution mass spectrometry of inorganic and organic substances. *Fresenius' Zeitschrift Analytical Chemistry*, *325*(8), 661–666. https://doi.org/10.1007/BF00470971

Heumann, K. G. (1992). Isotope dilution mass spectrometry. *International Journal of Mass Spectrometry and Ion Processes*, *118–119*, 575–592. https://doi.org/10.1016/0168-1176(92)85076-C

Hinsinger, P., Plassard, C., Tang, C., & Jaillard, B. (2003). Origins of root-mediated pH changes in the rhizosphere and their responses to environmental constraints: A review. *Plant and Soil*, *248*(1), 43–59. https://doi.org/10.1023/A:1022371130939

Hoagland, D. R., & Arnon, D. I. (1938). The water-culture method for growing plants without soil. *University of California, Colleage of Agriculture, Agricultural Experiment Station. Circular*, *347*, 1884–1949.

Hoff, R. Z. (1995). *Responding to oil spills in coastal marshes: The fine line between help and hindrance. HAZMAT Report 96-2.* (Vol. 96, Issue 1). Hazardous Materials Response and

Assessments Division, NOAA. https://response.restoration.noaa.gov/sites/default/files/Coastal_Marshes_508.pdf

Holubar, P., Grudke, T., Moser, A., Strenn, B., & Braun, R. (2000). Effects of bacterivorous ciliated protozoans on degradation efficiency of a petrochemical activated sludge process. *Water Research*, *34*(7), 2051–2060. https://doi.org/10.1016/S0043-1354(99)00378-4

Honda, M., & Suzuki, N. (2020). Toxicities of polycyclic aromatic hydrocarbons for aquatic animals. *International Journal of Environmental Research and Public Health*, *17*(1363), 23. https://doi.org/10.3390/ijerph17041363

Hussain, F., Tahseen, R., Arslan, M., Iqbal, S., & Afzal, M. (2019). Removal of hexadecane by hydroponic root mats in partnership with alkane-degrading bacteria: bacterial augmentation enhances system's performance. *International Journal of Environmental Science and Technology*, *16*(8), 4611–4620. https://doi.org/10.1007/s13762-018-2165-1

Ichor, T., Okerentugba, P. O., & Okpokwasili, G. C. (2016). Biodegradation of total petroleum hydrocarbon by a consortium of cyanobacteria isolated from crude oil polluted brackish waters of Bodo creeks in Ogoniland, Rivers State. *Research Journal of Environmental Toxicology*, *10*(1), 16–27. https://doi.org/10.3923/rjet.2016.16.27

Idomeh, J. E., Shittu, O. B., Oyedepo, J. A., Bada, B. S., Balogun, S. A., Idomeh, F. A., & Ezenweani, R. S. (2021). Petroleum hydrocarbon impacted aquatic ecosystem reveals Methylotenera as the dominant genera in the Niger Delta Region of Nigeria. *Geomicrobiology Journal*, *38*(10), 879–894. https://doi.org/10.1080/01490451.2021.1973614

Idowu, I., Francisco, O., Thomas, P. J., Johnson, W., Marvin, C., Stetefeld, J., & Tomy, G. T. (2018). Validation of a simultaneous method for determining polycyclic aromatic

compounds and alkylated isomers in biota. *Rapid Communications in Mass Spectrometry*, *32*(3), 277–287. https://doi.org/10.1002/rcm.8035

IISD Experimental Lakes Area. (2022). *IISD Experimental Lakes Area: Bathymetry Data Package, 1968-2022 ver 3.* https://doi.org/10.6073/pasta/e9898c78448cbbe544057e689d3c06df

Ijaz, A., Shabir, G., Khan, Q. M., & Afzal, M. (2015). Enhanced remediation of sewage effluent by endophyte-assisted floating treatment wetlands. *Ecological Engineering*, *84*, 58–66. https://doi.org/10.1016/j.ecoleng.2015.07.025

Jatav, K. S., & Singh, R. P. (2015). Phytoremediation using algae and macrophytes: II. In A. A. Ansari, S. S. Gill, R. Gill, G. R. Lanza, & L. Newman (Eds.), *Phytoremediation: Management of Environmental Contaminants* (Vol. 2, pp. 291–296). Springer International Publishing. https://doi.org/10.1007/978-3-319-10969-5

Jia-hua, L., Hong-yan, G., Xiao-rong, W., Hong, W. M., ShiHe, W., Da-qiang, Y., Ying, Y., & Jingfei, Z. (2009). Plant-promoted dissipation of four submerged macrophytes to phenanthrene. *Aquatic Ecosystem Health and Management*, *12*(4), 471–476. https://doi.org/10.1080/14634980903341293

Jobard, M., Rasconi, S., & Sime-Ngando, T. (2010). Diversity and functions of microscopic fungi: A missing component in pelagic food webs. *Aquatic Sciences*, *72*(3), 255–268. https://doi.org/10.1007/s00027-010-0133-z

Jones, L. A., Muhlfeld, C. C., & Hauer, F. R. (2017). Temperature. In F. R. Hauer & G. A. Lamberti (Eds.), *Methods in Stream Ecology: Volume 1: Ecosystem Structure. Third Edition* (Vol. 1, pp. 109–120). Elsevier Inc. https://doi.org/10.1016/B978-0-12-416558-8.00006-8

Jouanneau, Y., Willison, J. C., Meyer, C., Krivobok, S., Chevron, N., Besombes, J. L., & Blake, G. (2005). Stimulation of pyrene mineralization in freshwater sediments by bacterial and plant bioaugmentation. *Environmental Science and Technology*, *39*(15), 5729–5735. https://doi.org/10.1021/es050412d

Jousset, A., Lara, E., Nikolausz, M., Harms, H., & Chatzinotas, A. (2010). Application of the denaturing gradient gel electrophoresis (DGGE) technique as an efficient diagnostic tool for ciliate communities in soil. *Science of the Total Environment*, *408*(5), 1221–1225. https://doi.org/10.1016/j.scitotenv.2009.09.056

Juhasz, A. L., & Naidu, R. (2000). Bioremediation of high molecular weight polycyclic aromatic hydrocarbons: A review of the microbial degradation of benzo[a]pyrene. *International Biodeterioration and Biodegradation*, *45*(1–2), 57–88. https://doi.org/10.1016/S0964-8305(00)00052-4

Kachieng'a, L., & Momba, M. N. B. (2017). Biodegradation of petroleum hydrocarbon functional groups in contaminated water using selected protozoan isolates. *Journal of Environmental Chemical Engineering*, *5*(2), 1885–1891. https://doi.org/10.1016/j.jece.2017.03.022

Kachieng'a, L., & Momba, M. N. B. (2018). The synergistic effect of a consortium of protozoan isolates (Paramecium sp., Vorticella sp., Epistylis sp. and Opercularia sp.) on the biodegradation of petroleum hydrocarbons in wastewater. *Journal of Environmental Chemical Engineering*, *6*(4), 4820–4827. https://doi.org/10.1016/j.jece.2018.07.005

Kadri, T., Rouissi, T., Kaur Brar, S., Cledon, M., Sarma, S., & Verma, M. (2017). Biodegradation of polycyclic aromatic hydrocarbons (PAHs) by fungal enzymes: A review. *Journal of Environmental Sciences*, *51*, 52–74.

https://doi.org/10.1016/j.jes.2016.08.023

Kamalanathan, M., Schwehr, K. A., Labonté, J. M., Taylor, C., Bergen, C., Patterson, N., Claflin, N., Santschi, P. H., & Quigg, A. (2021). The interplay of phototrophic and heterotrophic microbes under oil exposure: A microcosm study. *Frontiers in Microbiology*, *12*, 675328. https://doi.org/10.3389/fmicb.2021.675328

Kassambara, A. (2023). *_ggpubr: "ggplot2" Based publication ready plots_. R package version 0.6.0*. https://cran.r-project.org/package=ggpubr

Kertesz, M. A., & Kawasaki, A. (2010). Hydrocarbon-degrading Sphingomonads: Sphingomonas, Spingobium, Novosphingobium, and Sphingopyxis. In K. N. Timmis (Ed.), *Handbook of Hydrocarbon and Lipid Microbiology* (pp. 1693–1705). Springer, Berlin, Heidelberg. https://doi.org/10.1007/978-3-540-77587-4_119

Kessler, J. D., Valentine, D. L., Redmond, M. C., Du, M., Chan, E. W., Mendes, S. D., Quiroz, E. W., Villanueva, C. J., Shusta, S. S., Werra, L. M., Yvon-Lewis, S. A., & Weber, T. C. (2011). A persistant oxygen anomaly reveals the fate of spilled methane in the deep Gulf of Mexico. *Science*, *311*, 312–315. https://doi.org/10.1126/science.1199697

King, G. M., Kostka, J. E., Hazen, T. C., & Sobecky, P. A. (2015). Microbial responses to the Deepwater Horizon Oil spill: From coastal wetlands to the deep sea. *Annual Review of Marine Science*, *7*, 377–401. https://doi.org/10.1146/annurev-marine-010814-015543

Koo, H., Mojib, N., Huang, J. P., Donahoe, R. J., & Bej, A. K. (2015). Bacterial community shift in the coastal Gulf of Mexico salt-marsh sediment microcosm in vitro following exposure to the Mississippi Canyon Block 252 oil (MC252). *3 Biotech*, *5*(4), 379–392. https://doi.org/10.1007/s13205-014-0233-x

Kösesakal, T., & Seyhan, M. (2023). Phenanthrene stress response and phytoremediation

potential of free-floating fern Azolla filiculoides Lam. *International Journal of Phytoremediation*, *25*(2), 207–220. https://doi.org/10.1080/15226514.2022.2069224

Kulichevskaya, I. S., Suzina, N. E., Liesack, W., & Dedysh, S. N. (2010). Bryobacter aggregatus gen. nov., sp. nov., a peat-inhabiting, aerobic chemo-organotroph from subdivision 3 of the acidobacteria. *International Journal of Systematic and Evolutionary Microbiology*, *60*(2), 301–306. https://doi.org/10.1099/ijs.0.013250-0

Lara, E., & Acosta-Mercado, D. (2012). A molecular perspective on ciliates as soil bioindicators. *European Journal of Soil Biology*, *49*, 107–111. https://doi.org/10.1016/j.ejsobi.2011.11.001

Lara, E., Berney, C., Harms, H., & Chatzinotas, A. (2007). Cultivation-independent analysis reveals a shift in ciliate 18S rRNA gene diversity in a polycyclic aromatic hydrocarbon-polluted soil. *FEMS Microbiology Ecology*, *62*(3), 365–373. https://doi.org/10.1111/j.1574-6941.2007.00387.x

Lee, K., Boufadel, M., Chen, B., Foght, J., Hodson, P., Swanson, S., & Venosa, A. (2015). *Expert Panel Report on the Behaviour and Environmental Impacts of Crude Oil Released into Aqueous Environments*. Royal Society of Canada, Ottawa, ON. ISBN: 978-1-928140-02-3.

Lemmel, F., Maunoury-Danger, F., Leyval, C., & Cébron, A. (2021). Altered fungal communities in contaminated soils from French industrial brownfields. *Journal of Hazardous Materials*, *406*, 124296. https://doi.org/10.1016/j.jhazmat.2020.124296

Levy, M. G., Litaker, R. W., Goldstein, R. J., Dykstra, M. J., Vandersea, M. W., & Noga, E. J. (2007). Piscinoodinium, a fish-ectoparasitic dinoflagellate, is a member of the class Dinophyceae, subclass Gymnodiniphycidae: Convergent evolution with Amyloodinium.

Journal of Parasitology, *93*(5), 1006–1015. https://doi.org/10.1645/GE-3585.1

Li, H., Hao, H., Yang, X., Xiang, L., Zhao, F., Jiang, H., & He, Z. (2012). Purification of refinery wastewater by different perennial grasses growing in a floating bed. *Journal of Plant Nutrition*, *35*(1), 93–110. https://doi.org/10.1080/01904167.2012.631670

Liu, J., Zhang, Z., Sheng, Y., Gao, Y., & Zhao, Z. (2018). Phenanthrene-degrading bacteria on root surfaces: a natural defense that protects plants from phenanthrene contamination. *Plant and Soil*, *425*(1–2), 335–350. https://doi.org/10.1007/s11104-018-3575-z

Liu, Z., & Liu, J. (2013). Evaluating bacterial community structures in oil collected from the sea surface and sediment in the northern Gulf of Mexico after the Deepwater Horizon oil spill. *MicrobiologyOpen*, *2*(3), 492–504. https://doi.org/10.1002/mbo3.89

Louvel, B., Cébron, A., & Leyval, C. (2011). Root exudates affect phenanthrene biodegradation, bacterial community and functional gene expression in sand microcosms. *International Biodeterioration and Biodegradation*, *65*(7), 947–953. https://doi.org/10.1016/j.ibiod.2011.07.003

LuminUltra. (n.d.). *2nd generation ATP® testing*. Retrieved August 30, 2023, from https://www.luminultra.com/tech/2nd-generation-atp/?gclid=Cj0KCQjw0bunBhD9ARIsAAZl0E1KvVsKRkEIWCdNv1ciTaXT-WYeXv8-_2tMGRwgOSqEIh69sTctNScaAhicEALw_wcB

LuminUltra. (2017). *Product instructions. PhotonMaster™ Luminometer & Bluetooth® Module*.

Lyu, Y., Zheng, W., Zheng, T., & Tian, Y. (2014). Biodegradation of polycyclic aromatic hydrocarbons by Novosphingobium pentaromativorans US6-1. *PLoS ONE*, *9*(7), e101438. https://doi.org/10.1371/journal.pone.0101438

Macek, T., Makova, M., & Kas, J. (2000). Exploitation of plants for the removal of organics in

environmental remediation. *Biotechnology Advances*, *18*(1), 23–34. https://doi.org/10.1016/S0734-9750(99)00034-8

Magar, V. S., Chadwick, D. B., Bridges, T. S., Fuchsman, P. C., Conder, J. M., Dekker, T. J., Steevens, J. A., Gustavson, K. E., & Mills, M. A. (2009). Technical guide: Monitored natural recovery at contaminated sediment sites. *ENVIRON International Corporation* (Issue May). https://apps.dtic.mil/sti/pdfs/ADA512822.pdf

Mahmoudi, N., Porter, T. M., Zimmerman, A. R., Fulthorpe, R. R., Kasozi, G. N., Silliman, B. R., & Slater, G. F. (2013). Rapid degradation of deepwater horizon spilled oil by indigenous microbial communities in louisiana saltmarsh sediments. *Environmental Science and Technology*, *47*(23), 13303–13312. https://doi.org/10.1021/es4036072

Malla, M. A., Dubey, A., Yadav, S., Kumar, A., Hashem, A., & Abd-Allah, E. F. (2018). Understanding and designing the strategies for the microbe-mediated remediation of environmental contaminants using omics approaches. *Frontiers in Microbiology*, *9*(1132), 1–20. https://doi.org/10.3389/fmicb.2018.01132

Mangiafico, S. (2023). *_rcompanion: Functions to support extension education program evaluation_. R Package version 2.4.21*. https://cran.r-project.org/package=rcompanion

Martin, B. C., George, S. J., Price, C. A., Ryan, M. H., & Tibbett, M. (2014). The role of root exuded low molecular weight organic anions in facilitating petroleum hydrocarbon degradation: Current knowledge and future directions. *Science of the Total Environment*, *472*, 642–653. https://doi.org/10.1016/j.scitotenv.2013.11.050

McConkey, B. J., Duxbury, C. L., Dixon, D. G., & Greenberg, B. M. (1997). Toxicity of a PAH photooxidation product to the bacteria Photobacterium phosphoreum and the duckweed Lemna gibba: Effects of phenanthrene and its primary photoproduct,

phenanthrenequinone. *Environmental Toxicology and Chemistry*, *16*(5), 892–899. https://doi.org/10.1002/etc.5620160508

McIlroy, S. J., & Nielsen, P. H. (2014). The gamily Saprospiraceae. In E. Rosenberg, E. F. De Long, S. Lory, E. Stackebrandt, & F. Thompson (Eds.), *The Prokaryotes: Other major lineages of bacteria and the archaea* (pp. 863–889). Springer-Verlag Berlin Heidelberg. https://doi.org/10.1007/978-3-642-38954-2

Miguez, F. (2023). *_nlraa: Nonlinear regression for agricultural applications_. R package version 1.9.3.* https://cran.r-project.org/package=nlraa

Moorhead, K. K., & Reddy, K. R. (1988). Oxygen transport through selected aquatic macrophytes. *Journal of Environmental Quality*, *17*(1), 138–142. https://doi.org/10.2134/jeq1988.00472425001700010022x

Moss, J. A., McCurry, C., Tominack, S., Romero, I. C., Hollander, D., Jeffrey, W. H., & Snyder, R. A. (2015). Ciliated protists from the nepheloid layer and water column of sites affected by the Deepwater Horizon oil spill in the Northeastern Gulf of Mexico. *Deep-Sea Research Part I: Oceanographic Research Papers*, *106*, 85–96. https://doi.org/10.1016/j.dsr.2015.10.001

Müller, K. (2020). *_here: A simpler way to find your files_. R package 1.0.1.* (1.0.1).

Müller, K., & Wickham, H. (2022). *_tibble: Simple data frames_.R package version 3.1.8*. https://cran.r-project.org/package=tibble

Muratova, A., Golubev, S., Wittenmayer, L., Dmitrieva, T., Bondarenkova, A., Hirche, F., Merbach, W., & Turkovskaya, O. (2009). Effect of the polycyclic aromatic hydrocarbon phenanthrene on root exudation of Sorghum bicolor (L.) Moench. *Environmental and Experimental Botany*, *66*(3), 514–521. https://doi.org/10.1016/j.envexpbot.2009.03.001

Murphy, S. M. C., Bautista, M. A., Cramm, M. A., & Hubert, C. R. J. (2021). Diesel and crude oil biodegradation by cold-adapted microbial communities in the Labrador Sea. *Applied and Environmental Microbiology*, *87*(20), 1–21. https://doi.org/10.1128/AEM.00800-21

Murray, M. W., Allan, J. D., & Child, M. (2018). *Potential ecological impacts of crude oil transport in the Great Lakes Basin*. Great Lakes Science Advisory Board, Science Priority Committee. https://www.ijc.org/sites/default/files/2019-01/Potential%20Ecological%20Impacts%20of%20Crude%20Oil%20Transport%20in%20the%20Great%20Lakes%20Basin%20-%20Oct%202018.pdf

Naczi, R. F. C. (1992). *Systematics of Carex section Griseae (Cyperaceae)*. [Doctoral Dissertation, University of Michigan]. ProQuest Dissertations & Theses, https://www.proquest.com/docview/303996217

Naranjo-Ortiz, M. A., & Gabaldón, T. (2019). Fungal evolution: diversity, taxonomy and phylogeny of the Fungi. *Biological Reviews*, *94*(6), 2101–2137. https://doi.org/10.1111/brv.12550

National Center for Biotechnology Information. (2023). *PubChem compound summary for CID 995, phenanthrene*. https://pubchem.ncbi.nlm.nih.gov/compound/Phenanthrene

Natural Resources Canada. (2019). *Oil supply and demand*. https://natural-resources.canada.ca/our-natural-resources/energy-sources-distribution/fossil-fuels/crude-oil/oil-supply-demand/18086

Natural Resources Canada. (2020). *Crude oil industry overview*. https://natural-resources.canada.ca/our-natural-resources/energy-sources-distribution/fossil-fuels/crude-oil/crude-oil-industry-overview/18078

Natural Resources Canada. (2022). *Statistical data: Forest inventory Boreal Shield*.

https://cfs.nrcan.gc.ca/statsprofile/inventory/borealshield

Newton, R. J., Jones, S. E., Eiler, A., McMahon, K. D., & Bertilsson, S. (2011). A guide to the natural history of freshwater lake bacteria. *Microbiology and Molecular Biology Reviews*, *75*(1), 14–49. https://doi.org/10.1128/mmbr.00028-10

Niehl, A., Liebe, S., Varrelmann, M., & Koenig, R. (2020). Benyviruses (Benyviridae). In D. H. Bamford & M. Zuckerman (Eds.), *Encyclopedia of Virology* (4th ed., Vols. 1–5, pp. 219–228). https://doi.org/10.1016/B978-0-12-809633-8.21298-3

Oberholster, P., Cheng, P., Truter, C., Hill, L., & Botha, A. M. (2014). Species specific responses of common freshwater wetland phytoplankton to crude oil by application of bioassays. In A. Clifton (Ed.), *Oil spills: Environmental issues, prevention and ecological impacts* (Issue August, pp. 87–119). Nova Science Publishers, Inc.

Ogle, D., Doll, J., Wheeler, A., & Dinno, A. (2023). *_FSA: Simple fisheries stock assessment methods_. R package version 0.9.4*. https://cran.r-project.org/package=FSA

Oliver Wyman. (2019). *Canadian crude oil transportation: Comparing the safety of pipelines and railways*. https://www.railcan.ca/wp-content/uploads/2019/08/Canadian-Crude-Oil-Transportation-Comparing-the-Safety-of-Pipelines-and-Railways-2.pdf

Ozaki, S., Kishimoto, N., & Fujita, T. (2006). Isolation and phylogenetic characterization of microbial consortia able to degrade aromatic hydrocarbons at high rates. *Microbes and Environments*, *21*(1), 44–52. https://doi.org/10.1264/jsme2.21.44

Paine, C. E. T., Marthews, T. R., Vogt, D. R., Purves, D., Rees, M., Hector, A., & Turnbull, L. A. (2012). How to fit nonlinear plant growth models and calculate growth rates: An update for ecologists. *Methods in Ecology and Evolution*, *3*(2), 245–256. https://doi.org/10.1111/j.2041-210X.2011.00155.x

Palace, V. P., Peters, L., Berard-Brown, N., Smyth, P., Shanoff, T., Wiseman, G., Tomy, G., Havens, S., Dettman, H., Greer, C. W., Kajpust, H., Black, T., Hanson, M., Rodriguez-Gil, J. L., & Taylor, E. (2021). Assessing monitored natural recovery (MNR) for remediating crude oil spills in freshwater environments: The Freshwater Oil Spill Remediation Study (FOReSt) at the Experimental Lakes Area, Canada. *2021 International Oil Spill Conference*, 1–20.

Park, B. S., Erdner, D. L., Bacosa, H. P., Liu, Z., & Buskey, E. J. (2020). Potential effects of bacterial communities on the formation of blooms of the harmful dinoflagellate Prorocentrum after the 2014 Texas City "Y" oil spill (USA). *Harmful Algae, 95,* 101802. https://doi.org/10.1016/j.hal.2020.101802

Pedersen, E. J., Miller, D. L., Simpson, G. L., & Ross, N. (2019). Hierarchical generalized additive models in ecology: An introduction with mgcv. *PeerJ, 7*, e6876. https://doi.org/10.7717/peerj.6876

Pedersen, E., Simpson, G., Ross, N., & Rodriguez-Sanchez, F. (2020). *Hierarchical Generalized Additive Models: an introduction with mgcv*. https://doi.org/10.5281/zenodo.2604627

Pedersen, T. (2022). *_patchwork: The composer of plots_. R package version 1.1.2*. https://cran.r-project.org/package=patchwork

Peixoto, R. S., Vermelho, A. B., & Rosado, A. S. (2011). Petroleum-degrading enzymes: Bioremediation and new prospects. *Enzyme Research*, *2011*, 475193. https://doi.org/10.4061/2011/475193

Peng, M., Zi, X., & Wang, Q. (2015). Bacterial community diversity of oil-contaminated soils assessed by high throughput sequencing of 16s rRNA genes. *International Journal of Environmental Research and Public Health*, *12*(10), 12002–12015.

https://doi.org/10.3390/ijerph121012002

Pérez-Hernández, V., Ventura-Canseco, L. M. C., Gutiérrez-Miceli, F. A., Pérez-Hernández, I., Hernández-Guzmán, M., & Enciso-Sáenz, S. (2020). The potential of Mimosa pigra to restore contaminated soil with anthracene and phenanthrene. *Terra Latinoamericana*, *38*, 755–769. https://doi.org/10.28940/terra.v38i4.603

Pérez-Pantoja, D., Donoso, R., Agulló, L., Córdova, M., Seeger, M., Pieper, D. H., & González, B. (2012). Genomic analysis of the potential for aromatic compounds biodegradation in Burkholderiales. *Environmental Microbiology*, *14*(5), 1091–1117. https://doi.org/10.1111/j.1462-2920.2011.02613.x

Pezeshki, S. R., Hester, M. W., Lin, Q., & Nyman, J. A. (2000). The effects of oil spill and clean-up on dominant US Gulf coast marsh macrophytes: A review. *Environmental Pollution*, *108*(2), 129–139. https://doi.org/10.1016/S0269-7491(99)00244-4

Phenrat, T., Teeratitayangkul, P., Prasertsung, I., Parichatprecha, R., Jitsangiam, P., Chomchalow, N., & Wichai, S. (2017). Vetiver plantlets in aerated system degrade phenol in illegally dumped industrial wastewater by phytochemical and rhizomicrobial degradation. *Environmental Science and Pollution Research*, *24*(15), 13235–13246. https://doi.org/10.1007/s11356-016-7707-9

Phillips, L. A., Greer, C. W., Farrell, R. E., & Germida, J. J. (2012). Plant root exudates impact the hydrocarbon degradation potential of a weathered-hydrocarbon contaminated soil. *Applied Soil Ecology*, *52*(1), 56–64. https://doi.org/10.1016/j.apsoil.2011.10.009

Pilon-Smits, E. (2005). Phytoremedation. *Annual Review of Plant Biology*, *56*(1), 15–39. https://doi.org/10.1146/annurev.arplant.56.032604.144214

Pinheiro, J., & Bates, D. (2000). *Mixed-effects models in S and S-PLUS*. Springer.

https://doi.org/10.1007/b98882

Pinheiro, J., Bates, D., & R Core Team. (2022). *_nlme: Linear and nonlinear mixed effects models_. R package version 3.1-160*. https://cran.r-project.org/package=nlme

Pokorný, J., & Květ, J. (2004). Aquatic plants and lake ecosystems. In P. E. O'Sullivan & C. S. Reynolds (Eds.), *The lakes handbook* (Volume I, pp. 309–340). Blackwell Publishing Ltd.

Posit Team. (2023). *RStudio: Integrated Development Environment for R.* http://www.posit.co/

Prince, R. C. (2018). Eukaryotic hydrocarbon degraders. In T. J. McGenity (Ed.), *Taxonomy, genomics and ecophysiology of hydrocarbon-degrading microbes, Handbook of hydrocarbon and lipid microbiology* (pp. 1–20). Springer. https://doi.org/10.1007/978-3-540-77587-4_150

Prince, R. C., Amande, T. V., & McGenity, T. J. (2018). Prokaryotic hydrocarbon degraders. In T. J. McGenity (Ed.), *Taxonomy, genomics and ecophysiology of hydrocarbon degrading microbes, handbook of hydrocarbon and lipid Mmcrobiology* (pp. 1–41). Springer. https://doi.org/10.1007/978-3-319-60053-6_15-1

Quast, C., Pruesse, E., Yilmaz, P., Gerken, J., Schweer, T., Yarza, P., Peplies, J., & Glöckner, F. O. (2013). The SILVA ribosomal RNA gene database project: Improved data processing and web-based tools. *Nucleic Acids Research*, *41*, 590–596. https://doi.org/10.1093/nar/gks1219

R Core Team. (2022). *R: A language and environment for statistical computing.* R Foundation for Statistical Computing.

Radice, R. P., Fabrizio, V. De, Donadoni, A., Scopa, A., & Martelli, G. (2023). Crude oil bioremediation : From bacteria to microalgae. *Processes*, *11*(2), 442.

https://doi.org/10.3390/pr11020442

Raju, M. N., & Scalvenzi, L. (2018). Petroleum degradation: Promising biotechnological tools for bioremediation. In M. Zoveidavianpoor (Ed.), *Recent insights in petroleum science and engineering* (pp. 351–369). Intech Open. https://doi.org/10.5772/intechopen.70109

Ramdahl, T. (1983). Retene- a molecular marker of wood combustion in ambient air. *Nature*, *306*(8), 580–582. https://doi.org/10.1038/306580a0

Randerson, P. F., Moran, C., & Bialowiec, A. (2011). Oxygen transfer capacity of willow (Salix viminalis L.). *Biomass and Bioenergy*, *35*(5), 2306–2309. https://doi.org/10.1016/j.biombioe.2011.02.018

Redmond, M. C., & Valentine, D. L. (2012). Natural gas and temperature structured a microbial community response to the Deepwater Horizon oil spill. *Proceedings of the National Academy of Sciences of the United States of America*, *109*(50), 20292–20297. https://doi.org/10.1073/pnas.1108756108

Rehman, K., Arslan, M., Müller, J. A., Saeed, M., Imran, A., Amin, I., Mustafa, T., Iqbal, S., & Afzal, M. (2021). Bioaugmentation-enhanced remediation of crude oil polluted water in pilot-scale floating treatment wetlands. *Water*, *13*(20), 2882. https://doi.org/10.3390/w13202882

Rehman, K., Imran, A., Amin, I., & Afzal, M. (2018). Inoculation with bacteria in floating treatment wetlands positively modulates the phytoremediation of oil field wastewater. *Journal of Hazardous Materials*, *349*, 242–251. https://doi.org/10.1016/j.jhazmat.2018.02.013

Rehman, K., Imran, A., Amin, I., & Afzal, M. (2019). Enhancement of oil field-produced wastewater remediation by bacterially-augmented floating treatment wetlands.

Chemosphere, *217*, 576–583. https://doi.org/10.1016/j.chemosphere.2018.11.041

Ribicic, D., McFarlin, K. M., Netzer, R., Brakstad, O. G., Winkler, A., Throne-Holst, M., & Størseth, T. R. (2018). Oil type and temperature dependent biodegradation dynamics - Combining chemical and microbial community data through multivariate analysis. *BMC Microbiology*, *18*(1), 1–15. https://doi.org/10.1186/s12866-018-1221-9

Richardson, E., Bass, D., Smirnova, A., Paoli, L., Dunfield, P., & Dacks, J. B. (2020). Phylogenetic estimation of community composition and novel eukaryotic lineages in Base Mine Lake: An oil sands tailings reclamation site in Northern Alberta. *Journal of Eukaryotic Microbiology*, *67*(1), 86–99. https://doi.org/10.1111/jeu.12757

Robinson, D., Hayes, A., & Couch, S. (2023). *_broom: Convert statistical objects in tidy tibbles_. R package version 1.0.3*. https://cran.r-project.org/package=broom

Robinson, C. V., Porter, T. M., McGee, K. M., McCusker, M., Wright, M. T. G., & Hajibabaei, M. (2022). Multi-marker DNA metabarcoding detects suites of environmental gradients from an urban harbour. *Scientific Reports*, *12*(1), 1–12. https://doi.org/10.1038/s41598-022-13262-6

Rodriguez-Gil, J. L., Stoyanovich, S., Hanson, M. L., Hollebone, B., Orihel, D. M., Palace, V., Faragher, R., Mirnaghi, F. S., Shah, K., Yang, Z., Black, T. A., Cederwall, J., Mason, J., Patterson, S., Timlick, L., Séguin, J. Y., & Blais, J. M. (2021). Simulating diluted bitumen spills in boreal lake limnocorrals - Part 1: Experimental design and responses of hydrocarbons, metals, and water quality parameters. *Science of The Total Environment*, *790*, 148537. https://doi.org/10.1016/J.SCITOTENV.2021.148537

Rogerson, A., & Berger, J. (1981). Effect of crude oil and petroleum-degrading micro-organisms on the growth of freshwater and soil protozoa. *Journal of General Microbiology*, *124*(1),

53–59. https://doi.org/10.1099/00221287-124-1-53

Rohrbacher, F., & St-Arnaud, M. (2016). Root exudation: The ecological driver of hydrocarbon rhizoremediation. *Agronomy*, *6*(19), 1–27. https://doi.org/10.3390/agronomy6010019

Rojas-Gätjens, D., Fuentes-Schweizer, P., Rojas-Jiménez, K., Pérez-Pantoja, D., Avendaño, R., Alpízar, R., Coronado-Ruíz, C., & Chavarría, M. (2022). Methylotrophs and hydrocarbon-degrading bacteria are key players in the microbial community of an abandoned century-old oil exploration well. *Microbial Ecology*, *83*, 83–99. https://doi.org/10.1007/s00248-021-01748-1

Rojo, F. (2021). A new global regulator that facilitates the co-metabolization of polyaromatic hydrocarbons and other nutrients in Novosphingobium. *Environmental Microbiology*, *23*(6), 2875–2877. https://doi.org/10.1111/1462-2920.15527

Rosenberg, E., & Ron, E. Z. (1996). Bioremediation of petroleum contamination. In R. L. Crawford & D. L. Crawford (Eds.), *Bioremediation: Principles and applications* (pp. 100–124). Cambridge University Press, UK.

Saleem, H., Arslan, M., Rehman, K., Tahseen, R., & Afzal, M. (2019). Phragmites australis — a helophytic grass — can establish successful partnership with phenol-degrading bacteria in a floating treatment wetland. *Saudi Journal of Biological Sciences*, *26*(6), 1179–1186. https://doi.org/10.1016/j.sjbs.2018.01.014

Saleem, H., Rehman, K., Arslan, M., & Afzal, M. (2018). Enhanced degradation of phenol in floating treatment wetlands by plant-bacterial synergism. *International Journal of Phytoremediation*, *20*(7), 692–698. https://doi.org/10.1080/15226514.2017.1413334

Sammarco, P. W., Kolian, S. R., Warby, R. A. F., Bouldin, J. L., Subra, W. A., & Porter, S. A. (2013). Distribution and concentrations of petroleum hydrocarbons associated with the

BP/Deepwater Horizon Oil Spill, Gulf of Mexico. *Marine Pollution Bulletin*, *73*(1), 129–143. https://doi.org/10.1016/j.marpolbul.2013.05.029

Sasse, J., Martinoia, E., & Northen, T. (2018). Feed your friends: Do plant exudates shape the root microbiome? *Trends in Plant Science*, *23*(1), 25–41. https://doi.org/10.1016/j.tplants.2017.09.003

Schindelin, J., Arganda-Carreras, I., Frise, E., Kaynig, V., Longair, M., Pietzsch, T., Preibisch, S., Rueden, C., Saalfeld, S., Schmid, B., Tinevez, J. Y., White, D. J., Hartenstein, V., Eliceiri, K., Tomancak, P., & Cardona, A. (2012). Fiji: An open-source platform for biological-image analysis. *Nature Methods*, *9*(7), 676–682. https://doi.org/10.1038/nmeth.2019

Schoch, C. et al. (2020). *NCBI Taxonomy: a comprehensive update on curation, resources and tools. Database*. https://www.ncbi.nlm.nih.gov/Taxonomy/Browser/wwwtax.cgi?mode=Root

Selala, C., Botha, A. M., De Klerk, L. P., De Klerk, A. R., Myburgh, J. G., & Oberholster, P. J. (2014). Using phytoplankton diversity to determine wetland resilience, one year after a vegetable oil spill. *Water, Air, and Soil Pollution*, *225*(8), 1–11. https://doi.org/10.1007/s11270-014-2051-5

Shahid, M. J., Arslan, M., Ali, S., Siddique, M., & Afzal, M. (2018). Floating wetlands: A sustainable tool for wastewater treatment. *Clean - Soil, Air, Water*, *46*(10), 13. https://doi.org/10.1002/clen.201800120

Shahzad, A., Siddiqui, S., & Bano, A. (2016). Rhizoremediation of petroleum hydrocarbon, prospects and future. *RSC Advances*, *6*(110), 108347–108361. https://doi.org/10.1039/c6ra12458e

Siano, R., Montresor, M., Probert, I., Not, F., & de Vargas, C. (2010). Pelagodinium gen. nov. and P. béii comb. nov., a dinoflagellate symbiont of planktonic foraminifera. *Protist, 161*(3), 385–399. https://doi.org/10.1016/j.protis.2010.01.002

silva. (2023). *silva. High quality ribosomal RNA databases*. https://www.arb-silva.de/

Simpson, G. (2023). *_gratia: Graceful ggplot-based graphics and other functions for GAMs fitted using mgcv_. R package version 0.8.1*. https://gavinsimpson.github.io/gratia/

Sohn, J. H., Kwon, K. K., Kang, J. H., Jung, H. B., & Kim, S. J. (2004). Novosphingobium pentaromativorans sp. nov., a high-molecular-mass polycyclic aromatic hydrocarbon-degrading bacterium isolated from estuarine sediment. *International Journal of Systematic and Evolutionary Microbiology, 54*(5), 1483–1487. https://doi.org/10.1099/ijs.0.02945-0

Song, M., Luo, C., Jiang, L., Zhang, D., Wang, Y., & Zhang, G. (2015). Identification of benzo[a]pyrene-metabolizing bacteria in forest soils by using DNA-based stable-isotope probing. *Applied and Environmental Microbiology*, *81*(21), 7368–7376. https://doi.org/10.1128/AEM.01983-15

Song, W. F., Wang, J. W., Yan, Y. C., An, L. Y., Zhang, F., Wang, L., Xu, Y., Tian, M. Z., Nie, Y., & Wu, X. L. (2018). Shifts of the indigenous microbial communities from reservoir production water in crude oil- and asphaltene-degrading microcosms. *International Biodeterioration and Biodegradation, 132*, 18–29. https://doi.org/10.1016/j.ibiod.2018.04.015

Spalinger, K., & Bouwens, K. A. (2003). *The roles of phosphorus and nitrogen in lake ecosystems* (Issue Regional Information Report No. 4K03-42). Alaska Department of Fish and Game. https://www.adfg.alaska.gov/fedaidpdfs/RIR.4K.2003.42.pdf

Srivastava, J. K., Chandra, H., Kalra, S. J. S., Mishra, P., Khan, H., & Yadav, P. (2017). Plant–microbe interaction in aquatic system and their role in the management of water quality: a review. *Applied Water Science*, *7*(3), 1079–1090. https://doi.org/10.1007/s13201-016-0415-2

Stainton, M. P., Capel, M. J., & Armstrong, F. A. J. (1977). *The chemical analysis of freshwater* (2nd ed.).

Stanley, M., Palace, V., Grosshans, R., & Levin, D. B. (2022). Floating treatment wetlands for the bioremediation of oil spills : A review. *Journal of Environmental Management*, *317*, 115416. https://doi.org/10.1016/j.jenvman.2022.115416

Starr, J. R., Naczi, R. F. C., & Chouinard, B. N. (2009). Plant DNA barcodes and species resolution in sedges (Carex, Cyperaceae). *Molecular Ecology Resources*, *9*(Suppl. 1), 151–163. https://doi.org/10.1111/j.1755-0998.2009.02640.x

Statistics Canada. (2011). Environment. In Statistics Canada (Ed.), *Canada Year Book, 2011* (pp. 168–179). https://www150.statcan.gc.ca/n1/pub/11-402-x/2011000/pdf/environ-eng.pdf

Stottmeister, U., Wießner, A., Kuschk, P., Kappelmeyer, U., Kästner, M., Bederski, O., Müller, R. A., & Moormann, H. (2003). Effects of plants and microorganisms in constructed wetlands for wastewater treatment. *Biotechnology Advances*, *22*(1–2), 93–117. https://doi.org/10.1016/j.biotechadv.2003.08.010

Stoyanovich, S. S., Saunders, L. J., Yang, Z., Hanson, M. L., Hollebone, B. P., Orihel, D. M., Palace, V., Rodriguez-gil, J. L., Mirnaghi, F. S., Shah, K., & Blais, J. M. (2023). Chemical weathering patterns of diluted bitumen spilled into freshwater limnocorrals. *Environmental Science and Technology*, *57*(25), 9266–9276. https://doi.org/10.1021/acs.est.2c05468

Stoyanovich, S., Yang, Z., Hanson, M., Hollebone, B. P., Orihel, D. M., Palace, V., Rodriguez-Gil, J. R., Mirnaghi, F., Shah, K., & Blais, J. M. (2022). Fate of polycyclic aromatic compounds from diluted bitumen spilled into freshwater limnocorrals. *Science of the Total Environment, 819*, 151993. https://doi.org/10.1016/j.scitotenv.2021.151993

Sun, K., Liu, J., Gao, Y., Jin, L., Gu, Y., & Wang, W. (2014). Isolation, plant colonization potential, and phenanthrene degradation performance of the endophytic bacterium Pseudomonas sp. Ph6-gfp. *Scientific Reports*, *4*, 5462. https://doi.org/10.1038/srep05462

Tanner, C. C., & Headley, T. R. (2011). Components of floating emergent macrophyte treatment wetlands influencing removal of stormwater pollutants. *Ecological Engineering*, *37*(3), 474–486. https://doi.org/10.1016/j.ecoleng.2010.12.012

Taylor, N. M., Toth, C. R. A., Collins, V., Mussone, P., & Gieg, L. M. (2021). The effect of an adsorbent matrix on recovery of microorganisms from hydrocarbon-contaminated groundwater. *Microorganisms*, *9*(1), 1–19. https://doi.org/10.3390/microorganisms9010090

Thompson, H., Angelova, A., Bowler, B., Jones, M., & Gutierrez, T. (2017). Enhanced crude oil biodegradative potential of natural phytoplankton-associated hydrocarbonoclastic bacteria. *Environmental Microbiology*, *19*(7), 2843–2861. https://doi.org/10.1111/1462-2920.13811

Tobiszewski, M., & Namieśnik, J. (2012). PAH diagnostic ratios for the identification of pollution emission sources. *Environmental Pollution*, *162*, 110–119. https://doi.org/10.1016/j.envpol.2011.10.025

Toyama, T., Furukawa, T., Maeda, N., Inoue, D., Sei, K., Mori, K., Kikuchi, S., & Ike, M. (2011). Accelerated biodegradation of pyrene and benzo[a]pyrene in the Phragmites

australis rhizosphere by bacteria-root exudate interactions. *Water Research*, *45*(4), 1629–1638. https://doi.org/10.1016/j.watres.2010.11.044

Trapp, S., & Karlson, U. (2001). Aspects of phytoremediation of organic pollutants. *Journal of Soils and Sediments*, *1*(1), 37–43. https://doi.org/10.1065/jss2001.04.007

Tremblay, J., & Yergeau, E. (2019). Systematic processing of ribosomal RNA gene amplicon sequencing data. *GigaScience*, *8*(12), 1–14. https://doi.org/10.1093/gigascience/giz146

Tso, S. F., & Taghon, G. L. (2006). Protozoan grazing increases mineralization of naphthalene in marine sediment. *Microbial Ecology*, *51*(4), 460–469. https://doi.org/10.1007/s00248-006-9058-4

Ulloa, M. J., Álvarez-Torres, P., Horak-Romo, K. P., & Ortega-Izaguirre, R. (2017). Harmful algal blooms and eutrophication along the mexican coast of the Gulf of Mexico large marine ecosystem. *Environmental Development*, *22*, 120–128. https://doi.org/10.1016/j.envdev.2016.10.007

United States Department of Transportation Pipeline and Hazardous Materials Safety Administration. (2022). *Pipeline incident 20 year trends. All reported incidents (2002-2021). Hazardous liquids (crude oil and refined petroleum products).* https://portal.phmsa.dot.gov/analytics/saw.dll?Portalpages&PortalPath=%2Fshared%2FPDM Public Website%2F_portal%2FSC Incident Trend&Page=All Reported

United States Environmental Protection Agency. (1996). *Ambient water quality criteria for dissolved oxygen*. https://www3.epa.gov/region1/npdes/merrimackstation/pdfs/ar/AR-1236.pdf

United States Environmental Protection Agency. (2014). *Priority pollutant list*. https://www.epa.gov/sites/default/files/2015-09/documents/priority-pollutant-list-epa.pdf

United States Environmental Protection Agency. (2023a). *Degradation kinetics equations*. https://www.epa.gov/pesticide-science-and-assessing-pesticide-risks/degradation-kinetics-equations

United States Environmental Protection Agency. (2023b). *Guidance to calculate representative half-life values and characterizing pesticide degradation*. https://www.epa.gov/pesticide-science-and-assessing-pesticide-risks/guidance-calculate-representative-half-life-values

Uzoh, C. V, Ifeanyi, V. O., Okwuwe, C. I., Oranusi, S. U., Braide, W., Iheukwumere, I. H., & Anyanwuocha, C. E. (2015). Effect of light on the biodegradation of crude oil by the algae Closterium species. *Journal of Natural Sciences Research*, *5*(22), 112–118.

Vander Zanden, M. J., Vadeboncoeur, Y., & Chandra, S. (2011). Fish reliance on littoral-benthic resources and the distribution of primary production in lakes. *Ecosystems*, *14*, 894–903. https://doi.org/10.1007/s10021-011-9454-6

Vandermeer, J. (2010). How populations grow: The exponential and logistic equations. *Nature Education Knowledge*, *3*(10), 15. https://www.nature.com/scitable/knowledge/library/how-populations-grow-the-exponential-and-logistic-13240157/

Vergnoux, A., Malleret, L., Asia, L., Doumenq, P., & Theraulaz, F. (2011). Impact of forest fires on PAH level and distribution in soils. *Environmental Research*, *111*(2), 193–198. https://doi.org/10.1016/j.envres.2010.01.008

Waigi, M. G., Kang, F., Goikavi, C., Ling, W., & Gao, Y. (2015). Phenanthrene biodegradation by sphingomonads and its application in the contaminated soils and sediments: A review. *International Biodeterioration and Biodegradation*, *104*, 333–349. https://doi.org/10.1016/j.ibiod.2015.06.008

Wang, M., Sha, C., Wu, J., Su, J., Wu, J., Wang, Q., Tan, J., & Huang, S. (2021). Bacterial community response to petroleum contamination in brackish tidal marsh sediments in the Yangtze River Estuary, China. *Journal of Environmental Sciences*, *99*, 160–167. https://doi.org/10.1016/j.jes.2020.06.015

Wang, Y., Wang, J., Leng, F., & Chen, J. (2021). Effects of oil pollution on indigenous bacterial diversity and community structure of soil in Fushun, Liaoning Province, China. *Geomicrobiology Journal*, *38*(2), 115–126. https://doi.org/10.1080/01490451.2020.1817196

Wickham, H. (2007). Reshaping data with the reshape package. *Journal of Statistical Software*, *21*(12), 1–20. https://doi.org/10.18637/jss.v021.i12

Wickham, H. (2016). *ggplot2: Elegant graphics for data analysis*. Spring-Verlag.

Wickham, H. (2022). *_stringr: Simple, consitent wrappers for common string operations_. R package version 1.5.0*. https://cran.r-project.org/package=stringr

Wickham, H., Averick, M., Bryan, J., Chang, W., McGowan, L., François, R., Grolemund, G., Hayes, A., Henry, L., Hester, J., Kuhn, M., Pedersen, T., Miller, E., Bache, S., Müller, K., Ooms, J., Robinson, D., Seidel, D., Spinu, V., … Yutani, H. (2019). Welcome to the Tidyverse. *Journal of Open Source Software*, *4*(43), 1686. https://doi.org/10.21105/joss.01686

Wickham, H., François, R., Henry, L., Müller, K., & Vaughan, D. (2023). *_dplyr: A grammar of data manipulation_. R package version 1.1.0* (1.1.0).

Wickham, H., & Henry, L. (2023). *_purrr: Functional programming tools_. R package version 1.0.1*. https://cran.r-project.org/package=purrr

Wickham, H., Hester, J., & Bryan, J. (2023). *_readr: Read rectangular text data_. R package*

version 2.1.4. https://cran.r-project.org/package=readr

Wickham, H., Vaughan, D., & Girlich, M. (2023). *_tidyr: Tidy Messy Data_. R package version 1.3.0.* https://cran.r-project.org/package=tidyr

Wieβner, A., Kuschk, P., & Stottmeister, U. (2002). Oxygen release by roots of Typha latifolia and Juncus effusus in laboratory hydroponic systems. *Acta Biotechnologica*, *22*(1–2), 209–216. https://doi.org/10.1002/1521-3846(200205)22:1/2<209::AID-ABIO209>3.0.CO;2-O

Wood, S. (2023). *mgcv Pacakge. Mixed GAM Compution Vehicle with GCV/AIC/REML/NCV smoothness estimation and GAMMS by REML/PQL. Version 1.9-0.* https://cran.rstudio.com/web/packages/mgcv/index.html

Wood, S. N. (2003). Thin plate regression splines. *Journal of the Royal Statistical Society. Series B: Statistical Methodology*, *65*(1), 95–114. https://doi.org/10.1111/1467-9868.00374

Wood, S. N. (2004). Stable and efficient multiple smoothing parameter estimation for generalized additive models. *Journal of the American Statistical Association*, *99*(467), 673–686. https://doi.org/10.1198/016214504000000980

Wood, S. N. (2011). Fast stable restricted maximum likelihood and marginal likelihood estimation of semiparametric generalized linear models. *Journal of the Royal Statistical Society. Series B: Statistical Methodology*, *73*(1), 3–36. https://doi.org/10.1111/j.1467-9868.2010.00749.x

Wood, S. N. (2017). *Generalized additive models: An introduction with R* (Second). Chapman and Hall, CRC Press. https://doi.org/10.1201/9781315370279

WoRMS Editorial Board. (2023). *World Register of Marine Species*. https://doi.org/doi:10.14284/170

Xia, Z., Idowu, I., Kerr, E., Klaassen, N., Assi, H., Bray, H., Marvin, C., Thomas, P. J., Stetefeld, J., & Tomy, G. T. (2021). New approaches to reduce sample processing times for the determination of polycyclic aromatic compounds in environmental samples. *Chemosphere*, *274*, 129738. https://doi.org/10.1016/j.chemosphere.2021.129738

Xiao, M., Zhang, Z. Z., Wang, J. X., Zhang, G. Q., Luo, Y. J., Song, Z. Z., & Zhang, J. Y. (2013). Bacterial community diversity in a low-permeability oil reservoir and its potential for enhancing oil recovery. *Bioresource Technology*, *147*, 110–116. https://doi.org/10.1016/j.biortech.2013.08.031

Yan, B., Abrajano, T. A., Bopp, R. F., Chaky, D. A., Benedict, Lucille, A., & Chillrud, S. N. (2005). Molecular tracers of saturated and polycyclic aromatic hydrocarbon inputs into Central Park Lake, New York City. *Environ. Sci. Technol.*, *39*(18), 7012–7019. https://doi.org/10.1021/es0506105

Yang, S., Jin, H., Wei, Z., He, R., Ji, Y., Li, X., & Yu, S. (2009). Bioremediation of oil spills in cold environments：A review. *Pedosphere*, *19*(3), 371–381. https://doi.org/10.1016/S1002-0160(09)60128-4

Yang, S., Wen, X., Shi, Y., Liebner, S., Jin, H., & Perfumo, A. (2016). Hydrocarbon degraders establish at the costs of microbial richness, abundance and keystone taxa after crude oil contamination in permafrost environments. *Scientific Reports*, *6*, 37473. https://doi.org/10.1038/srep37473

Yavari, S., Malakahmad, A., & Sapari, N. B. (2015). A review on phytoremediation of crude oil spills. *Water, Air, and Soil Pollution*, *226*(279), 1–18. https://doi.org/10.1007/s11270-015-2550-z

Yilmaz, P., Parfrey, L. W., Yarza, P., Gerken, J., Pruesse, E., Quast, C., Schweer, T., Peplies, J.,

Ludwig, W., & Glöckner, F. O. (2014). The SILVA and "all-species living tree project (LTP)" taxonomic frameworks. *Nucleic Acids Research*, *42*, 643–648. https://doi.org/10.1093/nar/gkt1209

Yunker, M. B., Macdonald, R. W., Vingarzan, R., Mitchell, H., Goyette, D., & Sylvestre, S. (2002). PAHs in the Fraser River basin: A critical appraisal of PAH ratios as indicators of PAH source and composition. *Organic Geochemistry*, *33*(4), 489–515. https://doi.org/10.1016/S0146-6380(02)00002-5

Zazouli, M. A., Ala, A., Asghari, S., & Babanezhad, E. (2023). Evaluation of Azolla filiculoides potential in pyrene and phenanthrene accumulation and phytoremediation in contaminated waters. *International Journal of Phytoremediation*, 1–10. https://doi.org/10.1080/15226514.2023.2257314

Zazouli, M. A., Asghari, S., Tarrahi, R., Lisar, S. Y. S., Babanezhad, E., & Dashtban, N. (2022). The potential of common duckweed (Lemna minor) in phytoremediation of phenanthrene and pyrene. *Environmental Engineering Research*, *28*(1), 210592. https://doi.org/10.4491/eer.2021.592

Zhang, S. Y., Wang, Q. F., Wan, R., & Xie, S. G. (2011). Changes in bacterial community of anthracene bioremediation in municipal solid waste composting soil. *Journal of Zhejiang University Science B*, *12*(9), 760–768. https://doi.org/10.1631/jzus.B1000440

Zhou, Y., & Gao, X. (2019). Characterization of biofilm formed by phenanthrene-degrading bacteria on rice root surfaces for reduction of pah contamination in rice. *International Journal of Environmental Research and Public Health*, *16*(11), 1–14. https://doi.org/10.3390/ijerph16112002

Zhou, Y., Kong, Q., Zhao, X., Lin, Z., & Zhang, H. (2022). Dynamic changes in the microbial

community in the surface seawater of Jiaozhou Bay after crude oil spills: An in situ microcosm study. *Environmental Pollution*, *307*, 119496. https://doi.org/10.1016/j.envpol.2022.119496

Zhu, X., Venosa, A. D., Suidan, M. T., & Lee, K. (2001). Guidelines for the bioremediation of marine shorelines and freshwater wetlands. *U.S. Environmental Protection Agency. Cincinnati, OH.* https://www.epa.gov/sites/default/files/2013-07/documents/guidelines_for_the_bioremediation_of_marine_shorelines_and_freshwater_wetlands.pdf

Zuur, A. F., Ieno, E. N., Walker, N. J., Saveliev, A. A., & Smith, G. M. (2019). *Mixed effects models and extensions in ecology with R* (M. Gail, K. Krickeberg, J. M. Samet, A. Tsiatis, & A. Wong (eds.)). Springer. https://doi.org/10.1007/978-0-387-87458-6

Appendix A- Chapter 3

A.1 Research Design

Figure A1. Example of a shoreline enclosure (Curry Industries Ltd., Winnipeg) in a rock cobble environment highlighting the floating collar attached to a polypropylene curtain sealed to the sediment and onto the shoreline, and EFW and sampling equipment.

A.1.1 Contingency Measures

In order to conduct such research, contingency measures were implemented with efforts to have no further impact to the ecosystem than the intended regions. The shoreline enclosures, representing the first level of containment, were sealed to the bottom sediment and five meters onto shore with sandbags. If oil were to be accidentally released from the enclosures three other contingency measures were in place, including a secondary containment boom that surrounded each region of the shoreline enclosures (Figure A1), a tertiary containment boom that was placed near the outflow, and a constructed underflow dam at the outflow of the lake. In addition, the IISD-ELA facilities were equipped with mechanical oil spill response equipment (e.g., sorbent pads) if required. Personnel in contact with fresh oil had proper personal protective equipment including Tyvek suit, nitrile gloves, eye protection, and a respirator.

A.2 Polycyclic Aromatic Compound Chemistry

Table A1. List of parent and alkylated PACs measured in water and sediments of the FLOWTER sites.

Compound	Parent or Alkylated	US EPA Priority PAC (2014)	Ring Number
Naphthalene	Parent	Yes	2
1-Methylnaphthalene	Alkylated	No	2
2-Methylnaphthalene	Alkylated	No	2
C2 Naphthalene	Alkylated	No	2
C3 Naphthalene (Trimethyl)	Alkylated	No	2
C4 Naphthalene (Tetramethyl)	Alkylated	No	2
Acenaphthene	Parent	Yes	3
Acenaphthylene	Parent	Yes	3
Anthracene	Parent	Yes	3
Dibenzothiophene*	Alkylated	No	3
C1 Dibenzothiophene*	Alkylated	No	3
C2 Dibenzothiophene*	Alkylated	No	3
C3 Dibenzothiophene*	Alkylated	No	3
Fluorene	Parent	Yes	3
C1 Fluorene	Alkylated	No	3
C2 Fluorene	Alkylated	No	3
Phenanthrene	Parent	Yes	3
1,7-Dimethylphenanthrene	Alkylated	No	3
1,8-Dimethylphenanthrene	Alkylated	No	3
1-Methylphenanthrene	Alkylated	No	3
2,6-Dimethylphenanthrene	Alkylated	No	3
2-Methylphenanthrene	Alkylated	No	3
3,6-Dimethylphenanthrene	Alkylated	No	3
3-Methylphenanthrene	Alkylated	No	3
9/4-Methylphenanthrene	Alkylated	No	3
C2 Phenanthrene	Alkylated	No	3
C3 Phenanthrene	Alkylated	No	3
C4 Phenanthrene	Alkylated	No	3
Retene	Alkylated	No	3
Benz[a]anthracene	Parent	Yes	4
Chrysene	Parent	Yes	4
C1 Chrysene	Alkylated	No	4

Compound	Parent or Alkylated	US EPA Priority PAC (2014)	Ring Number
C3 Chrysene	Alkylated	No	4
Fluoranthene	Parent	Yes	4
Pyrene	Parent	Yes	4
C1 Pyrene	Alkylated	No	4
C2 Pyrene	Alkylated	No	4
Benzo[a]pyrene	Parent	Yes	>4 (5)
C1 Benzo[a]pyrene	Alkylated	No	>4 (5)
Benzo[b]fluoranthene	Parent	Yes	>4 (5)
Benzo[g,h,i]perylene	Parent	Yes	>4 (6)
Benzo[k]fluoranthene	Parent	Yes	>4 (5)
Dibenzo[a,h]anthracene	Parent	Yes	>4 (5)
Indeno[1,2,3-c,d]pyrene	Parent	Yes	>4 (6)

* Parent and alkylated dibenzothiophenes are heterocyclic PACs (containing sulfur), but are included in the 28 aPAC grouping for visualization.

A.2.1 Water

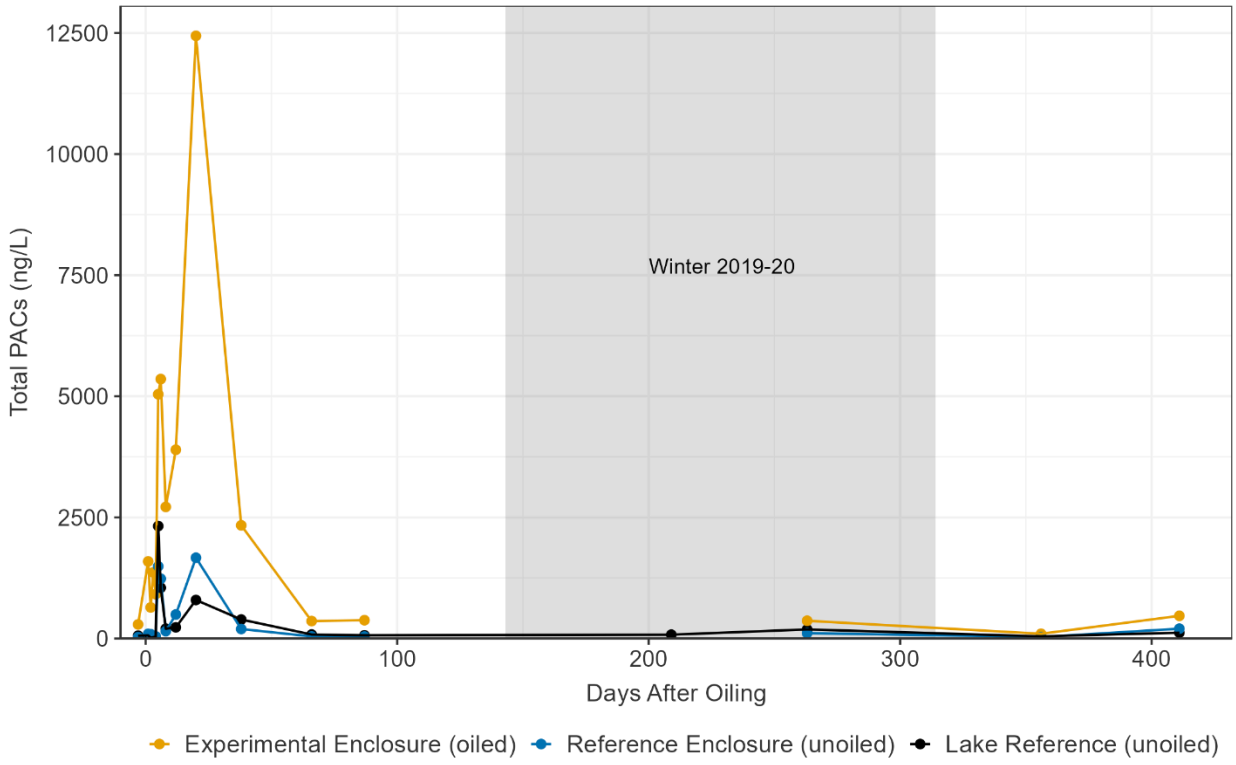

Figure A2. Total PAC (n=44) concentration in water over the duration of the 2019 dilbit experiment. GC-MS/MS runs for the EE and RE samples on day 209 failed, and are not included.

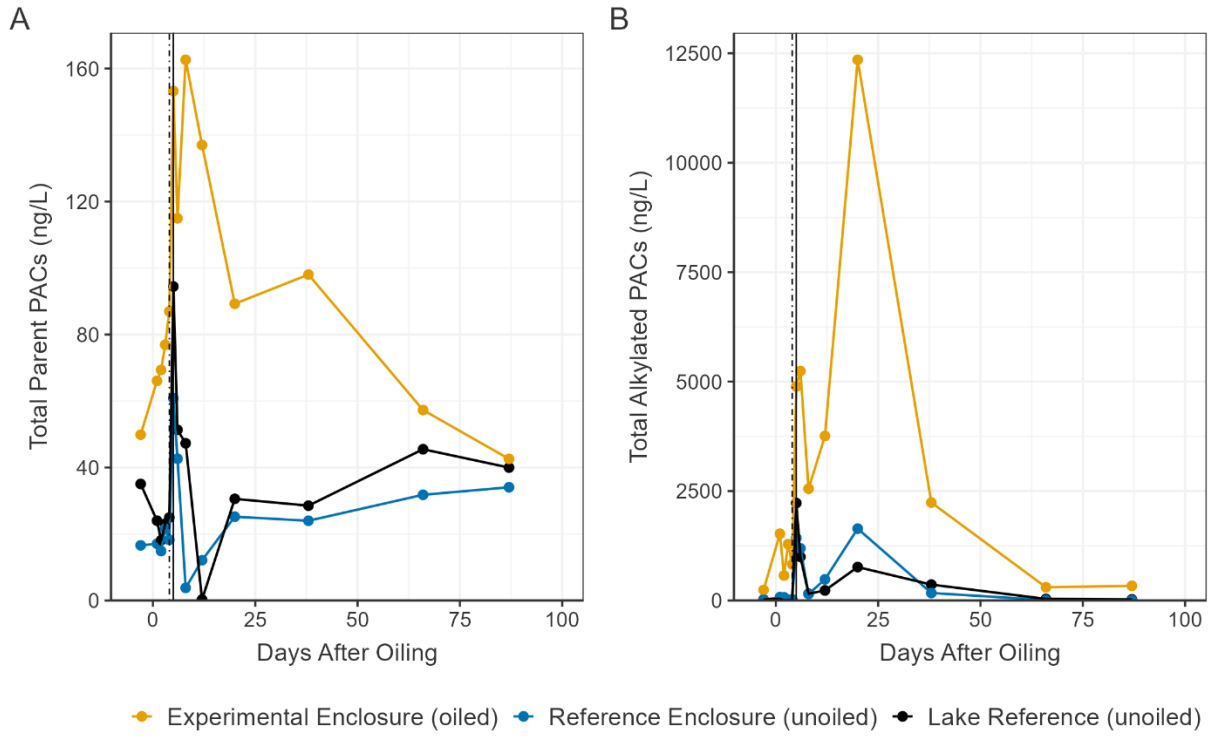

Figure A3. Total parent (A) and alkylated (B) PACs in the water from 3 days pre-oil addition to day 87 post-oil addition during the 2019 dilbit experiment. Vertical lines represent primary (dotted) and secondary (solid) remediation events.

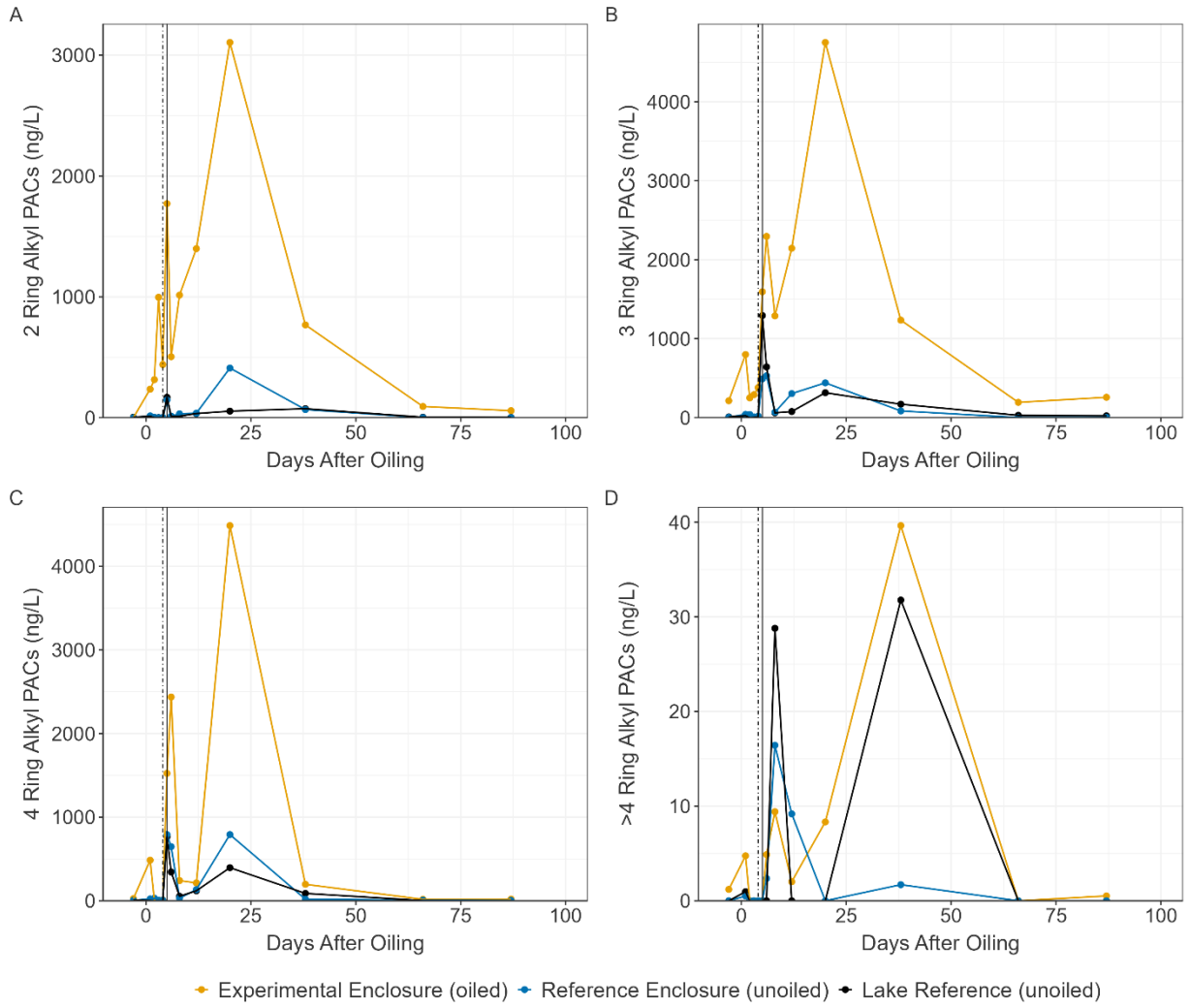

Figure A4. Total 2, 3, 4, and > 4 ring alkylated PACs in the water from 3 days pre-oil addition to day 87 post-oil addition during the 2019 dilbit experiment. Vertical lines represent primary (dotted) and secondary (solid) remediation events.

A.2.2 Sediment

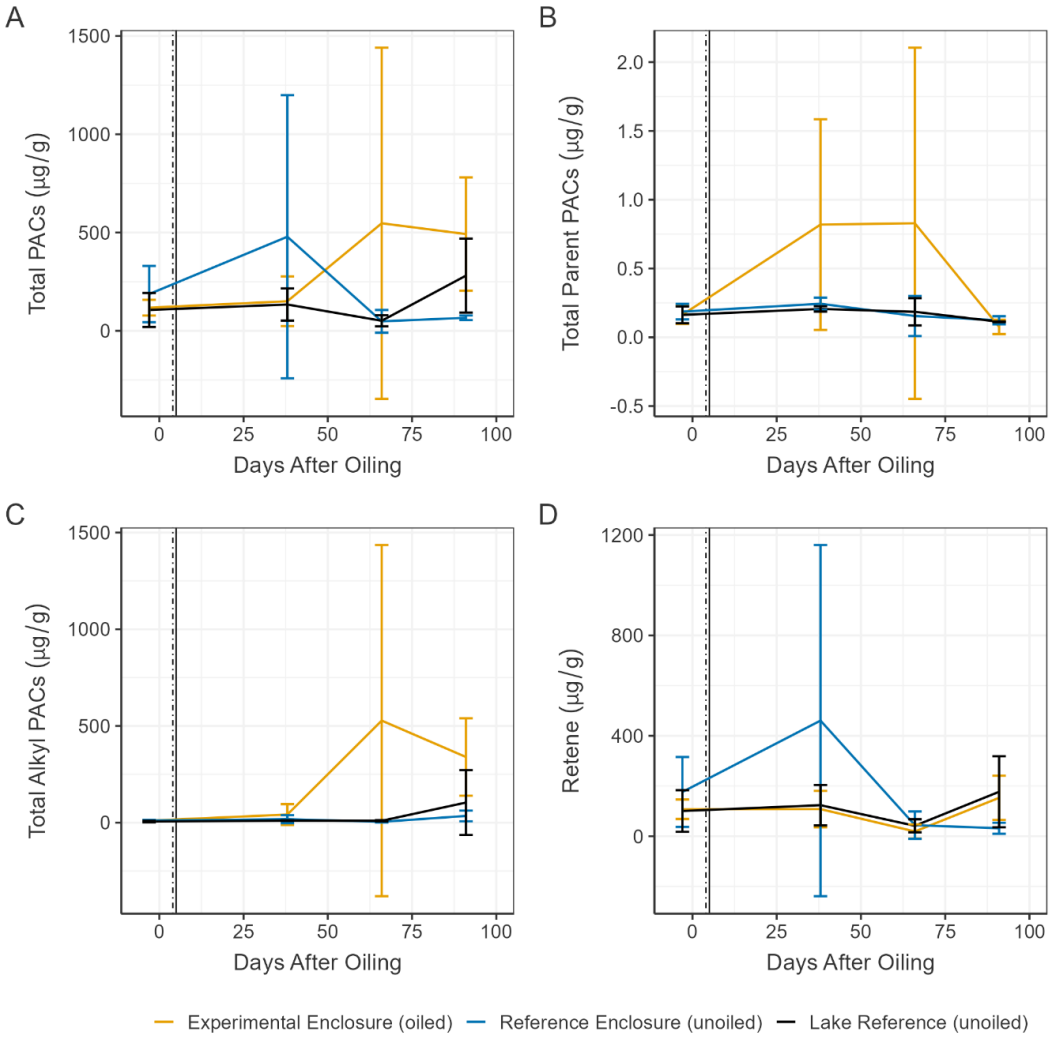

Figure A5. Mean (± SD) total PACs (A; n = 44), total parent PACs (B; n = 16), total alkylated PACs (C, minus retene, n = 27), retene (D) concentrations in the sediment from 3 days pre-oil addition to day 91 post-oil addition during the 2019 dilbit experiment. Error bars represent standard deviation of triplicate samples at each site. Vertical lines represent primary (dotted) and secondary (solid) remediation events. A single sediment sample day 91 from the EE was lost and error bars represent SD from 2 samples.

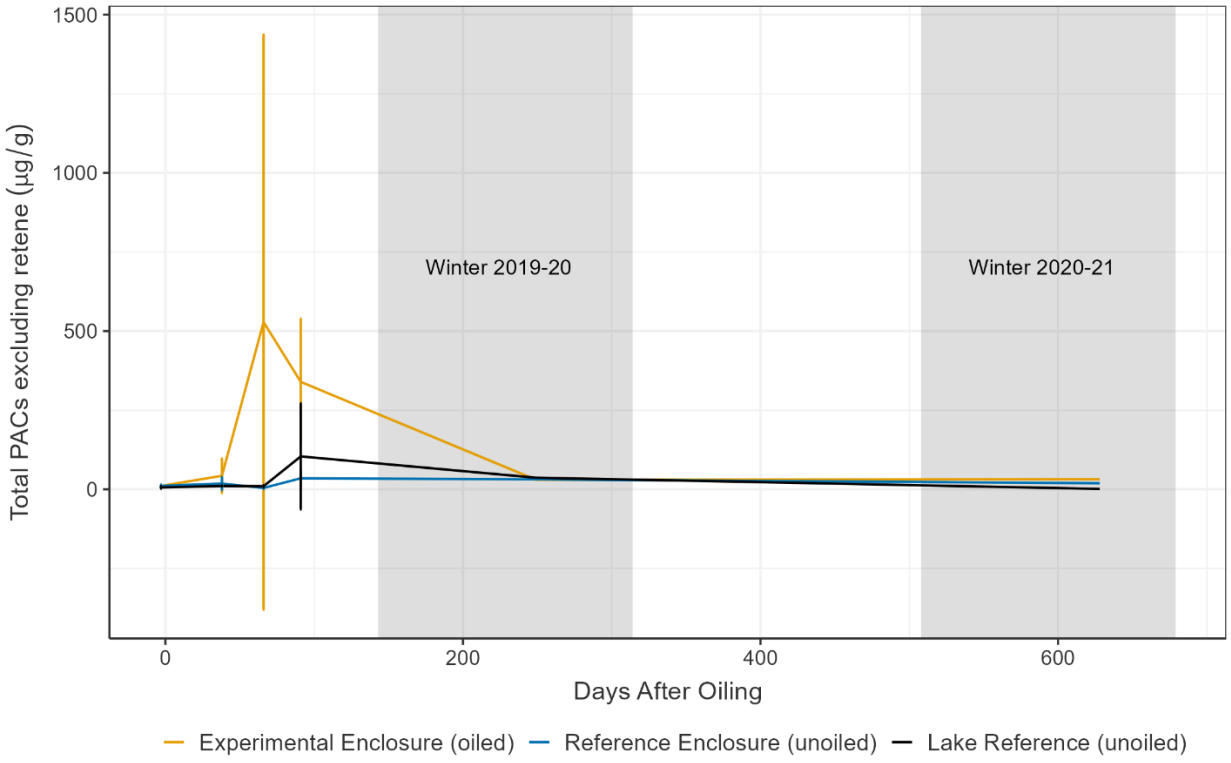

Figure A6. Mean (± SD) total PAC concentration (excluding retene, n=43) in sediment over the duration of the 2019 dilbit experiment. Error bars represent standard deviation of triplicate samples at each site. A single sediment sample day 91 from the EE was lost and error bars represent SD from 2 samples. Samples on days 249 and 628 represent a single sediment sample from each site.

A.2.2.1 Sediment PAC Ratios. In order to assess whether sediment PACs between sites arise from petrogenic (oil) or pyrogenic (combustion) sources, we assessed PAC concentration ratios including, retene/(retene+chrysene) and fluoranthene/(fluoranthrene+pyrene). The retene/(retene+chrysene) ratio can be used to identify sources of PACs from softwood combustion (>0.8) or petroleum burning/coal combustion (0.15 to 0.50) (Yan et al., 2005). All sediment samples had a ratio > 0.99, excluding one sample on day 66 in the EE (0.25),

suggesting sediment PAC sources were strongly influenced by wood combustion/forest fires in the region. The fluoranthene/(fluoranthene+pyrene) ratio can be used to assess petroleum, combustion, and environmental sources. Ratios >0.4 typically represent sources from combustion products (wood, coals, petroleum burning [excluding diesel which has a low ratio]), and < 0.4 typically indicate a petrogenic/petroleum source (the ratio for crude oil ranges from 0.14 to 0.26) (Yunker et al., 2002; Table 3 and citations therein).

During pre-oil conditions, all three sites had pyrogenic sources of PACs (Figure A7). On day 38, samples in the unoiled sites were also considered to be from pyrogenic origin, however some samples in the EE indicated petrogenic source (range: 0.17-0.54). On day 66 and 91, the RE indicated pyrogenic sources of PACs, while one sample in both the EE and LR indicated petrogenic source on day 66. Only one sample from the LR location was considered to be from a petrogenic source on day 91. One of the samples on day 38, 66 and 249, from the EE were within the ratio range for crude oil. On days 249 and 628, sediment sample PACs were all considered petrogenic sources, however these may be unreliable ratios at this point in the study. While these ratios should be used with caution, as environmental fate may vary by compound and over time (Tobiszewski & Namieśnik, 2012), the results suggest that much of the total PACs in the sediment, dominated by retene, was caused by pyrogenic sources/wood burning, and the EE had some samples with petrogenic sources, likely from dilbit application.

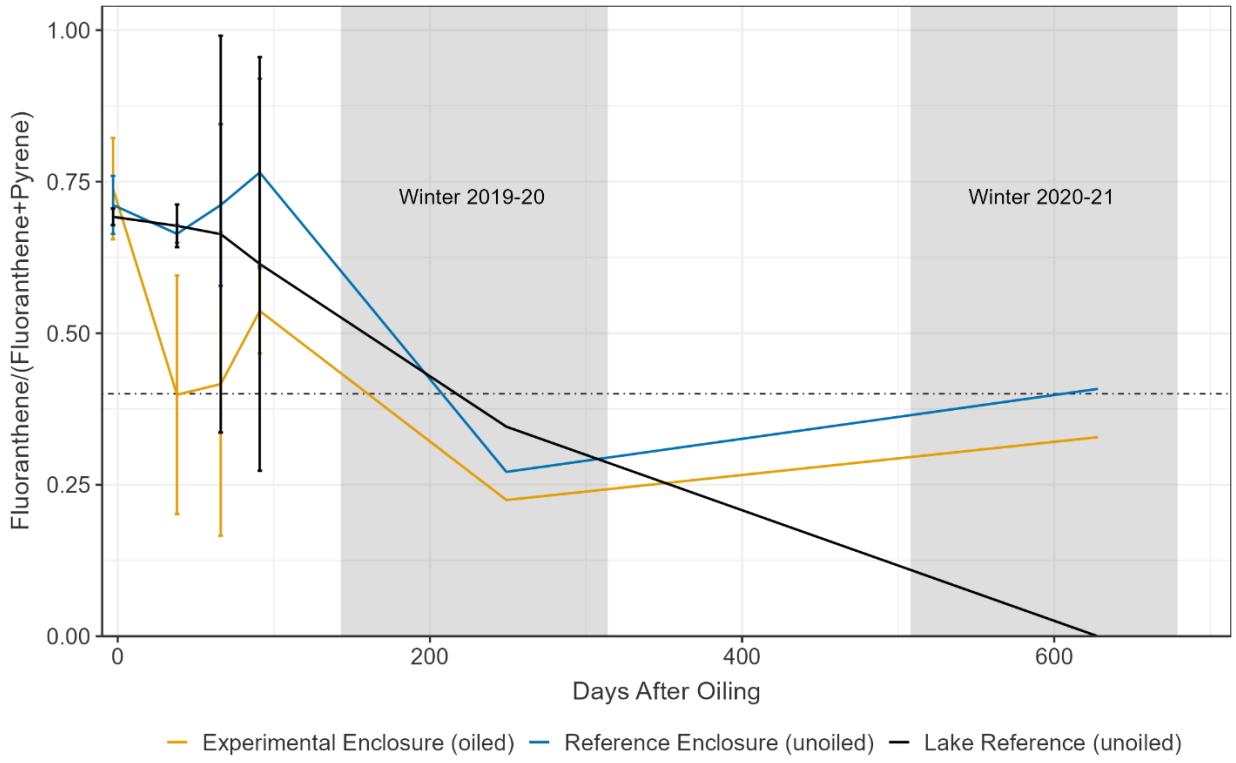

Figure A7. Mean (±SD) fluoranthene/(fluoranthene+pyrene) ratio in sediment over the duration of the 2019 dilbit experiment. Values above horizontal dashed line (0.4) indicate combustion sources, and below indicate petrogenic sources (Yunker et al., 2002). Error bars represent standard deviation of triplicate samples at each site. A single sediment sample on day 91 from the EE was lost and error bars represent SD from 2 samples. Samples on days 249 and 628 represent a single sediment sample from each site

A.3 Basic Water Quality

Far shore, surface water in each enclosure and lake reference were monitored regularly for water temperature (℃), dissolved oxygen (% and mg/L), specific conductivity (µS/cm), and pH using a Yellow Springs Instrument (YSI) Professional Series Plus multiparameter meter (YSI QUATRO, 18C100206. Xylem, Yellow Springs, Ohio) (Table A2).

Table A2. Basic water quality data recorded with a Yellow Spring Instrument (YSI) Professional Series Plus multiparameter meter (YSI QUATRO, 18C100206. Xylem, Yellow Springs, Ohio) during the 2019 dilbit experiment

Enclosure	Days After Oiling	Temperature	Dissolved Oxygen (%)	Dissolved Oxygen (mg/L)	Specific Conductivity (µS/cm)	pH
Experimental Enclosure (oiled)	-3	18.30	56.4	5.31	17.5	6.28
Reference Enclosure (unoiled)	-3	18.80	58.0	5.40	17.7	6.37
Lake Reference (unoiled)	-3	NA	NA	NA	NA	NA
Experimental Enclosure (oiled)	14	23.11	19.6	1.68	18.0	7.07
Reference Enclosure (unoiled)	14	22.78	18.5	1.60	18.0	7.01
Lake Reference (unoiled)	14	23.59	18.6	1.58	17.0	7.54
Experimental Enclosure (oiled)	19	22.40	69.1	5.99	NA	NA
Reference Enclosure (unoiled)	19	22.20	77.1	6.71	NA	NA
Lake Reference (unoiled)	19	23.00	93.4	8.02	NA	NA
Experimental Enclosure (oiled)	26	22.69	48.6	4.20	22.0	6.15
Reference Enclosure (unoiled)	26	22.46	55.9	4.85	23.0	6.09
Lake Reference (unoiled)	26	23.27	86.8	7.40	16.0	6.36
Experimental Enclosure (oiled)	28	22.40	46.8	4.07	NA	NA
Reference Enclosure (unoiled)	28	22.30	56.2	4.89	NA	NA
Lake Reference (unoiled)	28	23.10	90.7	7.76	NA	NA
Experimental Enclosure (oiled)	30	22.30	54.0	4.71	NA	NA

Enclosure	Days After Oiling	Temperature	Dissolved Oxygen (%)	Dissolved Oxygen (mg/L)	Specific Conductivity (µS/cm)	pH
Reference Enclosure (unoiled)	30	22.10	60.7	5.28	NA	NA
Lake Reference (unoiled)	30	NA	NA	NA	NA	NA
Experimental Enclosure (oiled)	33	22.52	67.0	5.80	22.0	6.45
Reference Enclosure (unoiled)	33	22.52	73.9	6.40	22.0	6.27
Lake Reference (unoiled)	33	23.19	100.1	8.56	16.0	6.69
Experimental Enclosure (oiled)	40	20.70	53.9	4.83	21.8	6.04
Reference Enclosure (unoiled)	40	20.80	65.4	5.86	23.0	5.92
Lake Reference (unoiled)	40	22.10	87.2	7.61	18.0	6.49
Experimental Enclosure (oiled)	47	22.60	54.4	4.70	22.7	6.15
Reference Enclosure (unoiled)	47	22.60	58.0	5.02	23.9	6.14
Lake Reference (unoiled)	47	23.50	86.8	7.37	18.3	6.54
Experimental Enclosure (oiled)	54	19.20	67.3	6.21	21.8	5.90
Reference Enclosure (unoiled)	54	19.00	70.1	6.49	23.7	6.06
Lake Reference (unoiled)	54	20.90	81.5	7.27	18.3	6.53
Experimental Enclosure (oiled)	61	20.60	68.9	6.20	21.1	5.97
Reference Enclosure (unoiled)	61	20.70	79.4	7.12	22.8	6.05
Lake Reference (unoiled)	61	21.20	86.5	7.68	18.1	6.24
Experimental Enclosure (oiled)	68	16.70	59.3	5.77	19.5	5.98
Reference Enclosure (unoiled)	68	16.50	68.2	6.66	21.1	5.83

Enclosure	Days After Oiling	Temperature	Dissolved Oxygen (%)	Dissolved Oxygen (mg/L)	Specific Conductivity (µS/cm)	pH
Lake Reference (unoiled)	68	17.50	77.1	7.38	18.2	6.23
Experimental Enclosure (oiled)	75	16.40	80.1	7.73	19.5	5.46
Reference Enclosure (unoiled)	75	16.90	84.4	8.00	20.9	5.71
Lake Reference (unoiled)	75	17.80	94.2	8.92	18.0	5.80
Experimental Enclosure (oiled)	84	12.70	77.3	8.21	19.2	5.68
Reference Enclosure (unoiled)	84	12.50	82.3	8.76	20.2	5.73
Lake Reference (unoiled)	84	NA	NA	NA	NA	NA
Experimental Enclosure (oiled)	90	18.60	70.5	6.60	19.7	5.58
Reference Enclosure (unoiled)	90	18.50	70.9	6.56	20.8	5.59
Lake Reference (unoiled)	90	NA	NA	NA	NA	NA

Temperature in the enclosures ranged from 12.50 ℃ to 23.11 ℃, and were above optimal temperatures for hydrocarbon biodegradation in freshwater (20-30 ℃; Atlas, 1985, as cited in Al-Hawash et al., 2018; Bartha & Bossert, 1984, and Cooney, 1984, as cited in Das and Chandran, 2011) for approximately the first 50 days of oil exposure. The LR typically had higher water temperature than the enclosures, suggesting there may be an enclosure effect, impacting wave and wind aeration. This was also observed for mean dissolved oxygen (DO) (% and mg/L) which were lower in the enclosures than the lake, similar to observations in Palace et al. (2021), and lowest in the EE. Oxygen is important for aerobic metabolism of PACs, required for the cleavage of aromatic rings (Cao et al., 2009; Das & Chandran, 2011; Lee et al., 2015), and may be lower in the EE due to microbial metabolism of oil, or from site variability. Mean (± standard deviation [SD]) DO (%) was 59.6 ± 15.0 % (n=15), 65.3 ± 16.1 % (n=15), and 82.1 ± 22.0 % (n=11) in the EE, RE, and LR site, respectively. Concentration of oxygen is an important metric for biota (e.g., fish), where the Coldwater criteria for ambient DO is 6.5 mg/L for early life stages (7 day mean for those exposed directly to the water column) and other life stages (30 day mean). While criteria for one day minimum can be 5.0 mg/L and 4.0 mg/L for early life stages (in the water column) and other life stages, respectively (US EPA, 1996). Mean (± SD; range) DO concentrations were 5.47 ± 1.58 mg/L (1.68 to 8.21 mg/L; n=15), 5.97 ± 1.65 mg/L (1.60 to 8.76 mg/L; n=15), 7.23 ± 1.95 mg/L (1.58 to 8.92 mg/L; n=11), respectively. DO reached quite low concentrations for biota on day 14 among all sites, which may have been a sensor or calibration error, however the remainder were above 4.07 mg/L. As discussed, there may be an enclosure effect influencing oxygen concentrations in the water column. The pH in the enclosures was also lower than the LR, however all had a declining trend over the first 90 days

of exposure. Mean (± SD; range) pH was 6.06 ± 0.43 (5.46 to 7.07; n=12), 6.06 ± 0.38 (5.59 to 7.01; n=12), and 6.49 ± 0.47 (5.80 to 7.54; n=9), respectively. The increased acidity in the enclosures may be due to the wetland/organic shoreline (Lee et al., 2015) with increased CO_2 production from root respiration, plant exudation products (e.g., photosynthetic products) (Hinsinger et al., 2003), metabolism (Al-Hawash et al., 2018; Das & Chandran, 2011; Lee et al., 2015), and/or reduced dilution/mixing. Specific conductivity was higher in the enclosures, with a mean (± SD) of 20.4 ± 1.72 µS/cm (n=12), 21.4 ± 2.05 µS/cm (n=12), and 17.54 ± 0.959 µS/cm (n=9), respectively.

A.4 Nutrient Chemistry

Water was collected bi-weekly from 3 days pre-oil addition to day 94 of exposure from the enclosures and from 4 days pre-oil addition to day 102 in the lake, and analyzed for a suite of parameters analyzed by the IISD-ELA chemistry facility and University of Alberta, Biogeochemical Analytical Services Lab (including anions, cations, particulate carbon, particulate nitrogen, and alkalinity). As nutrients (nitrogen (N) and phosphorus (P)) are often limited during an oil spill due to the influx of carbon (Lee et al., 2015) and are essential for biological growth, only total nitrogen (TN) and total phosphorus (TP) are discussed and remaining analyzed parameters are summarized in Table A3. Analytical methods used at the IISD-ELA laboratory are outlined in (Stainton et al., 1977).

Table A3. Nutrient chemistry summary data from day -3 to day 94 in the enclosures and from day -4 to day 102 in the lake epilimnion and day 87 in the metalimnion during the 2019 dilbit experiment.

Site	Parameter	Units	Mean	Std Dev	Min	Max	N
Experimental Enclosure (oiled)	Alkalinity	µEq/L	166	19.6	143	204	8
Lake Epilimnion	Alkalinity	µEq/L	116	20.1	67	126	8
Lake Metalimnion	Alkalinity	µEq/L	128	3.6	123	133	7
Reference Enclosure (unoiled)	Alkalinity	µEq/L	181	19.3	159	219	8
Experimental Enclosure (oiled)	Ammonia	µg/L	17.3	5.78	7.2	24.9	8
Lake Epilimnion	Ammonia	µg/L	18.8	11.53	<LOD*	43.6	8
Lake Metalimnion	Ammonia	µg/L	18.8	10.96	<LOD*	39.4	7
Reference Enclosure (unoiled)	Ammonia	µg/L	15.5	7.12	3.9	27.5	8
Experimental Enclosure (oiled)	Calcium	mg/L	2.4163	0.26832	2.1200	2.9200	8
Lake Epilimnion	Calcium	mg/L	1.7994	0.07312	1.7100	1.9000	8
Lake Metalimnion	Calcium	mg/L	1.8671	0.07158	1.7800	2.0000	7
Reference Enclosure (unoiled)	Calcium	mg/L	2.6263	0.32728	2.1400	3.0500	8
Experimental Enclosure (oiled)	Chlorine	mg/L	0.12	0.036	0.09	0.19	8
Lake Epilimnion	Chlorine	mg/L	0.15	0.014	0.14	0.18	8
Lake Metalimnion	Chlorine	mg/L	0.18	0.049	0.14	0.27	7
Reference Enclosure (unoiled)	Chlorine	mg/L	0.16	0.111	0.08	0.43	8
Experimental Enclosure (oiled)	Chlorophyll-a	µg/L	2.0	1.01	1.1	3.8	8
Lake Epilimnion	Chlorophyll-a	µg/L	2.1	0.67	1.3	3.2	8
Lake Metalimnion	Chlorophyll-a	µg/L	3.1	1.02	1.7	4.1	7
Reference Enclosure (unoiled)	Chlorophyll-a	µg/L	2.0	0.74	1.5	3.7	8

Site	Parameter	Units	Mean	Std Dev	Min	Max	N
Experimental Enclosure (oiled)	Conductivity	µS/cm	22.45	2.398	20.10	27.50	8
Lake Epilimnion	Conductivity	µS/cm	18.25	0.354	18.00	18.50	2
Lake Metalimnion	Conductivity	µS/cm	18.50	0.000	18.50	18.50	2
Reference Enclosure (unoiled)	Conductivity	µS/cm	22.96	2.142	20.50	27.00	8
Experimental Enclosure (oiled)	Dissolved Inorganic Carbon	µmol/L	299.5	43.34	240.0	358.0	8
Lake Epilimnion	Dissolved Inorganic Carbon	µmol/L	141.4	7.56	132.0	153.0	8
Lake Metalimnion	Dissolved Inorganic Carbon	µmol/L	174.6	34.66	146.0	245.0	7
Reference Enclosure (unoiled)	Dissolved Inorganic Carbon	µmol/L	305.1	48.69	257.0	411.0	8
Experimental Enclosure (oiled)	Dissolved Organic Carbon	µmol/L	755.6	86.76	580.0	899.0	8
Lake Epilimnion	Dissolved Organic Carbon	µmol/L	460.3	36.80	388.0	515.0	8
Lake Metalimnion	Dissolved Organic Carbon	µmol/L	441.7	24.98	401.0	477.0	7
Reference Enclosure (unoiled)	Dissolved Organic Carbon	µmol/L	731.8	82.98	629.0	890.0	8
Experimental Enclosure (oiled)	Iron	mg/L	0.13	0.063	0.07	0.22	8
Lake Epilimnion	Iron	mg/L	0.05	0.023	0.02	0.09	8
Lake Metalimnion	Iron	mg/L	0.09	0.033	0.04	0.14	7
Reference Enclosure (unoiled)	Iron	mg/L	0.09	0.043	0.03	0.14	8
Experimental Enclosure (oiled)	Magnesium	mg/L	0.6338	0.06457	0.5600	0.7600	8
Lake Epilimnion	Magnesium	mg/L	0.4575	0.01753	0.4300	0.4800	8
Lake Metalimnion	Magnesium	mg/L	0.4671	0.00951	0.4600	0.4800	7
Reference Enclosure (unoiled)	Magnesium	mg/L	0.6925	0.07440	0.5800	0.8000	8
Experimental Enclosure (oiled)	Manganese	mg/L	0.0185	0.01287	<LOD (0.0145)	0.0379	8
Lake Epilimnion	Manganese	mg/L	0.0073	0.00000	<LOD (0.0145)	0.0073	8
Lake Metalimnion	Manganese	mg/L	0.0156	0.01603	<LOD (0.0145)	0.0491	7
Reference Enclosure (unoiled)	Manganese	mg/L	0.0240	0.01995	<LOD (0.0145)	0.0662	8

Site	Parameter	Units	Mean	Std Dev	Min	Max	N
Experimental Enclosure (oiled)	Nitrate	µg/L	10.24	19.640	<LOD*	58.50	8
Lake Epilimnion	Nitrate	µg/L	11.24	13.614	1.10	34.00	8
Lake Metalimnion	Nitrate	µg/L	18.56	14.720	5.20	44.34	7
Reference Enclosure (unoiled)	Nitrate	µg/L	6.31	9.104	<LOD*	28.10	8
Experimental Enclosure (oiled)	Nitrite	µg/L	1.09	0.621	<LOD*	2.00	8
Lake Epilimnion	Nitrite	µg/L	1.10	0.629	<LOD*	2.10	8
Lake Metalimnion	Nitrite	µg/L	0.92	0.514	<LOD*	1.80	7
Reference Enclosure (unoiled)	Nitrite	µg/L	0.90	0.463	<LOD*	1.60	8
Experimental Enclosure (oiled)	Particulate Carbon	µg/L	713	403.1	365	1589	8
Lake Epilimnion	Particulate Carbon	µg/L	392	65.4	296	488	8
Lake Metalimnion	Particulate Carbon	µg/L	444	55.6	377	524	7
Reference Enclosure (unoiled)	Particulate Carbon	µg/L	749	340.3	475	1299	8
Experimental Enclosure (oiled)	Particulate Nitrogen	µg/L	57	37.5	30	144	8
Lake Epilimnion	Particulate Nitrogen	µg/L	39	13.4	23	59	8
Lake Metalimnion	Particulate Nitrogen	µg/L	44	10.0	29	59	7
Reference Enclosure (unoiled)	Particulate Nitrogen	µg/L	62	32.4	13	110	8
Experimental Enclosure (oiled)	Particulate Phosphorus	µg/L	4.3	1.58	2.0	7.0	8
Lake Epilimnion	Particulate Phosphorus	µg/L	2.4	0.52	2.0	3.0	8
Lake Metalimnion	Particulate Phosphorus	µg/L	3.1	0.69	<LOD*	4.0	7
Reference Enclosure (unoiled)	Particulate Phosphorus	µg/L	4.8	1.28	2.0	6.0	8
Experimental Enclosure (oiled)	pH	SU	6.219	0.1034	6.084	6.360	8
Lake Epilimnion	pH	SU	6.737	0.1489	6.448	6.962	8
Lake Metalimnion	pH	SU	6.608	0.3144	6.225	7.212	7
Reference Enclosure (unoiled)	pH	SU	6.237	0.1595	5.954	6.444	8

Site	Parameter	Units	Mean	Std Dev	Min	Max	N
Experimental Enclosure (oiled)	Potassium	mg/L	0.3900	0.10447	0.2900	0.5600	8
Lake Epilimnion	Potassium	mg/L	0.3006	0.01782	0.2700	0.3250	8
Lake Metalimnion	Potassium	mg/L	0.3014	0.01773	0.2800	0.3200	7
Reference Enclosure (unoiled)	Potassium	mg/L	0.3900	0.15297	0.2400	0.7000	8
Experimental Enclosure (oiled)	Sodium	mg/L	0.614	0.0920	0.510	0.760	8
Lake Epilimnion	Sodium	mg/L	0.686	0.0256	0.640	0.720	8
Lake Metalimnion	Sodium	mg/L	0.691	0.0186	0.670	0.730	7
Reference Enclosure (unoiled)	Sodium	mg/L	0.705	0.0978	0.580	0.900	8
Experimental Enclosure (oiled)	Soluble Reactive Silica	mg/L	0.512	0.1614	0.363	0.883	8
Lake Epilimnion	Soluble Reactive Silica	mg/L	1.482	0.1420	1.153	1.606	8
Lake Metalimnion	Soluble Reactive Silica	mg/L	1.560	0.0754	1.483	1.698	7
Reference Enclosure (unoiled)	Soluble Reactive Silica	mg/L	0.615	0.1373	0.293	0.721	8
Experimental Enclosure (oiled)	Sulfate	mg/L	0.52	0.173	0.40	0.88	8
Lake Epilimnion	Sulfate	mg/L	1.08	0.109	0.99	1.27	8
Lake Metalimnion	Sulfate	mg/L	1.15	0.114	1.01	1.34	7
Reference Enclosure (unoiled)	Sulfate	mg/L	0.46	0.177	0.32	0.81	8
Experimental Enclosure (oiled)	Total Dissolved Nitrogen	µg/L	396.1	53.78	338.0	476.5	8
Lake Epilimnion	Total Dissolved Nitrogen	µg/L	253.2	18.97	228.0	291.0	8
Lake Metalimnion	Total Dissolved Nitrogen	µg/L	271.9	25.52	233.0	317.0	7
Reference Enclosure (unoiled)	Total Dissolved Nitrogen	µg/L	370.4	61.31	284.0	497.0	8
Experimental Enclosure (oiled)	Total Dissolved Phosphorus	µg/L	5.97	1.748	<LOD*	8.40	8
Lake Epilimnion	Total Dissolved Phosphorus	µg/L	2.45	0.819	<LOD*	3.90	8
Lake Metalimnion	Total Dissolved Phosphorus	µg/L	2.46	0.479	<LOD*	2.87	7
Reference Enclosure (unoiled)	Total Dissolved Phosphorus	µg/L	4.44	1.909	<LOD*	7.50	8

Site	Parameter	Units	Mean	Std Dev	Min	Max	N
Experimental Enclosure (oiled)	Total Dissolved Solids	mg/L	25.88	11.837	16.00	53.00	8
Lake Epilimnion	Total Dissolved Solids	mg/L	17.56	6.695	2.00	23.00	8
Lake Metalimnion	Total Dissolved Solids	mg/L	21.14	4.634	16.00	28.00	7
Reference Enclosure (unoiled)	Total Dissolved Solids	mg/L	26.00	5.099	20.00	35.00	8
Experimental Enclosure (oiled)	Total Suspended Solids	mg/L	1.19	0.777	<LOD (0.05)	2.00	8
Lake Epilimnion	Total Suspended Solids	mg/L	0.83	0.948	<LOD (0.05)	2.00	8
Lake Metalimnion	Total Suspended Solids	mg/L	0.83	0.665	<LOD (0.05)	2.00	7
Reference Enclosure (unoiled)	Total Suspended Solids	mg/L	2.13	1.849	<LOD (0.05)	5.20	8
Experimental Enclosure (oiled)	Turbidity	NTU	0.67	0.237	0.41	0.99	8
Lake Epilimnion	Turbidity	NTU	0.39	0.101	0.31	0.62	8
Lake Metalimnion	Turbidity	NTU	0.55	0.153	0.41	0.86	7
Reference Enclosure (unoiled)	Turbidity	NTU	0.64	0.185	0.39	0.95	8

*Limit of Detection (LOD) was variable during each run based on the standard curve. Note, number of digits is based on decimal places for each analyte minimum limit of detection (LOD). Results <LOD were replaced with half LOD to calculate the mean and standard deviation.

During an oil spill, a large influx of carbon can alter nutrient ratios (C:N:P), impacting biodegradation potential (Lee et al., 2015). For every 1000 mg of hydrocarbons consumed by microorganisms, 150 mg nitrogen (N) and 30 mg phosphorus (P) are required, based on the Redfield Ratio of 106:16:1 (Rosenberg & Ron, 1996). Lake 260, and many boreal lakes at the IISD-ELA, are nutrient poor (oligotrophic). Mean (± SD) total nitrogen (TN) concentrations in Lake 260 were 292 ± 19.3 µg/L and 316 ± 31.1 µg/L, in the epilimnion (day -4 to 102; n= 8) and metalimnion (day -4 to 87; n=7), respectively, and mean (± SD) total phosphorus (TP) concentrations were 4.8 ± 1.06 µg/L and 5.6 ± 1.03 µg/L, respectively. Concentrations of TN and TP in the enclosures remained relatively stable over the first 94 days of the exposure period (June 18 to September 23, 2019; n=8), slightly declining over time. Mean (± SD) TN concentrations were 453 ± 59.1 µg/L and 432 ± 77.7 µg/L for the EE and RE, respectively. Mean (± SD) TP concentrations were 10.2 ± 2.95 µg/L and 9.2 ± 2.47µg/L , respectively.

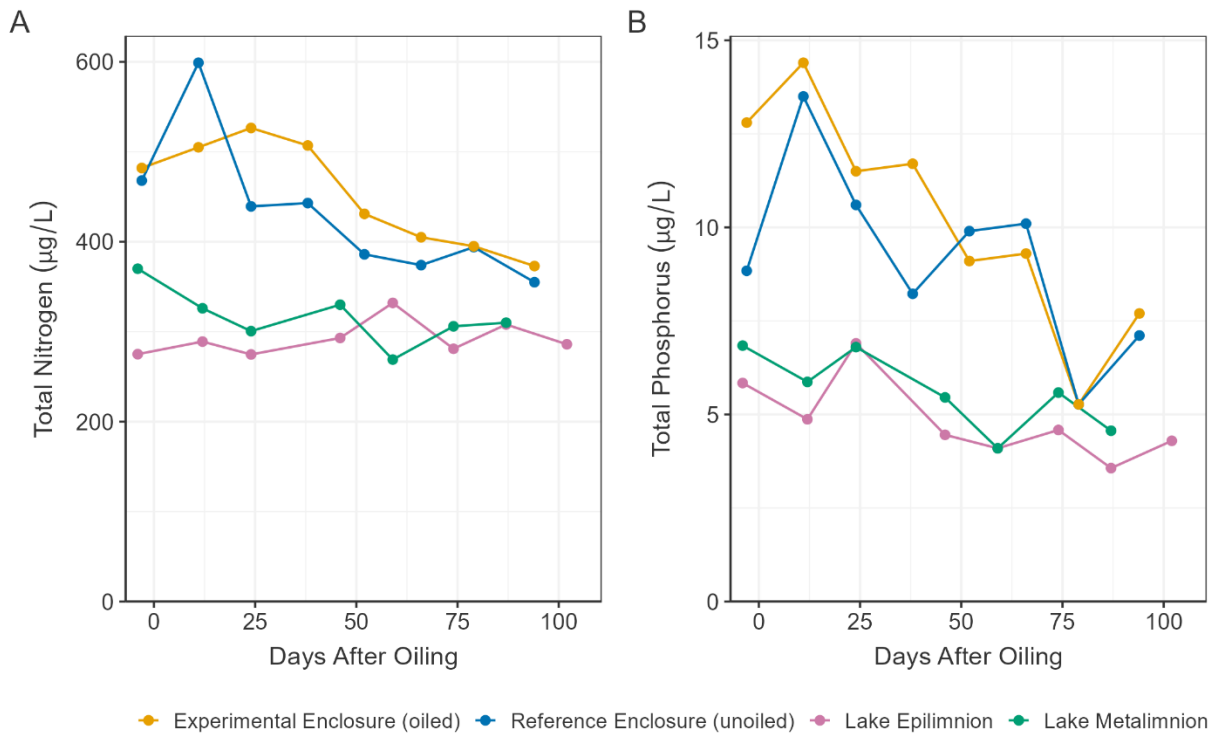

Figure A8. Total nitrogen (A) and total phosphorus (B) concentration in the FLOWTER enclosures and lake 260 center buoy epilimnion and metalimnion sites during pre-oil conditions and up to day 94 of exposure in the enclosures, day 87 in the lake metalimnion and 102 in the lake epilimnion during the 2019 dilbit experiment.

The enclosures and lake were almost always TP limited (Figure A9). However, due to the general limited nutrients in the lake and enclosures (oligotrophic classification based on Wetzel, 1983, in Spalinger & Bouwens, 2016), it was likely that nutrient availability may limit biodegradation. Enhancing nutrient availability through biostimulation (enhanced monitored natural recovery) may be an option to increase biodegradation.

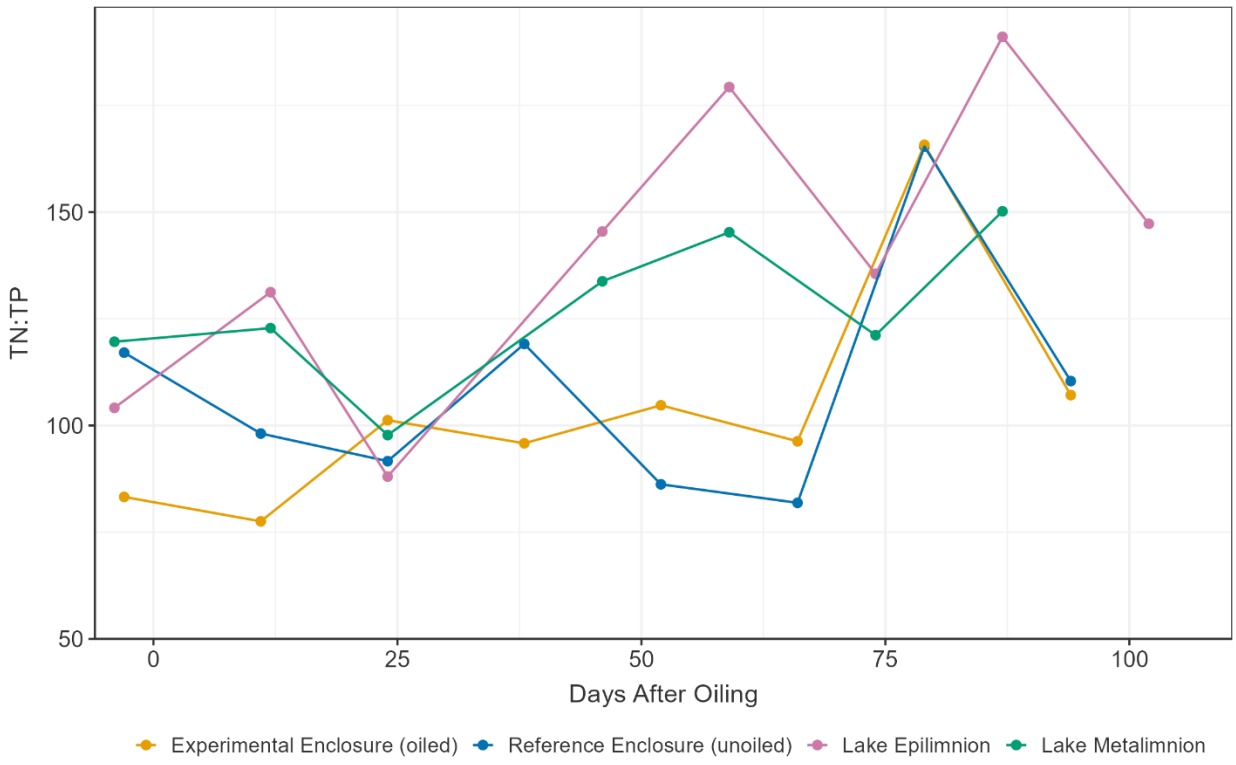

Figure A9. TN:TP molar ratio in the FLOWTER enclosures and Lake 260 center buoy epilimnion and metalimnion sites during pre-oil conditions and up to day 94 of exposure in the enclosures, day 87 in the lake metalimnion and 102 in the lake epilimnion during the 2019 dilbit experiment.

A.5 Root Microbial Community

Table A4. Mean (± SD of site replicates) prokaryotic and eukaryotic rarefied Alpha richness (observed ASVs), Chao 1 richness, Shannon diversity, and Simpson diversity in EFW root microbial biofilm for each sample period during the 2019 dilbit experiment.

Site	Days After Oiling	N	Alpha Richness	Chao1 Richness	Shannon Diversity	Simpson Diversity	Alpha Richness	Chao1 Richness	Shannon Diversity	Simpson Diversity
			Prokaryotes (16S)				Eukaryotes (18S)			
Experimental Enclosure (oiled)	-3	1	960	969	6.27	0.997	351	445	4.27	0.956
Experimental Enclosure (oiled)	38	3	979 ± 93.7	991 ± 96.8	6.22 ± 0.132	0.996 ± $9.03e^{-04}$	297 ± 128	315 ± 149	4.84 ± 0.490	0.981 ± $9.60e^{-03}$
Experimental Enclosure (oiled)	91	3	1242 ± 176.6	1270 ± 183.9	6.45 ± 0.199	0.996 ± $9.50e^{-04}$	350 ± 101	416 ± 142	4.25 ± 0.350	0.926 ± $2.98e^{-02}$
Reference Enclosure (unoiled)	-3	1	1009	1022	6.32	0.997	354	438	4.17	0.945
Reference Enclosure (unoiled)	38	3	994 ± 76.6	1005 ± 80.05	6.17 ± 0.0948	0.995 ± $9.71e^{-04}$	317 ± 40.8	338 ± 55.0	4.89 ± 0.161	0.980 ± $6.12e^{-03}$
Reference Enclosure (unoiled)	91	3	1253 ± 128.8	1280 ± 137.0	6.49 ± 0.127	0.997 ± $6.82e^{-04}$	387 ± 7.85	509 ± 33.6	4.10 ± 0.293	0.909 ± $5.46e^{-02}$

Site	Days After Oiling	N	Alpha Richness	Chao1 Richness	Shannon Diversity	Simpson Diversity	Alpha Richness	Chao1 Richness	Shannon Diversity	Simpson Diversity
			Prokaryotes (16S)				Eukaryotes (18S)			
Lake Reference (unoiled)	-3	1	986	996	6.27	0.996	337	384	4.61	0.971
Lake Reference (unoiled)	38	3	877 ± 111	883 ± 115	6.20 ± 0.105	0.996 ± $4.52e^{-04}$	235 ± 30.0	252 ± 37.9	4.48 ± 0.0991	0.975 ± $2.23e^{-03}$
Lake Reference (unoiled)	91	3	848 ± 9.84	853 ± 7.68	6.10 ± 0.0249	0.996 ± $1.92e^{-04}$	264 ± 13.3	309 ± 6.80	4.20 ± 0.373	0.950 ± $3.62e^{-02}$

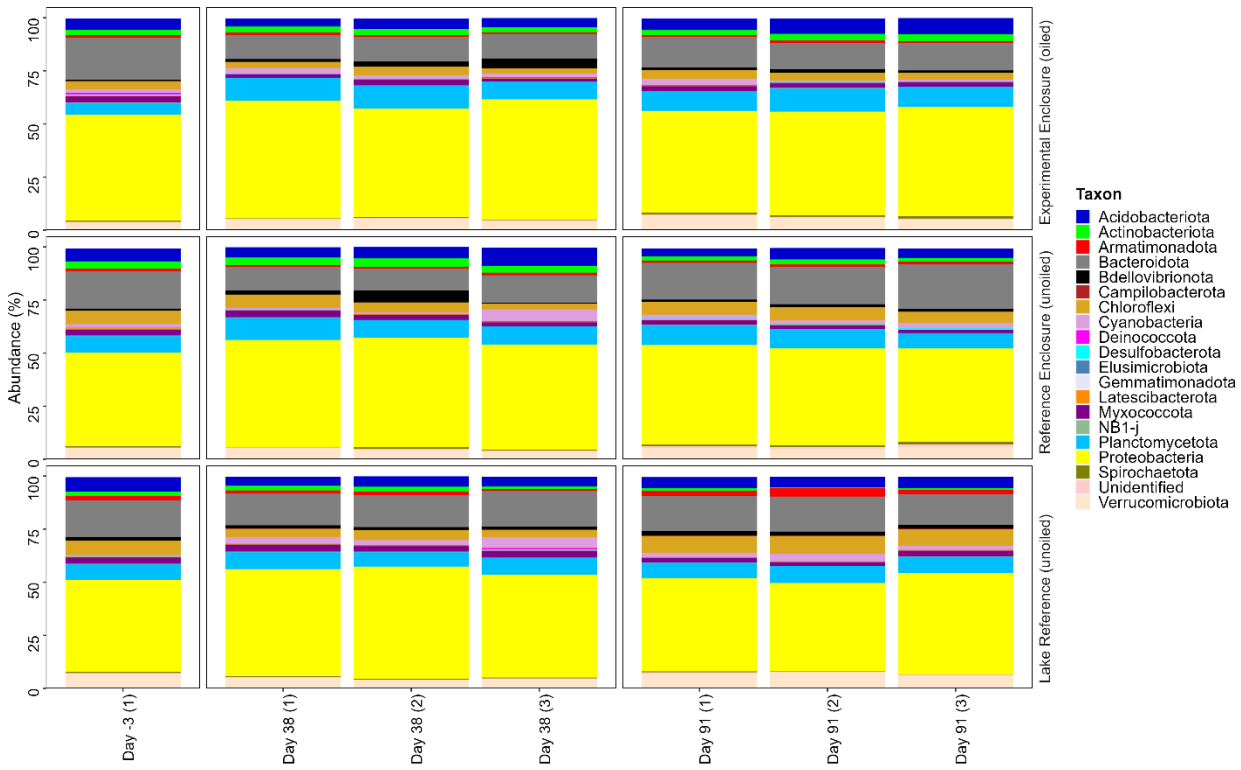

Figure A10. Taxonomic profile of the top twenty most relatively abundant 16S phyla in EFW root biofilm replicates from the EE, RE, and LR 3 days pre-oil addition, and on days 38 and 91 post-oil addition during the 2019 dilbit experiment.

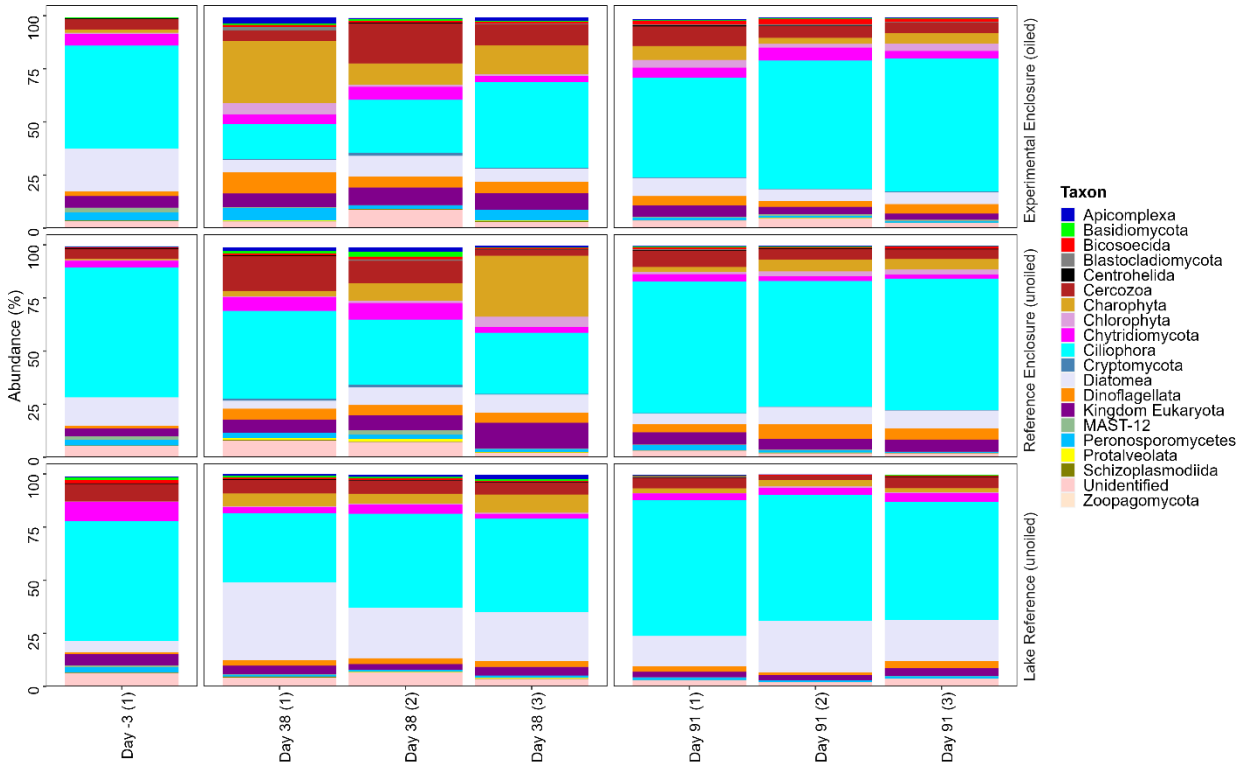

Figure A11. Taxonomic profile of the top twenty most relatively abundant 18S phyla in EFW root biofilm replicates from the EE, RE, and LR 3 days pre-oil addition, and on days 38 and 91 post-oil addition during the 2019 dilbit experiment.

Appendix B- Chapter 4

B.1 Research Design

Figure B1. Drone image of the FLOWTER 2021 shoreline enclosures (Curry Industries Ltd, Winnipeg) with deployed EFWs on Lake 260 at the IISD Experimental Lakes Area. LR EFW is to the right (west) of the photo. Source: IISD-ELA.

B.2 EFW Plant Development

Over the duration of the experimental period, the number of holes planted by species remained the same while the number of plants varied in all EFW sites (Figure B2). This variability likely arose from plant senescence, new shoot growth, insect activity, site conditions and nutrient availability, and/or potential toxicity in the oiled enclosure. Due to lack of site

replication, we are unable to confirm differences between sites. However, the total numbers of plants were highest in the LR site which increased over the experimental period, largely due to an increase of *Carex lasiocarpa*, which decreased and was variable in the enclosure sites. *Carex utriculata* plants decreased over the experimental periods in all three sites, while *Typha* sp. remained relatively stable, displaying some senescence on day 76.

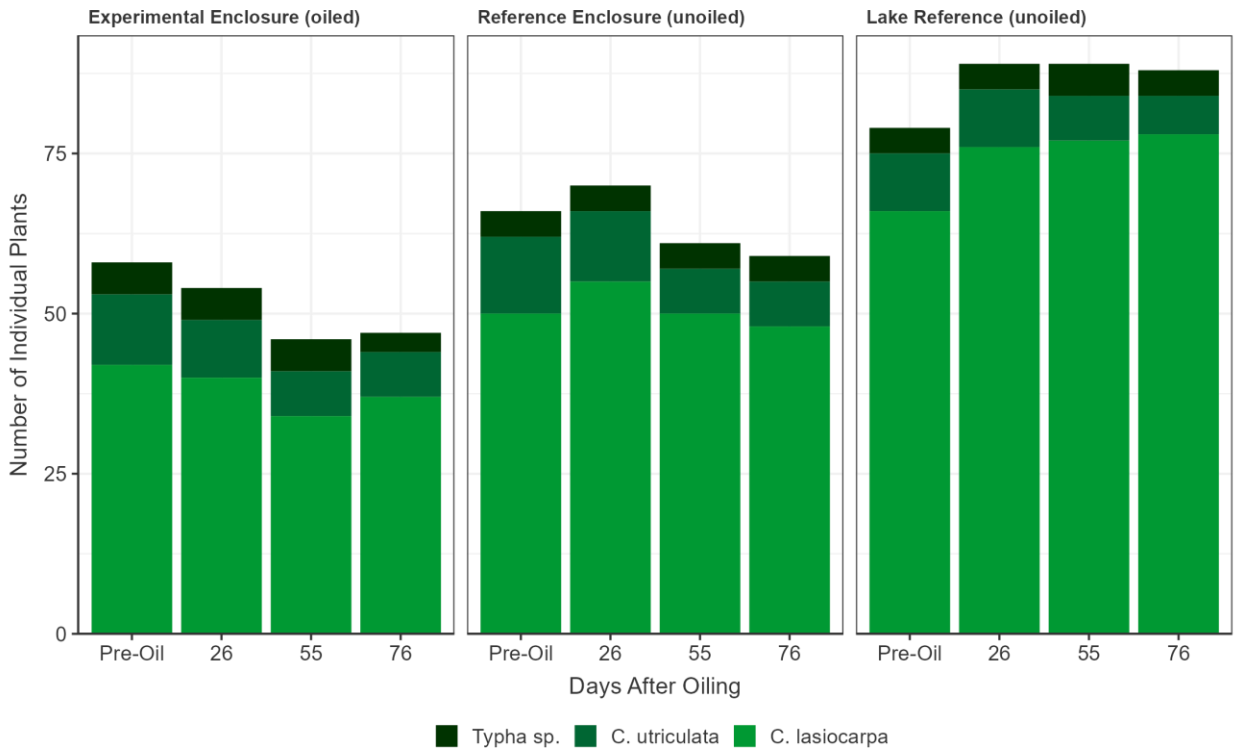

Figure B2. Number of individual plants by species on EFWs over the exposure period of the 2021 CHV experiment.

Mean and max heights increased for *C. lasiocarpa* in all three sites over the experimental period (Figure B3). Max heights of *Typha* sp. remained stable or slightly increased in each site, while the mean height declined in the LR, likely skewed by new shoot growth. Max heights of *C.*

utriculata declined and later increased in all three sites, while mean heights were variable. As there were no replicate treatments, there were no clear differences in plant growth or heights between oiled and unoiled sites, suggesting no obvious toxicity to EFW plants upon oil exposure. However, future replicated research should assess differences in growth and development of oil exposed and unexposed plants.

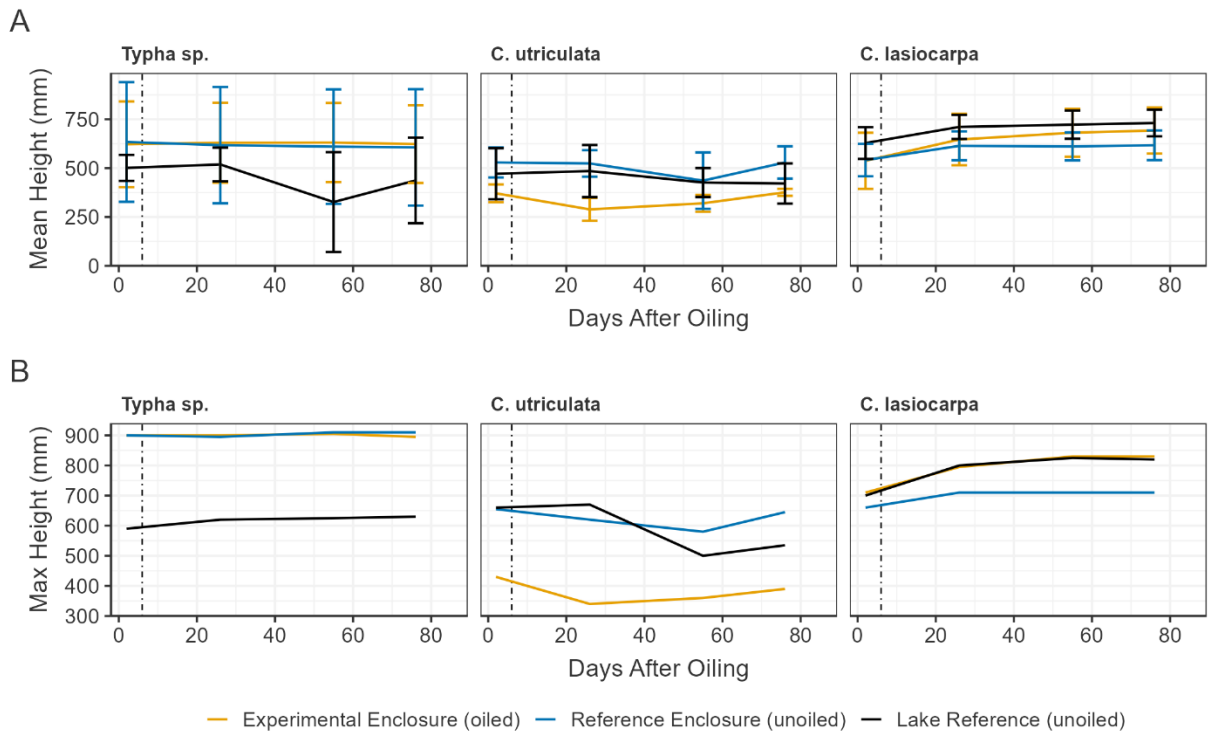

Figure B3. Mean (±SD) (A) and max (B) heights of *Typha* sp., *Carex utriculata*, and *C. lasiocarpa* on EFWs over the exposure period of the 2021 CHV experiment. Vertical dashed line represents EFW application to enclosures and LR locations.

B.3 Polycyclic Aromatic Compound Chemistry

Table B1. List of parent and alkylated PACs measured in water and sediments of the FLOWTER sites.

Compound	Parent or Alkylated	US EPA Priority PAC (2014)	Ring Number
Naphthalene	Parent	Yes	2
1-Methylnaphthalene	Alkylated	No	2
2-Methylnaphthalene	Alkylated	No	2
C2 Naphthalene	Alkylated	No	2
C3 Naphthalene (Trimethyl)	Alkylated	No	2
C4 Naphthalene (Tetramethyl)	Alkylated	No	2
Acenaphthene	Parent	Yes	3
Acenaphthylene	Parent	Yes	3
Anthracene	Parent	Yes	3
Dibenzothiophene*	Alkylated	No	3
C1 Dibenzothiophene*	Alkylated	No	3
C2 Dibenzothiophene*	Alkylated	No	3
C3 Dibenzothiophene*	Alkylated	No	3
Fluorene	Parent	Yes	3
C1 Fluorene	Alkylated	No	3
C2 Fluorene	Alkylated	No	3
Phenanthrene	Parent	Yes	3
1,7-Dimethylphenanthrene	Alkylated	No	3
1,8-Dimethylphenanthrene	Alkylated	No	3
1-Methylphenanthrene	Alkylated	No	3
2,6-Dimethylphenanthrene	Alkylated	No	3
2-Methylphenanthrene	Alkylated	No	3
3,6-Dimethylphenanthrene	Alkylated	No	3
3-Methylphenanthrene	Alkylated	No	3
9/4-Methylphenanthrene	Alkylated	No	3
C2 Phenanthrene	Alkylated	No	3
C3 Phenanthrene	Alkylated	No	3
C4 Phenanthrene	Alkylated	No	3
Retene	Alkylated	No	3
Benz[a]anthracene	Parent	Yes	4
Chrysene	Parent	Yes	4
C1 Chrysene	Alkylated	No	4

Compound	Parent or Alkylated	US EPA Priority PAC (2014)	Ring Number
C3 Chrysene	Alkylated	No	4
Fluoranthene	Parent	Yes	4
Pyrene	Parent	Yes	4
C1 Pyrene	Alkylated	No	4
C2 Pyrene	Alkylated	No	4
Benzo[a]pyrene	Parent	Yes	>4 (5)
C1 Benzo[a]pyrene	Alkylated	No	>4 (5)
Benzo[b]fluoranthene	Parent	Yes	>4 (5)
Benzo[g,h,i]perylene	Parent	Yes	>4 (6)
Benzo[k]fluoranthene	Parent	Yes	>4 (5)
Dibenzo[a,h]anthracene	Parent	Yes	>4 (5)
Indeno[1,2,3-c,d]pyrene	Parent	Yes	>4 (6)

* Parent and alkylated dibenzothiophenes are heterocyclic PACs (containing sulfur), but are included in the 28 aPAC grouping for visualization.

B.3.1 Water

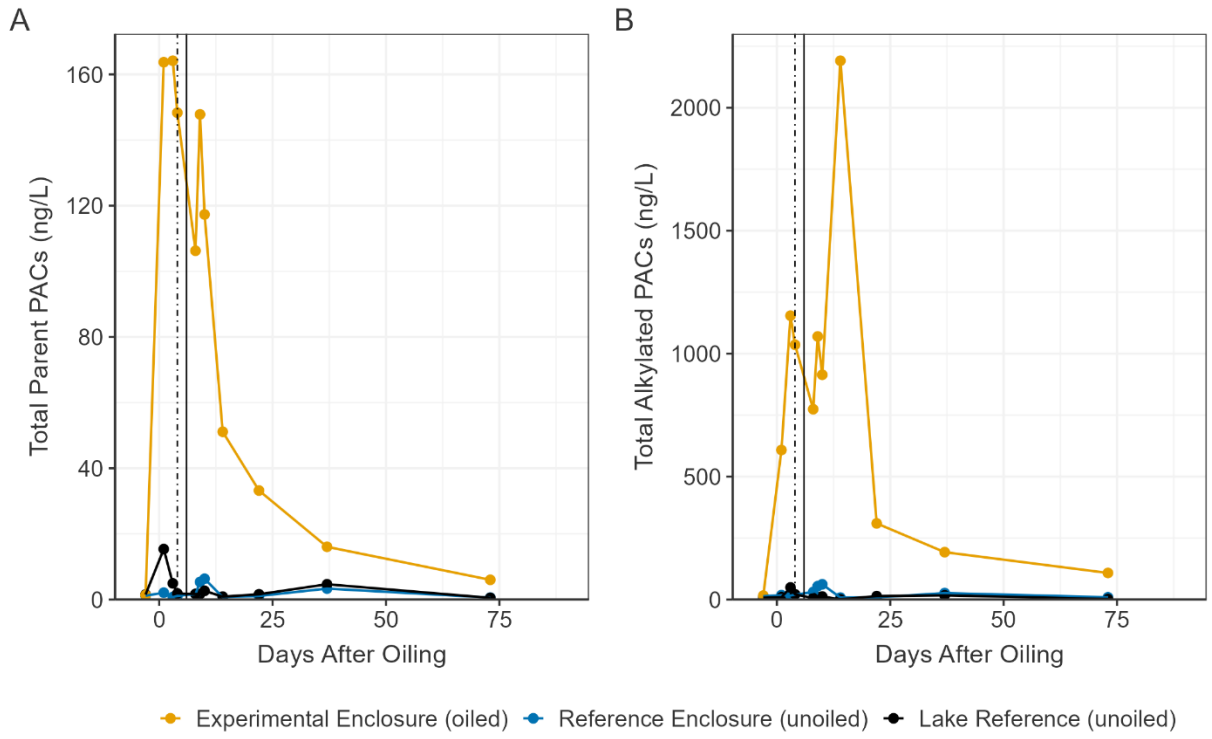

Figure B4. Total parent (A) and alkylated (B) PACs in the water from 3 days pre-oil addition to day 73 post-oil addition during the 2021 CHV experiment. Vertical lines represent primary (dotted) and secondary (solid) recovery events.

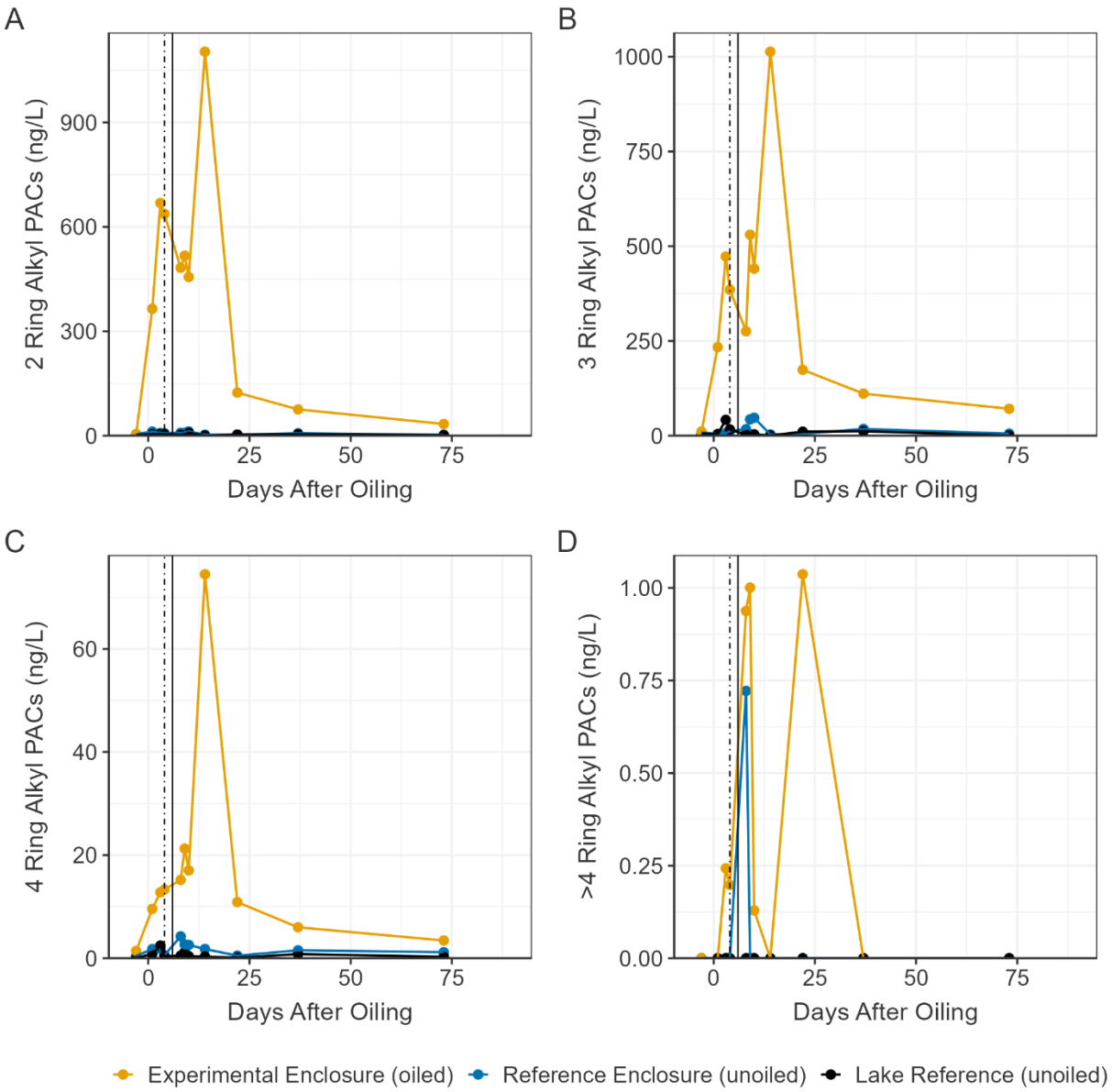

Figure B5. Total 2, 3, 4, and >4 ring alkylated PACs in the water from 3 days pre-oil addition to day 73 post-oil addition during the 2021 CHV experiment. Vertical lines represent primary (dotted) and secondary (solid) recovery events.

B.3.2 Sediment

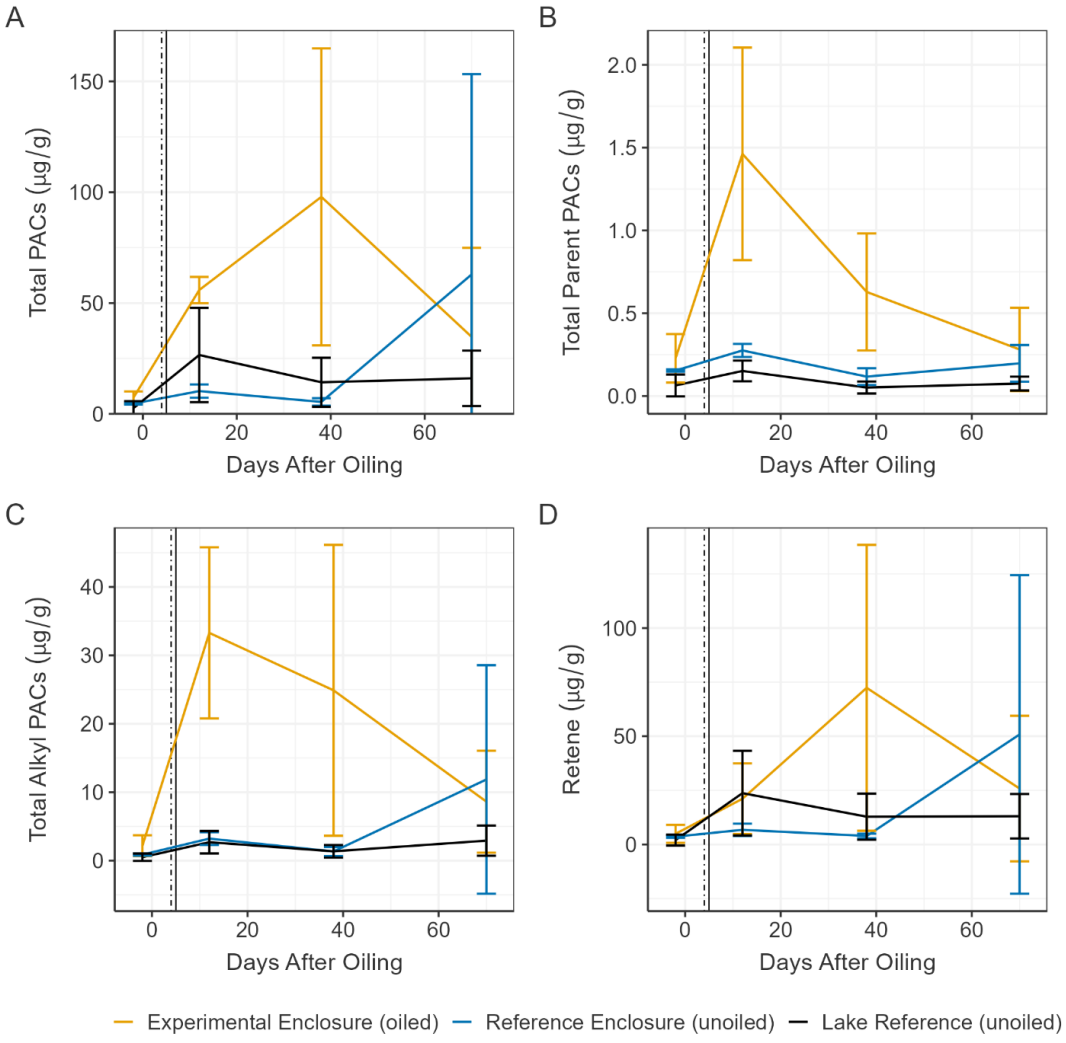

Figure B6. Mean (± SD) total PACs (A; n = 44), total parent PACs (B, n = 16), total alkylated PACs (C, minus retene, n = 27), and retene (D) concentrations in sediment from 2 days pre-oil addition to day 70 post-oil addition during the 2021 CHV experiment. Error bars represent standard deviation of triplicate samples at each site. Vertical lines represent primary (dotted) and secondary (solid) recovery events.

B.3.2.1 Sediment Ratios. In order to identify whether sediment PACs were contributed by pyrogenic (combustion) or petrogenic (oil/petroleum) sources, we assessed the

retene/(retene+chrysene) ratio to identify softwood (> 0.80) versus petroleum/coal (0.15-0.5) combustion sources (Yan et al., 2005), and fluoranthene/(fluoranthene+pyrene) ratio to identify combustion (>0.4) versus petrogenic (<0.4) sources (Yunker et al., 2002).

Of combustion sources in the sediment, the retene/(retene+chrysene) ratio suggests softwood combustion (0.93-1.00), indicating historic forest fires have significant impact on retene in the sediment (data not shown). Interestingly, when assessing the fluoranthene/(fluoranthene+pyrene) ratios, all sediment samples on days 12 and 38 (excluding one sample in LR) were considered to arise from petrogenic sources among all sites (Figure B7). However, ratios may only be appropriate to use in sites are exposed to PACs higher than background. Stoyanovich et al. (2023) found biodegradation ratios calculated for limnocorrals of low oil volumes may have been an artifact of the low concentrations and not necessarily biodegradation. In addition, Tobiszewski & Namieśnik (2012) note caution in using and interpreting these ratios, as environmental fate of these compounds can vary over time, as discussed in Chapter 3, and perhaps only appropriate for oiled sites. Following oil addition, all sediment samples in the EE sediment were indicative of a petrogenic source.

It is likely that sediment in Lake 260 is strongly influenced by pyrogenic combustion sources by nearby and historic forest fires influencing interpretation of PACs. However, there was clear oil influenced on sediment PACs in the EE.

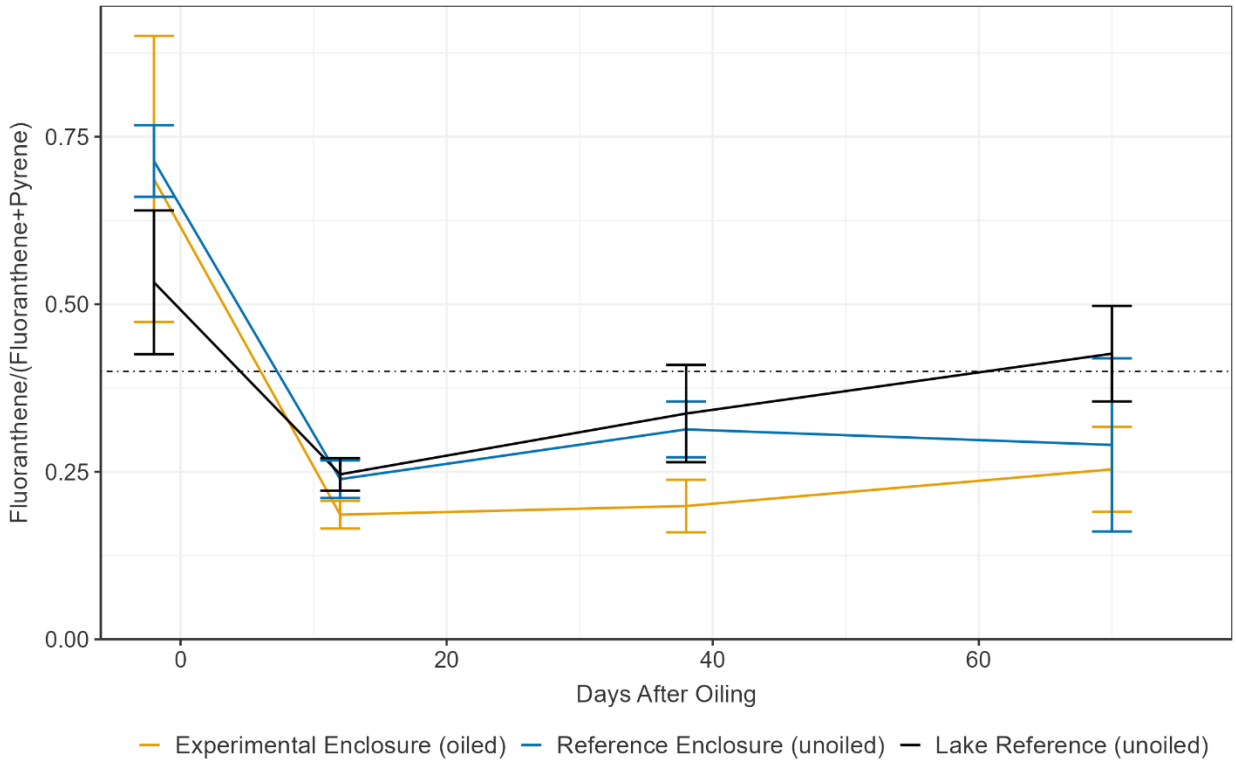

Figure B7. Mean (±SD) fluoranthene/(fluoranthene+pyrene) ratio in sediment over the duration of 2021 CHV experiment. Values above horizontal dashed line (0.4) indicate combustion sources, and below indicate petrogenic sources (Yunker et al., 2002). Error bars represent standard deviation of triplicate samples at each site.

B.4 Basic Water Quality

Surface waters in the far shore environment in each enclosure and lake reference were monitored weekly for water temperature (℃), dissolved oxygen (% and mg/L), specific conductivity (µS/cm), and pH using a Yellow Springs Instrument (YSI) Professional Series Plus multiparameter meter (YSI QUATRO, 18C100206. Xylem, Yellow Springs, Ohio). Temperatures in the enclosures and LR ranged from 14.3 to 23.7 ℃ and 16.2 to 24.0 ℃ from 2 days pre-oil addition to day 88 after oil addition, respectively (Figure B8). The lake was slightly

warmer than the enclosures, possibly due to greater mixing, however not as defined as in the 2019 dilbit enclosure experiments (Chapter 3), which may be due to differences in conditions between years. Water temperatures were within optimal temperature conditions for biodegradation until day 60 following oil addition (20-30 ℃; Atlas, 1985, as cited in Al-Hawash et al., 2018; Bartha & Bossert, 1984, and Cooney, 1984, as cited in Das and Chandran, 2011).

Dissolved oxygen (% and mg/L) was generally higher in the LR site than the enclosures with mean percent saturation (± standard deviation [SD]; n=13) of 85.0 ± 8.63 %, 81.5 ± 7.34 %, and 93.1 ± 4.99 % in the EE, RE, and LR, respectively (Figure B9). Mean concentrations of dissolved oxygen (± SD; n=13) were 7.75 ± 0.926 mg/L, 7.45 ± 0.795 mg/L, and 8.35 ± 0.630 mg/L, respectively (Figure B10), suggesting the enclosures may slightly reduce aeration from mixing and wind. However, mean concentrations are above criteria for Coldwater aquatic biota (6.5 mg/L for early life stages exposed to the water column (7 day mean) and other life stages (30 day mean) (US EPA, 1996), with only five measurements below 6.5 mg/L in the EE and RE sites (5.88-6.47; n=5). The pH between the lake and enclosures were relatively similar through the duration of exposure with a mean (± SD; n=13) of 6.29 ± 0.270, 6.30 ± 0.300, and 6.39 ± 0.243, respectively (Figure B11). Mean specific conductivity was highest in the RE and lowest in the LR, with a mean (± SD; n=13) of 31.8 ± 6.51 μS/cm, 36.3 ± 6.03 ± μS/cm, and 28.1 ± 7.11 μS/cm, respectively (Figure B12), potentially an enclosure effect of reduced dilution. Trends of conductivity increased over the experimental period in all three sites, which may result from seasonal climate conditions. Conductivity increases with water temperature (Barron & Ashton, 2005), and can change with precipitation and evaporation (Bennett et al., 2007; DataStream Initiative, 2021). Bennett et al. (2007) observed increasing conductivity in Nebraska lakes

generally towards the end of the summer drought, however response in freshwater lakes can be variable and can be related to lake connectivity.

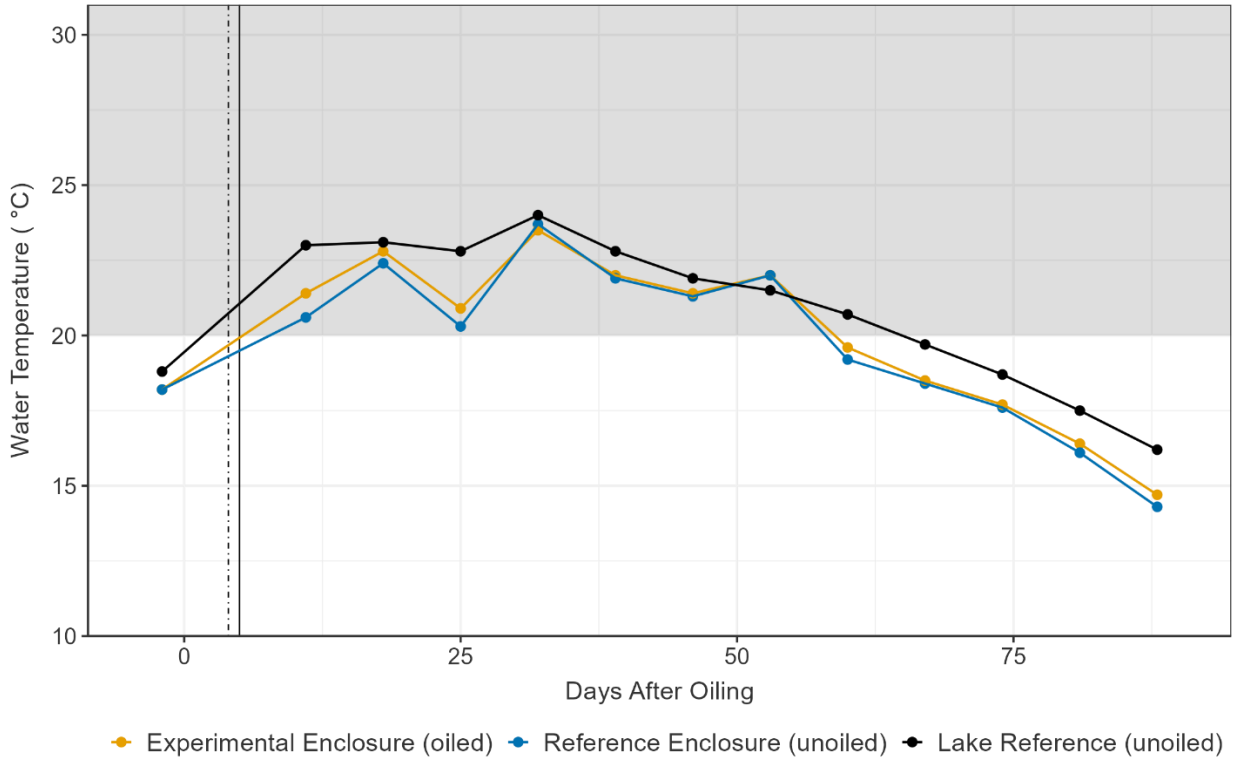

Figure B8. Water temperature in FLOWTER sites from 2 days pre-oil addition to day 88 post-oil addition during the 2021 CHV experiment. Vertical lines represent primary (dotted) and secondary (solid) recovery. Grey region indicates optimal temperature for biodegradation

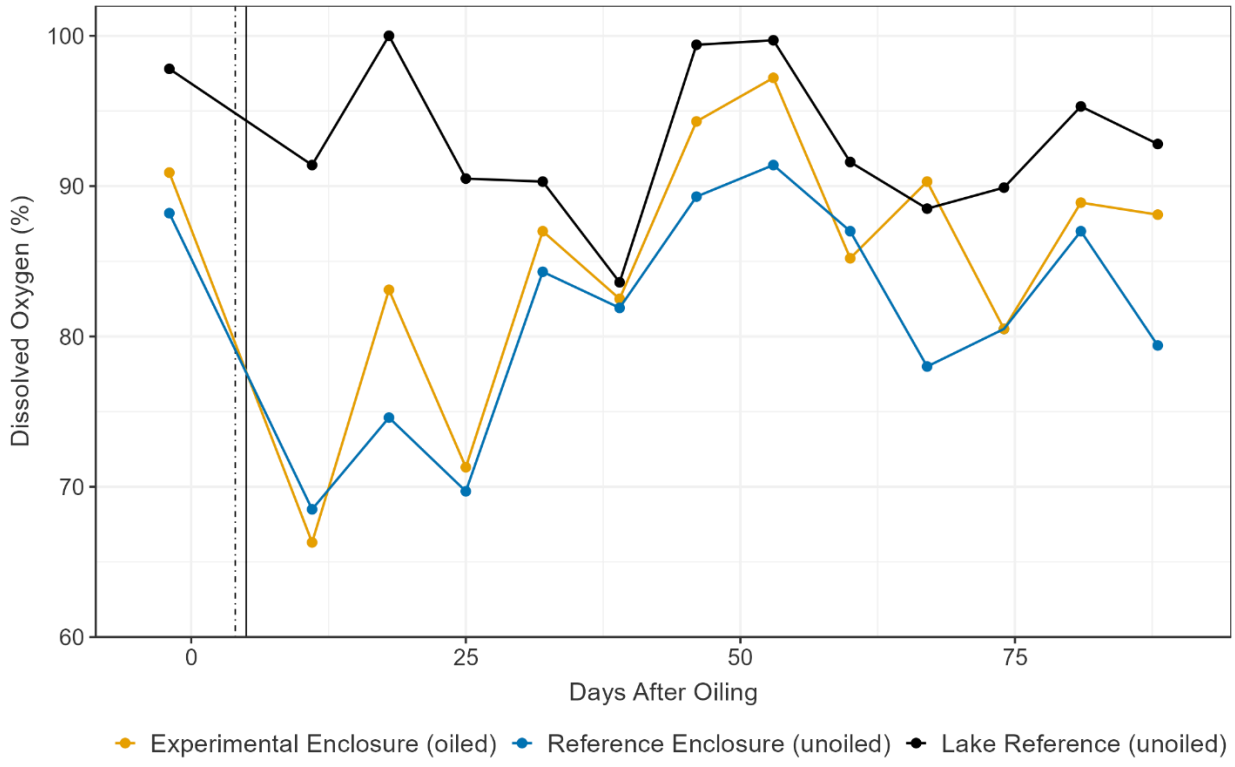

Figure B9. Dissolved Oxygen (%) in FLOWTER sites from 2 days pre-oil addition to day 88 post-oil addition during the 2021 CHV experiment. Vertical lines represent primary (dotted) and secondary (solid) recovery.

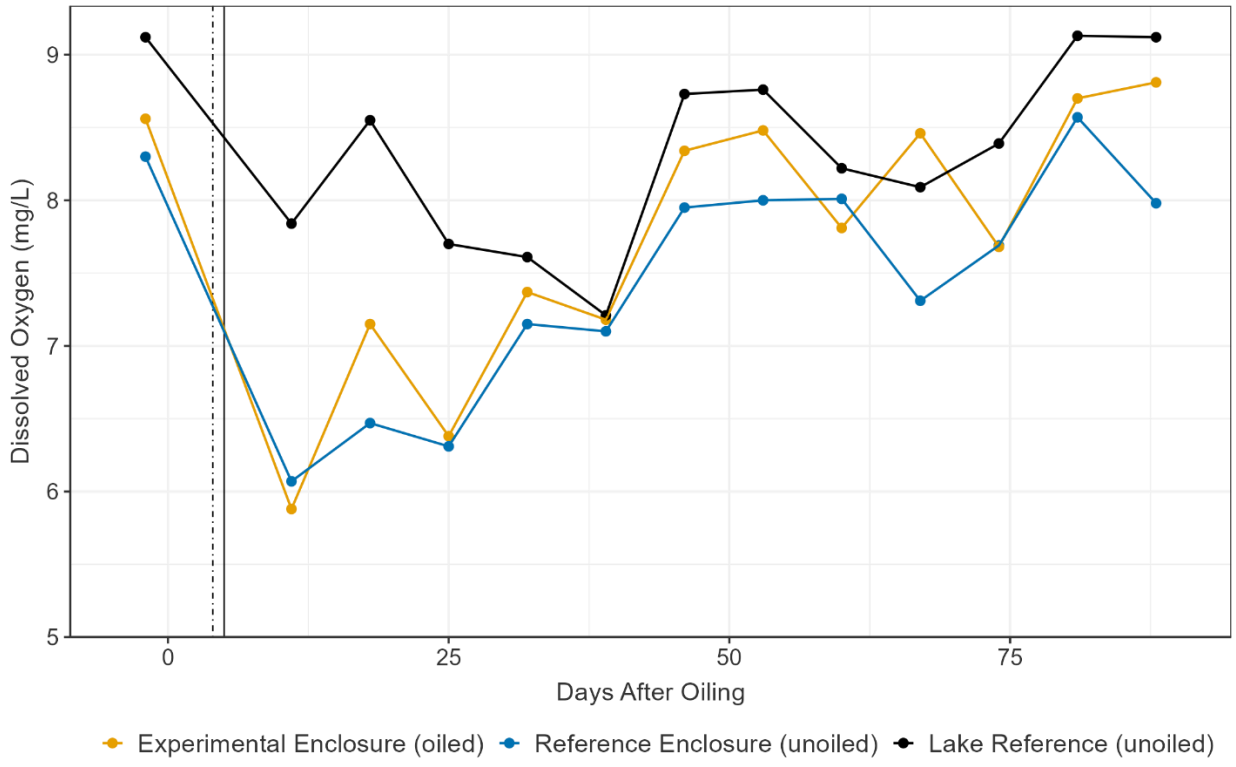

Figure B10. Dissolved oxygen concentration in FLOWTER sites from 2 days pre-oil addition to day 88 post-oil addition during the 2021 CHV experiment. Vertical lines represent primary (dotted) and secondary (solid) recovery.

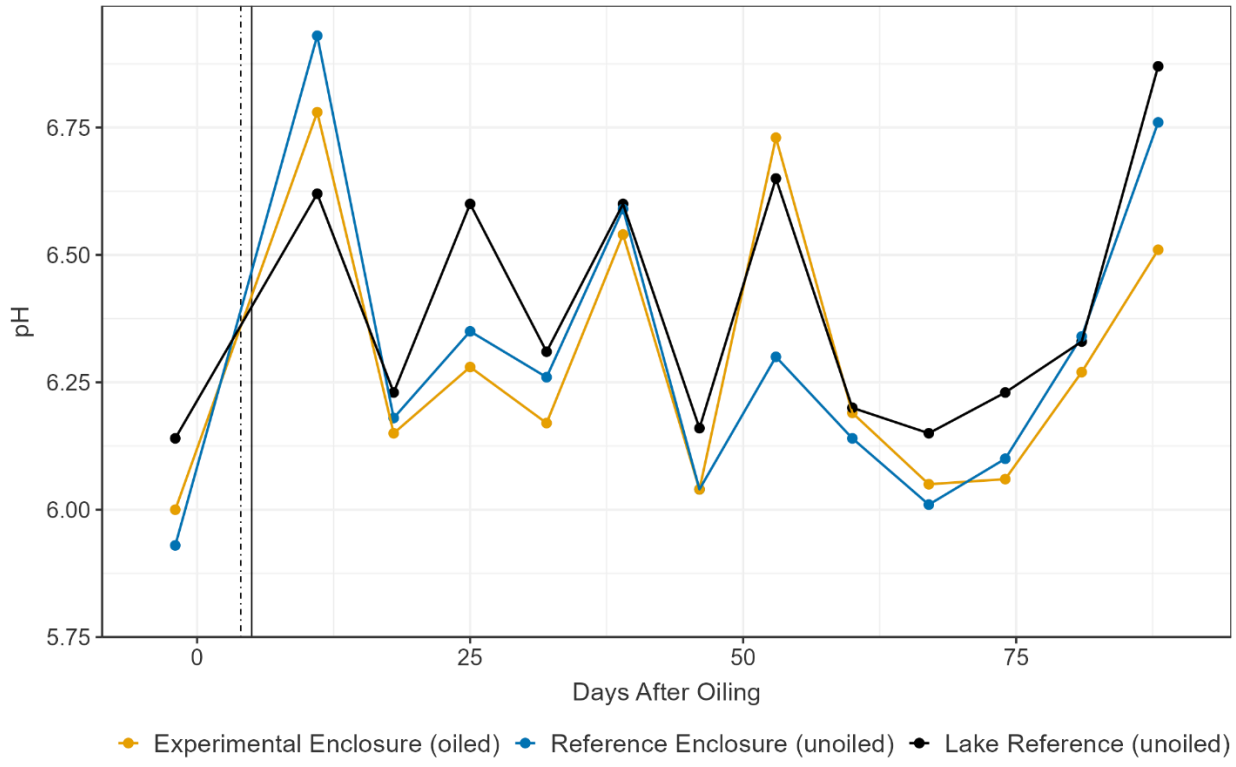

Figure B11. pH in FLOWTER sites from 2 days pre-oil addition to day 88 post-oil addition during the 2021 CHV experiment. Vertical lines represent primary (dotted) and secondary (solid) recovery.

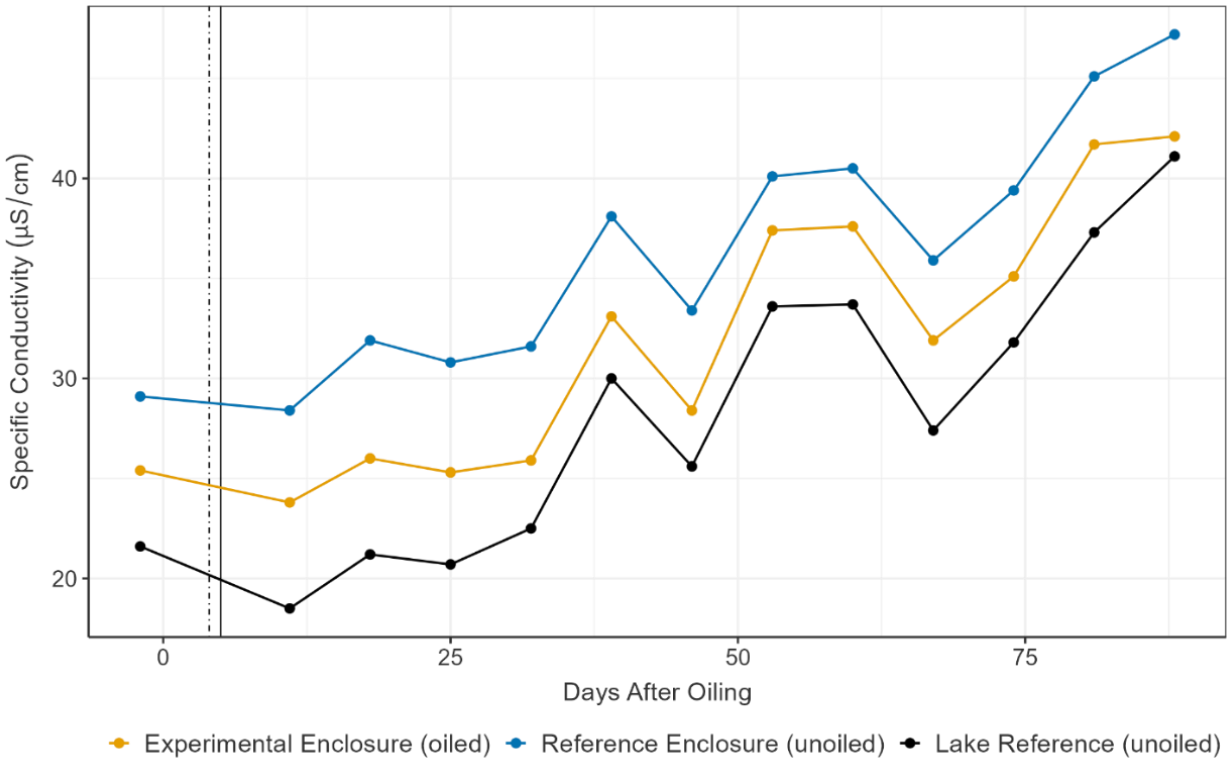

Figure B12. Specific conductivity in FLOWTER sites from 2 days pre-oil addition to day 88 post-oil addition during the 2021 CHV experiment. Vertical lines represent primary (dotted) and secondary (solid) recovery.

During the experiment, we experienced low precipitation, with total monthly rainfall below the 30 year normal (1991-2020) from June to September (data source: IISD-ELA) (Table B2). This may have caused greater evaporation than water contributed from precipitation, causing conductivity to increase over the season (Bennett et al., 2007; DataStream Initiative, 2021). Figure B13 overlays the relationship between temperature and conductivity, and highlights precipitation events over 10 mm. In the beginning of the study, conductivity increased with water temperature, but often observed slight declines during measurements that directly

followed a precipitation event. Once temperatures began to cool, conductivity continued to climb, possibly due to continued evaporation.

Table B2. Total monthly precipitation (mm; 2021) during the experimental period compared to 30 year climate normal (1991-2020). Data Source: IISD-ELA.

Month	**June**	**July**	**August**	**September**
Study Day	-24 to 5	6 to 36	37-67	68-97
2021 Precipitation (mm)	61.2	80.8	81.5	61.5
30 Year Normal (1991-2020) Precipitation (mm)	114.1	109.4	90.1	97.5

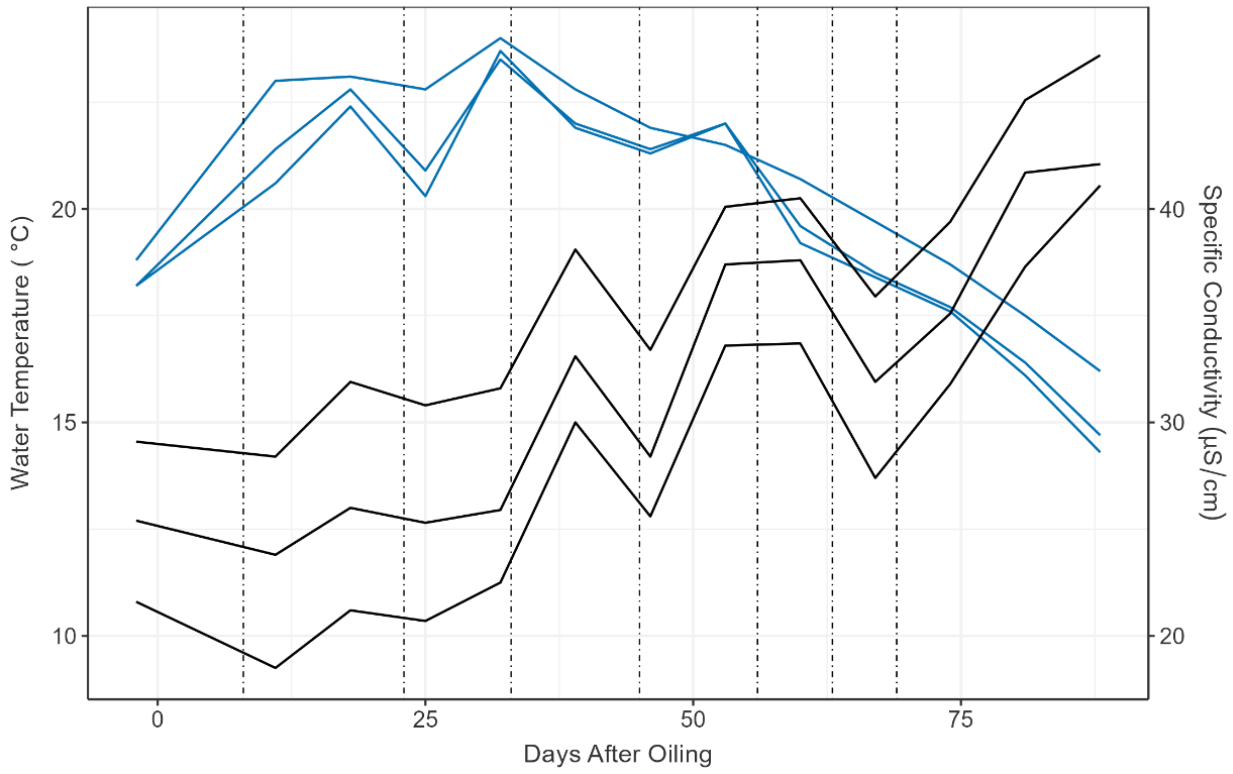

Figure B13. Trends of water temperature (blue) and specific conductivity (black) in FLOWTER sites from 2 days pre-oil addition to day 88 post-oil addition during the 2021 CHV experiment. Replicate lines represent all three FLOWTER sites. Vertical lines represent precipitation events >10 mm (Precipitation data source: IISD-ELA).

B.5 Nutrient Chemistry

Nutrient chemistry in the enclosure waters were analyzed biweekly from 3 days pre-oil addition to day 68 post-oil addition. Water was collected in the far shore environment from the FLOWTER enclosures and in the epilimnion and metalimnion at the center of the lake, and analyzed for a suite of parameters by the IISD-ELA chemistry laboratory (methods in Stainton, Capel, & Armstrong, 1977) and the Biogeochemical Analytical Service Laboratory at the University of Alberta (for anions, cations, particulate carbon, particulate nitrogen, and

alkalinity). Only total nitrogen (TN) and total phosphorus (TP) are described in detail due to their importance for biodegradation (Lee et al., 2015; Rosenberg & Ron, 1996), and summary data for other parameters in the FLOWTER sites are available in Table B3.

Lake 260 is oligotrophic, with a mean (± SD; n=3) TN of 287 ± 5.1 µg/L and 297 ± 15.0 µg/L, and TP of 5.2 ± 1.06 µg/L and 7.4 ± 0.85 µg/L in the epilimnion and metalimnion over the duration of the 2021 field season, respectively (July 6 to September 16, 2021). The EE and RE had greater nutrient concentrations, likely due to reduced dilution and mixing caused by the enclosure and the near shore environment. Mean (± SD; n=7) TN concentrations were 381 ± 19.3 µg/L and 483 ± 28.0 µg/L and TP concentrations were 8.6 ± 1.68 µg/L and 11.8 ± 2.71 µg/L, in the EE and RE, respectively (June 22 to September 1, 2021) (Figure B14). Concentrations of TN and TP were lower in the EE than the RE, and may be a result of enclosure variability or the consumption of nitrogen and phosphorus for biodegradation of petroleum hydrocarbons. It is likely caused by enclosure variability as concentrations displayed differences during pre-oil conditions. However, nutrient availability is particularly important for successful biodegradation, as during an oil spill the influx of carbon causes the C:N:P to shift (Lee et al., 2015). Based on the Redfield Ratio of 16:1 [N:P] (Rosenberg & Ron, 1996), Lake 260 and the FLOWTER enclosures were always TP limited (Figure B15). However, due to the low nutrient availability in Lake 260, and many boreal oligotrophic lakes, it is likely that both N and P are limiting and may impact biodegradation. The addition of nutrients, through biostimulation or enhanced monitored natural recovery (eMNR) as explored through the Freshwater Oil spill Remediation Study (FOReSt) may enhance oil recovery in low nutrient environments.

Table B3. Nutrient chemistry summary data from day -3 to day 68 in the enclosures and from day 11 to day 83 in the lake epilimnion and metalimnion during the 2021 CHV experiment.

Site	Parameter	Units	Mean	Std Dev	Min	Max	N
Experimental Enclosure (oiled)	Alkalinity	µEq/L	177	49.5	84	252	7
Lake Epilimnion	Alkalinity	µEq/L	137	1.9	135	138	3
Lake Metalimnion	Alkalinity	µEq/L	141	6.7	135	149	3
Reference Enclosure (unoiled)	Alkalinity	µEq/L	217	14.6	201	235	7
Experimental Enclosure (oiled)	Ammonia	µg/L	7.1	2.62	<LOD (6.6)	9.0	7
Lake Epilimnion	Ammonia	µg/L	4.5	2.14	<LOD (6.6)	7.0	3
Lake Metalimnion	Ammonia	µg/L	7.1	3.85	<LOD (6.6)	11.0	3
Reference Enclosure (unoiled)	Ammonia	µg/L	8.9	5.16	<LOD (6.6)	17.0	7
Experimental Enclosure (oiled)	Calcium	mg/L	2.64	0.118	2.47	2.81	7
Lake Epilimnion	Calcium	mg/L	2.09	0.081	2.00	2.15	3
Lake Metalimnion	Calcium	mg/L	2.15	0.131	2.00	2.25	3
Reference Enclosure (unoiled)	Calcium	mg/L	3.14	0.196	2.88	3.37	7
Experimental Enclosure (oiled)	Chlorine	mg/L	0.20	0.018	0.18	0.23	7
Lake Epilimnion	Chlorine	mg/L	0.19	0.02	0.17	0.21	3
Lake Metalimnion	Chlorine	mg/L	0.18	0.012	0.17	0.19	3
Reference Enclosure (unoiled)	Chlorine	mg/L	0.25	0.036	0.18	0.29	7
Experimental Enclosure (oiled)	Chlorophyll-a	µg/L	1.1	0.31	0.7	1.5	7
Lake Epilimnion	Chlorophyll-a	µg/L	1.1	0.44	0.8	1.7	3
Lake Metalimnion	Chlorophyll-a	µg/L	2.0	0.64	1.3	2.5	3
Reference Enclosure (unoiled)	Chlorophyll-a	µg/L	1.6	0.39	1.1	2.3	7
Experimental Enclosure (oiled)	Dissolved Inorganic Carbon	µmol/L	225	27.2	191	257	7

Site	Parameter	Units	Mean	Std Dev	Min	Max	N
Lake Epilimnion	Dissolved Inorganic Carbon	µmol/L	140	7.5	133	148	3
Lake Metalimnion	Dissolved Inorganic Carbon	µmol/L	201	70.0	136	275	3
Reference Enclosure (unoiled)	Dissolved Inorganic Carbon	µmol/L	265	29.6	225	305	7
Experimental Enclosure (oiled)	Dissolved Organic Carbon	µmol/L	560.6	53.53	494.0	657.0	7
Lake Epilimnion	Dissolved Organic Carbon	µmol/L	468.7	83.50	417.0	565.0	3
Lake Metalimnion	Dissolved Organic Carbon	µmol/L	453.3	93.47	393.0	561.0	3
Reference Enclosure (unoiled)	Dissolved Organic Carbon	µmol/L	634.1	17.26	604.0	654.0	7
Experimental Enclosure (oiled)	Iron	mg/L	0.09	0.044	0.03	0.16	7
Lake Epilimnion	Iron	mg/L	0.03	0.032	<LOD (0.02)	0.07	3
Lake Metalimnion	Iron	mg/L	0.09	0.093	0.03	0.20	3
Reference Enclosure (unoiled)	Iron	mg/L	0.08	0.039	0.03	0.14	7
Experimental Enclosure (oiled)	Magnesium	mg/L	0.69	0.035	0.65	0.75	7
Lake Epilimnion	Magnesium	mg/L	0.53	0.015	0.51	0.54	3
Lake Metalimnion	Magnesium	mg/L	0.53	0.020	0.51	0.55	3
Reference Enclosure (unoiled)	Magnesium	mg/L	0.87	0.054	0.76	0.92	7
Experimental Enclosure (oiled)	Manganese	mg/L	0.0116	0.00788	<LOD (0.0145)	0.0269	7
Lake Epilimnion	Manganese	mg/L	0.0121	0.00840	<LOD (0.0145)	0.0218	3
Lake Metalimnion	Manganese	mg/L	0.0300	0.02949	<LOD (0.0145)	0.0633	3
Reference Enclosure (unoiled)	Manganese	mg/L	0.0102	0.00784	<LOD (0.0145)	0.0280	7
Experimental Enclosure (oiled)	Nitrate	µg/L	2	1.9	1	6	7
Lake Epilimnion	Nitrate	µg/L	1	0.3	<LOD (1)	1	3
Lake Metalimnion	Nitrate	µg/L	4	3.1	1	7	3
Reference Enclosure (unoiled)	Nitrate	µg/L	3	2.3	<LOD (1)	7	7
Experimental Enclosure (oiled)	Nitrite	µg/L	0.44	0.313	<LOD (0.43)	1.00	7
Lake Epilimnion	Nitrite	µg/L	0.22	0.000	<LOD (0.43)	0.22	3

Site	Parameter	Units	Mean	Std Dev	Min	Max	N
Lake Metalimnion	Nitrite	µg/L	0.22	0.000	<LOD (0.43)	0.22	3
Reference Enclosure (unoiled)	Nitrite	µg/L	0.59	0.423	<LOD (0.43)	1.20	7
Experimental Enclosure (oiled)	Particulate Carbon	µg/L	477	72.7	374	586	7
Lake Epilimnion	Particulate Carbon	µg/L	366	37.9	337	409	3
Lake Metalimnion	Particulate Carbon	µg/L	500	64.5	446	571	3
Reference Enclosure (unoiled)	Particulate Carbon	µg/L	578	126.0	425	766	7
Experimental Enclosure (oiled)	Particulate Nitrogen	µg/L	61	12.9	42	83	7
Lake Epilimnion	Particulate Nitrogen	µg/L	44	9.3	33	50	3
Lake Metalimnion	Particulate Nitrogen	µg/L	58	11.6	46	68	3
Reference Enclosure (unoiled)	Particulate Nitrogen	µg/L	71	14.9	45	91	7
Experimental Enclosure (oiled)	Particulate Phosphorus	µg/L	5	1.1	3	6	7
Lake Epilimnion	Particulate Phosphorus	µg/L	2	0.6	2	3	3
Lake Metalimnion	Particulate Phosphorus	µg/L	4	0.0	4	4	3
Reference Enclosure (unoiled)	Particulate Phosphorus	µg/L	6	1.9	4	9	7
Lake Epilimnion	pH	SU	6.955	0.0301	6.920	6.974	3
Lake Metalimnion	pH	SU	6.536	0.3238	6.230	6.875	3
Experimental Enclosure (oiled)	Potassium	mg/L	0.42	0.034	0.37	0.47	7
Lake Epilimnion	Potassium	mg/L	0.37	0.006	0.36	0.37	3
Lake Metalimnion	Potassium	mg/L	0.36	0.006	0.36	0.37	3
Reference Enclosure (unoiled)	Potassium	mg/L	0.56	0.063	0.49	0.65	7
Experimental Enclosure (oiled)	Sodium	mg/L	0.85	0.033	0.82	0.90	7
Lake Epilimnion	Sodium	mg/L	0.83	0.025	0.81	0.86	3
Lake Metalimnion	Sodium	mg/L	0.82	0.000	0.82	0.82	3
Reference Enclosure (unoiled)	Sodium	mg/L	0.93	0.021	0.91	0.97	7
Experimental Enclosure (oiled)	Soluble Reactive Silica	mg/L	105.868	277.8620	0.734	736.000	7

Site	Parameter	Units	Mean	Std Dev	Min	Max	N
Lake Epilimnion	Soluble Reactive Silica	mg/L	1.375	0.0381	1.343	1.417	3
Lake Metalimnion	Soluble Reactive Silica	mg/L	1.374	0.1372	1.257	1.525	3
Reference Enclosure (unoiled)	Soluble Reactive Silica	mg/L	0.265	0.0637	0.168	0.333	7
Experimental Enclosure (oiled)	Sulfate	mg/L	1.02	0.042	0.93	1.05	7
Lake Epilimnion	Sulfate	mg/L	1.11	0.060	1.05	1.17	3
Lake Metalimnion	Sulfate	mg/L	1.16	0.105	1.05	1.26	3
Reference Enclosure (unoiled)	Sulfate	mg/L	1.02	0.124	0.91	1.26	7
Experimental Enclosure (oiled)	Total Dissolved Nitrogen	µg/L	320.3	27.49	270.0	354.0	7
Lake Epilimnion	Total Dissolved Nitrogen	µg/L	243.7	10.60	234.0	255.0	3
Lake Metalimnion	Total Dissolved Nitrogen	µg/L	238.3	3.51	235.0	242.0	3
Reference Enclosure (unoiled)	Total Dissolved Nitrogen	µg/L	411.4	33.29	349.0	447.0	7
Experimental Enclosure (oiled)	Total Dissolved Phosphorus	µg/L	4.0	0.71	3.1	5.1	7
Lake Epilimnion	Total Dissolved Phosphorus	µg/L	2.9	1.14	2.1	4.2	3
Lake Metalimnion	Total Dissolved Phosphorus	µg/L	3.4	0.85	2.8	4.4	3
Reference Enclosure (unoiled)	Total Dissolved Phosphorus	µg/L	5.4	1.12	3.9	6.9	7
Experimental Enclosure (oiled)	Total Dissolved Solids	mg/L	33.29	12.984	16.00	49.00	7
Lake Epilimnion	Total Dissolved Solids	mg/L	12.00	7.000	4.00	17.00	3
Lake Metalimnion	Total Dissolved Solids	mg/L	16.67	13.317	8.00	32.00	3
Reference Enclosure (unoiled)	Total Dissolved Solids	mg/L	35.29	16.173	17.00	64.00	7
Experimental Enclosure (oiled)	Total Suspended Solids	mg/L	1.15	0.597	<LOD (0.05)	2.00	7
Lake Epilimnion	Total Suspended Solids	mg/L	1.33	0.306	1.00	1.60	3
Lake Metalimnion	Total Suspended Solids	mg/L	1.47	0.513	0.90	1.90	3
Reference Enclosure (unoiled)	Total Suspended Solids	mg/L	1.51	0.958	0.40	3.40	7
Experimental Enclosure (oiled)	Turbidity	NTU	0.58	0.079	0.49	0.70	7
Lake Epilimnion	Turbidity	NTU	0.48	0.044	0.43	0.51	3

Site	Parameter	Units	Mean	Std Dev	Min	Max	N
Lake Metalimnion	Turbidity	NTU	0.86	0.255	0.69	1.15	3
Reference Enclosure (unoiled)	Turbidity	NTU	0.71	0.077	0.61	0.81	7

Note, number of digits is based on decimal places for each analyte minimum limit of detection (LOD). Results <LOD were replaced with half LOD to calculate the mean and standard deviation.

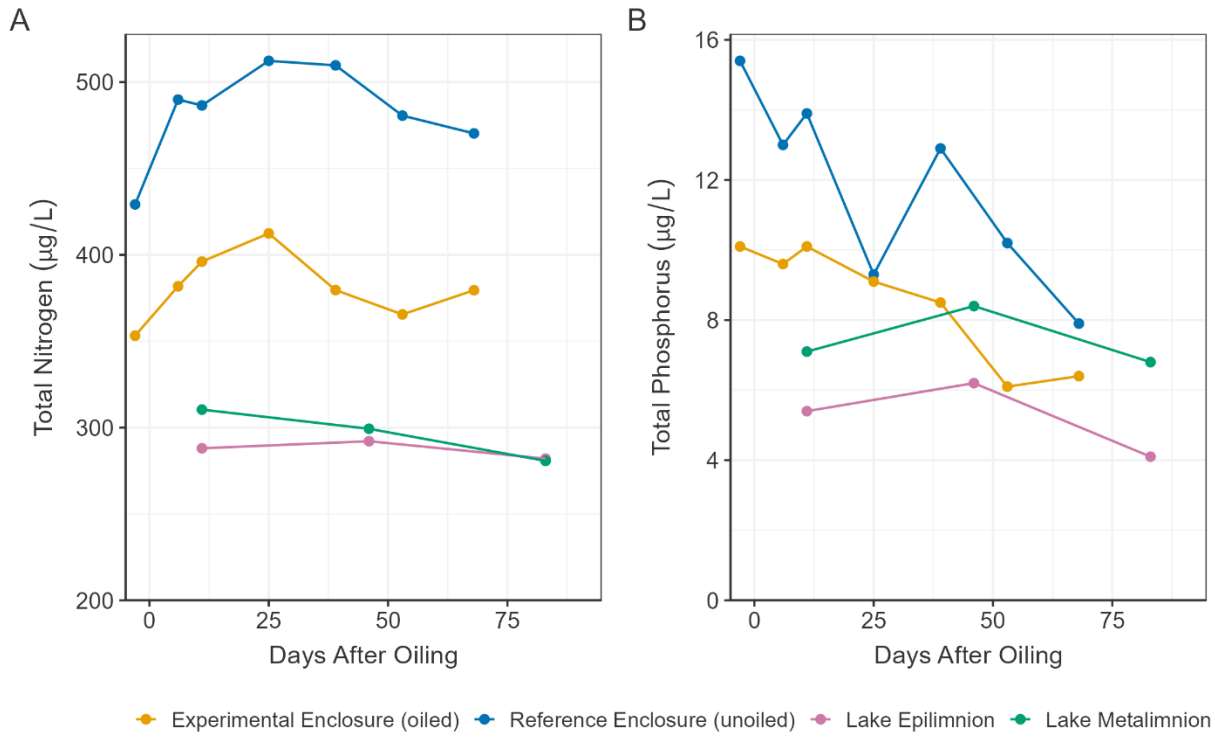

Figure B14. Total nitrogen (A) and total phosphorus (B) concentration in FLOWTER enclosures and Lake 260 epilimnion and metalimnion during pre-oil conditions and up to day 68 post-oil addition in the enclosures and day 83 in the lake during the 2021 CHV experiment.

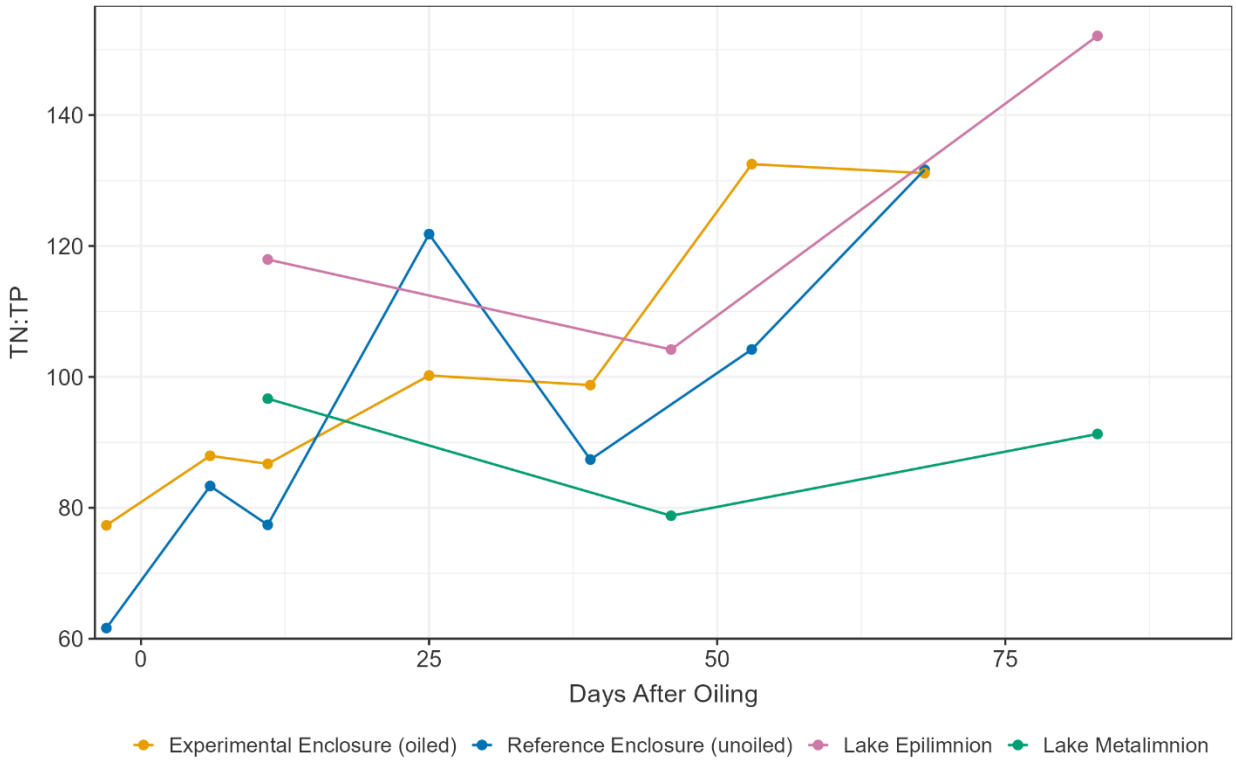

Figure B15. TN:TP molar ratio in the FLOWTER enclosures and Lake 260 epilimnion and metalimnion during pre-oil conditions and up to day 68 post-oil addition in the enclosures and from day 11 to day 83 in the lake during the 2021 CHV experiment.

B.6 Root Microbial Community

Table B4. Mean (±SD of site replicates; N=3) prokaryotic and eukaryotic rarefied Alpha richness (observed ASVs), Chao 1 richness, Shannon diversity, and Simpson diversity in the EFW root microbial biofilm for each sample period during the 2021 CHV experiment.

Site	Days After Oiling	Alpha Richness	Chao 1 Richness	Shannon Diversity	Simpson Diversity	Alpha Richness	Chao1 Richness	Shannon Diversity	Simpson Diversity
		Prokaryotes (16S)				Eukaryotes (18S)[a]			
Experimental Enclosure (oiled)	-11	1084 ± 258.9	1114 ± 279.9	5.97 ± 0.338	0.993 ± $4.25e^{-03}$	259 ± 83.4	364 ± 166	4.99 ± 0.284	0.988 ± $1.49e^{-03}$
Experimental Enclosure (oiled)	33	1512 ± 132.2	1540 ± 136.5	6.56 ± 0.162	0.997 ± $6.98e^{-04}$	232 ± 107	339 ± 199	4.54 ± 0.682	0.966 ± $2.73e^{-02}$
Experimental Enclosure (oiled)	84	1381 ± 97.67	1400 ± 103.5	6.55 ± $3.68e^{-02}$	0.997 ± $1.84e^{-04}$	253 ± 42.8	458 ± 104	4.41 ± 0.343	0.959 ± $1.59e^{-02}$
Reference Enclosure (unoiled)	-11	1286 ± 182.8	1326 ± 199.0	6.17 ± $8.52e^{-02}$	0.994 ± $1.08e^{-03}$	262 ± 26.2	408 ± 45.9	4.61 ± 0.352	0.968 ± $1.55e^{-02}$
Reference Enclosure (unoiled)	33	1180 ± 388.5	1192 ± 401.3	6.23 ± 0.394	0.994 ± $1.20e^{-03}$	224 ± 45.0	321 ± 105	4.26 ± 0.225	0.954 ± $7.22e^{-03}$
Reference Enclosure (unoiled)	84	1659 ± 95.00	1696 ± 96.68	6.73 ± 0.119	0.997 ± $6.85e^{-04}$	291 ± 2.76	479 ± 32.5	4.95 ± $4.14e^{-02}$	0.984 ± $2.76e^{-03}$

Site	Days After Oiling	Alpha Richness	Chao 1 Richness	Shannon Diversity	Simpson Diversity	Alpha Richness	Chao1 Richness	Shannon Diversity	Simpson Diversity
		Prokaryotes (16S)				Eukaryotes (18S)[a]			
Lake Reference (unoiled)	-11	1140 ± 95.12	1167 ± 104.6	6.11 ± 3.46e^{-02}	0.994 ± 7.18e^{-04}	266 ± 96.8	383 ± 200	4.75 ± 0.572	0.971 ± 2.06e^{-02}
Lake Reference (unoiled)	33	1106 ± 103.8	1127 ± 111.9	5.71 ± 0.347	0.981 ± 1.12e^{-02}	189 ± 12.0	290 ± 83.8	3.59 ± 1.21	0.818 ± 0.224
Lake Reference (unoiled)	84	1344 ± 478.3	1373 ± 500.1	6.17 ± 0.308	0.990 ± 2.76e^{-03}	229 ± 129	424 ± 378	4.46 ± 0.536	0.967 ± 9.32e^{-03}

[a] One replicate from both the RE and LR on day 33 were excluded from 18S richness and diversity analyses due to extremely low richness detected, skewing interpretation of the entire community.

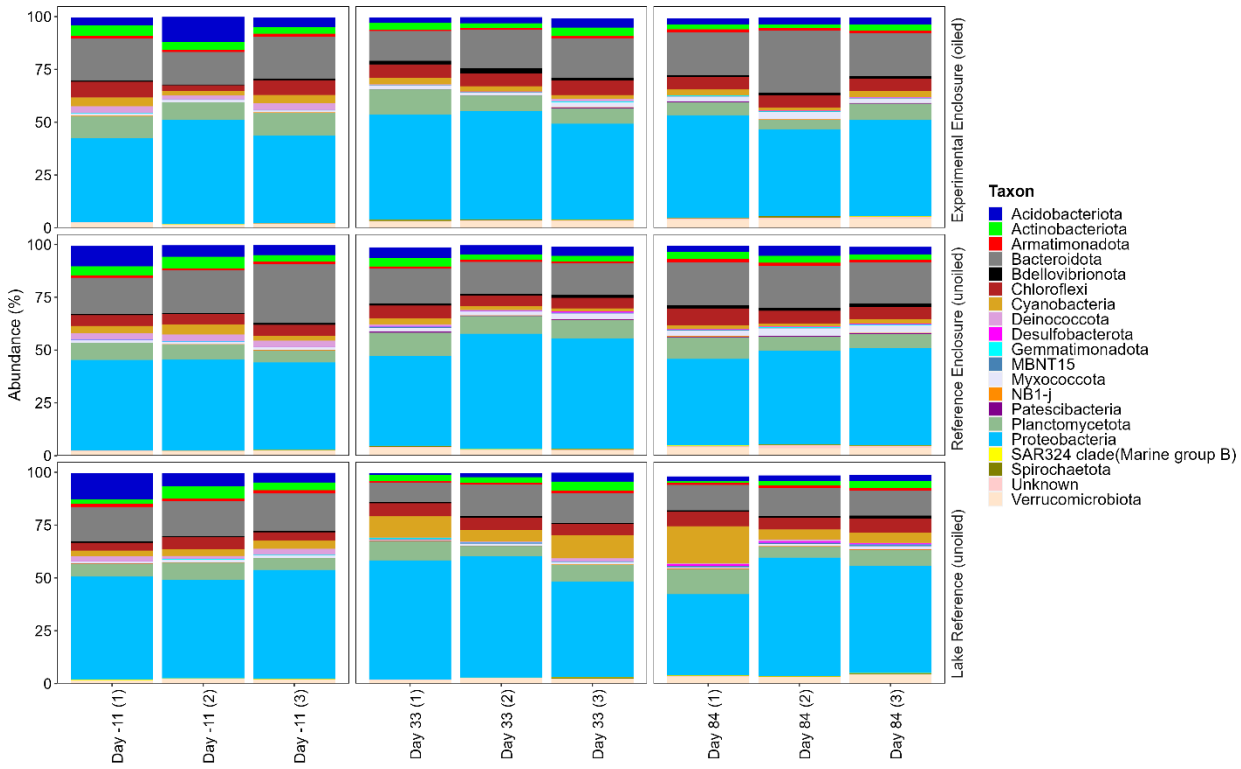

Figure B16. Taxonomic profile of the top twenty most relatively abundant 16S phyla in EFW root biofilm replicates from the EE, RE, and LR 11 days pre-oil addition, and on days 33 and 84 post-oil addition during the 2021 CHV experiment.

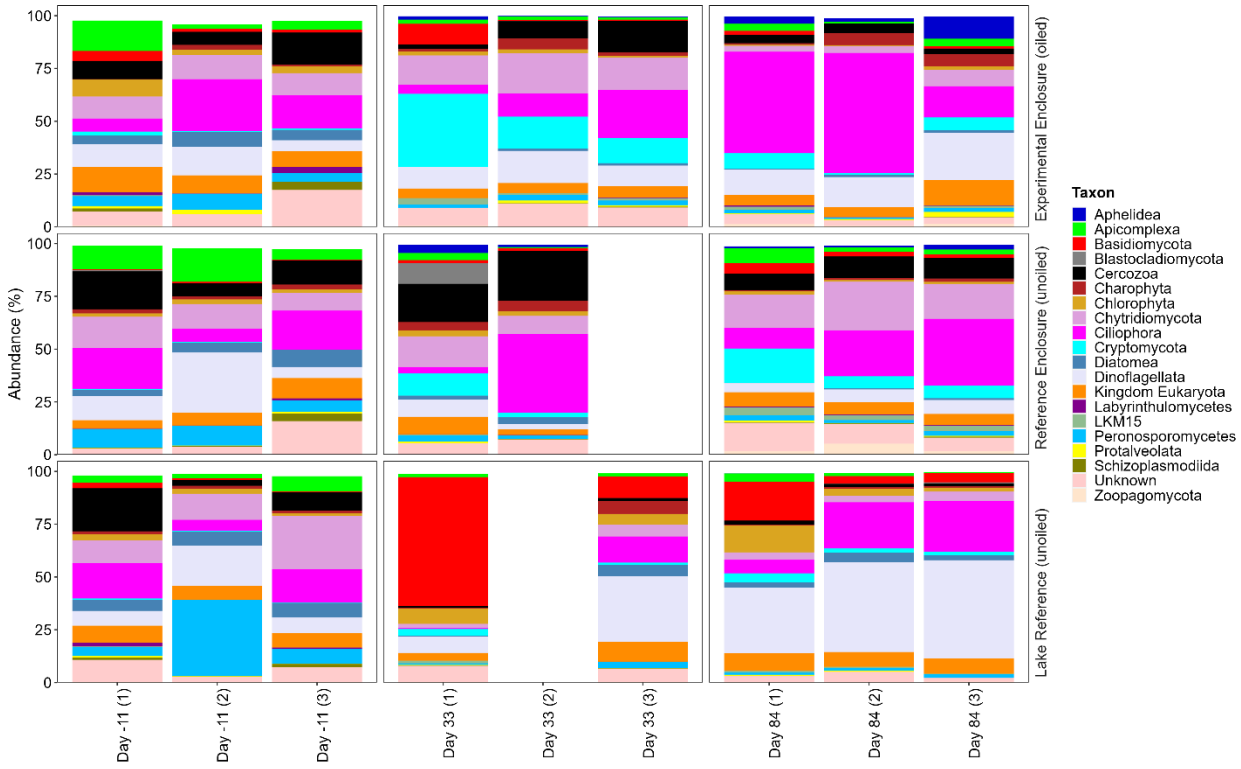

Figure B17. Taxonomic profile of the top twenty most relatively abundant 18S phyla in EFW root biofilm replicates from the EE, RE, and LR 11 days pre-oil addition, and on days 33 and 84 post-oil addition during the 2021 CHV experiment.

B.7 Microbial ATP

Adenosine triphosphate (ATP) on EFW roots was measured as a metric of microbial energy (pg ATP), using LuminUltra 2nd Generation ATP ® test kits and PhotonMaster Luminometer, which equates to microbial quantity/concentrations (LuminUltra, n.d., 2017). Following manufacturers guidelines for measured deposit, root clippings were made from EFW roots on days -11, 33, 62, and 84 of exposure, with efforts to collect cattail roots to minimize variability between plants species. Following the assay, roots were removed from the lysing agent and rinsed three times in deionized reverse osmosis water and gently dried using a

kimwipe. Root samples were weighed for wet biomass (mg) and photographed for surface area (cm^2) determined using Fiji software (v. 1.53c; Schindelin et al., 2012). Roots were then placed in a 60 ℃ drying oven for 24 hours, and weighed for dry biomass (mg). ATP in each root sample was calculated by manufacturers calculations and corrected for root dry weight to standardize between sample size.

ATP (ng ATP/mg dry root weight) showed high variability during each sample round (Table B5), likely a result of spatial diversity on EFW roots (Sasse et al., 2018). Mean ATP in the EE and RE were stable during the first two sampling rounds. ATP decreased on day 62, later increasing on day 84 in the EE, while the reference enclosure increased over the exposure period. The temporal increase is likely a result of biofilm growth over time, and likely not a reflection of site conditions. Mean ATP was often higher in the LR from day 33 to 84, but the high variability caused difficulty in assessing whether there were any seasonal trends. Since we cannot conduct statistical analyses, it cannot be confirmed whether differences were a result of seasonality or site conditions. However, the increased mean ATP in the LR on day 33 and 62 could be a result of rapid changes to the microbial community as observed in the diversity and taxonomic analyses, or the result of an enclosure effect decreasing microbial activity. Future replicated research should analyze ATP to see if there are significant differences of root microbial energy/quantity between oiled and unoiled EFWs.

Table B5. Mean (± SD of site replicates) total ATP (ng ATP/mg dry weight) of EFW cattail roots and biofilm over the exposure period of the 2021 CHV experiment.

EFW Site	**Pre Oil (Day -11)**	**Day 33**	**Day 62**	**Day 84**
	N=3	N=6	N=6	N=6
Experimental Enclosure (oiled)	117.4 ± 113.5	177.9 ± 173.3 (n=5)	52.41 ± 15.88	214.4 ± 165.3
Reference Enclosure (unoiled)	135.0 ± 88.78	137.5 ± 120.4	244.9 ± 373.4	304.1 ± 315.4
Lake Reference (unoiled)	63.85 ± 50.09	680.2 ± 1028	720.3 ± 525.9	361.5 ± 314.0

Appendix C- Chapter 5

C.1 Methods

Table C1. Final mols in 1 L of 5% and 10% strength modified Hoagland media based on (Hoagland and Arnon, 1938).

Compounds	5 % strength	10% strength
KNO_3	0.00025	0.0005
$Ca(NO_3)_2 \cdot 4H_2O$	0.00025	0.0005
$MgSO_4 \cdot 7H_2O$	0.0001	0.0002
KH_2PO_4	0.00005	0.0001
H_3BO_3	$2.31 e^{-06}$	$4.63 e^{-06}$
$MnCl_2 \cdot 4H_2O$	$4.64 e^{-07}$	$9.29 e^{-07}$
$ZnSO_4 \cdot 7H_2O$	$3.82 e^{-08}$	$7.65 e^{-08}$
$CuSO_4 \cdot 5H_2O$	$1.60 e^{-08}$	$3.20 e^{-08}$
$H_2MoO_4 \cdot 2H_2O$	$2.48 e^{-08}$	$4.96 e^{-08}$
$C_{12}H_{12}Fe_2O_{18}$	$4.50 e^{-07}$	$8.99 e^{-07}$

Figure C1. Experimental design including (A) foil covered glass jars/microcosms, (B) stainless steel hydroponic pots, (C) experimental set up in pool and greenhouse tent, (D) example microcosm at the end of the experiment.

C.2 Photoelectrochemical oxygen demand

Photoelectrochemical oxygen demand (peCOD) was analyzed using the peCOD ® COD Analyzer L50 (Mantech Inc, Guelph, Ontario) in 5 mL water samples from microcosms A, B, F, G, and H on days 0, 2, 5, 20 and 21 of exposure. Efforts were made to monitor rate of peCOD degradation as a metric of phenanthrene removal. However, the methanol in phenanthrene standard may have skewed the interpretation of peCOD removal rates. An oversite was not applying the same volume of methanol to microcosm replicates without phenanthrene, this would ensure comparability between microcosms and the same background carbon sources potentially used by the microbial community. Following these results, a replicated experiment was conducted to assess peCOD readings in milli-q water treated with (1) phenanthrene standard (in methanol), (2) Optima ™ methanol, and (3) milli-q alone in triplicate. A Kruskal Wallace ($\chi^2 = 5.42$, $p = 0.07$, df = 2) and Dunn Test identified no significant difference between methanol and phenanthrene treatments (unadjusted $p = 0.88$) (data not shown). Future research should be mindful of interpreting COD results in experiments with chemical standards in carbon-based solvents, and should add equal volumes of solvent into uncontaminated treatments, or include the analyte in chemical analyses.

C.3 Basic Water Quality

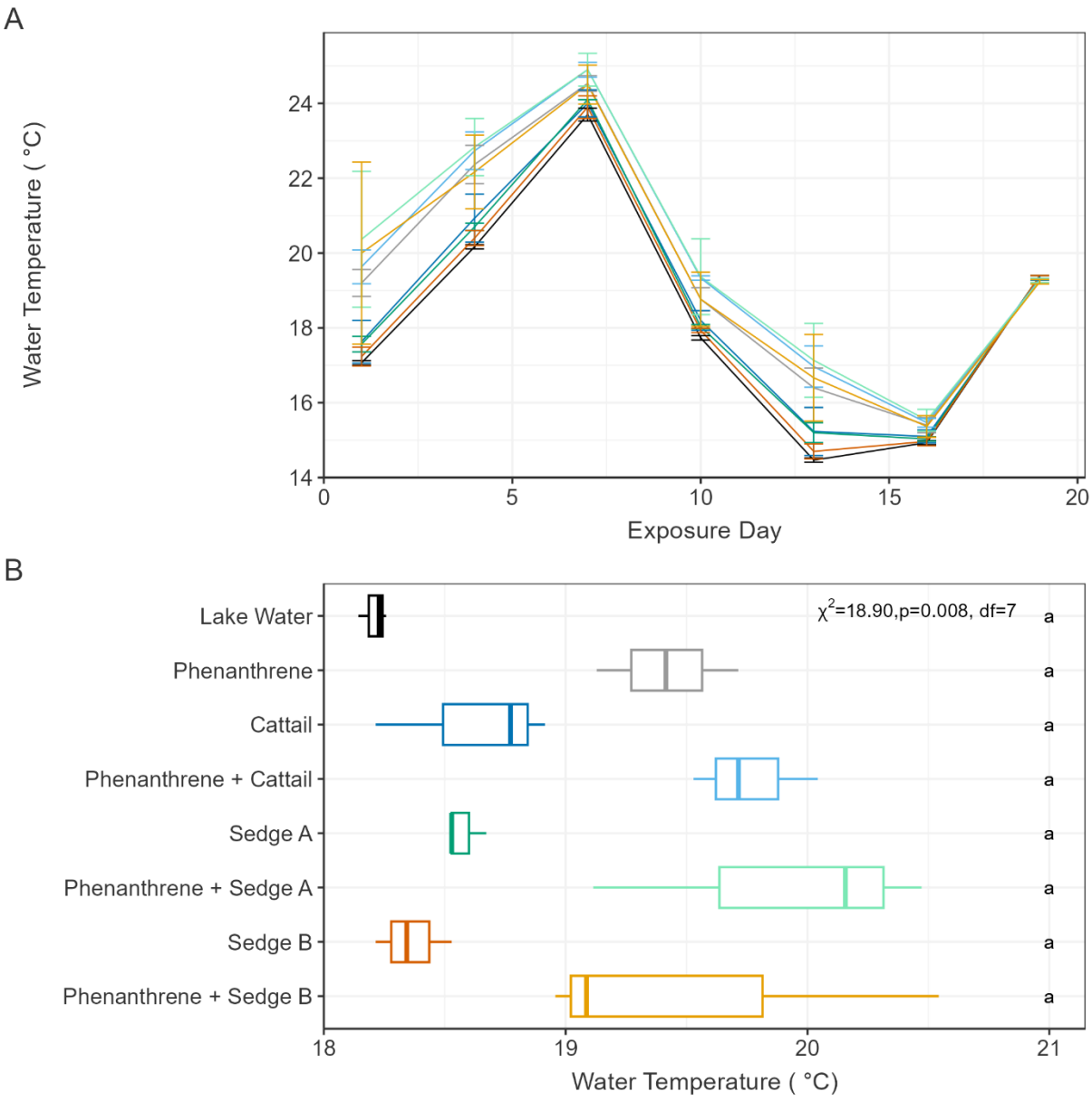

Figure C2. Mean trends and boxplots of water temperature in freshwater microcosms over the experimental period. Error bars in (A) represent standard deviation of microcosm replicates (n=3). Letters in (B) represent significant differences ($p < 0.05$) identified from Kruskal Wallace and Dunn Tests (holm *p*-value adjustment).

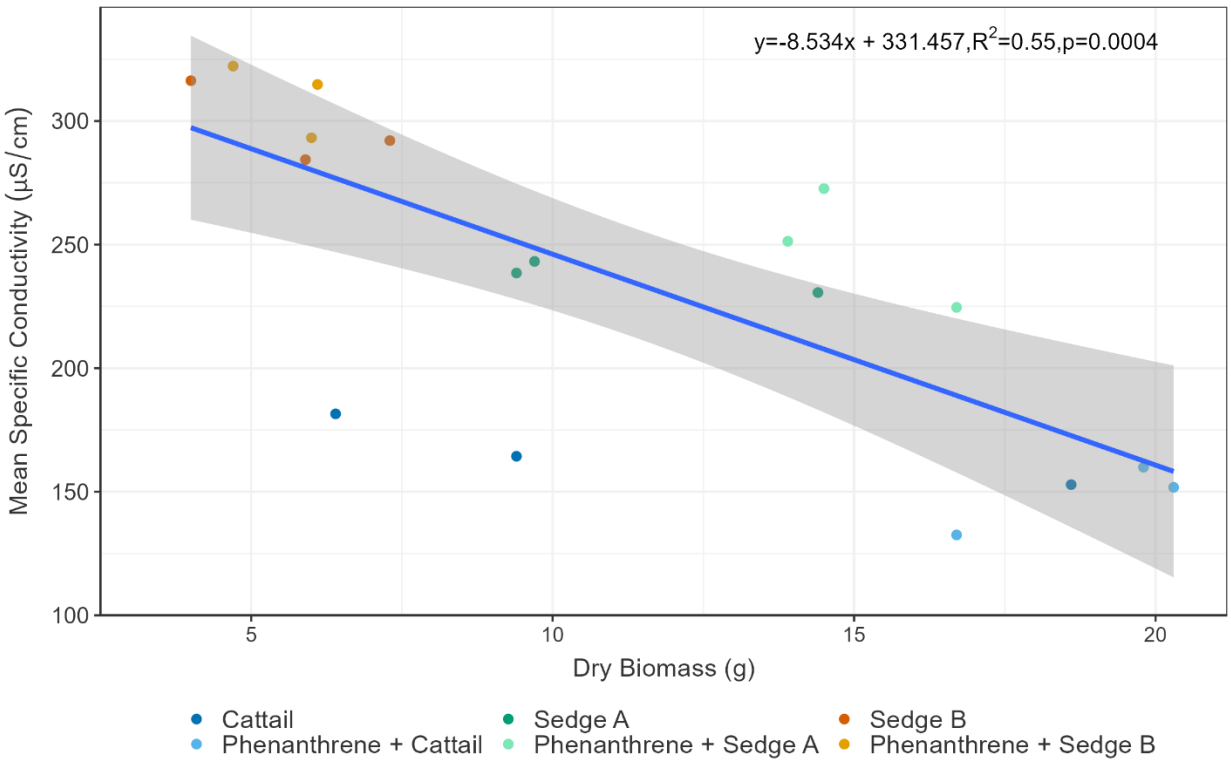

Figure C3. Linear relationship between mean specific conductivity (for each microcosm) and final dry biomass.

The following GAMM models were prepared to identify the relationship of time and treatment on specific conductivity, pH, and dissolved oxygen concentration using microcosms as a random effect. Each model was prepared using the maximum degrees of freedom for the k value for each smoothing term, however it is acknowledged that some models may be underfitting the trend based on k index values using gam.check in the *mgcv* package (v 1.9-0; Wood, 2023, 2017). For example, k index values for pH and DO are 0.91 and 0.92, respectively, however no significant *p*-values were identified in gam.check. In addition, *p*-values from the statistical test for each smooth (Ref Df and F) are approximate.

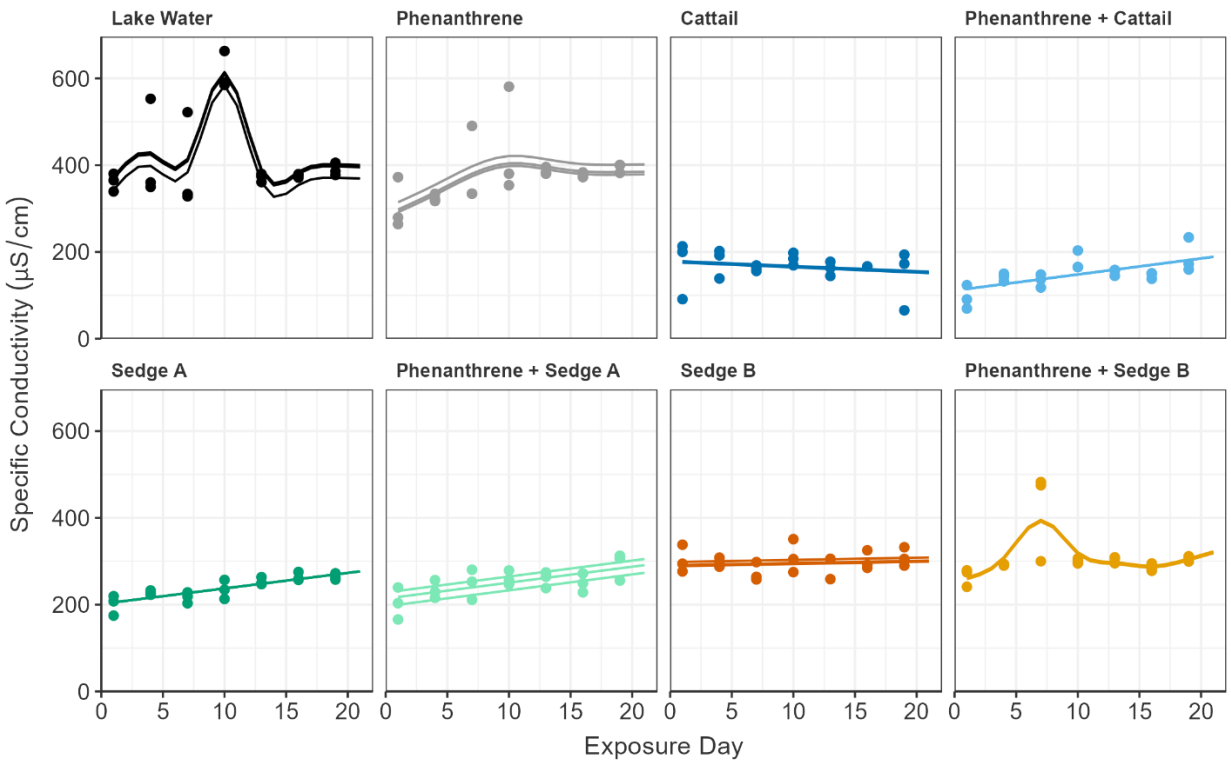

Figure C4. GAMM of specific conductivity over the experimental period for each treatment type. Main model fit (line) is presented for each microcosm replicate, predicted daily for 21 days. Model: conductivity ~ treatment + s(exposure day, by = treatment, k = 7, m = 2, bs = "tp") + s(microcosm, by = treatment, bs = "re"), R^2adj = 0.869, deviance explained = 89.3 %, -REML = 805.75, Scale est. = 1367.6, n = 167. Note: One Cattail microcosm replicate had a conductivity under range on day 16.

Table C2. Significance of parametric coefficients (treatment; A) and approximate significance of smooth terms (B) of conductivity GAMM (Figure C4).

A				
Parametric Coefficients	**Estimate**	**Standard Error**	**t value**	***p*-value**
Intercept	418.41	14.21	29.450	$< 2e^{-16}$ ***
Lake Water	NA	NA	NA	NA
Phenanthrene	-45.43	18.73	-2.425	0.0166 *
Cattail	-252.39	16.69	-15.122	$< 2e^{-16}$ ***
Phenanthrene + Cattail	-270.46	16.37	-16.522	$< 2e^{-16}$ ***
Sedge A	-181.10	16.34	-11.084	$< 2e^{-16}$ ***
Phenanthrene + Sedge A	-169.01	19.88	-8.504	$2.99e^{-14}$ ***
Sedge B	-120.82	17.16	-7.042	$8.67e^{-11}$ ***
Phenanthrene + Sedge B	-108.19	16.66	-6.495	$1.46e^{-09}$ ***
B				
Smooth Terms	**EDF***	**Ref Df**	**F**	***p*-value**
Exposure Day: Lake Water	5.806	5.984	16.131	$< 2e^{-16}$ ***
Exposure Day: Phenanthrene	2.860	3.517	5.915	$5.68e^{-04}$ ***
Exposure Day: Cattail	1.000	1.000	0.758	0.386
Exposure Day: Phenanthrene + Cattail	1.000	1.000	7.537	$6.87e^{-03}$ **
Exposure Day: Sedge A	1.000	1.000	7.083	$8.72e^{-03}$ **
Exposure Day: Phenanthrene + Sedge A	1.000	1.000	7.449	$7.19e^{-03}$ **
Exposure Day: Sedge B	1.000	1.000	0.145	0.704
Exposure Day: Phenanthrene + Sedge B	4.938	5.599	4.815	$1.04e^{-03}$ **
Microcosm: Lake Water	1.355	2.000	2.099	0.0483 *
Microcosm: Phenanthrene	1.125	2.000	1.287	0.106
Microcosm: Cattail	$2.117e^{-01}$	2.000	0.119	0.328
Microcosm: Phenanthrene + Cattail	$2.991e^{-02}$	2.000	0.015	0.365
Microcosm: Sedge A	$6.722e^{-05}$	2.000	0.000	0.813
Microcosm: Phenanthrene + Sedge A	1.326	2.000	1.966	0.0548
Microcosm: Sedge B	$5.929e^{-01}$	2.000	0.421	0.245

Smooth Terms	EDF*	Ref Df	F	*p*-value
Microcosm: Phenanthrene + Sedge B	$2.780e^{-01}$	2.000	0.161	0.316

*EDF: Estimated degrees of freedom. The larger the value, the less linear (Zuur et al., 2019).

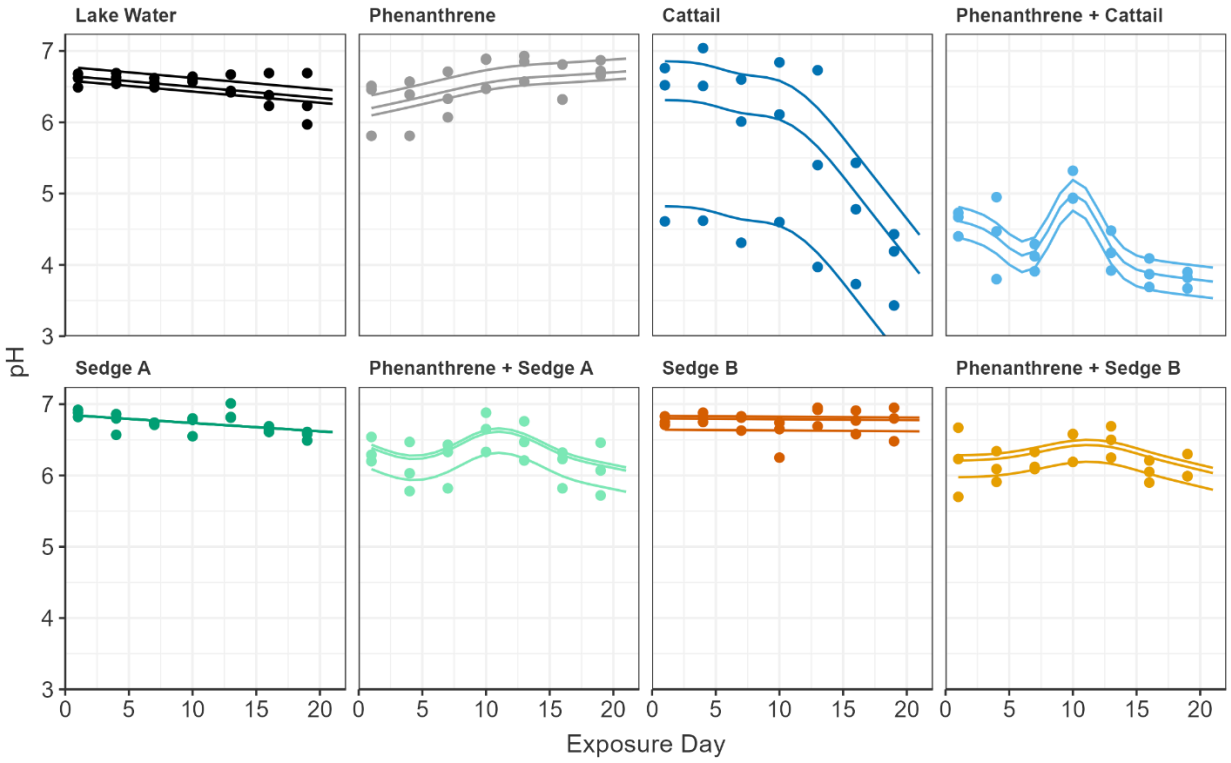

Figure C5. GAMM of pH over the experimental period for each treatment type. Main model fit (line) is presented for each microcosm replicate, predicted daily for 21 days. Model: pH ~ treatment + s(exposure day, by = treatment, k = 7, m = 2, bs = "tp") + s(microcosm, by = treatment, bs = "re"), R^2adj = 0.952, deviance explained = 96.3 %, -REML = 31.704, Scale est. = 0.04203, n = 168.

Table C3. Significance of parametric coefficients (treatment; A) and approximate significance of smooth terms (B) of pH GAMM (Figure C5).

A				
Parametric Coefficients	**Estimate**	**Standard Error**	**t value**	***p*-value**
Intercept	6.517	0.0807	80.717	$< 2e^{-16}$ ***
Lake Water	NA	NA	NA	NA
Phenanthrene	$4.286e^{-03}$	0.130	0.033	0.974
Cattail	-1.154	0.617	-1.871	0.0636
Phenanthrene + Cattail	-2.225	0.161	-13.861	$< 2e^{-16}$ ***
Sedge A	0.2181	0.0923	2.363	0.0196 *
Phenanthrene + Sedge A	-0.2405	0.148	-1.629	0.106
Sedge B	0.2310	0.116	1.992	0.0486*
Phenanthrene + Sedge B	-0.2929	0.137	-2.137	0.0345*
B				
Smooth Terms	**EDF***	**Ref Df**	**F**	***p*-value**
Exposure Day: Lake Water	1.000	1.000	4.441	0.0370 *
Exposure Day: Phenanthrene	1.845	2.291	6.549	$1.26e^{-03}$ **
Exposure Day: Cattail	3.615	4.379	54.860	$< 2e^{-16}$ ***
Exposure Day: Phenanthrene + Cattail	5.574	5.928	13.144	$< 2e^{-16}$ ***
Exposure Day: Sedge A	1.000	1.000	2.432	0.121
Exposure Day: Phenanthrene + Sedge A	3.827	4.606	2.910	0.0161 *
Exposure Day: Sedge B	1.000	1.000	0.024	0.878
Exposure Day: Phenanthrene + Sedge B	2.727	3.359	1.583	0.155
Microcosm: Lake Water	1.386	2.000	2.257	0.0417 *
Microcosm: Phenanthrene	1.614	2.000	4.182	$6.85e^{-03}$ **
Microcosm: Cattail	1.989	2.000	185.813	$< 2e^{-16}$ ***
Microcosm: Phenanthrene + Cattail	1.792	2.000	8.615	$1.29e^{-04}$ ***
Microcosm: Sedge A	$1.199e^{-05}$	2.000	0.000	0.799
Microcosm: Phenanthrene + Sedge A	1.738	2.000	6.629	$7.41e^{-04}$ ***

Smooth Terms	EDF*	Ref Df	F	*p*-value
Microcosm: Sedge B	1.422	2.000	2.462	0.0343 *
Microcosm: Phenanthrene + Sedge B	1.674	2.000	5.129	$2.87e^{-03}$ **

*EDF: Estimated degrees of freedom. The larger the value, the less linear (Zuur et al., 2019).

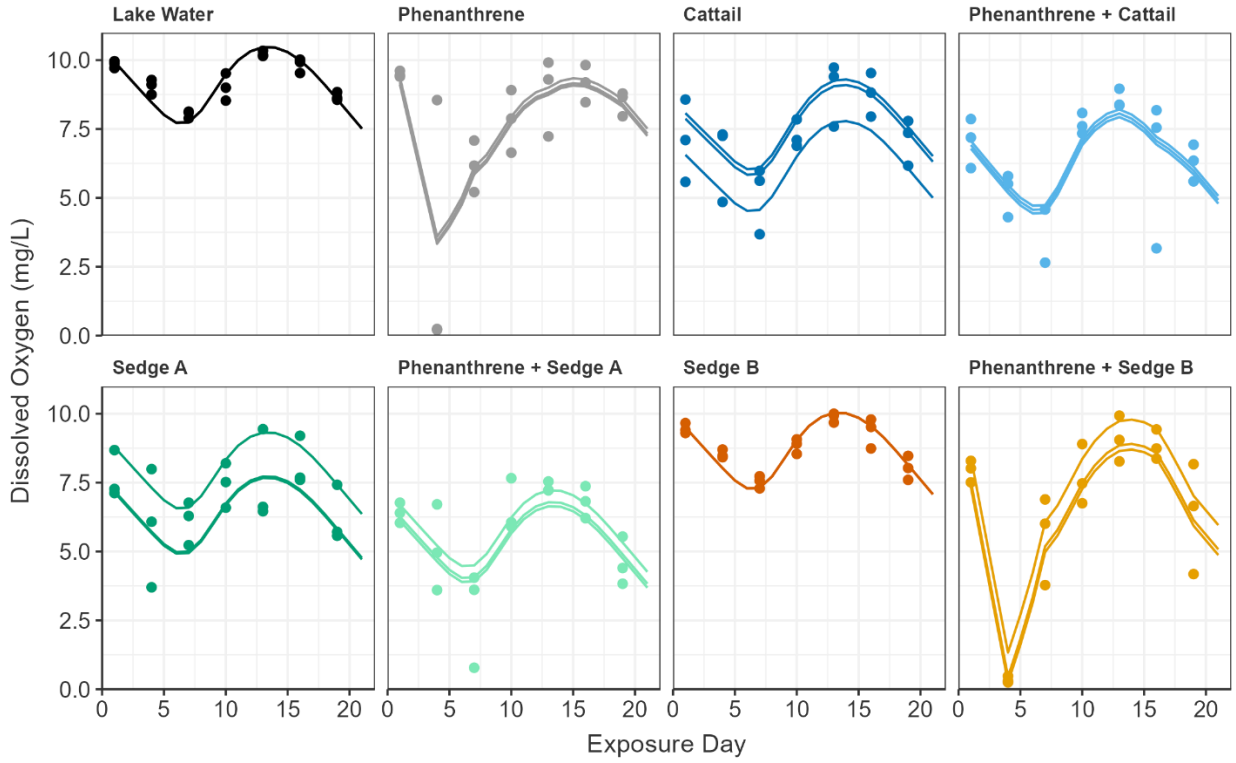

Figure C6. GAMM of dissolved oxygen over the experimental period for each treatment type. Main model fit (line) is presented for each microcosm replicate, predicted daily for 21 days. Model: dissolved oxygen ~ treatment + s(exposure day, k = 7, m = 2, bs = "tp")+ s(exposure day, by = treatment, k = 7, m = 1, bs = "tp") + s(microcosm, by = treatment, bs = "re"), R^2adj = 0.784, deviance explained = 82.8 %, -REML = 275.37, Scale est. = 1.0129, n = 168.

Table C4. Significance of parametric coefficients (treatment; A) and approximate significance of smooth terms (B) of dissolved oxygen GAMM (Figure C6).

A				
Parametric Coefficients	**Estimate**	**Standard Error**	**t value**	***p*-value**
Intercept	9.2400	0.2196	42.072	$< 2e^{-16}$ ***
Lake Water	NA	NA	NA	NA
Phenanthrene	-1.6838	0.3415	-4.930	$2.41e^{-06}$ ***
Cattail	-1.9967	0.6017	-3.318	$1.17e^{-03}$ **
Phenanthrene + Cattail	-2.8090	0.3431	-8.186	$1.95e^{-13}$ ***
Sedge A	-2.2333	0.6562	-3.403	$8.8e^{-04}$ ***
Phenanthrene + Sedge A	-3.5876	0.3905	-9.188	$7.08e^{-16}$ ***
Sedge B	-0.4381	0.3106	-1.411	0.161
Phenanthrene + Sedge B	-2.6952	0.4940	-5.455	$2.31e^{-07}$ ***
B				
Smooth Terms	**EDF***	**Ref Df**	**F**	***p*-value**
Exposure Day	5.242	5.741	17.546	$< 2e^{-16}$ ***
Exposure Day: Lake Water	$8.007e^{-05}$	6.000	0.000	0.694
Exposure Day: Phenanthrene	5.312	6.000	7.266	$< 2e^{-16}$ ***
Exposure Day: Cattail	1.325	6.000	0.507	0.0638
Exposure Day: Phenanthrene + Cattail	2.462	6.000	0.679	0.140
Exposure Day: Sedge A	$3.883e^{-05}$	6.000	0.000	0.911
Exposure Day: Phenanthrene + Sedge A	$3.354e^{-05}$	6.000	0.000	0.475
Exposure Day: Sedge B	$7.729e^{-05}$	6.000	0.000	0.684
Exposure Day: Phenanthrene + Sedge B	5.623	6.000	14.204	$< 2e^{-16}$ ***
Microcosm: Lake Water	$2.634e^{-05}$	2.000	0.000	0.767
Microcosm: Phenanthrene	0.5897	2.000	0.418	0.246
Microcosm: Cattail	1.693	2.000	5.506	$2.02e^{-03}$ **
Microcosm: Phenanthrene + Cattail	0.6122	2.000	0.441	0.240
Microcosm: Sedge A	1.748	2.000	6.928	$5.59e^{-04}$***

Smooth Terms	EDF*	Ref Df	F	*p*-value
Microcosm: Phenanthrene + Sedge A	1.074	2.000	1.161	0.119
Microcosm: Sedge B	$3.125e^{-05}$	2.000	0.000	0.679
Microcosm: Phenanthrene + Sedge B	1.507	2.000	3.060	0.0194 *

*EDF: Estimated degrees of freedom. The larger the value, the less linear (Zuur et al., 2019).

C.4 Plant Metrics

Table C5. Summary of final dry biomass (g) of plants by treatment.

Treatment	Mean ± SD	Range
Cattail (n=3)	11.5 ± 6.4	6.4 - 18.6
Phenanthrene + Cattail (n=3)	18.9 ± 2.0	16.7 - 20.3
Sedge A (n=3)	11.2 ± 2.8	9.4 - 14.4
Phenanthrene + Sedge A (n=3)	15.0 ± 1.5	13.9 - 16.7
Sedge B (n=3)	5.7 ± 1.7	4.0 - 7.3
Phenanthrene + Sedge B (n=3)	5.6 ± 0.8	4.7 - 6.1

C.5 Phenanthrene

Table C6. Mean (± SD of microcosm replicates) phenanthrene concentration (mg/L) in microcosms over 21 days of exposure.

Treatment	Day 0 (~hr 4)	Day 2	Day 5	Day 10	Day 21	% removal	% removal (nominal)
Lake Water (n=3)	$9.00e^{-04}$ ± $4.38e^{-04}$	$8.38e^{-04}$ ± $1.08e^{-04}$	$6.47e^{-04}$ ± $2.07e^{-04}$	$2.50e^{-04}$ ± $5.59e^{-05}$	$8.09e^{-05}$ ± $2.42e^{-05}$	NA	NA
Phenanthrene (n=3)	1.09 ± 0.326	1.21 ± 0.263	0.689 ± 0.274	0.179 ± 0.172	$5.66e^{-04}$ ± $2.13e^{-04}$	99.9 ± 0.0256	99.9 ± 0.0213
Phenanthrene + Cattail (n=3)	0.654 ± 0.0874	0.286 ± 0.0188	0.177 ± 0.0235	0.108 ± 0.0160	0.0554 ± $3.26e^{-03}$	91.5 ± 0.726	94.5 ± 0.329
Phenanthrene + Sedge A (n=3)	0.531 ± 0.113	0.280 ± 0.0531	0.187 ± 0.0420	0.101 ± $5.32e^{-03}$	0.0283 ± 0.0234	93.9 ± 5.34	97.2 ± 2.34
Phenanthrene + Sedge B (n=3)	0.688 ± 0.246	0.628 ± 0.0474	0.434 ± 0.0664	0.160 ± 0.0125	$3.57e^{-04}$ ± $1.01e^{-04}$	99.9 ± 0.0379	99.9 ± 0.0101
Method Blank (n=1)	$1.10e^{-03}$	$4.26e^{-04}$	$5.77e^{-04}$	$2.66e^{-04}$	$8.45e^{-05}$	NA	NA

Of note, on day 2 of exposure, a minor contamination occurred during extraction where some extract from sample 0053 (Lake Water + Phen + Sedge A) was transferred into 0056 (Lake Water + Phen). However, it is assumed no major influenced occurred, as concentrations in this microcosm were the lowest of the triplicate.

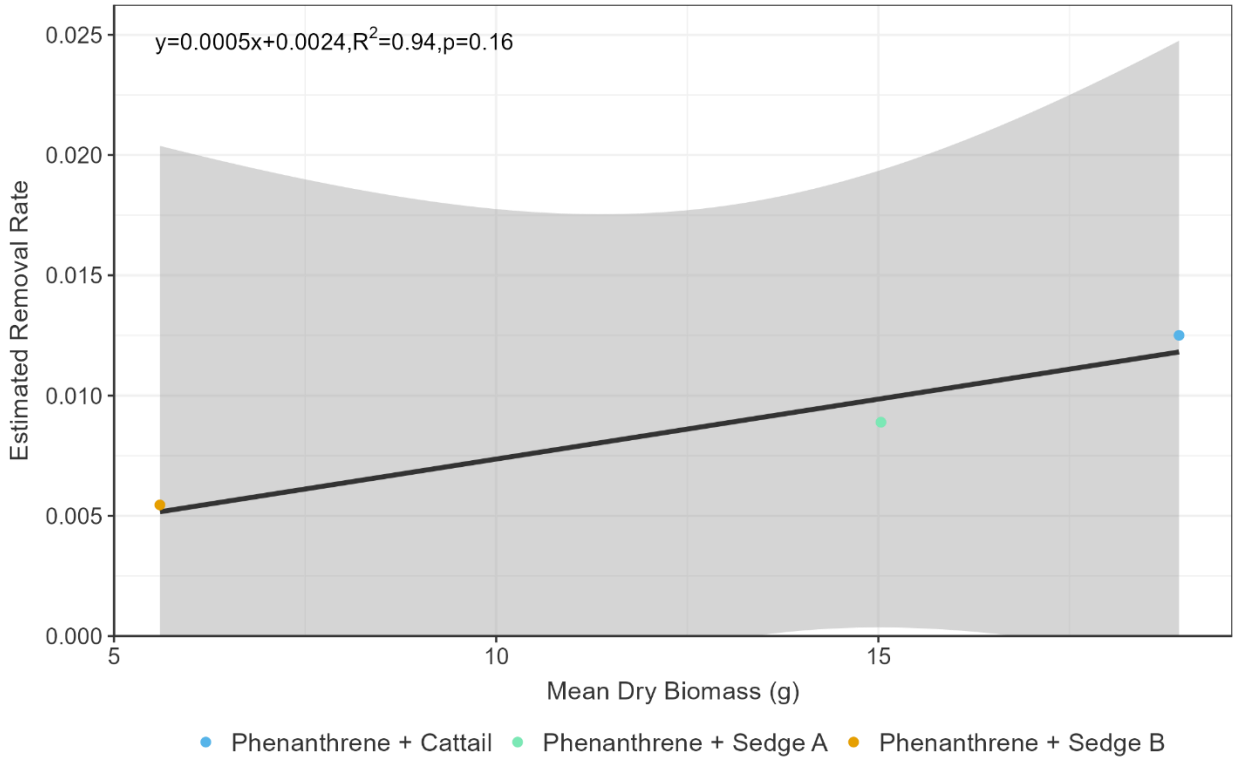

Figure C7. Linear relationship between mean dry biomass (n=3) and estimated phenanthrene removal rate.

C.6 Respirometry

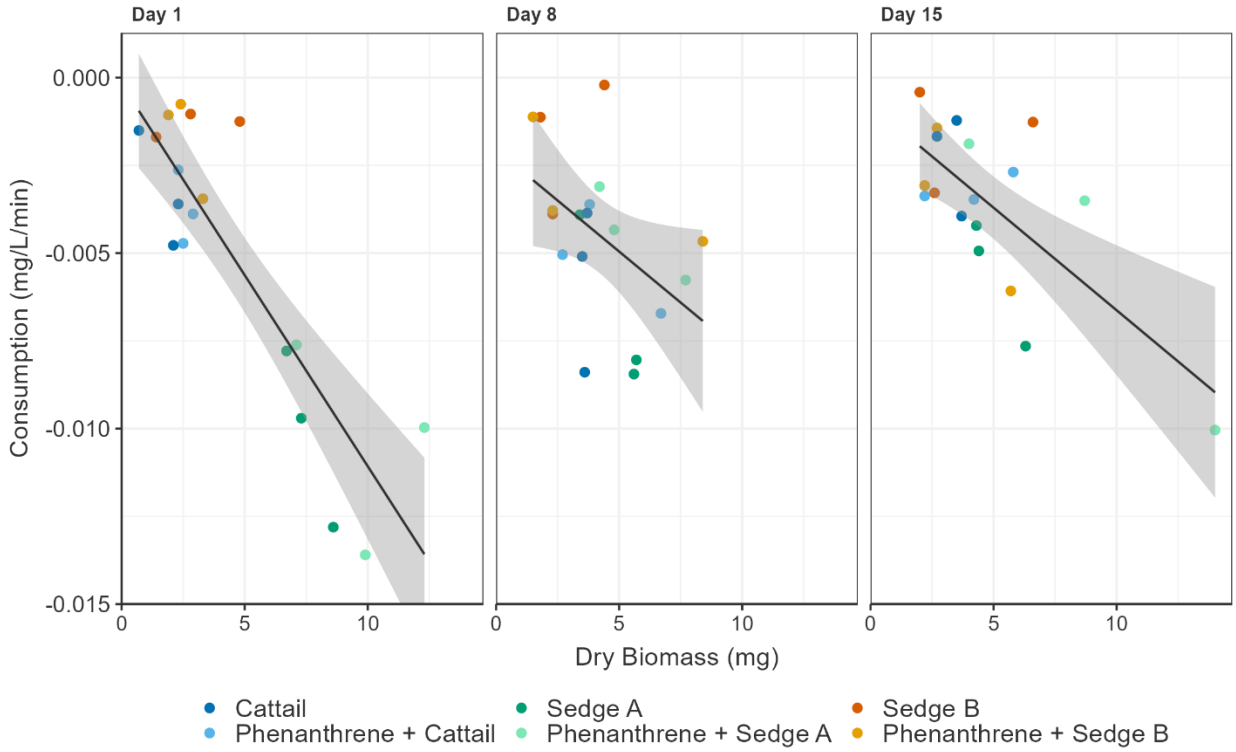

Figure C8. Linear relationship between root dry biomass and oxygen consumption on day 1 (r2 = 0.76, p = 2.61e-06, y = -0.001x-0.0002), day 8 (r2 = 0.23, p = 0.04, y = -0.0006x-0.002), and day 15 (r2 = 0.50, p = 0.001, y = -0.0006x-0.0008) of exposure. Note, negative values indicate oxygen removal.

Appendix D- Additional R packages used for data analyses and visualization not described in the main thesis.

Package	Version	Reference
broom	1.0.3	Robinson, Hayes, & Couch (2023)
data.table	1.14.8	Dowle & Srinivasan (2023)
dplyr	1.1.0	Wickham, François, Henry, Müller, & Vaughan (2023)
FSA	0.9.4	Ogle, Doll, Wheeler, & Dinno (2023)
ggpubr	0.6.0	Kassambara (2023)
gratia	0.8.1	Simpson (2023)
here	1.0.1	Müller (2020)
janitor	2.2.0	Firke (2023)
lubridate	1.9.2	Grolemund & Wickham (2011)
multcompView	0.1-8	Graves, Piepho, & Dorai-Raj (2019)
patchwork	1.1.2	Pedersen (2022)
purrr	1.0.1	Wickham & Henry (2023)
rcompanion	2.4.21	Mangiafico (2023)
readr	2.1.4	Wickham, Hester, & Bryan (2023)
reshape2	1.4.4	Wickham (2007)
stringr	1.5.0	Wickham (2022)
tibble	3.1.8	Müller & Wickham (2022)
tidyr	1.3.0	Wickham, Vaughan, & Girlich (2023)